"The Geology of Mexico has been but imperfectly studied"

Matias Romero, 1896

Cenozoic environmental evolution of the San Juan Raya Basin, south central Mexico

Thesis submitted for the degree of Doctor

of Philosophy at the University of Leicester

by

Javier Medina Sánchez

Department of Geography

University of Leicester

Supervisor Dr Sue McLaren

October 2010

Abstract

Cenozoic environmental evolution of the San Juan Raya Basin, south central Mexico

Javier Medina-Sánchez

This thesis was carried out to gain a better understanding of the Cenozoic environmental evolution of the San Juan Raya Basin, which is a sub-system of the Tehuacan Valley in central Mexico. The likely roles of tectonics and climate in the geomorphic processes of the basin were examined by analysing the geology, geomorphology, depositional environments, as well as other palaeo-records: palaeosols, fossils and geochemical deposits. The correlation of 11 sedimentary sections was established on the basis of 12 radiocarbon dates. A glyptodont (Xenarthra) fossil discovered as part of this study provided important palaeoenvironmental information.

The first hypothesis on the Neogene evolution of the basin is put forward, indicating that this system was formed by NE faults probably since the late Miocene or later. The asymmetry of the alluvial landforms indicates that the main factor controlling the development of Pleistocene fans from the north slope was tectonics. Late Pleistocene-Holocene deposits are more widely spread and represent environmental changes since 28.5 kyr ago. Macrofossil and stable isotopes suggest a mixed vegetation and high evaporative conditions under a poorly drained basin before the Last Glacial Maximum (LGM), probably under a colder than present climate. No records are available between the LGM and the end of the Pleistocene. Higher moisture availability was inferred in the early Holocene on the basis of high deposition rates and *in situ* tufa, followed by periods of intense deposition during the middle Holocene. A discrete alluvial fan reveals a combination of climate and tectonics. Alluvial incision since 2.3 kyr BP coincides with the establishment of current climatic and geomorphic conditions. Late Quaternary erosion and deposition suggest that climate and tectonics have played a dominant role in controlling the geomorphic processes of this basin.

Acknowledgments

CONTENTS

List of Figures

List of Tables

Acronyms

Climatology
GCM – General Circulation Models
ITCZ – Intertropical Convergence Zone
LGM – Last Glacial Maximum
LIS – Larentide Ice Sheet
MIS – Marine Isotope Stage
NADW – North Atlantic Deepwater Formation
SST – Sea Surface Temperature

Geologic formations
Kl-S – San Juan Raya Formation
Kl-Z – Zapotitlan Formation
Ku-C – Cipiapa Formation
Tom-T – Tehuacan Formation

Highlands
CC – Cerro Campanario
CGa – Cerro El Garambullo
CGo – Cerro Gordo
CM – Cerro Mezquite
CMe – Cerro La Mesa
COm – Cerro Ometepec
COt – Cerro Otate
CS – Cerro Salado
CSM – Cerro Santa Maria
CT – Cerro Tarantula
CV – Cerro Viejo
CX – Cerro Xentle

Regional geographical features
ATB – Atexcal Basin
COB – Coatxingo Basin
TEPB – Tepexi Basin
NPB – Nopala Basin
SJRB - San Juan Raya Basin
SMS - Sierra Madre del Sur
SSFB – San Sebastian Frontera Basin
TB – Tehuacan Basin
THB – Tehuitzingo Basin
TMVB – Trans Mexican Volcanic Belt
ZDLSB – Zapotitlan de las Salinas Basin

Rivers (barrancas)
BAI – Barranca Agua la Iglesia
BG – Barranca Grande
BSL – Barranca San Lucas
BZ – Barranca El Zapote

Settlements
PFv – Plan de Fierro village
SATv – Santa Ana Teloxtoc village
SGCv – San Gabriel Chilac village
SJRv – San Juan Raya village
SLTv - San Lucas Tetetitlan village
ZDLSv – Zapotitlan de las Salinas village

Sedimentary sections
ALB - Alberca
BIS - Bisonte
CAN - Candelilla
CAP - Capullos
PV – Palo Verde
SJII – San Juan II
SLC – San Lucas
SLT - Salitrillo
STC – Santa Cruz
TFR – Two Friends
TPX - Teponaxtle

Other
CAM – Crassulacean acid metabolism
ESS - Earth Surface System

CHAPTER I

INTRODUCTION

1.1. Background

Reconstructing the natural history has been central for Biological and Earth Sciences since they were formally established; essentially because the entities they study are formed through long-term processes. Lyell's famous maxim "the present is the key to the past", emerged from the paradigm of Hutton's work (Windley, 1993), and still persists as a guiding concept in Earth Sciences. On the basis of this idea, Lyell not only encouraged Geology as a scientific discipline (Rudwick, 1975), but certainly established the scientific programme that constitutes its foundations (Camardi, 1999). With the sub-title of his *Principles of Geology,* Lyell made clear his "attempt to explain the former changes of the Earth's surface, by reference to causes now in operation" (Lyell, 1832); an idea that forms the framework for modern environmental reconstructions (Lowe & Walker, 1997). However, given the complexity of the Earth Surface Systems (ESS) specific past processes do not always leave clear signatures in the palaeorecords, making it essential to consider multiple likely causal factors and a wider spectrum of evidence. Such is the approach adopted in this thesis, in which the landforms, sediments and other palaeorecords preserved in the SJRB (SJRB), in the arid region of Tehuacan in central Mexico (Fig. 1), are studied with the aim of gaining a better understanding of the evolution of this basin as an integrated ESS.
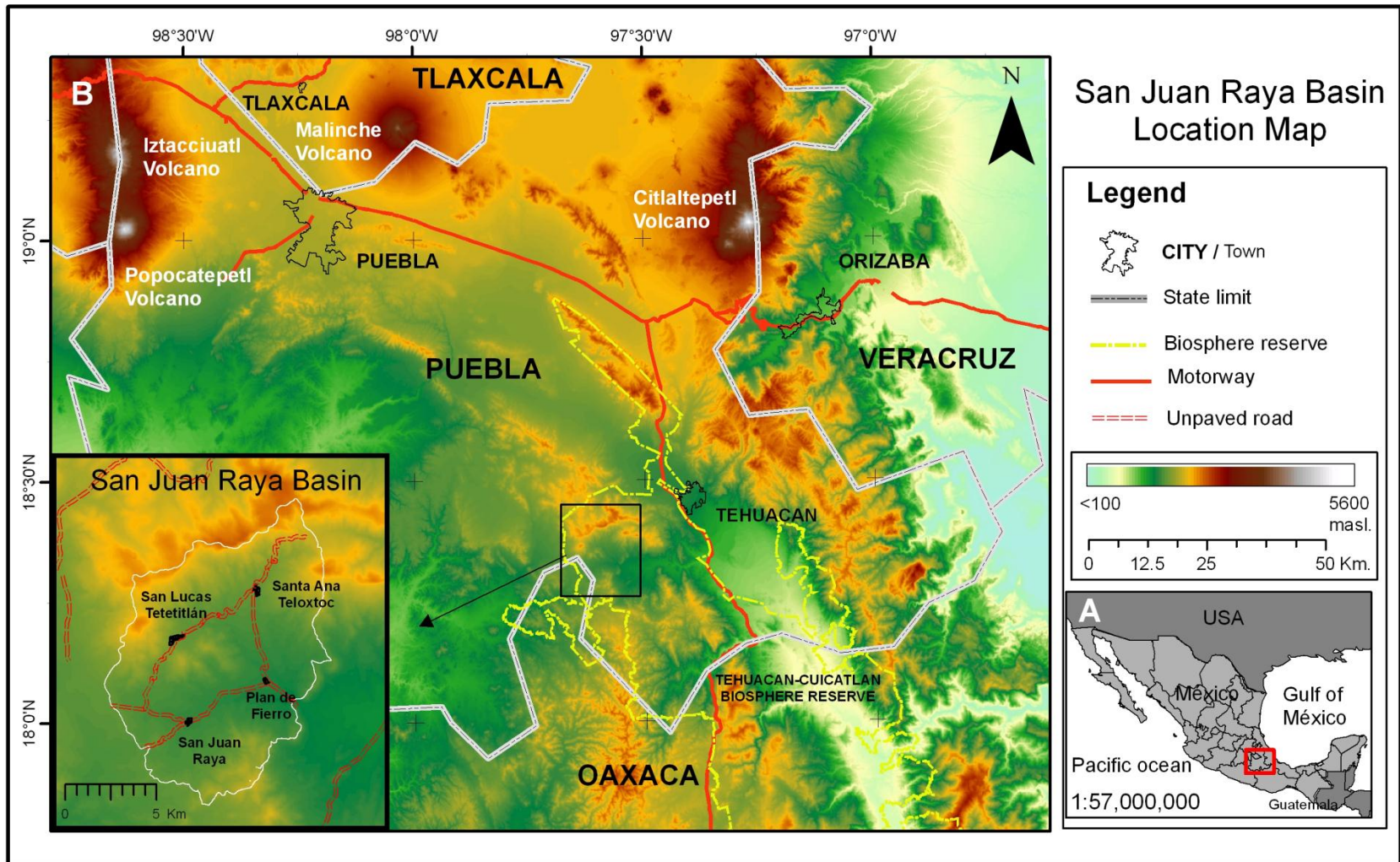
Figure 1. Geographical location of the San Juan Raya Basin. The approximate area of the Tehuacan region corresponds to the reserve boundaries.

The SJRB has to be understood as an ESS in which physical, biological and anthropogenic factors relate through feedback interactions as a thermodynamic system (von Bertalanffy, 1950). According to Phillip's conceptual categorisation (Phillips, 2009), an ESS shows four properties when subjected to changing forces: response, resistance, resilience and recursion. The first refers to the time it takes for a component to show modifications and the rate at which they occur under change-inducing forces; the second relates to the thresholds under which the system remains unchanged; the third is defined as the ability to recover stability after perturbation and the last comes from the possible internal and external feedback. A knowledge of these properties in a long-term perspective for the SJRB would allow for a better understanding of its evolution, how it was formed and what the likely future impacts may be of potential climatic changes on geomorphic events and human activities.

In order to study the evolution of the SJRB it has been crucial to consider that it has a complex assembly of landforms and sediments, which could be formed and modified as a response to processes linked to one, or to a combination of some of the main interacting components that characterise any ESS: geologic, geomorphologic, hydrological, pedological, climatic, biotic (Bull, 1991; Phillips, 2009) and anthropogenic (Phillips, 1997; Oldfield, 2005). The challenge is then to make an adequate interpretation of those records taking into account the complexity of the interacting factors involved and that many modern land-shaping processes, which would be the ideal present reference, are not completely understood. In the field of palaeoenvironmental reconstruction in arid lands one of the most challenging problems is to identify

3

the relative role of tectonics and climate in determining some landscape features. Rocks and landforms reflect changes in the tectonic setting that modify the landscape through time but also track changes in climate by preserving features of past depositional conditions, fossils as well as environment-related physical and chemical alterations of the original materials. An ideal retrospective study of ESS's is that in which independent or external variables are well controlled. For example, the formation of alluvial fans in areas with a long history of tectonic stability can be attributed to the climate with a certain confidence (Wysocka, 2009), whereas an inverse causal relationship can be drawn where independent sources provide reliable data on climate change. However, this ideal scenario is distant in the case of the present study given the potential polygenetic origin of sediments and landforms of the SJRB and the lack of detailed information on long-term tectonics and palaeoclimates. Instead, this research has adopted an alternative approach aiming to explore the likely genetic causes, tectonic *vs* climate, that could explain the formation of the landforms and sediments, and secondly to analyse those paleo-records in order to identify which past processes could be inferred from them.

A starting point in this research was to review the knowledge on geology and palaeoenvironmental change in neighbouring areas and to set out a number of research questions and hypotheses on the basis of previous studies and field observations, as will be detailed in later sections. Previous field observations showed that the SJRB has extensive stratigraphic records that include palaeosols, volcanic ashes and unconsolidated alluvial and fluvial deposits. Some of these records were previously dated at the latest Pleistocene and lay directly on marine Mesozoic rocks representing a depositional gap in

4

the order of tens of millions of years. These features contain the only palaeorecords of the basin and are investigated in this thesis from the view of the likely tectonic and environmental processes that ruled its evolution. It has been documented that in this part of central Mexico major tectonic processes during the Cenozoic formed a series of closed basins where lakes persisted since the Oligocene until the Quaternary. Later tectonics caused the opening and draining of these basins, with dramatic consequences in local environments. How those tectonic episodes influenced the landforms and environments of the SJRB and what the role of tectonics has been in forming the local depositional environments are some of the main questions that enhanced this research. On the other hand the late Quaternary unconsolidated sediments observed in the SJRB are known to represent the latest Pleistocene and the Holocene and showed clear differences among strata indicating contrasting depositional conditions and environments during this length of time. What particular environmental conditions may be reconstructed from those sediments and how they relate to the atmospheric climatic changes during the late Quaternary are also key questions in this thesis. The Tehuacan region is the only semi-desert in Mesoamerica and, given the lack of local and regional studies on palaeoenvironmental reconstruction, the records found in the SJRB are of high importance and deserve to be studied.

The former issues were addressed on the basis of a revision of literature, cartographic products, extensive field work, laboratory analyses and a chronology established by radiocarbon dating. Particular emphasis has been given to the characteristics of the basin geometry, alluvial landforms, terraces,

the stratigraphic record of the unconsolidated alluvial, fluvial and palaeosols deposited, stable isotopes and fossil evidence.

The thesis is structured into 7 chapters. The Literature Review (Chapter II) provides a synthesis of the most relevant published information on the Tehuacan Valley and related regions which can provide a reference for understanding the evolution of the SJRB. Chapter III outlines the research framework, defining the type of approach, setting the objectives, and clarifying the research questions that guided the investigation as well as the hypothesis to be tested. The study site is presented and followed by the methods employed in this research in Chapter IV. Results are detailed in Chapter V. The aim in Chapter VI is to integrate and analyse the evidence of the Cenozoic history of the SJRB. Conclusions are presented in Chapter VII. Separate sections are dedicated to listing the supporting bibliography and presenting detailed results in Appendices.

1.2. Justification

The only way to understand how particular earth systems have acquired their present structure and function is by means of palaeoenvironmental reconstructions (Oldfield, 2005). The need for these studies in the Tehuacan region is particularly important because the current environments are of a high natural and cultural relevance and because their vulnerability makes them especially susceptible to irreversible changes. This region is a complex mosaic of microclimates, landforms, vegetation and cultural features undergoing constant and dynamic interactions. However, although the present environment of the region has been relatively well studied, knowledge of how it has evolved is still very limited. This semi-arid area is one of the most important centres of

biological diversity and cultural development in Mesoamerica. Its location, landforms, rocks and sediments also make it a key area for understanding the geologic and environmental past of southern Mexico. However, despite more than 100 years of geological studies, intense biological research during the last two decades and small-scale studies carried out by anthropologists, to date there have not been any systematic palaeoenvironmental studies. By analysing the geomorphology and sedimentary records of the SJRB this thesis aims to make an initial contribution to establishing the past environmental frame in which the biodiversity, cultural development and future scenarios can be better understood, as well as calling to attention the enormous potential of the region for the development of future investigations.

In geological terms it is has been documented that this part of Mexico became continental land arround 70 million years ago through the tectonic uplift and compression of marine sedimentary rocks (Cerca *et al.*, 2007; Nieto-Samaniego *et al.*, 2006) and that currently some of the most active fault systems of the country cut through the region (Davalos-Álvarez *et al.*, 2007). Yet knowledge of which tectonic forces formed the present day basins and landforms is still poor. Of particular interest in this thesis is how the Cenozoic tectonic activity has contributed to shaping the geomorphology and sediments of the SJRB.

Research on the biotic aspect of the region also highlights the relevance of palaeoenvironmental reconstructions. Notoriously 30% of the plant species inhabiting Tehuacan cannot be found naturally anywhere else in the world (Davila *et al.*, 1993). It is also known that this region of 10,000 km^2 has been the centre of diversification of columnar cacti and hosts 36 different plant

communities (Valiente-Banuet *et al.*, 2000; 2009) formed by at least 2,650 species (Davila *et al.*, 1993). This former number represents 1 % of the world-wide known flowering plants and makes the region one of the most biodiverse arid systems in the world (Olson & Dinerstein, 1998; Davila *et al.*, 2002). It is crucial to understand what climates and geomorphic conditions provided the scenario for the convergence, evolution and development of such outstanding diversity during the last several thousands of years and how variable those conditions were during the past. This knowledge is essential for making decisions given the current function of local ecosystems and the vulnerability of the diversity under future changes.

The understanding of cultural development is another field of knowledge which would be enriched by environmental reconstructions. The first human settlements in the area are thought to have occurred at least 10,000 years ago (MacNeish, 1967) and their legacy includes the Tehuacan Viejo and Cuta pyramids, as well as the San Pedro Nodon cemetery. For years Tehuacan was claimed as the "cradle of maize" because of the discovery of the oldest maize remains in Coxcatlan cave (MacNeish, 1967; Iltis, 1983). More recently, the neighbouring Balsas region has been put forward as the more likely location for the initial domestication of maize on the basis of pollen, phytoliths and starch grains (Ranere *et al.*, 2009; Piperno *et al.*, 2009). Because these last studies were based only on isolated fossils found in a few caves, the potential of sediments in the Tehuacan region including the SJRB, which before this study were known to date back to at least 28 thousand years, in providing more continuous records of maize presence has yet to be explored. Again, well-dated

and characterised sedimentary records could provide very useful sources of environmental information on such an important topic.

It has been suggested that pre-Columbian and modern land management practices have caused massive soil erosion (McAuliffe *et al.*, 2001). Such an assertion was based on a study with poor stratigraphic and chronological control and observations at micro-scale level, and did not consider the landscape as a system in which different variables can account for the erosion-deposition events, such as climate and tectonics. More extensive data on sedimentation chronology, tectonic, climatic and human controls on landscape processes, like erosion, are urgently needed in order to test the reliability of those ideas.

Important findings on the present conditions need palaeoenvironmental reconstructions in order to understand the long-term processes that have given the region its current form. It is not known how variable the climatic conditions were under which this evolutionary and ecological phenomena occurred during the last thousands of years. Also, the climate regime, hydrologic and erosion dynamics and landform conditions under which pre-Columbian agriculture was developed remain as important gaps in information. The role of environmental change studies for providing key information for management and forecasting future scenarios is unquestionable; especially for arid zones like the Tehuacan Valley which have been experiencing high rates of population growth, intensive erosion and loss of biodiversity among other problems. For these and other important questions to be addressed the information provided by late Quaternary environmental reconstructions is crucial.

This thesis focuses on the records of the evolution of the SJRB firstly because this locality is a representative sub-basin of the Tehuacan region; secondly because its landforms and sedimentary sequences constitute a palaeoenvironmental record formed over at least tens of thousands of years; and thirdly because as a first order basin, in the sense defined by Horton (1945), it does not receive fluvial sedimentary inputs from other basins because it is located at the highest topographic position in the drainage system and allows inferences at intra-basin level to be made. This ESS is also suitable because it shows little evidence of anthropogenic disturbance compared with neighbouring localities. Thus the SJRB displays all the characteristics that make this Earth Surface System a suitable place for retrospective environmental studies and a valuable source of information on the processes that have been active during its evolution.

CHAPTER II

LITERATURE REVIEW

2.1. Introduction

Situating the SJRB in the context of the main geological and environmental changes at a regional level is crucial in order to unravel its Cenozoic evolution as an ESS. This chapter summarises the most relevant works and observations which provide ideas on some of the various aspects of the past that can help to give a better interpretation of the palaeorecords. In turn, this may help to explain the main tectonic and climatic processes implicated in the formation and shaping of this basin. This chapter is sub-divided into three parts. The first (2.2) describes the main geological structures related to the kinetic changes. The second (2.3) provides details on the main tectonic and environmental episodes of southern Mexico before the Quaternary. This period of time was treated separately, because of the potential of long-term geological processes to provide clues about the evolution of this basin, and because of the depositional gap between the Cretaceous rocks and the Quaternary sediments in the SJRB. Thirdly, a previous work showed that the Quaternary unconsolidated sediments of the basin cover the last 25 kyr. This interval is relatively small in geological terms, but very important in terms of the climate changes and how they have induced current conditions. For that reason a separate sub-section (2.4) is dedicated to exploring the last tens of thousands of years of environmental change. Also, the distinctions mentioned above relate to the type of analysis and approach. For pre-Quaternary palaeorecords it involves the study of geological formations, faults and geomorphology, whereas the study of

unconsolidated records required other tools like sedimentology, radio carbon dating and fossils.

2.2. Structural setting

The evolution of the SJRB is directly linked to the tectonic processes at a regional level and can be traced in the rocks and geological structures of this part of southern Mexico. The SJRB is located in the Sierra Madre del Sur (SMS) physiographic province (Fig. 2.1), which is one of the most extensive mountain chains in Mexico (de Cserna, 1989). These highlands are formed of a number of tectono-stratigraphic terrains which are defined as regional fault-bound groups of rocks that underwent an independent sedimentary and tectonic history during important periods of the Palaeozoic (Sedlock *et al.*, 1993; Keppie, 2004). Structurally the SJRB is part of the Mixteco terrain, located near the border with the Oaxaca terrain (Figs. 2.2, 2.3). Originally being part of the Earth's crust which now corresponds to the Pacific tectonic plate, the tectono-stratigraphic terrains Guerrero (composed of several smaller ones), Mixteco, Oaxaca and Juarez amalgamated to form continental southern Mexico (Keppie, 2004) (Fig. 2.2). The Oaxaca terrain was the core to which the Mixteco terrain accreted during the early Permian (Elias-Herrera & Ortega-Gutiérrez, 2002; Centeno-García *et al.*, 2009), followed by the Juarez during the Jurassic (Alaníz-Álvarez *et al.*, 1996), and other smaller sections like Xolapa during the early Cretaceous (Ortega-Gutiérrez & Elias-Herrera, 2003). The major faults Caltepec and Oaxaca are the boundaries between the Oaxaca terrain with the Mixteco and Juarez respectively (Fig. 2.2 & 2.3). These two faults are very important because although they have formed since the Paleozoic, their activity has had major implications in forming and altering the current Cenozoic basins.
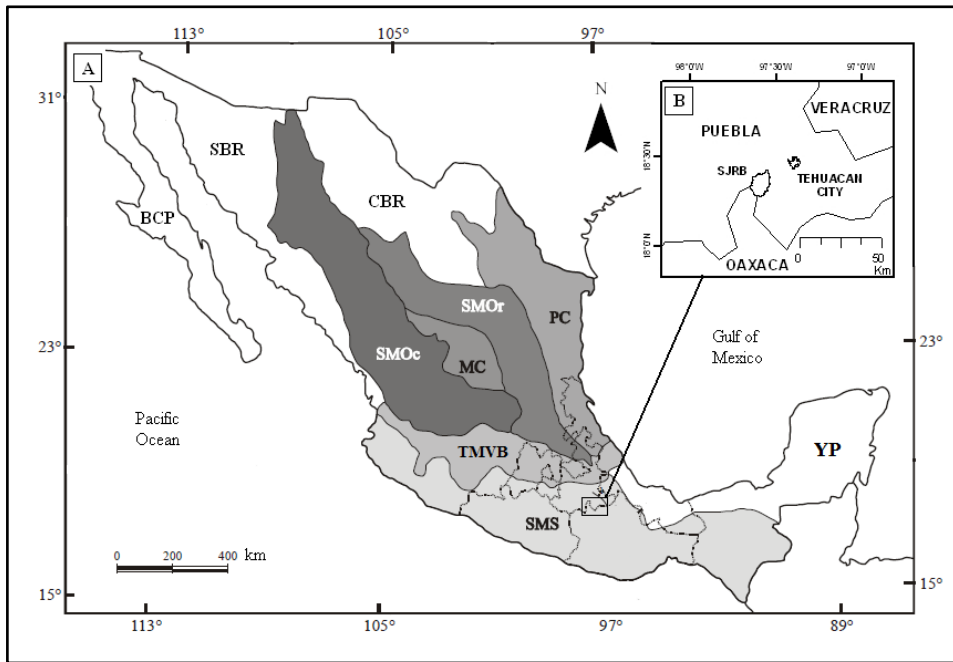
Figure 2.1. A: Physiographic provinces of Mexico. BCP: Baja California Peninsula; SBR: Sonora Basin and Range; CBR: Chihuahua Basin and Range; SMOc: Sierra Madre Occidental; MC: Mesa Central; SMOr: Sierra Madre Oriental; TMVB: Trans Mexican Volcanic Belt; SMS: Sierra Madre del Sur; YC: Yucatan Peninsula. B: Location of the SJRB in the highlands of the SMS and political boundaries. Figure modified from Dávalos-Álvarez (2006).
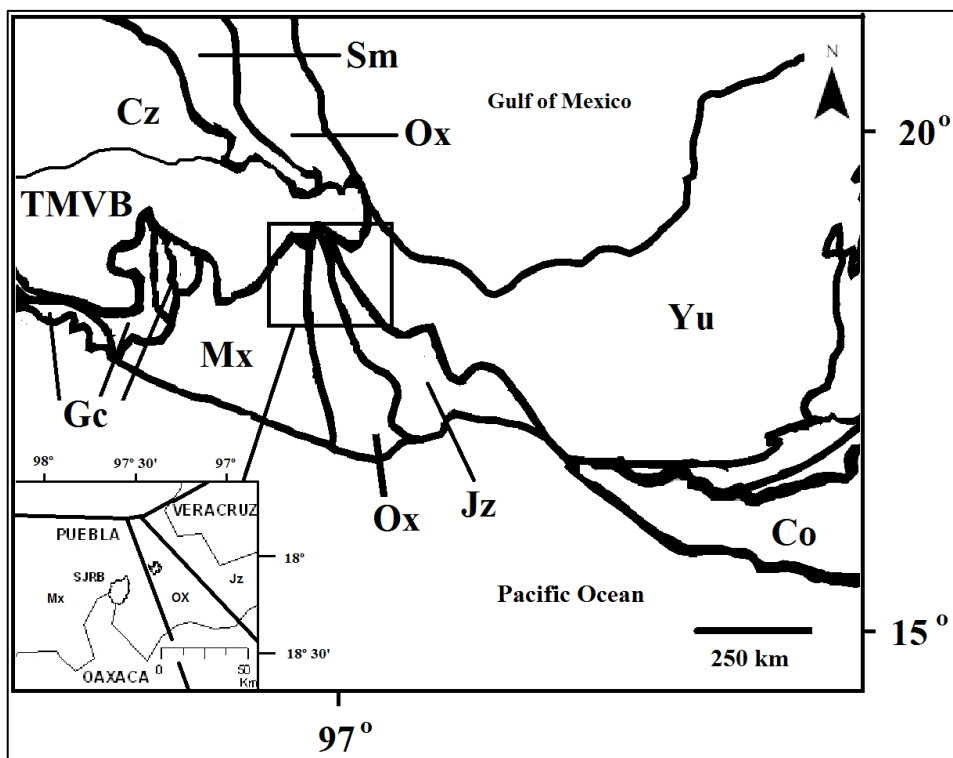
Figure 2.2. Tectonostratigraphic terrains of Mexico. Co: Cocos plate; Cz: Cortez; Sm: Sierra Madre; Ox: Oaxaca; TMVB: Trans Mexican Volcanic Belt; Gc: Guerrero composite terrain; Mx: Mixteco; Jz: Juarez; Yu: Yucatan Peninsula. The San Juan Raya Basin (SJRB) is shown as part of the Mx terrain.

This will be detailed in further sections. As shown in Figure 2.3 these terrains are a mosaic of rocks formed in three geologic Eras. The following section will describe the most important episodes of its evolution.

2.3. Geologic and environmental evolution

2.3.1. Pre-Cenozoic geology

Synopses of the regional geology from Ortega-Gutiérrez, *et al.* (1995) and Nieto-Samaniego *et al.* (2006) and stratigraphy from Ortega-Gutiérrez (1978), Sedlock *et al.* (1993) and Dávalos-Álvarez *et al.* (2007) are presented in Figures 2.3 and 2.4. The oldest Palaeozoic rocks of the SMS are grouped into the metamorphic Acatlán and Oaxaca complexes, which as stated before, constitute the base of the Mixteco and Oaxaquia terrains respectively (Ortega-Gutiérrez, 1978; Sedlock *et al.*, 1993), and surround the SJRB (Fig. 2.3). The metamorphism shown by these rocks was the result of a series of deformation phases on pre-existing marine sedimentary rocks during the Palaeozoic (Yañez *et al.*, 1991; Ortega-Gutiérrez *et al.*, 1999). These two complexes were not in contact geographically until the late Palaeozoic (Elias-Herrera & Ortega-Gutiérrez, 2002; Centeno-García *et al.*, 2009), when the deformation phase ended giving rise to the early Permian Matzitzi Formation (Centeno-García *et al.*, 2009) (Fig.2.4), which did not experience the Paleozoic metamorphism (Sedlock *et al.*, 1993). The rich plant fossil assemblage found in the Matzitzi rocks is evidence of an early phase of continental enviroments and a rapid change that prevented deposition, leaving a hiatus in the area of the Acatlan and Oaxaca terrains (Figs. 2.3). A small outcrop of Paleozoic schists observed in the centre of the SJRB is assumed to belong to the Acatlan complex (pers. observ.). However this outcrop was of a few metres, less than the minimum

mapable area. The Mesozoic rocks show important tectonic and environmental changes. Most of the Triassic and Jurassic in the Oaxaquia terrain is a depositional hiatus (Dávalos-Álvarez *et al*., 2007) (Fig. 2.4), whereas in the Mixteco terrain the Matzitzi Formation is covered unconformably by volcano-sedimentary ignimbrites (Corona-Esquivel, 1983) and by terrestrial alluvial and
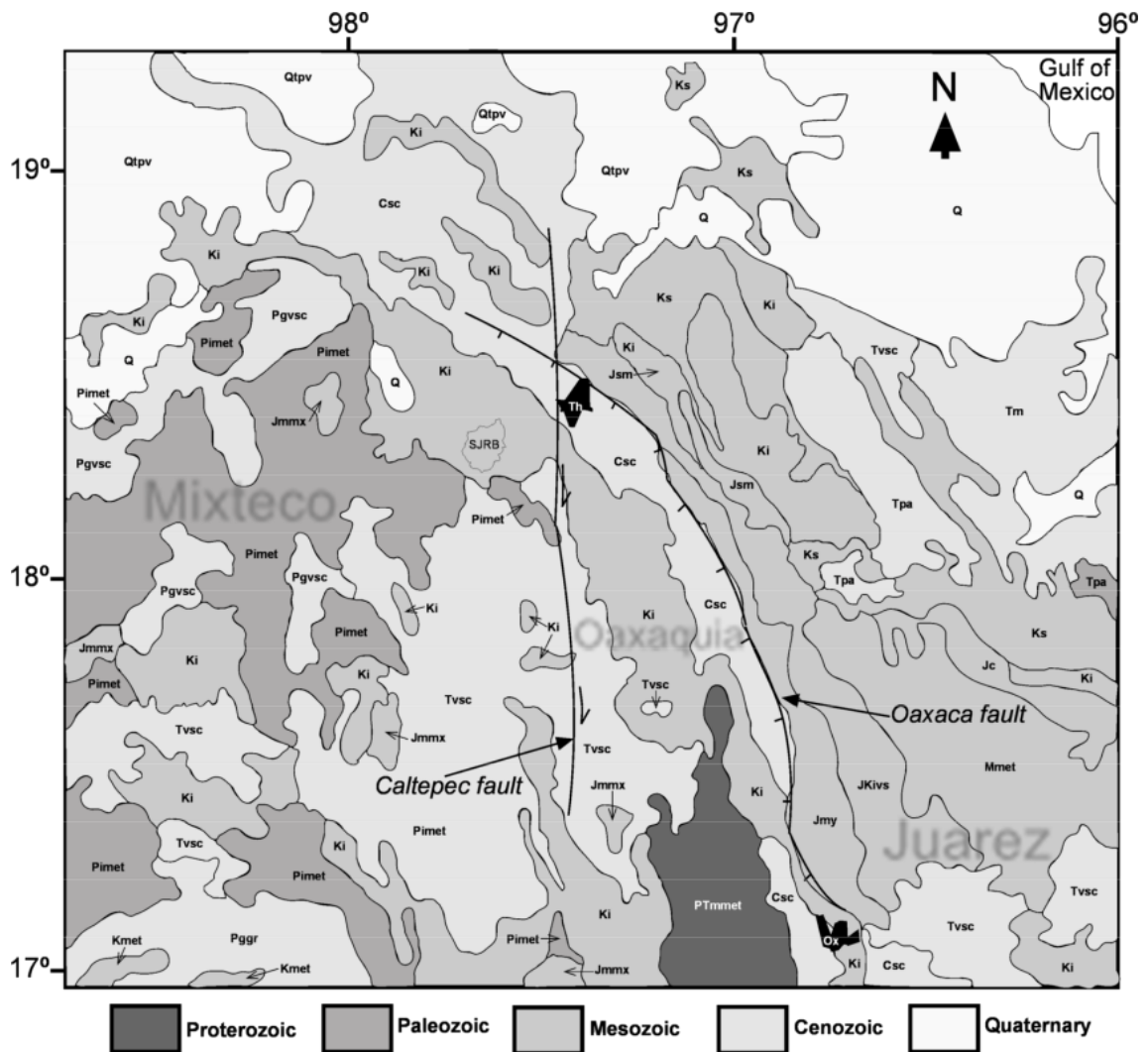
Figure 2.3. Geology of south central Mexico. Summarised from Ortega-Gutiérrez *et al*. (1992) and Nieto-Samaniego *et al*. (2006) and location of the SJRB in the Mixteco terrain. Ptmmet: Proterozoic-Oaxaca metamorphic complex; Pimet: Paleozoic-metamorphic; Jc: Jurasic- continental; Jmmx: Middle Jurasic-continental and marine; Jsm: Late Jurasic-Early Cretaceous-continental and marine; J-Kivs: Late Jurasic-Early Cretaceous marine volcanosedimentary; Mmet: Mesozoic-metamorphic; Kmet: Cretaceous-Xolapa metamorphic complex; Ki: Early Cretaceous-marine; Ks: Late Cretaceous-marine sedimentary; Tpa: Paleocene marine; Pgvsc: Paleogene-continental volcanosedimentary; Pggr: Paleogene granite; Tvsc: Tertiary- continental volcanosedimentary; Tm: Tertiary-marine; Csc: Cenozoic-undifferentiated continental; Qtpv: Quaternary-volcanic; Q: Quaternary-alluvial. Oaxaca (Ox) and Tehuacan (Th) cities are shown for reference.
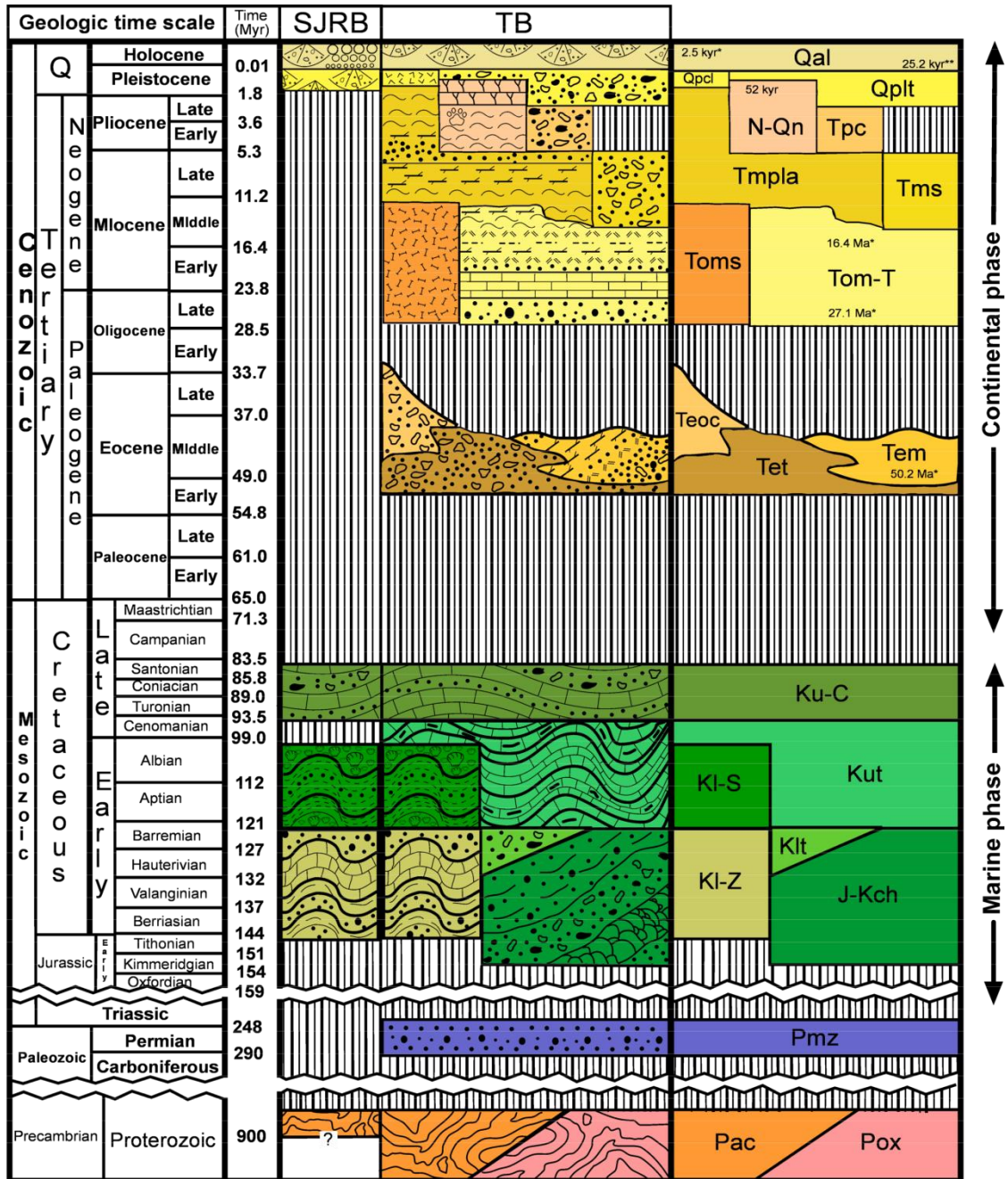
Figure 2.4. General stratigraphy of the Tehuacan (TB) and San Juan Raya (SJRB) basins. Paleozoic section after Ortega-Gutiérrez (1978) and Sedlock *et al*. (1993). Post-Mesozoic section after Dávalos-Álvarez *et al*, (2006).

Stratigraphic codes

Code	Description		Code	Description
Qal	Quaternary alluvial deposits		Tet	Tilapa red beds
Qplt	Teotitlan conglomerates		Ku-C	Cipiapa Formation
Qpcl	Cuayucatepec conglomerates		Kut	Upper Tamaulipas
N-Qn	Neogene-Quaternary lacustrine		Kl-S	San Juan Raya Formation
Tpc	Coyoltepec conglomerates		Klt	Tecachi conglomerates
Tmpla	Altepexi lacustrine		Kl-Z	Zapotitlan Formation
Tms	San Isidro conglomerates		J-Kch	Chivillas Formation
Tom-T	Tehuacan Formation		Pmz	Matzitzi Formation
Toms	Atzingo andesite		Pox	Oaxaca Complex
Teoc	El Campanario conglomerates		Pac	Acatlan Complex
Tem	Mesquitongo Formation			

Igneous

Andesite   Basalt   Pilow lavas

Volcano-sedimentary

Tuff

Sedimentary

Alluvial   Calcareous conglomerate   Coquina   Fluvial

Gypsum   Lacustrine   Limestone   Lutite

Mudstone   Polymictic conglomerate   Sandstone   Tufa

Metamorphic

Metamorphic complex   Flint and onyx
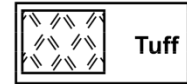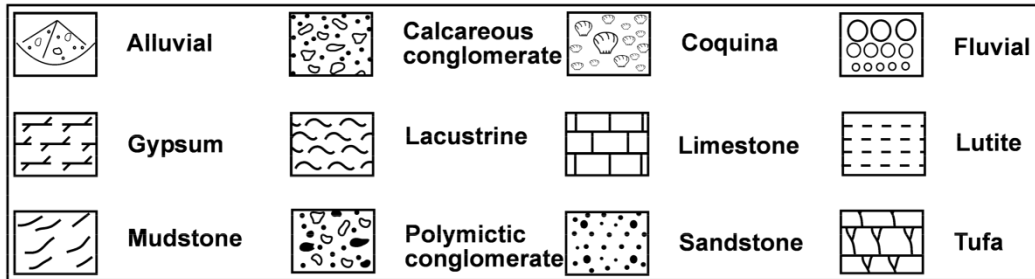
Fossils

Ichnofossils

Figure 2.4. (cont.).

17

fluvial conglomerates hosting metamorphic clasts of the older Acatlán complex (Calderón-García, 1956; Moran-Zenteno *et al.*, 1993 Centeno-García *et al.*, 2009). The change to a tropical low depth coastal environment is clearly shown by the middle Jurassic carbonaceous shale and marine quartz conglomerates and by the upper Jurassic limestones (Sedlock *et al.*, 1993; Omaña & González-Arreola, 2008). The dominant outcrops of the SJRB and the immediate surrounding areas were formed during the early to late Cretaceous and represent a warm tropical shallow coast (Aguilera *et al.*, 1896). Sandstone and lutite are the main components of the San Juan Raya formation (Kl-S) which occupies most of the area of the SJRB (Fig. 2.5), preserving a rich assemblage of marine invertebrate fossils of Aptian age. This diversity includes *Nerinea*, *Tylostoma*, *Turritela* and other members of Mollusca, as well as Decapoda and abundant coral and equinoid fossils (Aguilera *et al*, 1896; Aguilera, 1906; Biutrón & Barceló-Duarte, 1980; Feldmann *et al.*, 2007; Löser, 2009). The Zapotitlan formation (Kl-Z) and Kl-S are overlain discordantly by up to 600 metres of compact calcareous limestone. This formation of marine origin was first named Cipiapa Formation (Kl-C) (González-Arreola, 1974; Buitrón and Barceló-Duarte, 1980), but later mapped as undifferentiated upper Cretaceous (Dávalos-Álvarez, 2006). These rocks represent the last phase of the marine environments in the south of Mexico and their later deformation was caused by the beginning of the continental orogeny.

2.3.2. Cenozoic regional tectonic and environmental evolution

2.3.2.1. Late Cretaceous and Cenozoic orogeny and basin formation
A series of tectonic episodes since the late Cretaceous caused the uplift of the marine sedimentary rocks to give rise to the SMS and also structured the blocks
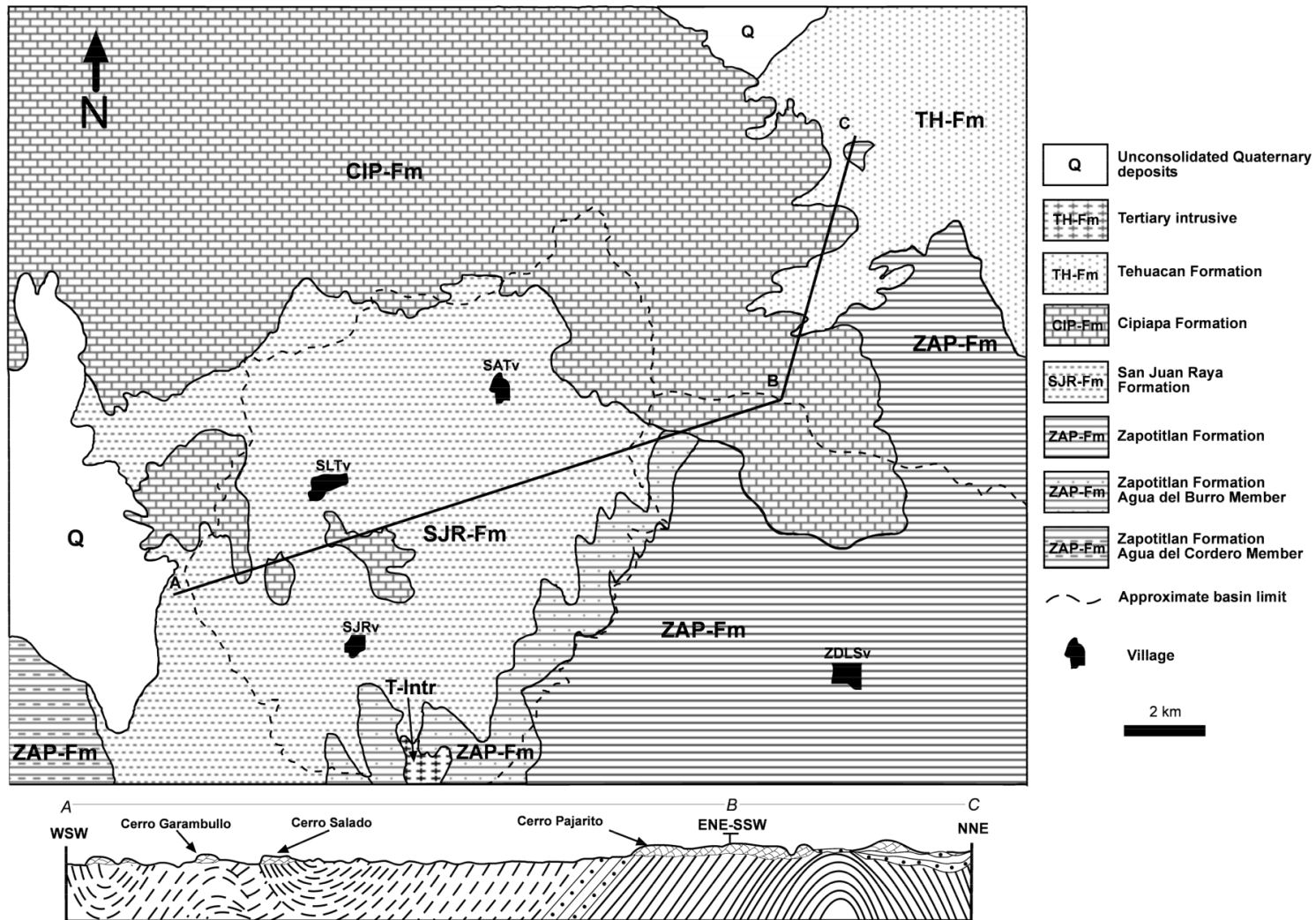
Figure 2.5. Simplified geological map of part of the San Juan Raya and Zapotitlan area after Mauvois (1977) and INEGI (1998c). Lower Cretaceous KI-S and KI-Z geologic units occupy most of the basin areas of San Juan Raya and Zapotitlan respectively. See Acronims section for reference to the village names.

19

around the SJRB. Three tectonic events have been argued to be the likely cause of this orogeny: the subduction of the Kula plate under the North American plate that produced the Laramide orogeny (Nieto-Samaniego *et al.*, 2006); the collision of the Guerrero terrain against the Mixteco-Oaxaca terrain (Campa & Coney, 1983) and the eastern migration of the Chortis block (Cerca *et al.*, 2007). Although it is still uncertain as to which major tectonic events dominated, there is consensus concerning the main intra-continental effects: 1) A E-W compressive shortening of the early Cretaceous marine rocks that commenced during the Coniacian (~88 Myr) to the west margin of the Mixteco-Oaxaca block, migrated eastwards to end at the western part of the Veracruz state at the earliest Paleogene (Nieto-Samaniego *et al.*, 2006; Cerca *et al.*, 2007); 2) a weaker shortening between the Paleocene and earliest Eocene accompanied by gentle folding and clockwise rotation of the pre-deformed structures caused by transpressional left lateral strike-slip faults aligned in a general north to south trend (Cerca *et al.*, 2007); 3) a shift of the shortening trend to NE-SW and strike-slip fault activity since the early Eocene until the middle Oligocene (Nieto-Samaniego *et al.*, 2006) and 4) a change from previous contraction to a NE-SW extension caused by active normal faults since the middle Eocene until middle Miocene (Nieto-Samaniego *et al.*, 2006). The result of events 1-3 was the uplift, compression and faulting of the SMS province, which in the SJRB can be observed as the folding of Cretaceous formations (Fig. 2.5). The fourth event accounts for the opening of the continental depositional basins.

The Caltepec fault (Fig. 2.3) stretches at least 150 km from the west of Tehuacan city in Puebla State to Juchatengo town in Oaxaca State (Ortega-

Gutiérrez, 1981) and is the other main structure related to the post-Cretaceous tectonics. It represents the contact between the basal Acatlán and Oaxaca complexes (Elias-Herrera & Ortega-Gutiérrez, 2002), and also showed weak extensional activity during the Oligocene between 26 and 29 Myr (Elias-Herrera & Ortega-Gutiérrez, 2002; Santamaría-Díaz *et al.*, 2008). Near Tamazulapa town this fault was studied by Santamaria-Diaz *et al.* (2008) using Cinematic Compatibility Diagrams (CCD), which allow the calculation of the likely main direction of the strength of a group of structures. They showed that the structural block to the east (Oaxaca complex and overlaying Mesozoic and Cenozoic strata) had a localised activity, synchronic with the Oaxaca fault kinematics (Santamaria-Diaz *et al.*, 2008). The block to the west of the fault, where the SJRB is located, experienced two main deformation events: a compressive episode during the late Eocene to early Oligocene and a later extension active during the late Oligocene. Given that the SJRB is located on the block west to the Caltepec fault, evidence of these deformation episodes would be expected in its outcrops. In fact, as shown in Figure 2.5, the predicted folding of the Mesozoic rocks is clear and has been reported before. However, as will be seen below, the late Oligocene extensional tectonism that could explain the formation of the SJRB is less clear, particularly because there are no mapped rocks of continental basin origin. These deposits are present in areas surrounding the SJRB and show the tectonic origin and evolution of those basin systems.

In the region of interest a number of important depositional basins were formed in the previously shaped highlands as a consequence of the fourth tectonic major event. Those basins resulted from the regional extensional

tectonism caused by left lateral and normal faulting during Eocene to Miocene times (Silva-Romo *et al.*, 2000; Dávalos-Álvarez *et al.*, 2007). Because these faults were roughly aligned north-south (Fig. 2.6), the basins opened in an east to west trend. The most prominent basin formed under this tectonic regime is the half graben known as the Tehuacan Basin (TB) located to the east of the SJRB. The widening of TB commenced around 27 Myr ago as a product of the re-activation of the Oaxaca fault (Nieto-Samaniego *et al.*, 2006). This fault of north-northwest orientation can be traced for at least 250 km from Oaxaca City to Perote in Veracruz State (Fig. 2.6) and is one of the most active tectonic features in Mexico (Nieto-Samaniego *et al.*, 2006). Structurally, this fault is the contact between the Oaxaca and Juarez terrains and topographically defines the western edge of the Sierra de Juarez (also known as Mazateca Mountain Range) where it meets the TB (Dávalos-Álvarez *et al.*, 2007). According to Dávalos-Álvarez *et al.* (2007) this normal fault resulted in a vertical displacement of the TB floor (hanging wall) to a lower position with respect to the Mazateca mountains block (foot wall) in at least four deformation phases, from early Eocene until the Pleistocene. In the first phase (late Paleocene to early Eocene) the Tilapa red beds formed as the first Cenozoic deposits in the young TB. The second and third episodes were characterised by very active tectonism, with the expansion of the Oaxaca fault during the middle Eocene until early Oligocene and the formation of the Tilapa and Calipam fault ramps, followed by a strong tilting of Eocene units and a later deposition of lake sediments of the Tehuacan Formation. The fourth stage produced the northward expansion of the fault and the deveopment of the Tehuacan ramp. The start of this last phase was dated to during the second half of the Miocene;

and as the youngest rocks affected by this event are the Villa Alegría lake sediments, their upper limit is considered to represent the boundary of the Pliocene-Pleistocene. Basins to the west of SJRB are also Cenozoic structures
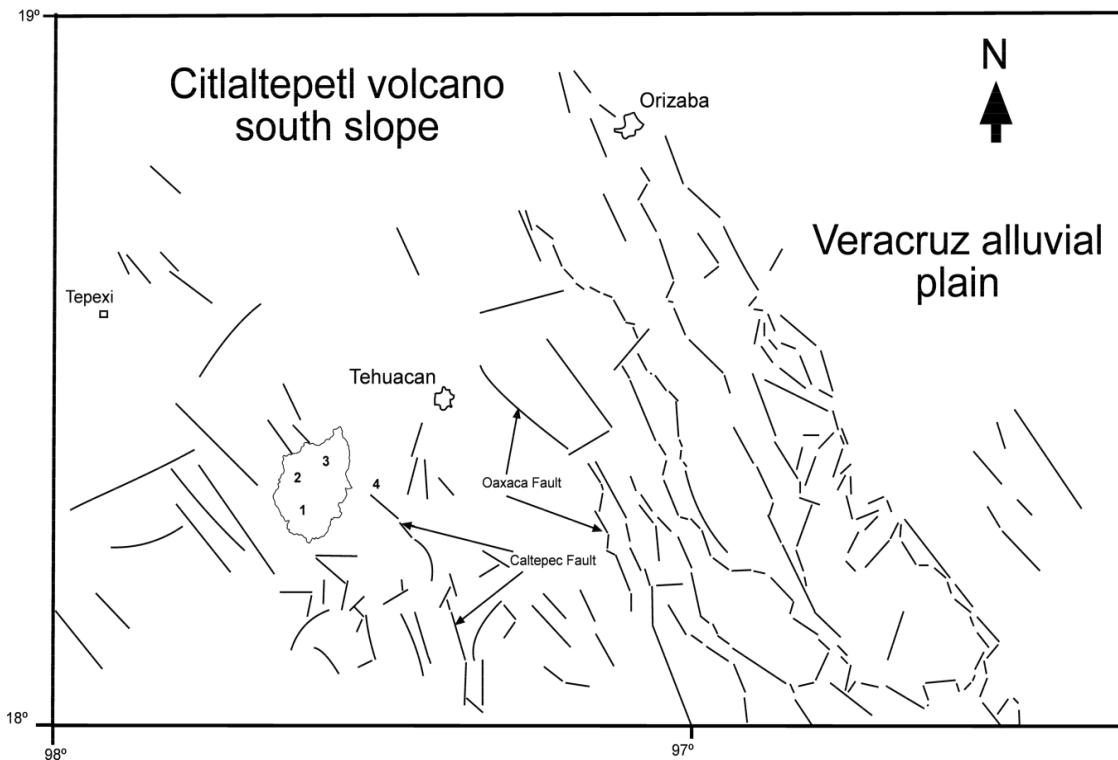
Figure 2.6. Major faults in the Tehuacan and surrounding regions extracted from the map of Martínez *et al*. (2001). San Juan Raya (1), San Lucas Tetetitlan (2), Santa Ana Teloxtoc (3) and Zapotitlan de las Salinas (4) villages are indicated for reference. Note the NW-SE regional pattern.

formed by active faults during the Eocene and Oligocene (Pantoja-Alor, 1990; Silva-Romo *et al*., 2000). A number of northeast to southwest oriented faults experienced left lateral displacements that gave rise to the Coatxingo, Tepexi and Tehuitzingo basins (COB, THB & TEB). In these three basins lakes were developed under an endorheic geometry (Silva-Romo *et al*., 2000). By the late Oligocene the TEB, COB and TB had already developed basin deposits. However, as stated before, the SJRB shows no records of this type (Fig. 2.4), indicating that this area was probably not a depositional basin. These contrasts suggest a non-contemporaneous basin formation of the SJRB in relation to

23

other basins in this part of the SMS. The relationship between the Cenozoic tectonics described above, their role in the formation of the SJRB, and the consequences on the setting of internal landforms like alluvial fans, has not been addressed before and constitutes a main area to be investigated in this thesis.

The first insights into the tectonic controls in the SJRB come from the spatial fault pattern and the already mentioned depositional hiatus. In structural terms a number of faults in areas arround the SJRB show a NW-SE trend (Fig. 2.7), which is consistent with the alignment of the regional kinematic structures (Fig. 2.6). The SJRB is part of the structural block to the west of the Caltepec fault, and it would be easy to assume that late Oligocene tectonic activity of this fault caused its opening as a continental basin. However, the observations of the fault spatial pattern suggest that the formation of the SJRB could have been independent of the formerly explained tectonic episodes. The structural interpretation by Buitrón and Barceló-Duarte (1980) presented in Figure 2.7 shows that the fault alignment of the SJRB does not match with the regional NW-SE pattern. The north and south fault systems that limit the SJRB appear to be the structures that broke the continuity of the highlands forming the basin. These faults are aligned in a NE-SW trend and to date it is unknown if they were formed by the same processes that created the surrounding basins, through normal activity of the NW-SE faults during the Paleogene. On the other hand, the Cretaceous to late Quaternary hiatus is compatible with the hypothesis put forward here that the SJRB was formed by more localised tectonic processes, not described previously. The presence of sedimentary endorheic basin-type rocks are well represented elsewhere in the region, as will

be seen in the following section. Those Cenozoic rocks are an abundant source of records of basin evolution for at least the last 27 Myr. Given the broad scale of previous maps, a more detailed study of the geological records and structures of the SJRB would provide key information on how this ESS worked during that period. If the SJRB was a depositional basin during the Cretaceous-Quaternary interval, sedimentary rocks of Tertiary age would be found and the internal geological structures, blocks and faults would show a trend
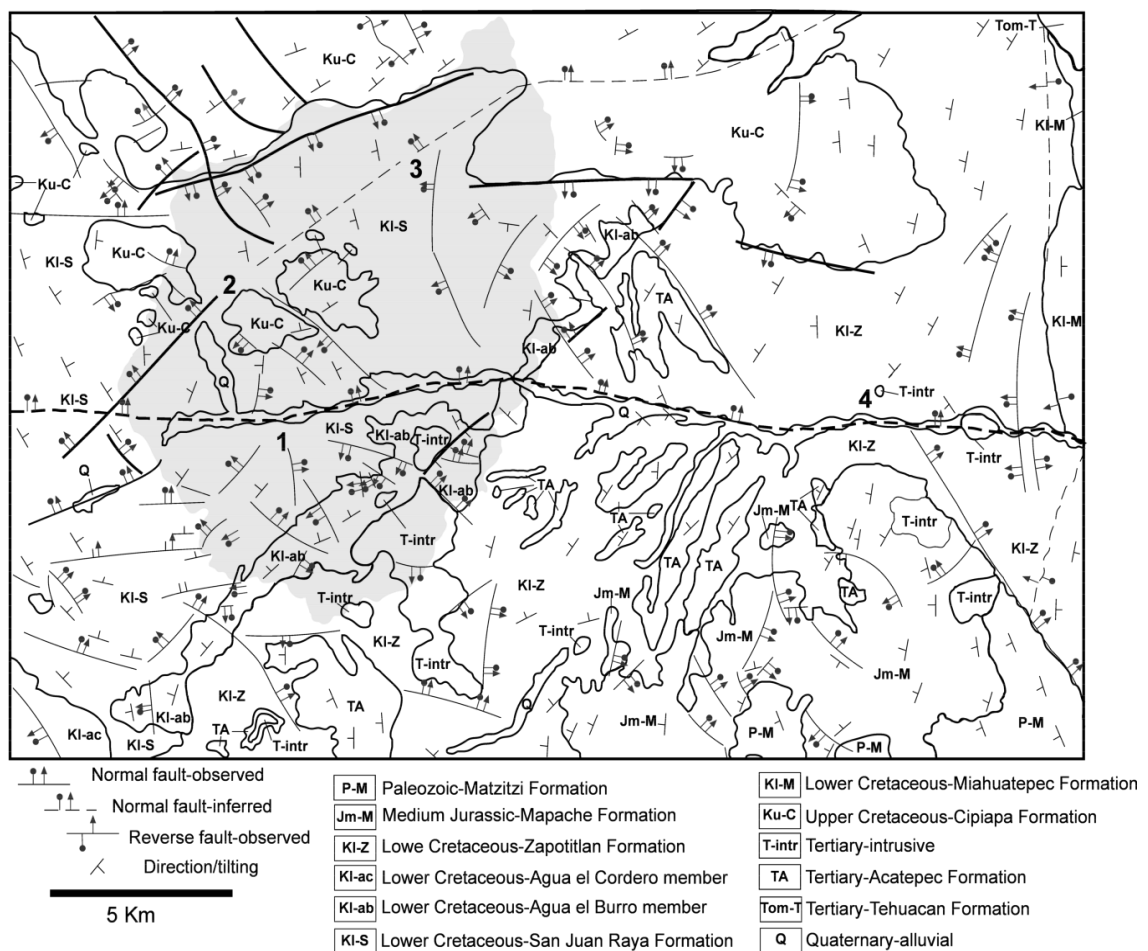
Figure 2.7. Summary of the original interpretation of the structural geology of the SJRB and ZDLSB by Buitrón and Barceló-Duarte (1980). San Juan Raya (1), San Lucas Tetetitlan (2), Santa Ana Teloxtoc (3) and Zapotitlan (4) villages are indicated for reference. Note the NE-SW trend of the major normal faults that border the SJRB (shaded area) and the E-W central fault.

corresponding to the kinetic episodes previously detailed. This hypothesis was tested in this thesis through an extensive field recognition of the lithology, geologic structures and mapping.

2.3.2.2. Tertiary palaeoenvironments in the Tehuacan region

Notoriously the vast continental sediments of Tehuacan have not been subjected to palaeoenvironmental interpretation despite the high potential for studies on pollen, sedimentology and geochemistry. A novel palaeocological approach based on phylogenetic relationships of co-existing modern plants in the mediterranea-type vegetation in Tehuacan puts forward the idea that the Tehuacan region was wetter during the Tertiary, turning more arid towards the Quaternary (Valiente-Banuet *et al.*, 2006). Although this approach provides an independent line of evidence on a long-term, at the moment it is constrained by the low resolution and the big timescale it covers. Complementary studies of sediments are then necessary and possible through detailed reconstruction, considering that the Cenozoic rocks in the TB cover at least the last 27 million years and are widely distributed (Figs. 2.3 & 2.4). The fact that those geological records include lake deposits means that they are a major source of continuous archives of the environmental evolution of the region, not yet studied. Such studies have been carried out in other basins of the region as explained below.

The only Mesozoic rocks of the region from which palaeoenvironmental studies have been published correspond to the COB and TB. Rocks outcropping there are of late Eocene-early Oligocene age and have been subjected to sedimentological (Beraldi-Campesi *et al.*, 2006) and a palynological analysis (Ramírez-Arriaga *et al.*, 2006); providing the only consistent palaeoenvironmental reconstruction of the Cenozoic in southern

Mexico. According to Beraldi-Campesi *et al.* (2006), the upward fining shown in the sedimentary sequence "Axamilpa section", which belongs to the Coatzingo Formation (referred as "Pie de Vaca" in other studies), records four phases of change. The bottom conglomerates and sandstones indicate alluvial and fluvial deposition in a continental closed basin. Evaporites formed in this system have been correlated to late Eocene-early Oligocene. The pollen from these evaporites indicates a semi-arid, but wetter than present climate, with an altitudinal moisture gradient. The landscape was dominated by grassland and thorn scrub with Acacia, as well as neighbouring communities of tropical deciduous forest, chaparral (also known as *mexical*) and pine and cloud mesophillous forest (Ramírez-Arriaga *et al.*, 2006). According to this reconstruction, coniferous forest colonised the temperate highest parts, whereas in the canyons and lowlands more available moisture allowed the development of mesophyllous vegetation. Areas close to the lake were drier with sclerophyllous shrubland and tropical deciduous forest (Martínez-Hernandez & Ramírez-Arriaga, 1999). These reconstructions suggest warm conditions with a marked inverse relationship between temperature and altitude for the region. It also suggests a wetter than present climate on a regional scale, considering that mesophyllous vegetation requires high amounts of precipitation. These climatic and vegetation reconstructions correspond to conditions that occurred at least 33 Myr ago. Nowadays there are no coniferous forests in the area and the tropical deciduous forests in south-central Mexico dominate the Balsas basin to the west slope (Rzedowski, 1978), but are constrained to small areas in the more mesic parts of the southwest of the Cuicatlan region (Valiente-Banuet *et al.*, 2000; 2009). As will be seen in section

4.1.6, the vegetation in the Tehuacan region is at present dominated by arid communities like scrub, chaparral-type and columnar cacti forests. There are still many chronological gaps in the environmental history of this part of Mexico, particularly the Pleistocene. Prior to this study the oldest date obtained from the sediments of SJRB clearly indicates that this system has the potential to provide records of the last tens of thousands of years.

2.3.3. Summary of geological and environmental evolution

Studies on the regional collection of metamorphic, igneous and sedimentary rocks in the Tehuacan area show that this part of the crust was a continental margin during the Palaeozoic and until the first part of the Mesozoic (Ortega-Gutiérrez et al., 1995); turned into a shallow tropical coast during the early Cretaceous (Aguilera et al., 1896); emerged as a continental mountain chain since the late Cretaceous and was affected by important NW-SE faults like the Oaxaca and Caltepec systems that, between 85 and 33 million years ago formed the currently active depositional basins (Nieto-Samaniego et al., 2006; Cerca et al., 2007). These basins show a wide variety of rocks corresponding to lake, alluvial and fluvial deposits and record changes towards more arid conditions during the Tertiary. However, the fault pattern and the Cretaceous-Quaternary hiatus observed in the SJRB raise the hypothesis that this particular basin was formed later by neo-tectonic activity. The fact that Cenozoic rocks have not been reported in the SJRB raises the question of what particular processes have prevented the formation or preservation of sedimentary rocks during this period. One likely cause of this hiatus could be a long-term lack of deposition as a result of prevailing folded structures, taking the shape of highlands without a well-defined valley floor where sedimentary environments

would be formed. If topographic conditions did not constrain the formation of a valley, intense erosion and associated tectonics could also be responsible for such lack of deposition. However, remnants of this phase should be preserved somewhere in the basin. This thesis tests such hypotheses by analysing the main regional tectonic events and the structures and lithology of the SJRB.

2.4. Quaternary environmental change

Considering that the sedimentary palaeorecords of the SJRB cover the latest Pleistocene and the Holocene, a revision of the the climate pattern becomes relevant. The revision below will focus only on the environmental change over the last 30 kyr. Because there are no published palaeoclimatic studies of the Tehuacan region, some insights into the past climatic conditions can come from the revision of General Circulation Models (GCMs) and study cases in neighbouring regions that are currently affected by the same atmospheric and oceanic phenomena.

2.4.1. Quaternary palaeoenvironments of central Mexico and surrounding regions

Given that the sedimentary record of the SMS is extensive, and the fact that the SJRB in particular has experienced active sedimentary deposition for at least the last 25,000 years, the potential for reconstructing past landscapes has not been exploited. In fact, to-date, Quaternary research in Mexico faces three main problems. Firstly, there are still few studies in general; secondly, the spatial cover is very limited. A decade ago Metcalfe *et al.* (2000) pointed out that Quaternary studies in Mexico had focused on three contrasting continental regions; 1) the northern great deserts of Chihuahua (CHD), Sonora and Baja California (S-BCD); 2) the Trans-Mexican Volcanic Belt (TMVB) and 3) the Yucatan Peninsula (YP). This situation has not changed since (Fig. 2.3). On the

other hand, marine sediments from the Gulf of Mexico have proven to be an ample source of data for palaeoclimatic models (Brunner, 1982), but their use in explaining past environments at meso and micro regional levels is limited. With very few exceptions, the research has concentrated only on systems that provide continuous sedimentary records like lakes, paleolakes or marine basins based on the available proxies in those water bodies like pollen, diatoms, geomagnetism and geochemistry. Those proxies cannot be applied to disentangling the environmental past of the SJRB because the sedimentary records are mainly alluvial. Finally, another central problem is that the majority of studies mentioned only cover the period since the late Pleistocene, particularly since the Last Glacial Maximum (LGM), to the present, mainly because those studies have been restricted by coring depth and/or because a wider spectrum of localities and different sedimentary environments have not been approached.

The Tehuacan region is defined by particular climatic and ecological conditions whose environmental past is unknown. However, because it has no Quaternary lacustrine palaeorecords, it has received no attention, despite the fact that there are other types of sedimentary records like alluvial, fluvial and chemical deposits which contain important archives of past environments. A first approach to the palaeoenvironments of the region necessitates the revision of past and present climatic phenomena on a wider scale. The present day climate of the Tehuacan will be detailed in Section 4.1.5, but in general it has been described as warm semi-arid and highly seasonal. Its sub-tropical position confers it warm temperatures while the primary source of moisture is the easterly winds (Fig. 2.3.1). Rain falls in summer and is provided by those winds
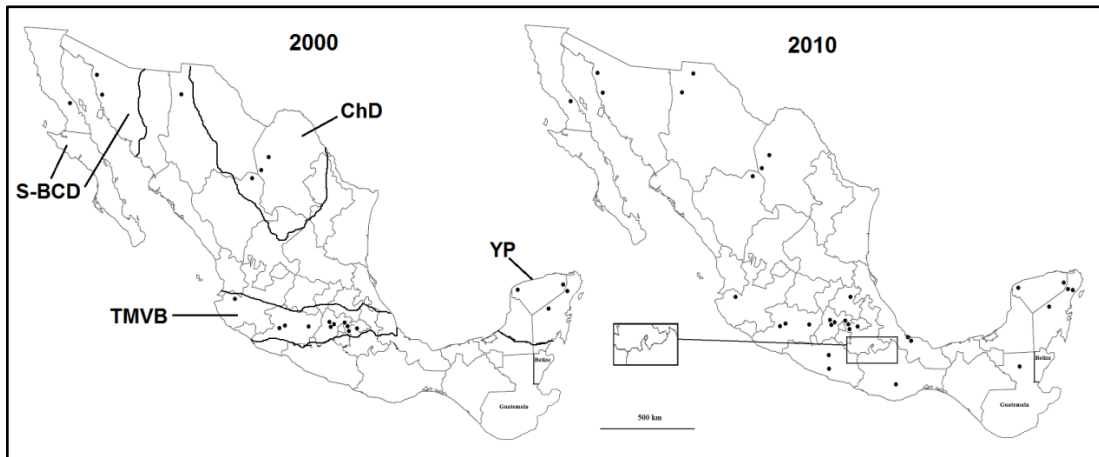
Figure 2.3. Localities of continental Quaternary studies in Mexico based on lakes and palaeolakes proxies before 2000 (Metcalfe *et al.*, 2000) and 2010. Dot in Guatemala indicates the (overlapping) location of Quetxil and Peten lakes, which are mentioned in the text (Leyden *et al.*, 1994; Rosenmeier *et al.*, 2002). For region codes see Section 2.3. Insert between maps shows the location of the SJRB.

carrying moisture from the Gulf of Mexico (Mosiño-Aleman & García, 1981); although strong storms generated in the Pacific Ocean make a secondary contribution with episodic rains (Englehart & Douglas, 2001). The rain shadow at the east and west flanks of Tehuacan enhance its aridity. In order to understand when this climatic regime established in the region and what conditions prevailed, it is necessary to refer to the established ideas on late Quaternary climate change in this part of Mexico.

2.4.2. Late Pleistocene

The most dramatic global climatic changes during the late Quaternary are linked to the shift from a glacial to an interglacial stage. Global cold conditions had an impact in central Mexico. In particular, different palaeosols in Tlaxcala (TMVB-approximately 150 km north of the SJRB) showed characteristics that indicate cold and wet conditions during the second half of the isotope stage 3 (with palaeosols dated between 38 and 24 kyr) under relative geomorphic stability (Sedov *et al.*, 2009). Caballero *et al.* (1999) and Bradbury (2000) both suggest that central Mexico highlands were cold and more humid between around 38

31

and 25 kyr, glacial times, based on their analysis of different proxies like diatoms, pollen assortments and magnetic susceptibility in Patzcuaro and Tecomulco lakes. However, the climatic conditions of the TMVB cannot be directly extrapolated to the SMS because of its geographical position and relief
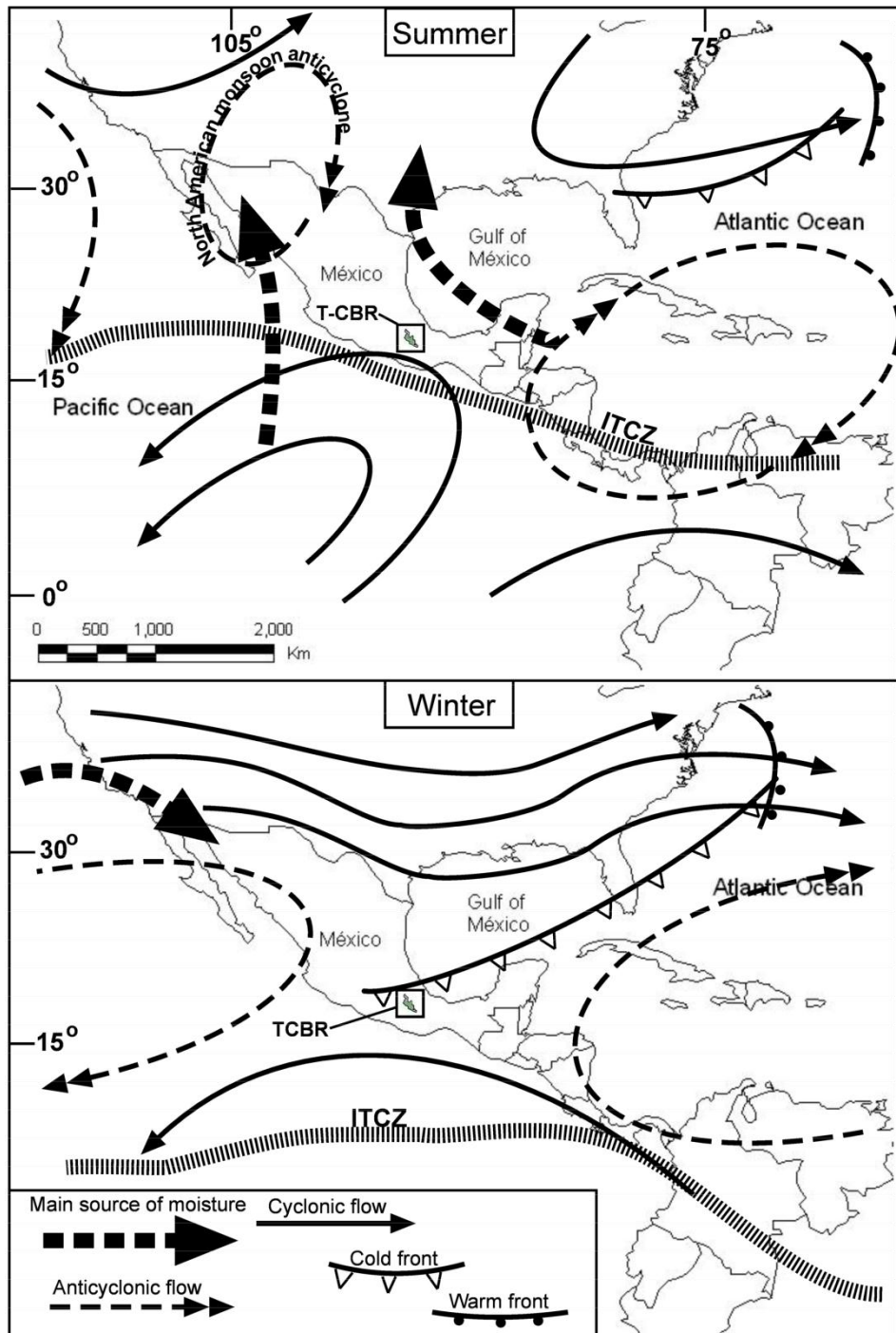
Figure 2.3.1. Present day summer and winter atmospheric features of Mexico. Modified from Metcalfe *et al*. (2000) and Haug *et al*. (2001). ITCS: Intertropical Convergent Zone; TCBR: Tehuacan-Cuicatlán Biosphere Reserve.

features. For example, rain patterns and abundances during the late Pleistocene between north and south Mexico seemed to have been opposite (Metcalfe *et al.*, 2000). In one of the few studies that discuss detailed links between orbital and internal mechanisms to explain detected environmental changes, Leyden *et al.* (1994) relate the pollen assemblages of temperate vegetation at 27,450 ^{14}C yr BP form lake Quexil, to the cold and relatively dry climate for the Circum-Caribbean region as a response to low seasonality (lower isolation gradient between summer and winter) in the Yucatan peninsula. Lower temperatures in the Gulf of Mexico waters caused reductions in humidity and cloud formation (Leyden *et al.*, 1994). As mentioned above, this region and south central Mexico (and SMS highlands of east facing slopes) are influenced by the same atmospheric precipitation, and by analogy, we would expect general colder and semi-arid conditions in the Tehuacan region for at least several thousand years before the LGM.

A rapid global decrease in temperature 30 kyr ago, an interstadial event at the end of the isotope stage 3 (Johnsen *et al.*, 1992), culminated in the establishment of the LGM (Martinson *et al.*, 1987) between around 21 to 18 kyr BP (isotope stage 2) (Lowe & Walker, 1997). According to the GCM (Kutzbach & Guetter, 1986), the most important climatic changes over American mid-latitudes were influenced by the Laurentide Ice Sheet (LIS), which reached its maximum extent with an elevation of up to 2900 masl near 58N, 90W (CLIMAP, 1976; Gates, 1976). During LGM times an anticyclonic system developed over the LIS, relocating the jet stream southwards, pushing the moisture to lower latitudes from its original position in the middle American Northwest (Gates, 1976) and promoting an increase in water discharge, a dry summer-wet winter

regime and the development of pluvial lakes in nearly 100 basins in areas that are now occupied by the Mexican and North American "Great Deserts" (Ortega-Ramírez, 1995;1998; 2001; Metcalfe *et al.*, 1997; 2002; Palacios-Fest *et al.*, 2002; Tchakerian & Lancaster, 2002). The effects of the LIS were also recorded in mountain glacials and lake sediments in the highlands of central Mexico. The advance of mid-latitude alpine glacials was synchronous with that of the highest peaks in the TMVB during the LGM (Vázquez-Selem & Heine, 2004). Studies of pollen records in the lakes of the TMVB also indicate that the region was colder than today during the LGM (Bradbury, 2000; Lozano-García *et al.*, 2005). The establishment of winter rains in the American Southwest during the last glacial (Meyer, 1973), also seem to appear in central Mexico, as evidenced by the abundance of planktonic deep-freshwater diatoms that flourish with winter rains, found in the sediments of lake Pátzcuaro between 25 and 13 ^{14}C kyr BP. (Bradbury, 2000). However, studies from Lozano-García *et al.* (1993, 2005) and Lozano-García and Ortega-Guerrero (1998) based on multi-proxy analyses of Chalco, Chignahuapan and Texcoco lakes respectively, coincide with a cold end of the Pleistocene but suggest lower precipitation between 19 and 16 ^{14}C kyr BP. This pluvial regime was due to the westerly's movement mentioned above, which brought high effective moisture during most of the last glacial (Bradbury, 2000), but there are no records to suggest influence at latitudes below the TMVB. Apparently for areas where the North American westerly winds were not the primary source of precipitation, the LGM represented a drier climate (Metcalfe *et al.*, 2000).

During the LGM the water forming the LIS caused a decrease in sea levels of approximately 100 metres. With temperatures in the Gulf of Mexico

around 23.6 ºC, compared to present values of 29 ºC (Flower *et al.*, 2004), and with the added low seasonality (Leyden *et al.*, 1994), it is likely that the Tehuacan region experienced enhanced aridity at those times. This analogy finds a base from patterns found in other regions whose moisture provenance is the Gulf of Mexico. For example, Huang *et al.* (2006) argue that for central Florida, the low precipitation inferred during the LGM caused more xeric C_4 plants to dominate. Also, the eastern portion of Mexico, the Yucatan peninsula, as well as other parts of Central America, are thought to be colder and drier at 18 ^{14}C kyr BP. (Emiliani *et al.* 1975; Leyden, 1985; Grimm *et al.*, 1993; Lachniet & Seltzer, 2002; Vélez *et al.*, 2006). These ideas harmonise with the anticyclone circulation caused by cooler and more saline conditions in the Gulf of Mexico during the LGM. Piperno *et al.* (2007) studied the pollen, phytoliths and charcoal in the sediments of three lakes in the Balsas Basin and report cold and dry conditions at the end of the Pleistocene, between 14,000 and 10,000 yr BP. A similar climate is hypothesised for the Tehuacan region.

2.4.3. Pleistocene-Holocene transition

The major climate changes that followed the end of the LGM were attributed to the higher insolation that produced relatively rapid melting of the LIS (Brunner & Cooley, 1976) and an increase in seasonality (Leyden *et al.*, 1994). In general terms, the latest Pleistocene (post-LGM) was a period of high climatic instability. Although the LIS melting is thought to have occurred in a number of phases (Jansen & Veum, 1990), only the inputs since 16.1 until 15.6 kyr BP., since 15.2 until 13 kyr BP and between 12.7 and 12.1 ^{14}C kyr BP. drained to the Gulf of Mexico via the Mississippi river (Marchitto & Wei, 1995; Flower *et al.*, 2004). The trend of rising sea water temperatures in the Gulf of Mexico to the present

value of 29 °C in summer (Brunner, 1982) was not gradual, but markedly fluctuating; peaking at around 15, 12.5 and 10 kyr ^{14}C BP. (Flower *et al.*, 2004). The fresh water input from the ice melting into the western Atlantic Ocean also altered sea salinity; decreasing the North Atlantic Deep Water (NADW) formation when the water drained through the north eastern outlets and enhancing it when it flowed into the Gulf of Mexico (Clark *et al.*, 2001). Hence, when NADW formation was reduced, the heat transfer associated to the global thermohaline circulation was lowered, promoting a rainfall decrease in tropical (Street-Perrott & Perrott, 1990) and extra-tropical Mexico (Galloway, 1983). Even when the NADW formation was higher during the Mississippi flows; it occurred during spring and summer, cooling the Gulf waters (Emiliani *et al.*, 1978) and perhaps decreasing the warm water available for regional rains north of the Gulf of Mexico like Florida. This low NADW could be related to the low seasonality and aridity that persisted in the Caribbean until the end of the Pleistocene (~13 kyr) (Leyden *et al.*, 1994).

With the last significant freshwater input into the North Atlantic around 11 ^{14}C kyr BP. (Marchitto & Wel, 1995; Sionneau *et al.*, 2010), the resulting higher sea surface temperatures and evaporation from the ocean waters at these latitudes (Street-Perrott & Perrott, 1990) allowed the establishment of the current summer precipitation pattern at the Pleistocene-Holocene inter-phase in northern Mexico (Ortega-Ramírez *et al.*, 2001; 2004; Metcalfe *et al.*, 2002). In the American Southeast a series of oscillations in humidity, at 900 ±200 year intervals until 11 ^{14}C kyr BP., indicate episodic events of air penetration from the Gulf of Mexico (Wang *et al.*, 2000), suggesting a change in the rain provenance. Evidence of a cold Pleistocene-Holocene transition at lower latitudes comes

from Venezuela, where Lake Valencia had been cold and shallow from 12.6 until 10 ^{14}C kyr BP.; suggesting relatively drier conditions during the Pleistocene-Holocene transition (Curtis *et al.*, 1999).

Climatic changes during the latest Pleistocene are less clear in central Mexico. It appears the shifts in the pollen record of the lake Chignahuapan, relate to a relatively dry level at 12 kyr BP. (Lozano-García *et al.*, 2005). According to Lozano-García *et al.* (2005), at this time the vegetation in the TMVB corresponded to a cold climate; being arid until 9.5 ^{14}C kyr BP. (Lozano-García & Vázquez-Selem, 2005) and wetter by 7 kyr BP. (Lozano-García & Ortega-Guerrero, 1994; Lozano-García *et al.*, 2005). On the other hand, Metcalfe *et al.* (2007) suggested that at the end of the Pleistocene and early Holocene the same region was more humid, promoting high lake levels in Pátzcuaro. The cold Pleistocene-Holocene transition was followed by a warmer and wetter environment (Lozano-García *et al.*, 2005), interrupted by a middle Holocene dry interval since 6.5 to 5 cal. kyr BP. (Lozano-García & Vázquez-Selem, 2005). The fact that inferred paleoclimates for the TMVB in central Mexico are still unclear due to the contradictory evidence of pluvial regimes especially during the early Holocene (Bradbury, 2000; Lozano-García *et al.*, 2005), suggests that factors other than just the temperature and rain patterns influence pollen records. This is even more dramatic for the poorly studied southern Mexico highlands (SMS).

2.4.4. Holocene
Once the LIS was in its final melting phase until around 7 ^{14}C kyr BP. (Flower *et al.*, 2004), with no important flow to the Gulf of Mexico, the atmospheric conditions associated with variations in solar radiation became more important

in driving the climate in middle and high latitudes of the American continent (Leyden *et al.*, 1994; Kirby *et al.*, 2002). During the Holocene, North Atlantic hydrography has been under the influence of solar outputs, altering thermal currents in 1,500-2,000 year cycles, with important global implications (deMenocal *et al.*, 2000; Bond *et al.*, 2001; Asmeron *et al.*, 2007). With increasing summer insolation, sea levels rose and the Gulf of Mexico became warmer, with the peak seasonality in the Circum-Caribbean occurring during the early Holocene, between 10.4-8.2 kyr. This has been the highest for the last ten thousand years (Leyden *et al.*, 1994). This warmer climate forced the Intertropical Convergence Zone (ITCZ) to move northwards sending warm water from the Caribbean to the Gulf of Mexico by means of a loop current resulting in more precipitation (but still colder than present temperatures) in the Yucatan peninsula (Leyden *et al.*, 1994; 1998, Hodell *et al.*, 2005), Haiti (Higuera-Gundy *et al.*, 1999; Poore *et al.*, 2003) and Venezuela (Leyden, 1985; Curtis *et al.*, 1999). These conditions persisted until roughly 8,000 years ago and by homology to the modern circulation pattern, probably to central Mexico. Evidence of a warmer and wetter climate at the beginning of the Holocene came also from other regions. Associated with the Gulf of Mexico moisture source, the Florida lakes remained shallow because of low precipitation until ~ 8.0 ky BP., when the wetter modern climate was established (Watts & Hansen, 1994). Lake Valencia became deeper with high water levels until 8.2 kyr BP. (Curtis *et al.*, 1999). Higher levels of precipitation in the Circum-Caribbean region occurred around ca. 7.0 kyr BP.; indicating an increase in moisture at early Holocene (Leyden, 1985; 1993; Curtis *et al.*, 1999; Lachniet *et al.*, 2004); perhaps caused by the orbital changes in isolation, which stressed seasonality

(Curtis *et al.*, 1999). It is assumed that as summer insolation decreased after 5.0 ^{14}C kyr BP., the ITCZ was located southwards, reaching its present position (Haug *et al.*, 2001). The reduced role of the easterlies in bringing moisture implied a drier climate after the maximum inward movement of the Loop current into the Gulf of Mexico between 6.5 and 4.5 ^{14}C kyr BP.; which is considered to be a period of high summer precipitation in the region (thermal maximum) (Poore *et al.*, 2003; 2005); followed by a fall after 3 kyr ^{14}C BP. (Higuera-Gundy *et al.*, 1999). The late Holocene has also been marked by alternating wet and dry periods, related to monsoonal rains and to El Niño Southern Oscillations (Haug *et al.*, 2001). Arid phases at the late Holocene have been recorded in palaeosols, as pedogenic carbonate accumulation at the north (1,310 ^{14}C yr BP-Sedov *et al.*, 2010) and south (4,650[14]C yr BP-Sedov *et al.*, 2009) flanks of the TMVB. By studying the oxygen stable isotopes ($\delta^{18}O$) of ostracod shells, Curtis *et al.* (1996) recognised three main phases of late Holocene climate change in the Yucatan Peninsula. A relatively wet period between 3.3 and 1.7 kyr BP., followed by an abrupt change to arid conditions between 1.7 and 0.9 kyr BP. and then a return to a wetter than previous environment, that continues until the present. Hodell *et al.* (2005), studying the oxygen stable isotopes of ostracods in a lake core, identified an arid episode in the middle of the fifteenth century, associated to the Little Ice Age. For the same period, Conserva and Byrne (2002) infer an increase in precipitation at the eastern most range "Sierra Madre Oriental". However, this slope with a mesouphyllous type of vegetation is one of the most humid parts of Mexico, since it faces directly to the Gulf of Mexico and receives additional moisture from tropical air masses, which cause semi-permanent fog. Relatively high levels of precipitation persisted until 3.0 ^{14}C kyr

BP., when lake levels decreased until today (Curtis *et al.*, 1999). For the Balsas region, east slope-facing the Pacific Ocean, Piperno *et al.* (2007) report changes in pollen indicating dry conditions at 2,000 yr BP. from a previous moist climate. Other pollen based studies in the Balsas Basin covering the last 3.0 ^{14}C kyr BP. suggest a general trend towards arid conditions since 2.7 kyr, with an intermediate wet period (1950-1070 cal. yr BP) and relatively constant warm temperatures (González-Quintero, 1980; Berrio *et al.*, 2006.). Berrio *et al.* (2006) point out that their pollen assemblages suggest an opposite pattern to the intense drought in Yucatan peninsula at around 1 kyr, and are conservative in suggesting a link to the shift of the ITCZ. However, the Balsas slope faces southwest and lies in the influence area of the Pacific storms, and not the moist winds from the Gulf of Mexico like Yucatan. Concordant with the patterns described above, the records indicate cold-dry environments before 10 kyr ^{14}C BP., followed by more humid conditions during the middle Holocene and drier conditions in the late Holocene.

2.4.5. Quaternary studies in the Tehuacan region

Only four studies have mentioned aspects of the Quaternary of the Tehuacan region. Based on field observations but not data, Brunet (1967), suggested that the sediments of the "Tertiary-closed lake" basin in the area now occupied by the Tehuacan Valley, were eroded head-wards by the river Santo Domingo to the southeast; draining to the Gulf of Mexico via the Papaloapan river. He also asserts that because of a lack of other evidence indicating climate change causes, dynamic geomorphic processes account for the enhanced aridity of the Tehuacan Valley during the late Quaternary. Vita-Finzi (1970) highlights the generalised late Quaternary alluvial deposition in different localities of central

Mexico, including the Tehuacan region and notices the depositional hiatus at the LGM. He provides a date of 540 ± 95 AD for unconsolidated sediments near Tehuacan city. However, to-date, there has been no systematic attempt to explain the origin of these depositions and still few numerical dates have been obtained.

A study conducted by McAuliffe *et al.* (2001) aimed to understand the soil erosion and vegetation change in the SJRB and ZDLSB. They compared hill slope soils and valley deposits in the southern portion of the ZDLSB against the westernmost section of the SJRB. On the basis of observations of present day methods of land management these authors considered that human agriculture had impacted on the first basin during the last millennia, while the second represented a more unspoiled environment. In summary, they suggested that the late Pleistocene landscape of the SJRB was of stable slopes and highlands, showing well developed soils, and a valley zone filled with alluvial sediment. An initial period of intense erosion and valley incision was inferred during the Pleistocene-Holocene transition followed by alluvial sedimentation. This alluvial activity was determined based on a charred material dated at 9,170 ± 80 ^{14}C yr BP from a sample taken at a depth of approximately 3.5 metres in a sedimentary section at the valley bottom. McAuliffe *et al* (2001) propose that this valley continued filling and was followed by deep valley incision, giving rise to the present day landscape. However, no numerical dates are given to these last events. McAuliffe *et al.* (2001) recognise active phases of late Quaternary alluvial activity but no dates are provided for these episodes nor the causes clarified. By observing the current agricultural methods in other parts of the Tehuacan region and the literature, they presume that land management and

climate change during the Pleistocene-Holocene were the likely causes, but do not provide direct or empirical evidence. Apart from the small scale and poor stratigraphic and chronological controls, such conclusions were also limited because although the hill slope soils were properly described, the valley alluvial deposits were not studied in sedimentological terms. In this thesis the study of the SJRB will include: a more detailed sedimentological analysis of those and related deposits, more dates, and a landscape perspective in order to increase the knowledge of the sedimentary processes and the likely role of other factors, including climate and tectonics.

More recently, Canúl (2008) analysed the pollen of the sedimentary profiles San Lucas (SLC) and Candelilla (CAN) located in the SJRB providing the first late Quaternary reconstruction of the palaeoenvironmental changes in the region. She found a mixed pollen assemblage of *Pinus*, grasses and riparian plants in a sedimentary unit dated at 25,220 ± 60 ^{14}C yr BP by Valiente-Banuet and Ortega-Ramírez (unpublished); and associated them with a cold and wet climate. This pollen zone was followed by an increase in *Pinus* pollen dominance until 12,980 ± 190 ^{14}C yr BP (date by Valiente-Banuet and Ortega-Ramírez, unpublished). The pollen composition bracketed between 12,980 ± 190 ^{14}C yr BP. and 6,790 ± 60 ^{14}C yr BP (dates by Valiente-Banuet and Ortega-Ramírez, unpublished) is represented mostly by mesophylous forest type. At the base of the sedimentary unit CAN, dated at 6,790 ± 60 ^{14}C yr BP., this pollen mixture overlaps with tropical deciduous forest until after 6,790 ± 60 ^{14}C yr BP., when *Pinus* disappears and grasses increase their presence. Grasses and tropical deciduous forest pollen dominated around 5,020 ± 40 ^{14}C yr BP.

Several considerations need to be made to increase the value of the late Quaternary pollen assemblages from CAN and SLC reported by Canúl (2008). If representative and well-preserved pollen and no re-deposition are assumed, Canúl's conclusions that cold and more humid than present conditions prevailed locally before the LGM and persisted until middle Holocene (6790 ± 60 ^{14}C yr BP.) are correct. Under the same view, the establishment of the current arid conditions and open vegetation is inferred since the middle Holocene (5,020 ± 40 ^{14}C yr BP.). However, although a consistent pattern of change between the Pleistocene and Holocene is observed, the fact that the pollen samples come from alluvial terraces means that a series of issues must be addressed. First, the pollen collections may not represent absolute *in situ* deposition, increasing the potential presence of contamination with reworked pollen (pre-deposited). The sedimentary context of the pollen deposition has not been addressed in the environmental interpretation by Canúl (2008). Also, the referred study faces the problem of not reporting modern pollen rain, making it difficult to compare the relative abundance of fossil pollen along the sedimentary sections with present day pollen input. In terms of the current vegetation the region is dominated by thorn scrub and locally by columnar cacti forests. However, these types of plant communities are absent in the pollen records reported by Canúl (2008). Instead pine and mesophyllous forests are reported; two types of vegetation which require as much as twice the amount of rain received in the area. In addition, the idea of a wet latest Pleistocene contradicts the hypothesis of relatively dry condition given that the atmospheric and oceanic processes mentioned previously implied reduced moisture input from the Circum-Caribbean region. It is important to stress that chronology and shifts in pollen assemblages across

both sections studied by Canúl (2008) present a clear pattern and could represent regional changes. However, the sedimentary context of the sampled sites, an extended analysis, and more proxies are essential in order to widen the discussion and increase the reliability of these pollen records.

2.4.6. Summary of regional palaeoenvironmental history

To date, there are very few published studies on the Quaternary environmental change of the Tehuacan region despite the high potential of the extensive sedimentary records. Because most studies of this type focus on lake sediments of north and south Mexico and the Caribean region, and are based on lake-related proxies, the alluvial records of past conditions of Tehuacan have not attracted attention and virtually no data is available. Hypotheses on late Quaternary climatic patterns have to be inferred from changes in neighbouring regions. Palaeoenvironmental reconstruction for parts where climate influences are shared with Tehuacan indicate that for several thousand years before the LGM (between around 28 kyr to 18 kyr) the climate was in general colder than present and relatively dry with low seasonal contrast, becoming even colder during the LGM and probably drier than present. Although there is little data between 18 to 13 kyr, proxies in different regions suggest that Late Pleistocene conditions could have been governed by high climatic instability caused by higher solar insolation and more seasonality. Higher temperatures than before, but still colder than present, and enhanced summer precipitation are more likely to have prevailed between 11 to 8 kyr ago. Around 5 kyr before present, the peak in summer insolation caused higher than present precipitation. The decline in insolation after middle Holocene was accompained by a decrease in moisture and the arrival of El Niño episodes. Current climate conditions were probably

established around 3 kyr ago. This inferred chronology of climatic events is the hypothetic scenario of change during the late Quaternary in the Tehuacan region. The duty of this thesis is to search for likely signatures of the environments associated with those changes documented in the unconsolidated deposits of the SJRB, sedimentological, pedogenic, fossils, etc. It is unknown how the late Quaternary atmospheric and marine circulation changes affected the local climate and environments, what unequivocal evidence is preserved, and the extent to which other factors like tectonics have contributed to forming the sedimentary records. Hence, the likely roles of other factors like tectonics are considered during the interpretation of those stratigraphic records. Details on the approach and methods of this investigation are presented in Chapter III.

CHAPTER III

RESEARCH FRAMEWORK

3.1. Introduction

In previous chapters the evolution of the SJRB was recognised as the product of its internal and external components interacting over different time and spatial scales; and finally the state of the knowledge from previous works on the regional history was revisited. With this framework it has now become possible to stress the particular hypotheses and objectives that have delineated and guided the research process.

3.3. Research questions and hypothesis

3.3.1. Was the SJRB formed by the pre-Neogene extensional tectonism of central Mexico?

The way in which the SJRB has evolved has not been studied before. This issue needs to be addressed in this research because the tectonics that formed the internal basins of the SMS determined the type of landforms on which the depositional environments developed, forming records of past processes. This was the case with the Tehuacan and Tepexi basins which were formed after the late Cretaceous-middle Oligocene shortening orogeny (Cerca *et al.*, 2007; Silva-Romo *et al.*, 2000). As explained in Section 2.3.2.1, a series of normal faults aligned in a NW-SE trend (Oaxaca, Caltepec, Tamazulapa) have displayed evidence of major activity since the middle of the Oligocene until the middle of the Miocene (~13 Myr ago) forming some of the closed basins of the SMS. The depositional hiatus between the late Cretaceous and Quaternary in the SJRB suggest that this system was not a basin and/or that very intense erosion has eliminated Tertiary rocks. Another line of evidence supporting the

idea that the SJRB formation was probably not contemporaneous with its neighbouring basins is that it shows a different faulting pattern and responded to different tectonic events. The fault system associated with the structural blocks that define the basin shape would reflect an independent pattern, not congruent with the regional extensional trend. Under the same hypothesis, post-late Cretaceous deposits should reflect Cenozoic lacustrine, fluvial and alluvial environments related to the evolution of the basin morphology.

To test such a hypothesis it is necessary to find evidence of tectonism related to the opening of the SJRB, and to revisit early structural maps in view of recent tectonic reconstructions. However, this is not a study based on geophysical methods and, provided that there is no data available on the internal structures, the first approximation needs to be based on the surface geology of the basin. Hence, a detailed revision of the geology of the SJRB was carried out by extensive field recognition, description of the spatial distribution of the rock formations, their stratigraphic relationships, major faults and other morphological features related to kinematic processes. On the other hand, if the SJRB was contemporaneous with its neighbouring basins and its Tertiary deposits were eroded, remnants of continental basin type rocks should be found in the system. An extensive and detailed field exploration was also carried out to test the presence of that phase.

3.3.2. What has been the role of tectonics and climate in producing the sedimentary records and landforms of the SJRB?

The focus of this section is the geomorphic nature of the SJRB and its environmental significance. The SJRB shows a number of surfaces like alluvial fans and fluvial terraces that can contain important information on basin evolution. These landforms keep records of soil formation, erosion, as well as

47

chemical and sediment deposition that can potentially be related to tectonic, climatic or human forces. Emphasis will be put on exploring the main geometry of the alluvial forms, terraces, rivers and other geomorphic features. As regional tectonics and climate have played an important role during the Cenozoic in the region, it is expected that their signature can be found in the landscape. The lack of tectonic studies and/or climatic controls from independent sources makes it difficult to distinguish clearly the relative role of each forming factor. The option adopted was to analyse the geometry, spatial distribution and other features of the alluvial fans and terraces. For example, the presence of correlated and widely distributed sedimentary units in different parts of the basin could be linked more closely to climate changes whereas localised non-correlatable landforms would more likely have been formed by tectonics. Given that contrasting litologies dominate different flanks of the basin, it could also be useful to distinguish local tectonic processes from regional phenomena. The sedimentary landforms have firstly been classified, their characteristics have been identified and their likely forming processes interpreted.

3.3.3. How did late Quaternary climate change modify local environments and which records are preserved?

This part will explore the potential for reconstruction of local past environmental changes of the SJRB. The sequences of deposited material in a basin system are the product the lithology, tectonic motion, climate change, and/or anthropogenic activity, constituting invaluable records of past environments. Following the hypothesis outlined in section 3.3.1, which states that the SJRB was likely to have been formed as a sedimentary basin after the SMS orogeny during the Cenozoic, it is proposed here that the exposed sediments document different phases of late Quaternary environmental change of the basin. A further

step is to analyse the links between the local environmental history and the inferred modifications on climatic patterns based on prevailing ideas on the atmospheric patterns that determined those changes during the late Quaternary. According to those climatic patterns, the most plausible hypothesis earlier stated (Section 2.4.6) and summarised in Table 1, is that south central Mexico, and consequently the geographical region where the SJRB is located, remained colder and relatively wetter than today for several thousand years until it moved towards cold and semi-arid conditions, culminating this period during LGM. Later changes implicated a relatively stable late Pleistocene, dry and with colder than present temperatures. The transition from Pleistocene to Holocene was accompanied by more solar insolation and probably increased temperatures and precipitation, especially at the early Holocene. The early-mid Holocene was the most likely period when the modern summer rain pattern established across the country. The period of highest precipitation during the Holocene in the SJRB is inferred to coincide with the highest summer insolation between 6.5 and 4.5 kyr BP recorded in regions whose moisture source is primarily the same as for south central Mexico. The establishment of a highly seasonal climate and increasing aridity in the region should have occurred after the middle Holocene. The correspondence with this hypothetical scenario and the palaeoenvironmental archives of the SJRB will be discussed and a cause-effect relationship and/or alternatives will be established on the basis of the findings of the present thesis and published studies. Preliminary observations in the SJRB show a number of stratigraphic sections of contrasting strata with fluvial, alluvial fans and palaeosols and it is expected that those strata represent different phases of late Quaternary environmental change. As mentioned

before, although discontinuously, at least one of those sections covers the last 25 kyr. Hence, the different facies of a number of sedimentary profiles will be analysed in order to interpret their palaeoenvironmental significance. Key alluvial and fluvial deposits and palaeosols will be analysed in terms of the environments under which they were formed; periods of climatic stability, and changes in fluvial/alluvial regime, etc. Evidence other than sedimentological, such as chemical precipitates of tufa and fossils, will be also interpreted in terms of the palaeoenvironmental context. The dates in which some of those environmental changes occurred will be established using a geochronological framework based on radiocarbon dating.

Table 1. Main late Quaternary climatic patterns for south central Mexico and hypothetical environmental and geomorphic responses in the Tehuacan region. The expected response in the SJRB are based on the available published works, which in turn provided data from marine and terrestrial proxies. MIS*- Marine Isotope Stage.

Time (approx. kyr BP)	Global climatic phenomenon	Hypothetical conditions in continental central Mexico	Hypothetical geomorphic response and records in the SJRB
End of MIS* 3 (30-20)	Interglacial conditions and shift to glacial, trend towards colder temperatures	Cold and dry with low seasonality	Geomorphic instability and soil erosion following changes in vegetation
LGM (18)	Glacial conditions. Lowest global temperatures in the last 130 kyr	Drier and colder than before with low seasonality	Low to medium intensity erosion and basin filling as a response to likely changes in vegetation cover
Latest Pleistocene (16-11)	Increase in solar insolation	Climatic instability with increasing precipitation and temperatures	Alternated periods of erosion and basin filling with soil formation
Early Holocene (10-8)	End of glacial conditions	Highest seasonality, more precipitation and warmer climate	Intense initial erosion followed by geomorphic stability and soil formation
Middle Holocene (5)	Peak in solar insolaton	Highest temperature and precipitation of the last 30 kyr	Initial basin filling; increase in plant cover and soil development
Late Holocene (4-3)	Gradual decrease in insolation and establishment of current conditions	Increase in aridity and establishment of summer rain pattern	Decrease in plant cover and intense erosion

3.5. Objectives

3.5.1. General

The aim of this thesis is to study the lithology, landforms, sediments and fossils in the SJRB as the end products of the key environmental processes. The main interest is to generate information on what geologic processes gave shape to the current geometric configuration of the SJRB and what fluvial, alluvial and pedogenic processes are recorded in the landforms and sediments of the basin; when they occurred and how they link to climatic and tectonic activity. In order to achieve this purpose a number of components of the basin with palaeoenvironmental significance are characterised. This includes the geology, geomorphology, alluvial and fluvial sediments, palaeosols, tufa as well as fossils. With this collection of information the aim is to produce a rational palaeoenvironmental reconstruction of the basin and to provide a discussion of the relevant implications of the evolution of the SJRB.

3.5.2. Particulars

- To carry out a detailed characterisation of the geology of the SJRB in terms of the rock types, their spatial distribution and stratigraphic relationships and to represent this information in a spatially explicit model, testing the presence of Tertiary continental sedimentary rocks.

- To identify the main structural features of the SJRB and to analyse if they correspond to the regional Paleogene tectonics or are the result of neo-tectonic activity.

- To characterise the geomorphology of the SJRB, to present it as a map and to analyse the different sedimentary landforms in terms of the genetic mechanisms, tectonic and climatic.

- To carry out field identification and description of key sedimentary sections that record fluvial, alluvial and pedogenic phases.

- To determine the stratigraphic relationships of the different sedimentary sections on the basis of numerical chronologies provided by radiocarbon dates.

- To characterise the different depositional and palaeosol environments along the sedimentary section by means of the physical characteristics; including description of hand specimens and granulometric parameters.

- To analyse the relationships between the environmental changes in the SJRB with other geological, climatic, ecological and anthropogenic factors on a local and regional scale.

CHAPTER IV

STUDY SITE AND METHODS

4.1. Study site

4.1.1. Location

The system under study is an intramontane basin of the Sierra Madre del Sur, in the region known as Tehuacan Valley (Fig. 4.1). The SJRB is in fact a first-order sub-basin of the Tehuacan Basin, which in turn belongs to the Papalopapan basin, which drains to the Gulf of Mexico. The SJRB forms part of the northwest boundary of this hydrographic system with the Balsas basin immediately to its west flank. In physical terms, the SJRB is located between 18º 16'-18º 25' N and 97º 32'-97º 39' W. According to the classification connectivity basins by Horton (1945), the SJRB is of first order because it is the upwards terminal basin of the hydrological network and does not receive water or sedimentary input from other basins (Fig. 4.1.2).

4.1.2. Geology

The first geological and structural maps of the SJRB were sketched by Mauvois (1977) and by Buitrón and Barceló-Duarte (1980) and for decades were the only available detailed maps of the SJRB. The Zapotitlan Formation (Kl-Z) of Barremian age consists of intercalated strata of polymictic conglomerates, sandstone, limestone, marl and grey micaceous siltstone (Aguliera, 1906; González-Arreola, 1974; Buitrón & Barceló-Duarte, 1980). A group of beds of grey calcareous limestone alternated with sandstone have been named Agua del Burro and Agua del Cordero and are considered members of the Kl-Z (Buitrón & Barceló-Duarte, 1980). The San Juan Raya Formation (Kl-S) is a sequence of greenish grey siltstone alternated with greywacke-sandstone and

coquina (Calderón, 1956 in González-Arreola, 1974; Buitrón & Barceló-Duarte, 1980) which outcrop locally in the basin (Fig. 2.1.2.2; 2.1.2.3). In the first published study Aguilera *et al.* (1896) described a 360-metre sequence of the KI-S, composed of 103 intercalated layers.

4.1.3. Topography

The altitude gradient goes from 1,600 at the basin outlet to the east to 2,720 masl in the Cerro Viejo (CV) and Cerro Santa Maria (CSM) north highlands. The most prominent topographic features are the highlands to the north, and the semi-conical Cerro Gordo (CGo) and Cerro Tarantula (CT) to the west and east respectively (Fig. 4.1.3). The Cerro El Garambullo (CGa), Cerro Mezquite (CM) and Cerro Salado (CS) are three internal minor highlands that divide the basin into two sections; southwest and northeast. A series of faulted highlands mark the east (Cerro Campanario-CC; Cero La Mesa-CMe; Cerro Xentle-CX) and south (Cerro Otate-COt, Cerro Ometepec-COm) boundaries of the basin, whereas the west limit is marked by a fracture that breaks the continuity of a plateau which extends into the neighbouring basin (Fig.4.1.2; 4.1.3). Three small villages are established inside the SJRB, named San Juan Raya (SJRv), Santa Ana Teloxtoc (SATv) and San Lucas Tetetitlan (SLTv). A small group of recently constructed houses are known as Plan de Fierro (PFv).

4.1.4. Hydrology

In terms of the hydrological system, the basin shows a network of intermittent rivers, locally named "barrancas", which carry water for short periods (minutes to hours) after episodic rains. The main river which connects the south network is Barranca Agua la Iglesia (BAI), while the secondary rivers to the north and east drain to Barranca El Zapote (BZ), Barranca San Lucas (BSL) and Barranca

Grande (BG) (Fig. 4.1.2). The main barrancas join up a few tens of metres before the basin outlet, which drains to ZDLSB, under the name Barranca Grande (BG). This intermittent river runs across the ZDLSB and drains to the Tehuacan Basin (TB) near San Gabriel Chilac (SGCv), where it takes the name of Rio Zapotitlan.

4.1.5. Climate

The regional warm dry climate is governed by its geographical position and by the surrounding physiographic features (García, 1981), although because of the high internal geomorphic heterogenetity, a wide variety of microclimates are found in different parts of the region. The importance of such heterogeneity is in fact that it partially explains the high biological diversity. The inter-tropical position (below 19 degrees, north latitude) and the relatively low altitude of the Tehuacan Valley (between 1400 and 1700 masl) cause warm temperatures and no winter frosts (Valiente, 1991). The climate is classified as semi-arid with summer rains (Bs_1(h')w''(w)eg) and a mean annual temperature of 24.7 ^{o}C (García, 1981). The summer monsoon rains originate primarily in the Gulf of Mexico, although some moisture has a Pacific Ocean provenance (Valiente, 1991; Englehart & Douglas, 2001). The annual average precipitation is 376 mm and is very seasonal, distributed during the summer months from June to September, with an intermediate short dry period (Valiente, 1991). The rain shadow is due to the surrounding Sierra Mazateca mountains to the east and the Cuicatlán and La Mixteca ranges to the south and west respectively. Annual precipitation in the SJRB for 2002 was 385 mm and showed a typical monthly distribution for a locality of the Tehuacan region (Medina-Sánchez, 2004) (Fig.

4.1.1). This monthly distribution has a seasonality index of 76.5 according to the following formula by Bull (1991):

$$Sp = \frac{Pw}{Pd}$$

where *Pw* is the average total precipitation for the three wettest consecutive months and *Pd* is the same value for the driest three months; and corresponds to a strongly seasonal pattern (Bull, 1991).

4.1.6. Vegetation

The Tehuacan Valley is enclosed in what Rzedowski (1978) named the phytogeographic "Xerophytic Mexican Region"; characterised by a mosaic of arid plants of Neo-tropical affinity (Rzedowski, 1978). The vegetation types
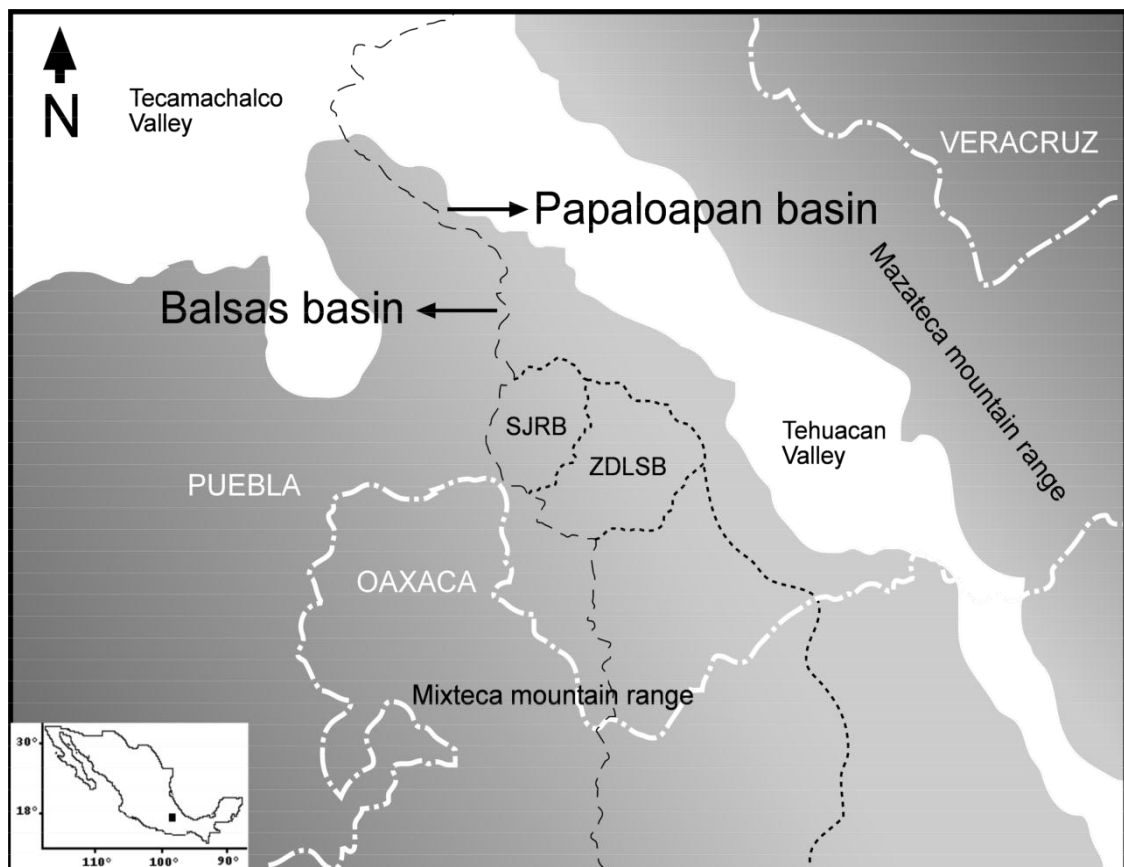
Figure 4.1. Regional context of the SJRB and ZDLSB. The white broken line indicates States boundaries. The black broken line marks the water divide between the Balsas and Papaloapan basins. Grey areas correspond to major highlands.

include thorny scrubs, tropical deciduous forests, sclerophillous scrubs (Mediterranean type) and columnar cacti forests among others (Valiente-Banuet *et al.*, 2000; 2009). Considering that the area covered by the Tehuacan Valley is of approximately 10,000 km^2 (Valiente-Banuet *et al.*, 1996) and that the number of plant species is very similar to that of the Sonoran desert (with 275,000 km^2) with 1,000 fewer species than the Chihuahuan desert (with an area of 453, 000 km^2), the region is the most diverse dry land in Mexico and one of the richest in the world (Davila *et al.*, 2002). The vegetation associations found in the SJRB, according to the classification by Valiente-Banuet *et al.* (2000; 2009) are columnar cacti forests, varying according to the dominant species: *Neobuxbaumia macrocephala* and *Neobuxbaumia mezcalaensis*; "Isotales", dominated by *Beaucarnea gracilis* or *Yuca periculosa*; thorny scrubs of *Mimosa sp.*, "Fouquieriales" where *Fouquieria formosa* is the dominant tree and *Equinocactus platiacanthus* thorny scrubs among others.
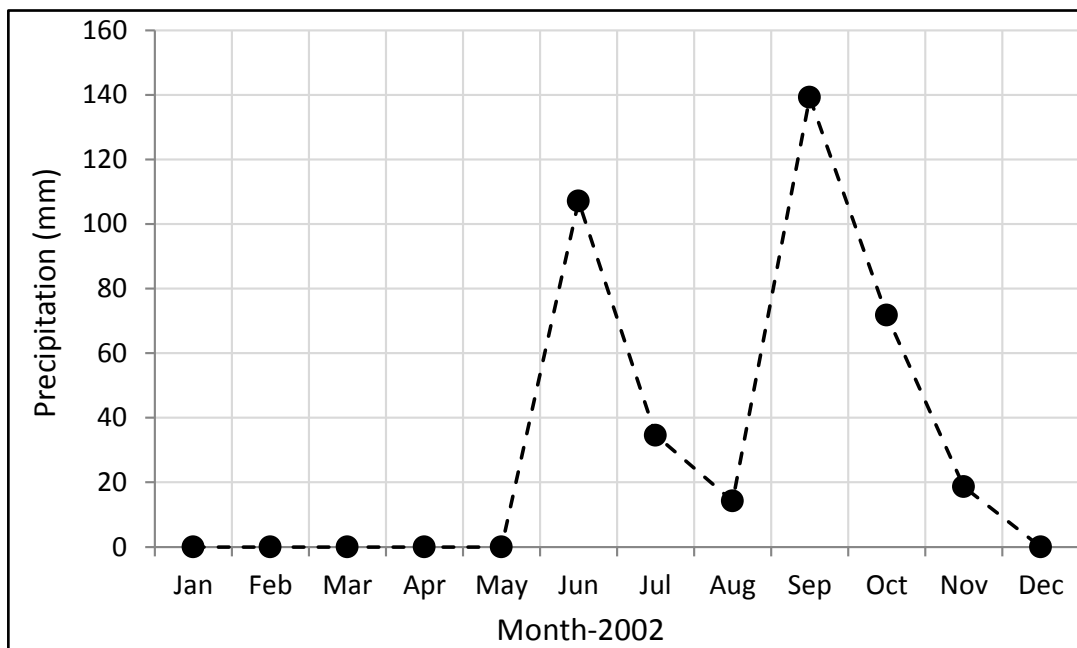
Figure 4.1.1. Rain distribution during 2002 in the SJRB (Medina-Sanchez, 2004).

57
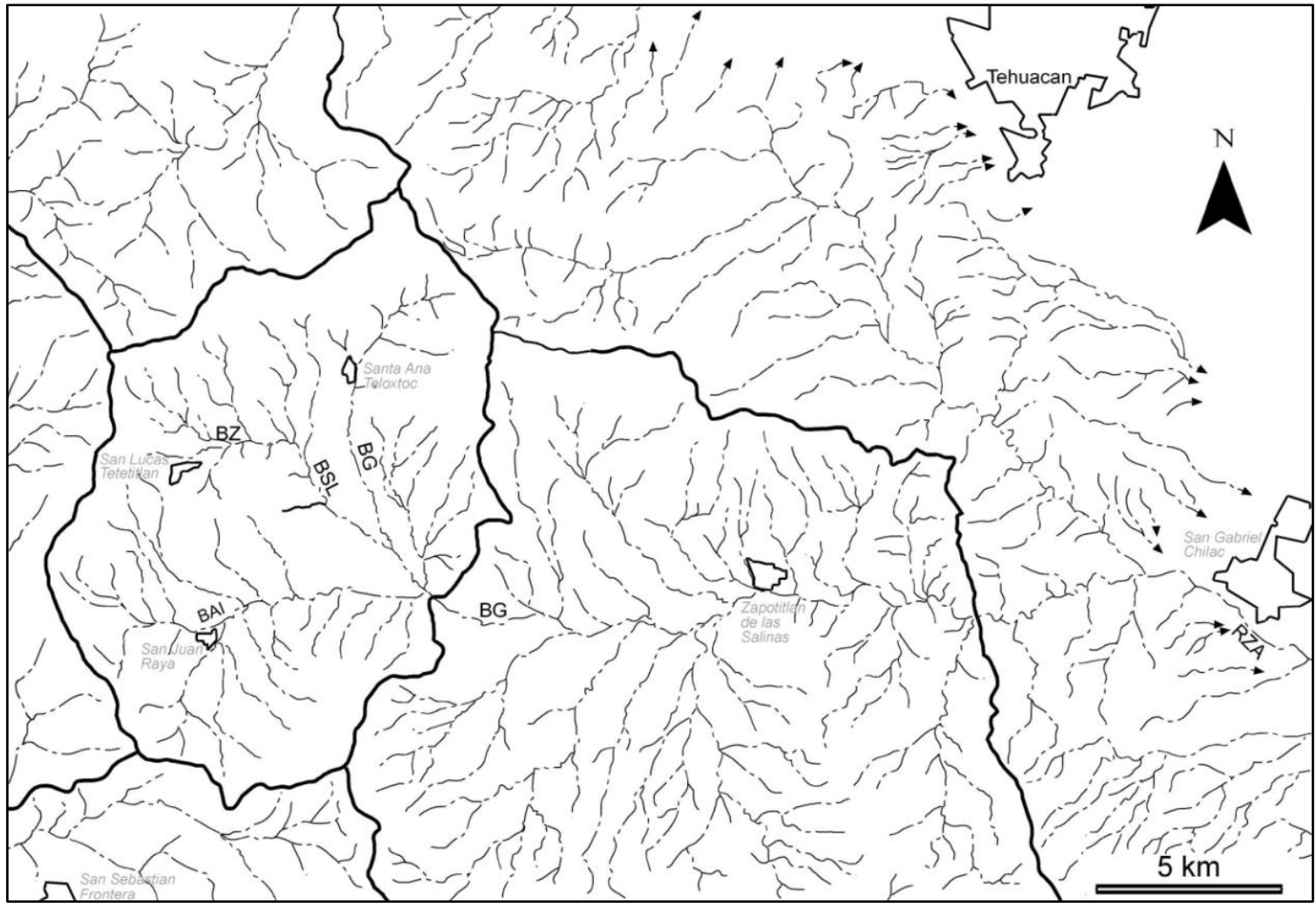
Figure 4.1.2. Simplified drainage network of the SJRB and adjacent basins. See text for abbreviations.
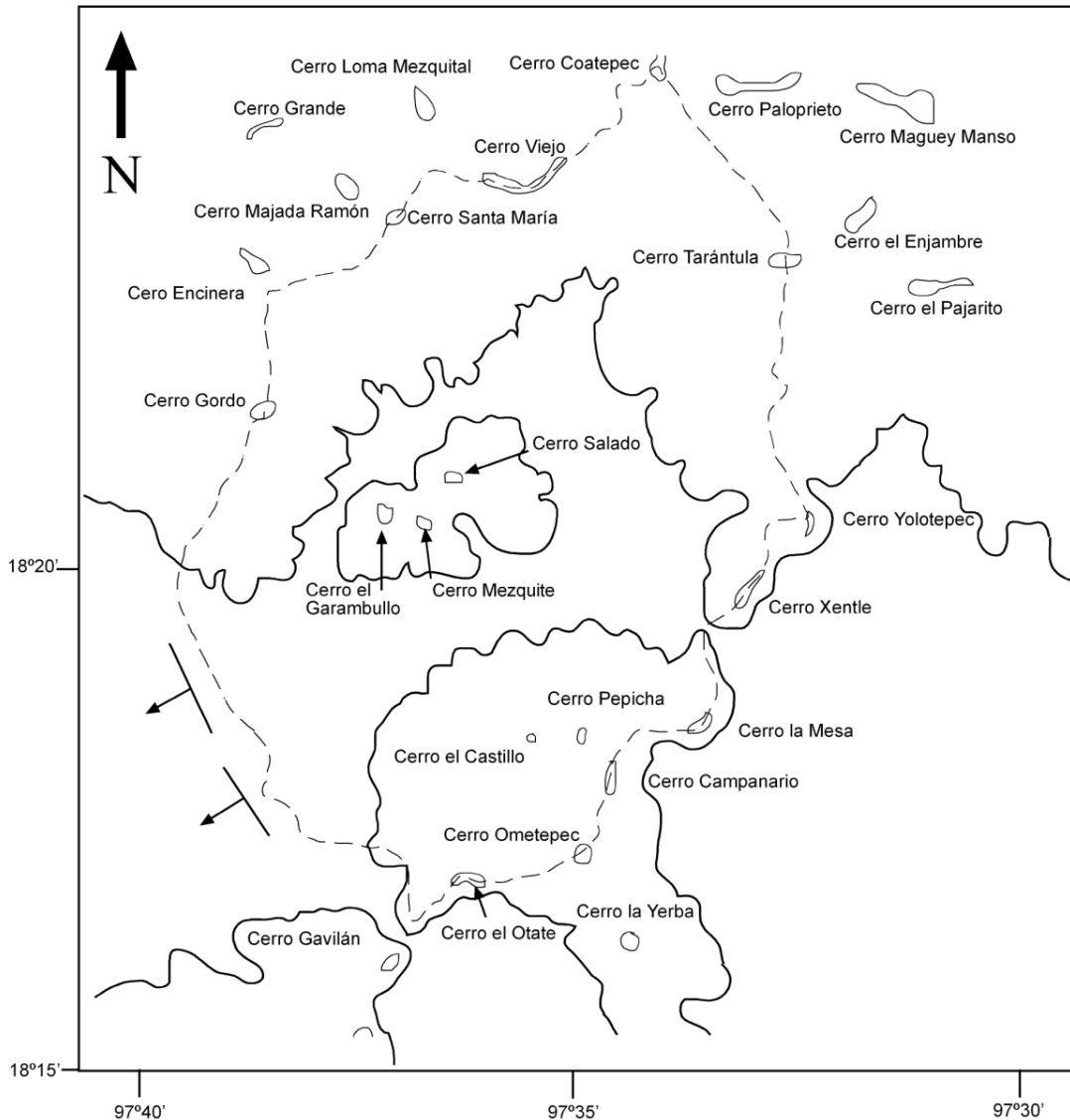
Figure 4.1.3. Highlands surrounding the SJRB. Summits are enclosed by thin lines and the basin border is marked by a dotted line. Arrows indicate drainage direction on the plateau to the west. Maximum altitude of the highlands decreases southwards from 2,700 in Cerro Viejo to 2,020 in Cerro Gavilán.

4.2. Methods

4.2.1. Geologic and geomorphologic setting of the San Juan Raya Basin

To analyse the evolution of the main geologic and geomorphic structures of the SJRB, an in-depth revision of the literature on regional geology was carried out and detailed maps on topography, hydrology, geology, geomorphology and a digital elevation model (DEM) were produced. The geology, geomorphology and hydrology maps were based on the interpretation of aerial photographs, scale

59

1:20,000, taken in 1997. The interpreted features were drawn in opaque mica on the photographs, using a standard stereoscope, and the resulting polygons, lines and points were scanned and geo-referenced on screen using ERDAS 8.7 and ArcMap 9.2. In the field, verification points were recorded with a Garmin 12 GPS. Base topographic maps, scales 1:250,000 ("Orizaba", INEGI, 1998a) and 1:50,000 ("Tehuacan", INEGI, 1998b), were used for rectification and location. Additional regional information was obtained from the following geology maps, scale 1:250,000: "Orizaba" by INEGI (1998c) and Martínez *et al.* (2001), "Oaxaca" (González *et al.*, 2000) and the structural geology "Tehuacan-Cuicatlan" map by Dávalos-Álvarez *et al* (2007). The age and stratigraphic position of the rock units of the SJRB were established on the basis of field observations and information provided in the literature and previously mentioned maps. Part of the information contained in the maps of the geology of the SJRB by Mauvois (1977) and Buitrón and Barceló-Duarte (1980) was revisited and incorporated in the geology map. Intensive fieldwork was carried out from May to August 2007, February to May 2008 and December 2008 to February 2009 to corroborated lithology, landforms, structures, descriptions and also to perform field descriptions and sampling. The DEM was taken from the STRM-V2 (NASA, 2009) and manipulated with the "Hydrotools" module of ARGIS 9.0 software. This model allowed the outlining of the basin borders. Landsat (USGS-NASA, 2009) satellite images of the study area were integrated to the model using ERDAS 8.7 and ARGIS 9.0 software.

4.2.2. Stratigraphic sections
The landforms were surveyed during the above mentioned fieldwork seasons. Surface characteristics and selected stratigraphic sections in rivers or other

exposed cuts were recorded. A number of stratigraphic sections were chosen, described and sampled in the field after extensive field recognition. Only those sections which showed a more complete and diverse set of depositional environments and hence more potential for reconstruction were included. Section names were assigned arbitrarily: Alberca (ALB), Bisonte (BIS), Capullos (CAP), Palo Verde (PV), Salitrillo (SLT), San Juan II (SJII), Santa Cruz (STC), Two Friends (TFR) and Teponaxtle (TPX). The sections Candelilla (CAN) and San Lucas (SLC) are currently undergoing a sedimentological a study by Canúl *et al.* (Canúl, per. comm.). For that reason those sections where only described in the field as part of the present study. A radiocarbon date was recently obtained from a section named PV, which corresponds to the top part of the alluvial terraces a few hundred metres from the section TPX according to Valiente-Banuet (per. comm.). The PV section was not visited during the fieldwork of the present thesis.

Samples were independently taken for sedimentological analysis (particle size distribution, organic matter, and hand specimen descriptions) and radiocarbon dating. The combined description in profile and of hand specimens included bedding, horizontal contacts, grading, sorting, structure, porosity, sedimentary and pedogenic features according to Graham (1988) and McManus (1988). For fluvial deposits, roundness, shape and sphericity were also recorded. Sedimentary profiles were correlated on the basis of their sedimentary characteristics, radiocarbon dates and stratigraphic positions.

4.2.3. Organic matter content

Organic matter was measured by Loss On Ignition (LOI). Samples were dried out on aluminium trays overnight at 110° C in an oven (Gallenkamp Hotbox

Oven S2). Pre-ignited crucibles of known weight were placed on an analytical balance (Sartorius U5000D), tared to zero. Three replicates per sample of twenty five grams were put inside the crucible, which represented the initial weight (*wi*). Crucibles with dry samples were then placed in a pre-heated furnace (Carbolite ELF 11/148) at 550 ºC for 4 hours. The crucibles with the sample were immediately weighed and the crucible mass discounted to obtain the final weight (*wf*). The organic matter (OM) content was then calculated with the following formula:

$$OM = \frac{wi - wf}{wi} \; 100$$

4.2.4. Particle size analysis

Samples for determination of particle size distribution were oven-dried at 110º C overnight in a Gallenkamp Hotbox Oven S2. Samples were split into representative sub-samples using a riffle box. For fine-grained samples (containing only particle < 2 mm) 20 grams were taken, while for coarser samples (containing particles < and > 2 mm) 100 grams or more were the initial amount. All weight measurements for these procedures were carried out using an analytical balance (Sartorius U5000D). In order to eliminate organic matter, carbonates and to break down aggregates before size frequencies were determined, the samples were pre-treated according to a modification of Konert and Vandenberghe (1997). Samples were placed in 500 ml Erlenmeyer flasks and aliquots of 10 ml 30 % H_2O_2 solution per each 20 grams of sample were added until all the organic matter was destroyed. Samples were then boiled on a hot plate for 30 minutes with distilled water to remove the excess H_2O_2. Carbonates were eliminated by boiling the samples in water and adding 10 ml aliquots of 10 % HCl whilst boiling until no reaction was visible. To eliminate

dissolved salts and excess hydrochloric acid, the samples were left to stand and water was decanted after three days avoiding loss of sediment particles. This procedure was carried out three times before further treatments. All samples were then wet-sieved through a 1 mm sieve and separated in two fractions; fine, >-1 Φ (< 2 mm), and coarse, <-1 Φ (> 2 mm). Separated fractions were oven-dried overnight and weights were recorded for percentage adjustment of size fractions measured by dry sieving (coarse fraction) and laser diffraction method (fine fraction). Although sieving and laser diffraction methods separate size classes by weight and volume respectively, the same density was assumed for both fractions. Coarse fractions were dry-sieved through the following sieves (ASTM modules Endecotts LTD): -1 Φ (very fine pebbles ≥ 2 mm); -1.4 Φ (very fine pebbles > 2.8 mm); -2 Φ (fine pebbles ≥ 4 mm); -2.4 Φ (fine pebbles > 5.6 mm); -3 Φ (medium pebbles > 8 mm); -3.4 Φ (medium pebbles > 11.2 mm) and -4 Φ (coarse pebbles > 16 mm). Particles bigger than -4 Φ were measured with a calliper. These sieve sizes were selected because they include approximate regular intervals of the coarse fraction. Particles of each size class were weighed and the percentage was calculated.

Particle size distribution was determined by the laser diffraction method: samples were dispersed by boiling them for 10 minutes in an Erlenmeyer flask with aliquots of 15 ml of 0.12M sodium hexametaphosphate ($Na_4P_2O_7 \cdot 10H_2O$) per 20 g of sample. The samples were then placed on a shaker plate (Chiltern) for two hours. Each sample was agitated and homogeneous aliquots were taken and processed with the laser equipment. Particle size measurements took place after the samples were cooled at room temperature in the laser equipment (Beckman-Coulter LS Series). Water was employed as fluid and

samples were subjected to sonication while fluxing; 60 seconds prior to and 90 seconds during laser measurements. Three or more replicates of each sample were measured following the former technique. Percentages of each size class were calculated from the adjusted coarse and fine fractions. Particles were classified according to the Friedman & Sanders classes (McManus, 1988)

4.2.5. Chronologic framework

4.2.5.1. Radiocarbon dates

Organic sediment and/or charcoal fragments were sampled for radiocarbon dating. Samples were extracted from the different facies of the sedimentary sections with clean blades to avoid contamination, covered with thick foil and put into plastic bags and transported to the laboratory of Community Ecology (UNAM), where they were oven dried at 110° C and packed again. Samples were transported to the UK and kept sealed in a cold room at 4 ° C until shipped to Beta Analytic facilities where dating was performed.

4.2.5.2. Tephrocrhonology

In the sedimentary sections CAN, SLT, SJII and TFR a volcanic ash layer was found. This promised to be an alternative source of numeric chronology from an independent method; thermoluminiscence. However, as this technique requires the presence of sanidine crystals of at least 200 μm and because no minerals of this size could be found in the tephras sampled, thermoluminescence could not be applied. In an attempt to constrain ages of the deposition of these ashes, a revision in the literature was carried out, focusing on the dated eruptive events of the closest volcanoes. Grain size distribution of the ashes by laser diffraction was carried out to obtain a first characterisation. A provisional correlation of the

tephras was put forward after radiocarbon dates from overlain and overlaid strata were obtained.

4.2.6. Other environmental proxies

On the14[th] of March 2008, a mammal fossil was found as part of the field explorations of this research in the previously described and sampled sedimentary section BIS. The discovery was immediately reported to the local authorities and the National Institute of Anthropology and History (INAH), according to Mexican law. In coordination with Dr. Joaquin Arroyo-Cabrales (INAH), the exposed bones were stabilised and, after the corresponding permits had been issued, they were transported to the laboratory of Archaeozoology-INAH in Mexico City for identification by Dr. Arroyo-Cabrales. A new *in situ* sample for radiocarbon dating was taken from the sediment in which the fossil was preserved and treated as described above.

CHAPTER V

RESULTS

5.1. Introduction

The results of this investigation are presented in this Chapter. The main products relating to the geological aspect appear in Section 5.2. Sections 5.3 and 5.4 include the characterisation of the geomorphology and stratigraphic sections respectively. The most relevant information is presented in this chapter while the complete set of data can be found in the Appendices.

5.2. Geologic evolution of the San Juan Raya Basin

Previous investigations into the geology of the SJRB did not analyse the tectonic controls of its geomorphology because data on regional tectonics was not yet available. According to the hypothesis outlined in Section 3.3.1, if the SJRB was not formed during the late Cretaceous to middle Miocene E-W extensional tectonism that affected the region, the topographic relationships between the geologic units outcropping in the basin would show an alignment different to the regional pattern. Under the same hypothesis, continental basin-type rocks of Tertiary age would be absent. A number of cartographic products that describe the relief and superficial geology of the basin are presented below with the aim of testing this working hypothesis.

5.2.1. Digital Elevation Model

The first approach to the geometry of the SJRB is through the visual representation of the system. The DEM (Fig.5.2.1) shows the internal heterogeneity of the geological and geomorphological structures, their geometry and relative positions. The north half of the SJRB corresponds to the mountain front of the locally named Sierra de Zapotitlan. This area of highlands was
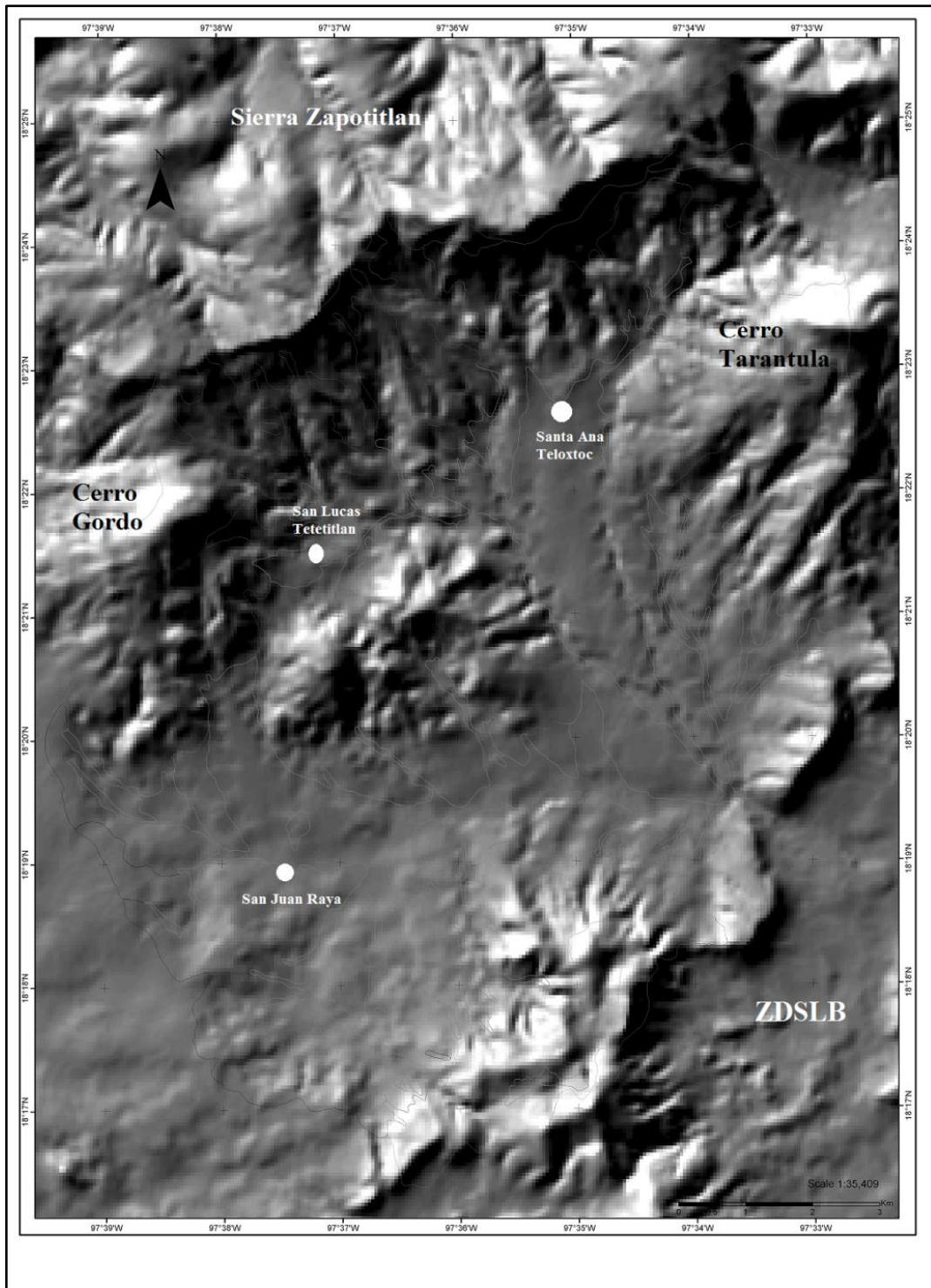
Figure 5.2.1. Digital elevation model of the SJRB.

formed by post late Cretaceous shortening and lifting (See section 2.3.2.1) and

shows a series of abrupt changes in the topography. In the area of the SJRB

the Sierra Zapotitlan is represented by a nearly vertical scarp, which limits the

basin wash. From north to south, four contrasting landforms can be

distinguished: the upper highlands of the Zapotitlan range, the fault scarps, the steeped slopes and the low valley section. The south shows a valley area, both in the SJRB and the adjacent ZDSLB. In the central portion the SJRB and ZDSLB are separated by structural isolated blocks and by a group of highlands to the south-centre. These highlands show abrupt scarps and a NE-SW alignment. Notoriously, the southwest limit of the SJRB is diffused at the scale presented in the DEM. This limit is given by a fracture on the plateau which extends towards the southwest (Fig. 5.2.1).

5.2.2. Hypsographic Model

The generalisation by iso-lines of similar altitude gave rise to the hypsographic image of the SJRB (Fig. 5.2.2), which highlights the internal altitudinal gradient, ranging from 1600 to 2780 masl and the asymmetry of the elevations. The north section of the basin is represented by the highest local structures CV and CSM (Figs. 4.1.3 and 5.2.2), which at some parts coincide with the water divide. The inclination of north and south slopes of these highlands are strongly contrasting, descending gently to the northwest and abruptly towards the basin because of the nearly vertical scarp that delineates the basin border (Fig. 5.2.1, 5.2.2). Other areas of approximately the same altitude (above 2,500 masl) are the conical CT and CGo mountains bordering the basin to the northeast and northwest (Fig. 4.1.3). The CC, COm and COt are the highest elevations in the south and despite being considerably lower than the northern highlands, their slopes have a similar pattern, gently tilting towards the northwest and abruptly falling to the southeast face. The steep slopes of the north mountain front and the gentler hills of the south, east and west mountains dominate the middle altitudes of the basin. The central portion seems topographically more

homogeneous. Deposits from the highlands, including alluvial fans and terraces, form the valley level at the lowest elevations. The valley is divided into two sections by the CGa, CM and CS (Fig. 4.1.3), which merge at the eastern margin of the basin. Deposits forming the valley floor show a very gentle and constant slope towards the basin outlet to the east. It is noticeable that the western limit of the basin forms a nearly topographic continuum with the adjacent basin, whose slope tilts gradually towards the southwest.
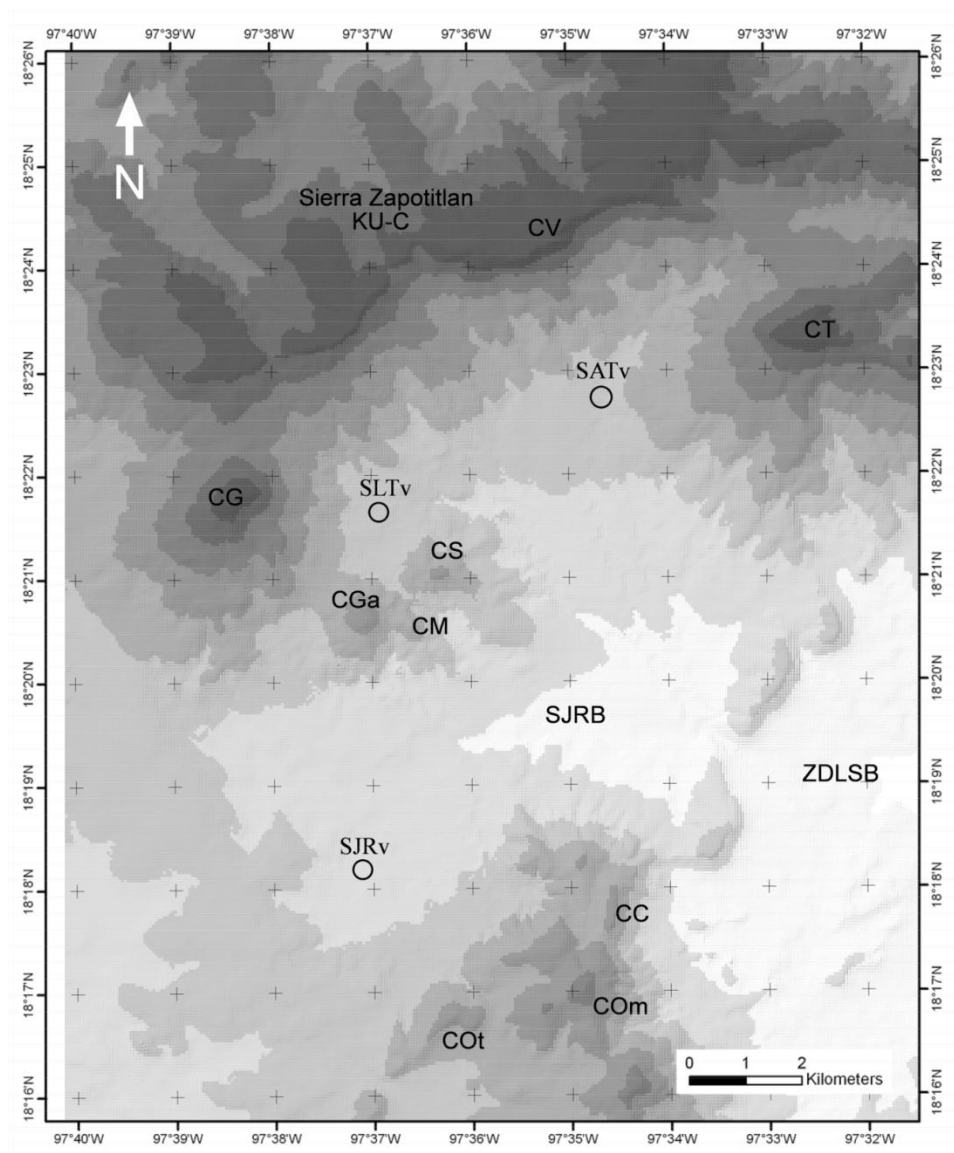
Figure 5.2.2. Hypsographic model of the SJRB. The isopatches represent generalisations of 100 metres. Labelled highlands: CC: Cerro Campanario; CV: Cerro Viejo; CT: Cerro Tarantula; CGo: Cerro Gordo; COm: Cerro Ometepec; COt: Cerro el Otate; CGa: Cerro Garambullo; CM: Cerro Mezquite; CS: Cerro Salado.

5.2.3. Geology

In previous maps the area of SJRB was almost entirely drawn as part of the Kl-S (Figs. 2.5 & 2.7) (Mauvois, 1977; Butrón & Barceló-Duarte, 1980). However, the detailed map presented here (see SJR-Geology map in Appendix A1) shows that other lithologies form an important proportion of the total area. Most of them correspond to Cretaceous formation and no Tertiary sedimentary rocks were found after extensive field exploration. The stratigraphic record of the basin covers from the lower Precambrian through the late Holocene, while the Tertiary depositional hiatus was corroborated. During the field explorations for this study, a small outcrop of schist, which this research has apportioned to the Acatlan complex, was found directly overlain by lower Cretaceous rocks. This schist outcrop was smaller than two metres in diameter, not big enough to be mapped. However, it was included in the local stratigraphy considering that the SJRB is part of the Mixteco terrain whose basal metamorphic rocks are grouped in the Acatlan complex. The oldest mappable strata are the Agua del Burro limestones, which are members of the Kl-Z. These compact rocks of marine origin border the west and south parts of the SJRB and according to Buitrón and Barceló-Duarte (1980) can reach up to 200 metres in thickness. In the field these rocks were observed as grey calcareous limestone with abundant calcite filaments. The Kl-Z is covered conformably by the Kl-S of Aptian age, which includes greenish mudstone, very fine-grained sandstone and coquina. The limestones and siltstones (lutite) of the Kl-S and Kl-Z are clearly folded and fractured (Fig. 5.2.3), covering most of the basin area and are found mainly in its central part (SJR-Geology map-Appendix A1). The Kl-Z and Kl-S are discordantly overlain by up to 600 metres of compact calcareous limestone, which can be observed to the north, west and east limits of the basin forming

the westward continuation of the Zapotitlan range. This formation of marine origin was first named as Cipiapa Formation (González-Arreola, 1974; Buitrón & Barceló-Duarte, 1980), but later mapped as "undifferentiated upper Cretaceous" limestone by Dávalos-Álvarez (2006). Given that the former author does not explain the reasons for re-naming this formation and because no radiometric data on its age have been reported, the name Cipiapa is respected here. No sedimentary strata could be identified, or have been reported, covering this formation in the region. In fact, the Cipiapa rocks represent the last sedimentary record of consolidated strata since the end of the Cretaceous and imply a depositional hiatus until the Quaternary. The northwest border of the basin shows breccia rocks containing coarse and angular clasts of the Ku-C and are interpreted as colluvial deposits of unknown age. These rocks do not correspond to depositional basin environments of valley type. The only post Cretaceous rocks in the locality are a series of small igneous structures at the south limit of the basin, intruding the Agua del Burro rocks. The age of these outcrops has not been accurately determined. Buitrón and Barceló-Duarte (1980) map these units and give them a Tertiary age. However, the igneous activity in the SMS migrated northwards during the Cenozoic and according to Morán-Zenteno *et al.* (1999) the region in which SJRB is located was affected by magmatism during the Oligocene to early Miocene. Another characteristic of this magmatism is that it was andesitic and basaltic (Ferrusquilla-Villafranca, 1976; Morán-Zenteno *et al.*, 1999), coinciding with the nature of the igneous outcrops in the SJRB. An Oligocene-early Miocene age is thus proposed for these outcrops as a result of this research. Other similar outcrops of basalt and basaltic andesite were reported in Zapotitlan Palmas (97º 48' 29'' -17º 53' 23'')

71

and Huajuapan de León (97º 41' 46'' – 18º 04' 51'') of 31+/- 1 Myr (Morán-Zenteno *et al.*, 1999), which also fit in with this tentative age. At the upper part of the stratigraphic column and covering a significant area of the floor of the SJRB, we found a series of Quaternary unconsolidated deposits. The distribution of these deposits can be divided into northeast and southwest main sections, and although they are widely distributed at the lower levels of the basin, some deposits can be found near the upper basin limit. The earliest age obtained from the Quaternary strata of the SJRB was 28,550 ± 200 ^{14}C yr BP and came from a sedimentary section named BIS (Section 5.4.2). As will be detailed in Section 5.3, the Quaternary stratigraphic sections studied here are located in the southwest. Because of the lack of radiocarbon dating, the stratigraphic relationship of the sedimentary units from the northeast portion was based on relative spatial positions and was possible only for the oldest units.

Figure 5.2.3. Siltstone (lutite) exposed along Barranca Grande. The axial folding plane is oriented north-south. Bottom line is one metre.

5.2.4. Structural Geology

The major regional structures are the blocks and fault contacts that separate them (Section 2.3). These faults have had normal activity during the Cenozoic, regulating the opening of the basins of this part of the SMS and controlling the main geomety. However, the fault system of the SJRB (Fig. 5.2.4) does not match with the regional fault NW-SE. On the basis of the faults and the relative position of the rocks of the SJRB a series of structural blocks have been inferred (Fig. 5.2.4.1). Under this new model the basin is composed of half graben blocks with a general tilting towards the southeast and perpendicular to the fault plane. The axial planes of the synclines and anticlines are northwest to southeast trending, indicating a west-southwest compression (see section 2.3.2), while the rupture of the structural blocks is along the main faults. The north, west, south and southwest limits of the basin are defined by fault scarps that almost invariably take the shape of vertical walls. The north scarp is apparently the continuation of a fault along the upper south facing mountain front of the Zapotitlan range (Fig. 5.2.4), up to the proximities of Tehuacan City. This fault was not mapped in previous works. The southwest facing scarps also represent a segment of an extended northeast to southwest oriented fault. The scarp that borders the southwest marks a rupture of the plateau of the adjacent basin and probably the lowering of the southwest segment of the SJRB as a result of normal faulting. Crossing the valley floor, another major fault divides the basin in north and south asymmetric fractions (Fig. 5.2.4). Although observed slicken sides are evidence of its activity (Fig. 5.2.4.2), it was not possible to determine the relative displacement of the blocks in contact because this part of the basin is mostly covered by alluvial sediments. In the structural
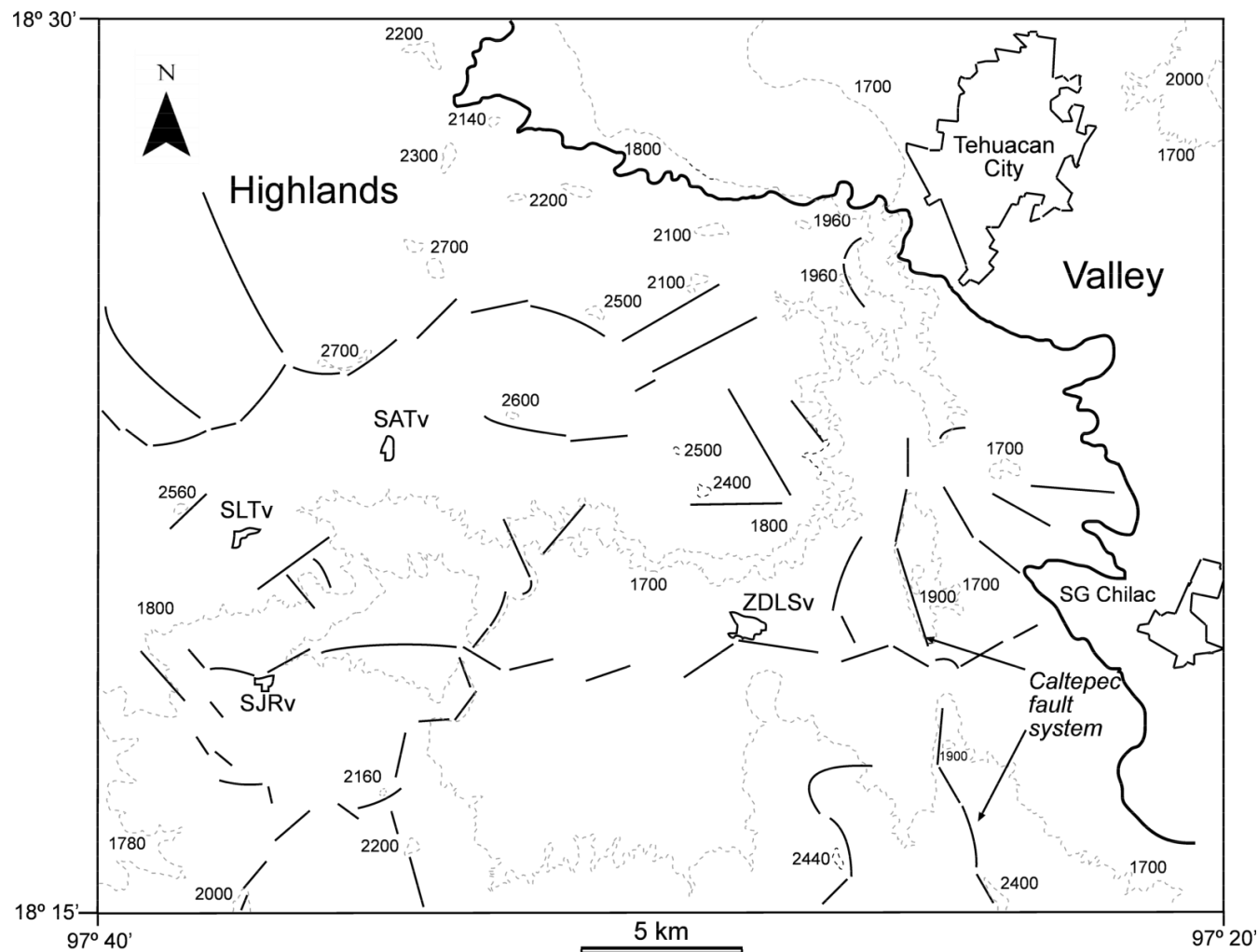
Figure 5.2.4. Fault pattern across the SJRB and ZDLSB. Note the NE-SW trend of the faults of the SJRB. Polygons indicate the main localities (see text for definitions). Altitude values (masl) are indicated next to the contour intervals (dotted lines).
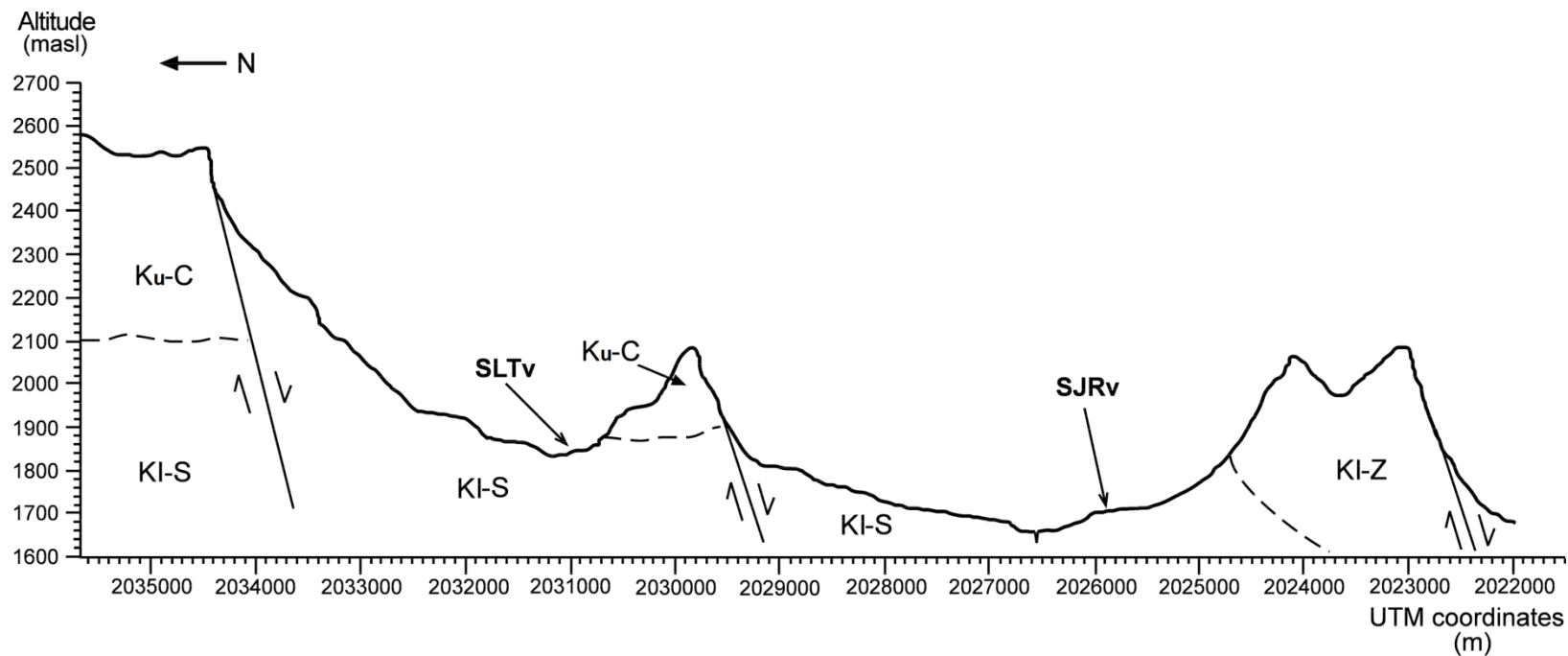
Figure. 5.2.4.1. Topographic N-S cross section of the SJRB showing the main inferred structures. Kl-S: Lower Cretaceous San Juan Raya Formatio; Kl-Z: Lower Cretaceous Zapotitlan Formation; Ku-C: Undifferentiated upper Cretaceous Cipiapa Formation outcropping as Cerro Garambullo in the central part of the basin. The profile corresponds to the topographic cross section showed in Figure 5.3.1.

Figure 5.2.4.2. Slicken side on the surface of a coquina on the river bed of BAI. Hammer for scale.

model presented in Figure 5.2.4.1, this fault is the contact where the southern structural block deepens. The normal faulting behaviour of the north fault is proposed on the basis of the downwards displacement of the central highlands (CGa, CM and CS), which constitute tectonic klippes located in the central part of the basin. The upper part of these highlands is limestone of the Ku-C, which according to Mauvois (1977), has a maximum thickness of 600 metres. As can be observed in Figure 5.2.4.1, the Ku-C klippes (highlands CG, CM & CS) show a negative vertical displacement with respect to the north highlands. The fault cutting these central highlands also shows a northeast to southwest trend and the rocks to its north flank deepen perpendicularly to this direction. It must be stressed that this model is based on published surface geological maps complemented with field observations and mapping derived from this work and that further seismic and/or gravity studies are necessary to provide detailed data on the subsurface structures (blocks and faults) to test this model.

5.2.5. Summary and key findings-Geological evolution of the SJRB

Viewed in the context of the surrounding highlands, the SJRB is a depression formed at the edge between the Balsas and Papaloapa basins. It is also part of a structural system that extends up to the proximities of the Tehuacan basin, connected by an east to west fault. Early Cretaceous lutite and sandstones of the KI-S are the main rocks outcropping in the basin, although other marine calcareous rocks of early and late Cretaceous can be found in the perimeter. After the folding and lifting of the Mesozoic rocks, no Tertiary sedimentary rocks were preserved in the area, confirming the Cretaceous-Quaternary hiatus. Late Quaternary sediments filled the valley bottom. The geometry of the basin is clearly asymmetric and defined by a series of faults of east-northeast and east orientations which also affect other structures of the ZDLSB. These faults seem to have had a normal behaviour and are interpreted as responsible for the tectonic opening of the basin as demonstrated by the klippes at the centre of the basin. The opening pattern of the SJRB does not coincide with the Palaeogene east-west opening of other SMS basins (caused by NW-SE), which leads to suggesting a Neogene age for the SJRB under a normal faults system that gave rise to a half graben system.

5.3. Geomorphic processes

As outlined in section 3.3.2., considering the tectonic evolution of the SJRB and the climate changes that occurred during the late Quaternary, the depositional landforms of the system may reflect some of those important changes. In order to understand the role of the different geomorphic processes that occurred during this period of the evolution of the basin, the geomorphology is described and analysed here.

5.3.1. Topography

In order to study the depositional landforms it is necessary to consider the topography because the elevation and slope of the sediment sources determine the initial potential energy for transportation. As mentioned in the previous section, the landscape of the SJRB is a product of different processes. The formation of the highlands is related to the SMS orogeny, while recent tectonism produced fault-related landforms like scarps and changes in base level (Section 5.2). The basin shows a topographic gradient of more than 1000 metres (Fig. 5.3.1) and clear asymmetry regarding the elevations. The northern portion is characterised by the highest elevations of up to >2,700 masl, while the south summits are nearly 500 metres below the north upper limit. The southwest border is defined by the fracture of a plateau that extends westwards into the San Sebastian Frontera basin (SSFB), which has a very gentle slope tilting towards its internal part (Fig. 5.3.1). The area below the 1,800 m topographic line covers most of the basin surface. The basin floor shows a gentle slope that maintains a constant rate and extends eastwards up to the outlet of the ZDLSB. Notably, the SJRB outlet is a very narrow discontinuity of the Kl-Z east highlands, forming a "bottleneck" (Fig. 5.3.1).

5.3.2. Hydrography

A number of distinctions can be made by observing the fluvial network. Perhaps the most obvious one is that the drainage pattern of the SJRB is divided into a northeast and a southwest sub-basin of similar area (Fig. 5.3.2.). The fluvial pattern in both sub-systems is also heterogeneous, reflecting the local differences in landforms and processes. Another distinction can be drawn between structurally defined rivers which follow the rock deformations in the hill slopes and the streams that dissect the unconsolidated depositional landforms.
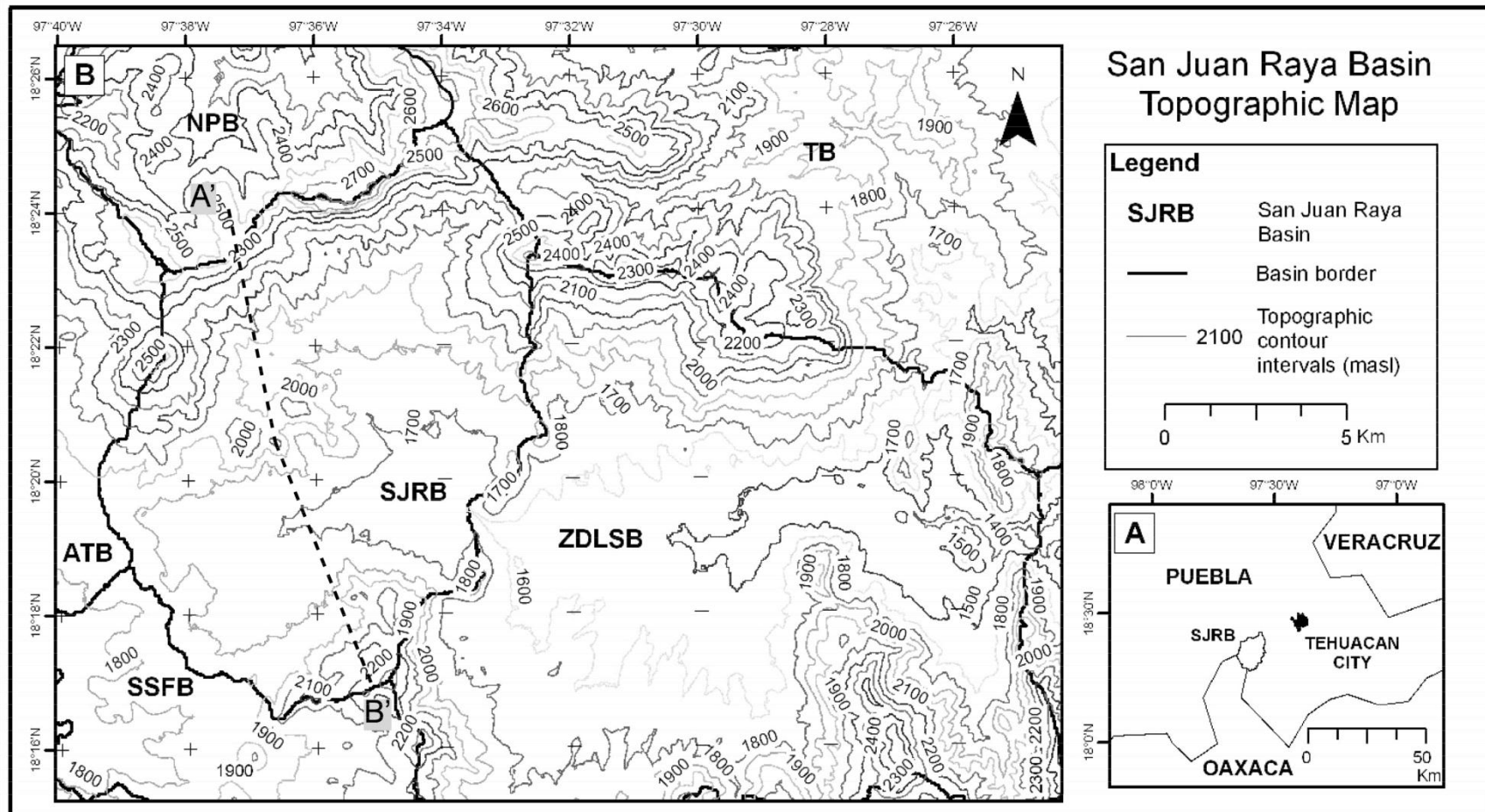
Figure 5.3.1. Simplified topography map of the SJRB showing surrounding basins: ATB: Atexcal Basin; NPB: Nopala Basin; SSFB: San Sebastian Frontera Basin; TB: Tehuacan Basin; ZDSLB: Zapotitlan de las Salinas Basin. The A'-B' transect corresponds to the structural model in Figure 5.2.4.1.

The first type is clear in the north and south highlands of the basin and will be described here, while the second group, a feature of the lowland sedimentary forms will be treated in section 5.3.3.

The northernmost scarp wall guides a series of nearly parallel rivers that drain down the basin and connect with other second order washes to form a dendritic pattern. This type of spatial arrangement is commonly governed by bedrock layers that respond similarly to erosive forces (Howard, 1967; Schumm *et al.*, 2000), which in the present case are the Ku-C calcareous limestones and Kl-S lutite. These dendritic washes, however, do not extend below the 1800 masl topographic level. From there downwards, the 3rd order main intermittent rivers adopt a parallel and less branched pattern, reflecting the elongated nature of the alluvial landforms they cut.

With regards to the southwest sub-basin, the only portion that shows a dense dendritic behaviour is the small network to the southwest limit, which corresponds to gentle slopes of the San Juan Raya sandstone. Some of the rivers in the west part of the sub-basin change direction, forming right angles. This behaviour has been associated with fault and/or joints that regulate the course (Howard, 1967; Schumm *et al.*, 2000), as observed in the tilted block located between 18°18'-18°19' and 97°38'-97°39', in which the wash runs following the main fracture. The slopes of the northern and southern halves of this sub-basin determine the approximate dendritic river pattern, which adopts this form and shows a reduced network density as it reaches the lower valley levels. The river dissections in the upper parts of the basin show a higher density compared with the lowlands. Some of the landforms near the basin floor are not cut by rivers. It is important to highlight that under the current semi-arid
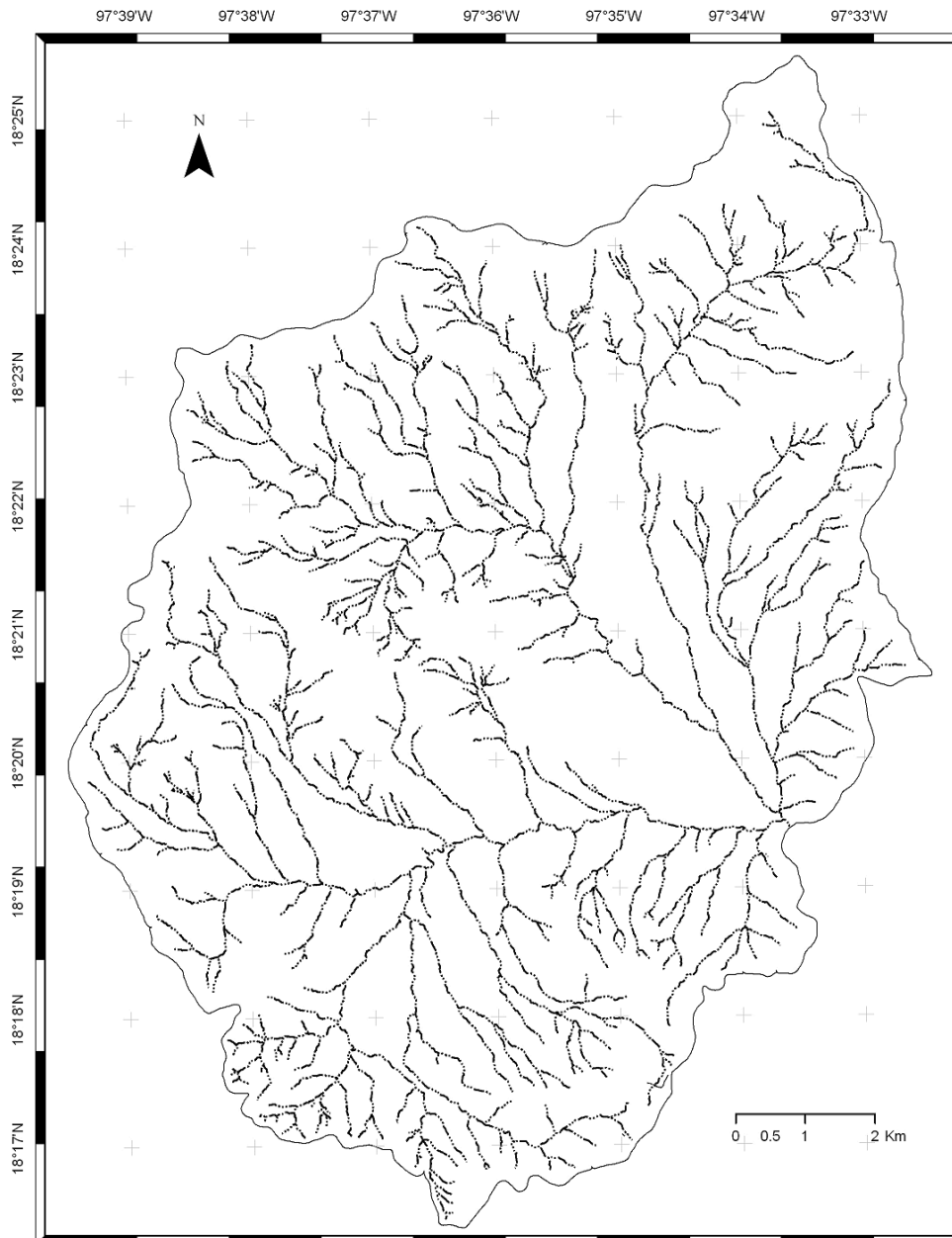
Figure 5.3.2. Hydrographic network of the SJRB.

climate the rivers are intermittent and rains episodic and of high intensity (pers.
obs.), causing important erosion of the unconsolidated surfaces.

5.3.3. Alluvial geomorphology and morpho-chronology

As reviewed in Section 5.2, the geometric arrangement of the structural blocks
of the SJRB suggests a tectonic origin, defining the basin shape, topography
and fluvial network. The SJRB summits and slopes of the limestone highlands
mark the boundaries of the geomorphic system, form the primary source of

81

sediment yield and provide the potential energy that gives rise to the depositional landforms observed in the lower parts of the basin (see SJR-Geomorphology map in Appendix A2). The previously mentioned asymmetry of the basin is also reflected in the sedimentary landforms, as can be seen in the geomorphologic map. Two prominent alluvial fans can be observed at both sub basins. The origin of the extended fans is invariably sediment from the south-facing slope of the north highlands; while the alluvial deposits of south provenance are limited to smaller fluvial terraces distributed along the fluvial network. These fans and other alluvial terraces represent generations whose relative age was determined on the basis of their comparative positions and surface characteristics. QaI surfaces correspond to the Pleistocene alluvial fans, QaII to a latest Pleistocene phases of alluvia re-activation, and finally QaIII defines a discrete alluvial fan formed during the Holocene. The most important geomorphic processes are related to erosion and sedimentation, while palaeosols are scarce. Notably, the south facing slope of the basin, and in general the north sub-basin, is characterised by extensive areas of badlands (Fig. 5.3.3).

5.3.3.1. QaI surfaces-Pleistocene

Surfaces QaI are alluvial fans that occupy a higher terrace level than the younger deposits (Geomorphology map-Appendix A), and extend longitudinally for more than 2 km and up to 1 km laterally. The surface of these fans is capped by a highly indurated calcrete that encloses poorly sorted, sub-angular to rounded clasts, supported by a finer matrix. Most of these clasts are limestone of the Ku-C, confirming that the north highlands are the source of this material (Fig. 5.3.3.1). The depth of the central part of the major fans (east and west) are

82
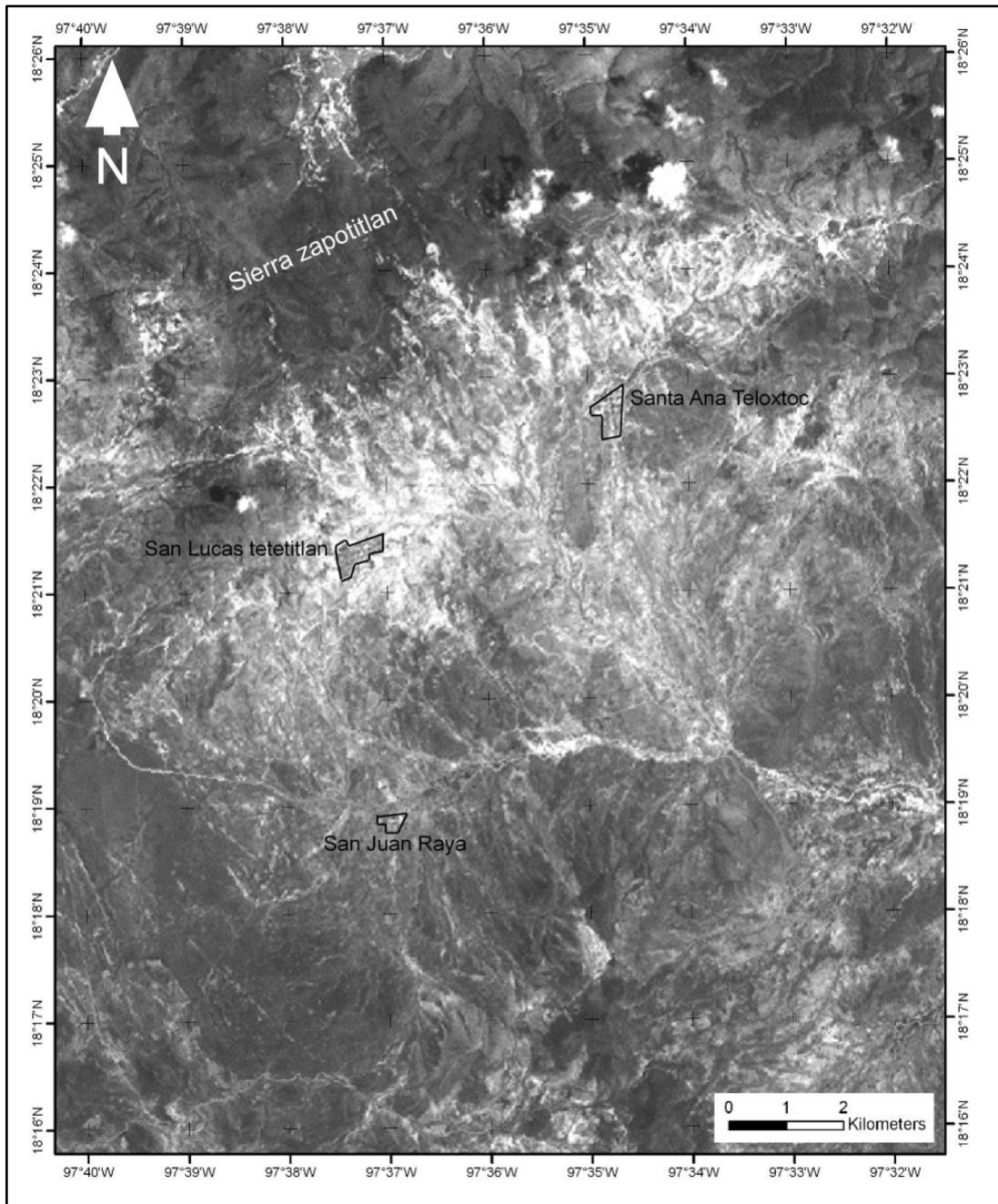
Figure 5.3.3. Landsat image of the SJRB. Areas of high reflectance in the north sector of the SJRB correspond to badlands.

estimated in more than 30 metres based on the presence of Mezquite (*Prosopis laevigata.*) (Fig. 5.3.3.2). These phreatophitic trees require very deep substrate to sustain their root system, which can reach up to 40 m (Pavon & Briones, 2001). Stratigraphic sections of these fans visualised at different parts along the river cuts show a series of alluvial deposits of different textures, colours and structures, alternated with redish palaeosols. Although a number of suitable
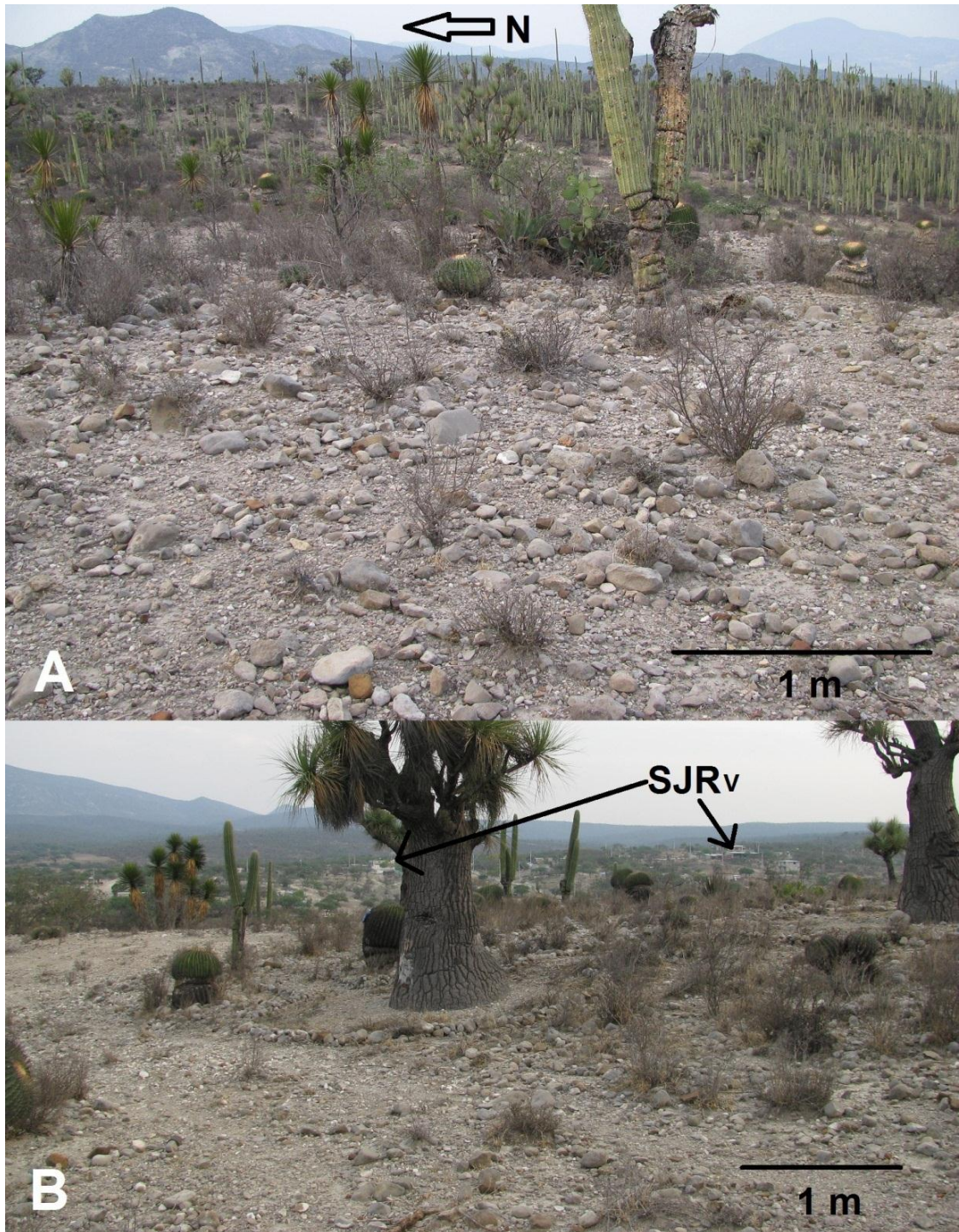
Figure 5.3.3.1. A: Northeast view on the distal-most fan Qal, north of SJRv. Top calcrete has been removed here exposing alluvial fan material, mostly composed of rounded calcareous limestone clasts from the Ku-C north highlands. Calcrete fragments can be observed. Background highlands are CT (upper right) and CM (upper left). B: South view from the same point as A. Note the lobe slope of the distal alluvial fan. SJRv at the middle background.
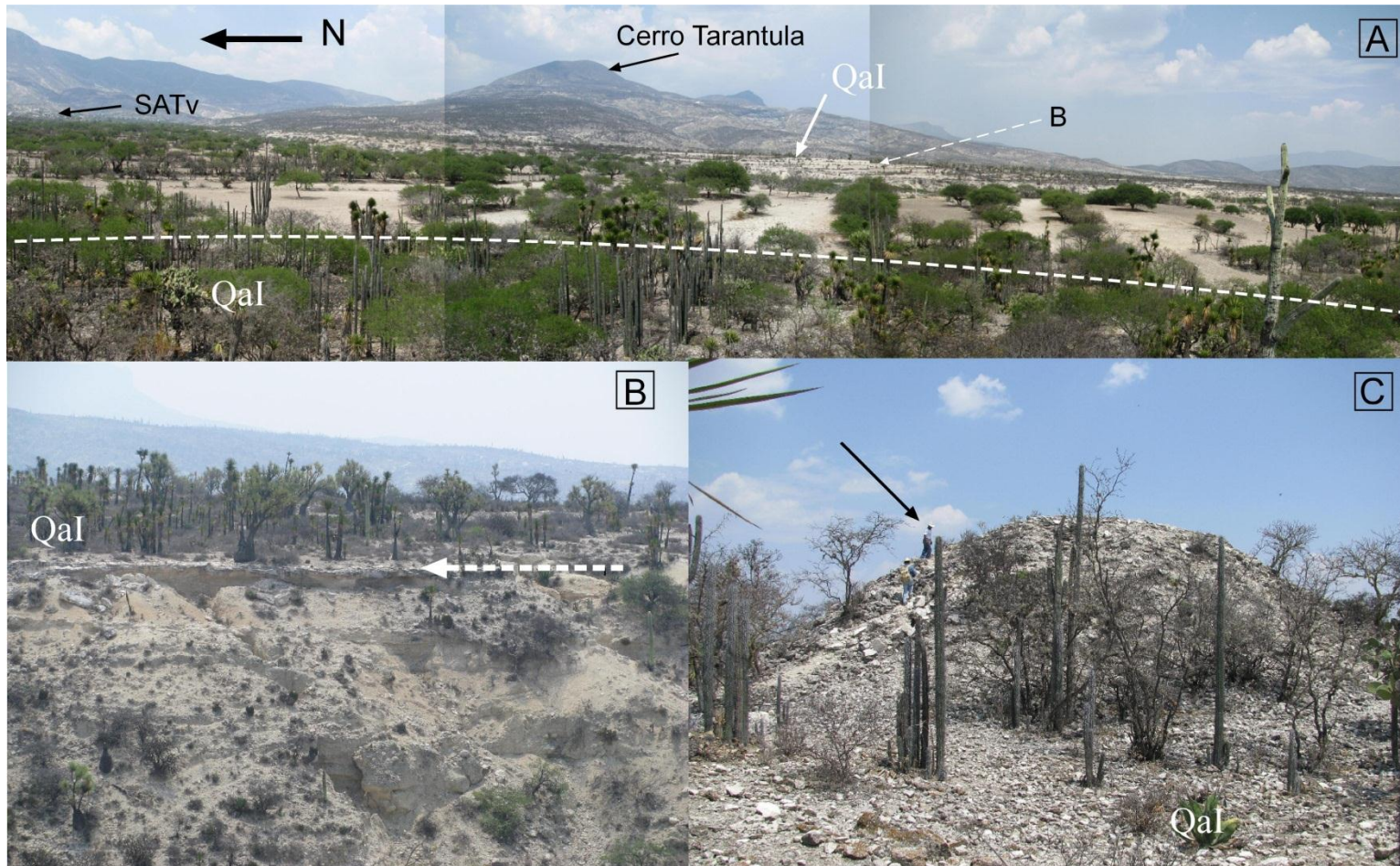
Figure 5.3.3.2. A: Panoramic east view of the QaI alluvial fan to the east of the SJRB. Dotted line indicates the approximate border of the remnant surface where calcrete is preserved. Mezquite trees are established where calcrete has been removed. Dashed arrow indicates location of image B. B: Eastern section of the dissected QaI shown in A. Dashed arrow points out the calcrete layer. C: Pre-Columbian dome (of possible ceremonial use built from calcrete crust fragments from QaI) from which panoramic photos of A were taken. Person pointed out for scale in C.

sections for study were identified, time and logistical limitations did not allow for the description and sampling of the sedimentary layers. These stratigraphic sections should be studied in detail in the future because they pre-date the oldest QaII alluvial deposits, maintaining sedimentary records before 28 kyr (Table 5.4.12). On top of these extensive fans the calcrete has been removed from considerable areas near the borders leaving uncovered layers exposed to intensive erosion and re-working. These exhumed surfaces have been labelled as QaI but their lateral contacts with more recent alluvial fans (QaII) were not always clear because of the erosion. Although QaI are considered the oldest fan generation, no numerical dates were obtained as part of this study because permission to access their sedimentary sections was issued by the local authorities only at the end of the last field season. The interpretations presented here are then based on the remote geomorphological survey and field observations.

5.3.3.2. QaII surfaces-Pleistocene-Holocene

Surfaces QaII are less spatially distributed forming a lower terrace level bordering the QaI surfaces (SJR-Geomorphology map-Appendix A2). These alluvial deposits take the shape of terraces along the fluvial network and isolated fans of smaller dimensions than the QaI units. The QaII terraces bordering the QaI are in general formed of finer sediment and in profile view show alternated alluvial and fluvial deposits and buried soils (See Section 5.4 for details). Following the terraces upstream the layering and textural characteristics are uniform, contrasting with the increase in the proportion of coarse material, upstream in QaI fans. Notoriously, alluvial terraces have not been exclusively formed at the valley bottom in the south part of the basin. In

fact, at the east and south, close to the highlands and basin water divide, it is possible to observe this type of landform. The fact that these alluvial deposits are confined to the upper parts of the basin, in topographic sections which normally act as the source or transit of sediments, suggests that the mobility of the sediment was constrained, perhaps due to low energy flows and the predominance of filling the basin. Given that terraces QaII are not covered by calcrete, in some parts they have been used for agriculture and their surface characteristics have been modified. A detailed characterisation of the sedimentary and edaphic facies of a number of profiles of different QaII landforms will be presented in section 5.4. The presence of charcoal and organic sediments in those sedimentary sections allowed the age of the terraces in which they formed to be determined. A basal age of 28,550 ± 200 ^{14}C yr BP in section BIS constrains the QaI fans to late Pleistocene. The minimum age of 1,660 ± 40 ^{14}C yr BP came from section PV and indicates a late Holocene deposition of QaII.

Other QaII terraces have formed along the channels of the west and east highlands, covering small depressions in some parts of these mountains. Some of the channel terraces were followed upstream and they show a consistent pattern of dominance of fine-grained alluvial beds alternated with some medium-poorly sorted ones. Although numerical dates were not acquired from these deposits, lateral continuity with QaII, similar sedimentological characteristics to QaII profiles, and the sporadic presence of pre-Columbian pottery indicates a Holocene age. On the basis of these observations those deposits were correlated and labelled as QaII.

5.3.3.2. QaIII surfaces-Holocene

A single alluvial fan located at the central part of the basin was classified as QaIII (Appendix A2; Fig. 5.3.3.3). The QaIII occupies a lower terrace level bordering an upper alluvial remnant composed of limestone of the tectonic klippes of the Cipiapa rocks. Downslope the QaIII takes a radial fan shape with a gentle tilt to the southeast. Its longitudinal extension is constrained by the sandstone slope of the south mountain front. The lithology of the QaIII fan is composed entirely of siltstones (lutite) because its provenance is the badlands between Cerro Mezquite and Cerro Salado, which are limestone of the KI-S. In the field, triangular facets were clearly observed at the contact between these rock formations indicating a tectonic fault (Figs. 5.3.3.4). This faulting cuts through an older alluvial terrace composed of clast from the Cipiapa dolomite. This can be observed near the apex of the QaIII (Fig. 5.3.3.4). The QaIII fan shows the typical pattern of decreasing clast grain size with increase distance from the source. This can be observed along the west channel incision as a transition from poorly sorted angular to sub-angular gravels up-fan to a braided pattern, massive structureless facies in the middle section, and very fine and structureless strata at the most distal part. As shown in Figure 5.4.8.2 (Section 5.4.8), three phases of incision of the valley floor are identified from this fan. A tectonic activation of the faults surrounding the QaIII and subsidence of a central small block and incision of the previous floodplain deposits occurred before 9 kyr is inferred by the earliest date of TPX. Another incision is observed before 3,680 ± 40 ^{14}C yr BP, while the end of the fan aggradation dates back to 2,300 ± 40 ^{14}C yr BP, pre-dating the modern incision of the valley floor (Fig. 5.4.8.2-Section 5.4.8). A fault trace runs parallel to QaIII and is clearly exposed at its distal part.
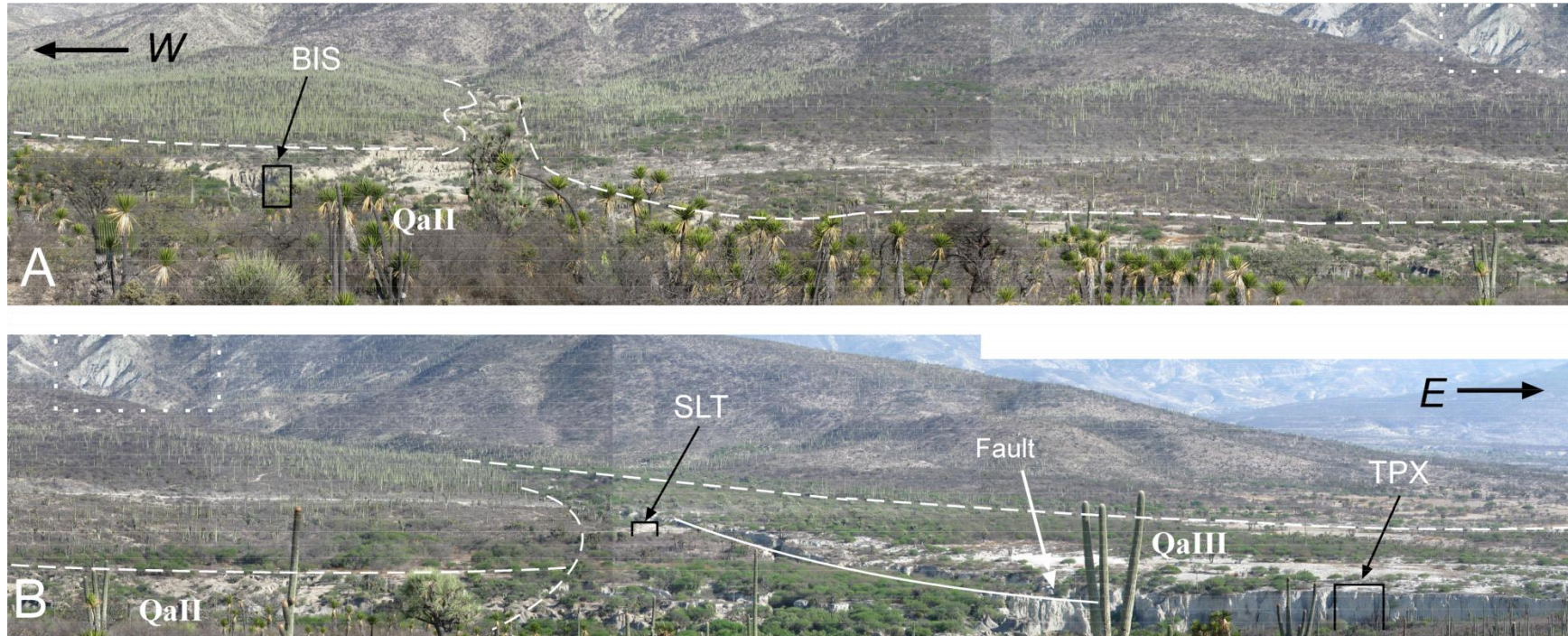
Figure 5.3.3.3. Panoramic view of the central part of the SJRB showing the central highlands and QaII (A) and QaIII (B) alluvial landforms. Location of BIS, SLT and TPX sections are indicated. The dotted square in A and B corresponds to the triangular facets of Figure 5.3.3.4. Note the A and B overlap. TPX is cut by the BAI intermittent river. The white arrow points out the approximate fault plane. Substrate nature can be identified by vegetation cover. Background siltstone and dolomite with shallow soil mantle support a *Neobuxbaumia mezcalaensis* forest; intensively eroded soil on sandstone are colonised by a thorn scrub with *Yucca periculosa*, *Beaucarnea gracilis*, *Mimmosa sp.* and *N. macrocephala* (foreground). The deep flood plains host a patchy mesquite forest (*Prosopis laevigata*).
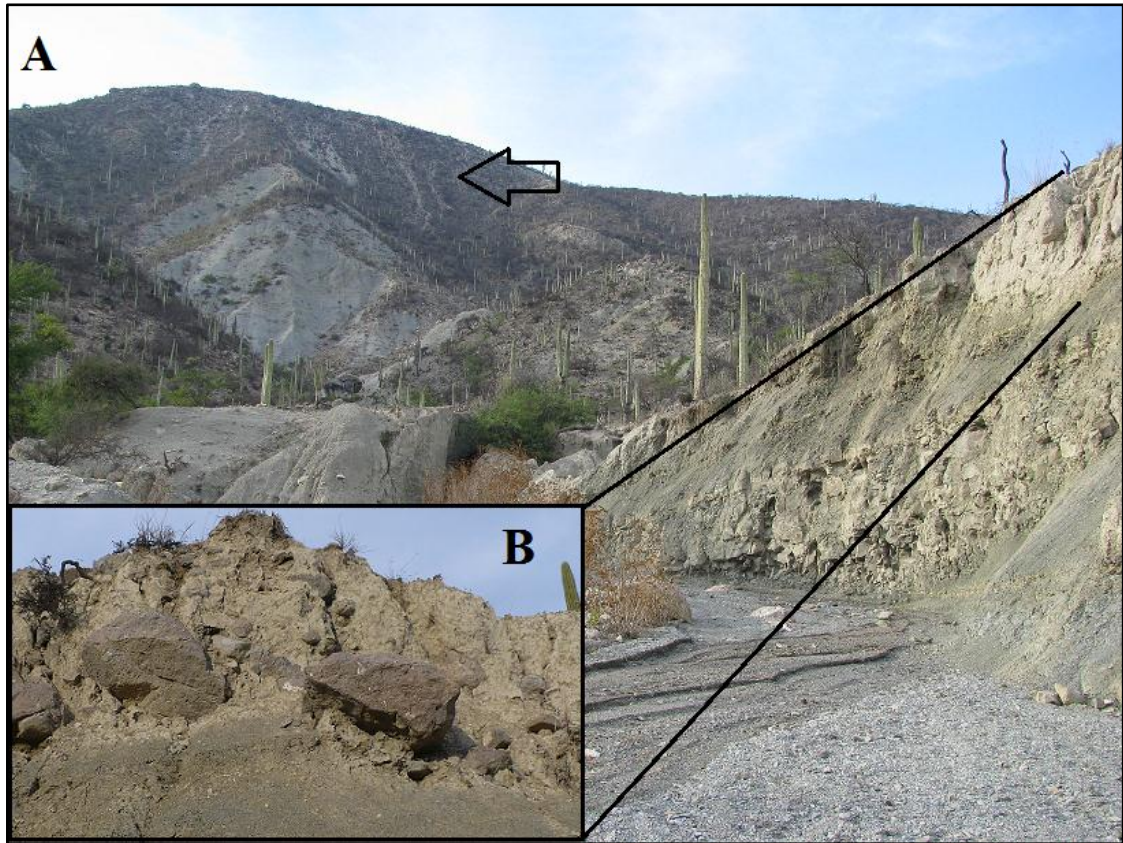
Figure 5.3.3.4. A: North view of the fault contact between lutite (Kl-S) and dolomite (Ku-C) at the source of QalII. The open arrow indicates the fault plane. Photo taken at a proximal location in the alluvial fan QalII. B: Older terrace remnant (probably contemporaneous with QaI) containing boulders of Cipiapa dolomite incrusted in a matrix of lutite.

5.3.3.3. Modern fluvial processes

As mentioned in section 5.3.2, the river system has two components. One comprises the structural washes that follow the pattern of blocks, joints and faults in the highlands; and the other is defined by rivers which cut through the alluvial deposits. In particular, the alluvial channels of the basin floor cut different fans and terraces, along which most of the sedimentary sections were studied (section 5.4). The ground morphology of these rivers shows primarily a tectonic origin. These rivers show a meandering pattern, carrying a mixed load and forming bars at the bend points, which is characteristic of medium to high energy streams (Schumm *et al.*, 2000). This behaviour has been confirmed in the field during summer rain episodes.

5.3.4. Summary and key findings-Geomorphic processes

The SJRB is very complex in geomorphological terms. The structural aligniation of the geological structures divides the basin into two hydrological systems, northeast and southwest. Main landforms include highlands, hill slopes and a basin floor. The north and south highlands form the water-divide and are the source of detrital material and potential energy for the Quaternary sediments that form the lowlands alluvial surfaces. Three cohorts of alluvial surfaces were identified, the oldest (QaI) being older that approximately 30 kyr, while the second (QaII) represents the latest Pleistocene until the middle Holocene. A single alluvial fan corresponds to the third episode (QaIII), formed during the late Holocene. The asymmetry and spatial distribution of the alluvial surfaces suggests that both tectonics and climate have played an important role in forming the sedimentary record. QaI and QaII are alluvial fans spatially constrained to the front of localised faulted mountains while QaII are widely distributed along the basin, suggesting a dominance of tectonic force in the first case and climatic in the second. QaI fans are extensive surfaces capped with a well-developed calcrete and were formed exclusively in the north slope with no contemporaneous surfaces from the south. This is interpreted as differential tectonic activity between the north and south highlands. More active normal faulting in the north basin border during the Pleistocene released important amounts of debris material from the Ku-C forming the QaI; while relative quiecense at the south prevented alluviation. A late Pleistocene-Holocene period of generalised basin filling involved the remotion of pre-deposited material of (QaI) and formation of the QaII alluvial terraces in a lower topographyc position. QaIII represents a very punctual and spatially defined alluvial fan made almost entirely of lutite from the central part of the basin. The

sediment forming this fan was clearly released after the tectonic activation of a focalised normal fault where the Cipiapa klippes and the KI-S join in the central part of the basin.

5.4. Depositional and palaeoenvironmental records: sedimentary sections.

The hypothesis put forward in Section 3.3.3 assumed that this continental basin developed a sedimentary record in which local palaeoenvironmental changes through the Cenozoic could be tracked. It was put forward that if the SJRB shared a tectonic history with adjacent basins, the palaeoenvironmental archives would cover the time span since post-orogeny basin opening, probably initiated at some point in the Miocene. However, after field examination of the sedimentary sections and the acquisition of numerical chronologies it became clear that such records cover only the late Quaternary. The palaeoenvironmental significance of 11 exposed sections of those records surveyed as part of this thesis is presented below. A chrono-stratigraphic sequence of the SJRB based on the main sedimentological characteristics and radiocarbon dates is presented in order to provide a sequential description of the environmental change. Figure 5.4.12 summarises the stratigraphic correlation of the 11 sedimentary sections studied.

5.4.1. Section ALB

A well-developed palaeosol has been preserved and exhumed at the lowlands of the west basin margin (Fig. 5.4.1; 643562W-2026294N). This palaeosurface occurs as an isolated outcrop, underlain by sandstone bedrock. This unit represents a period of geomorphic stability and correlates with a palaeosol of section TFR (Section 5.4.7.). The profile ALB reaches a depth of at least 80 cm and is composed of two distinctive pedogenic horizons (Bt1 and Bt2), showing
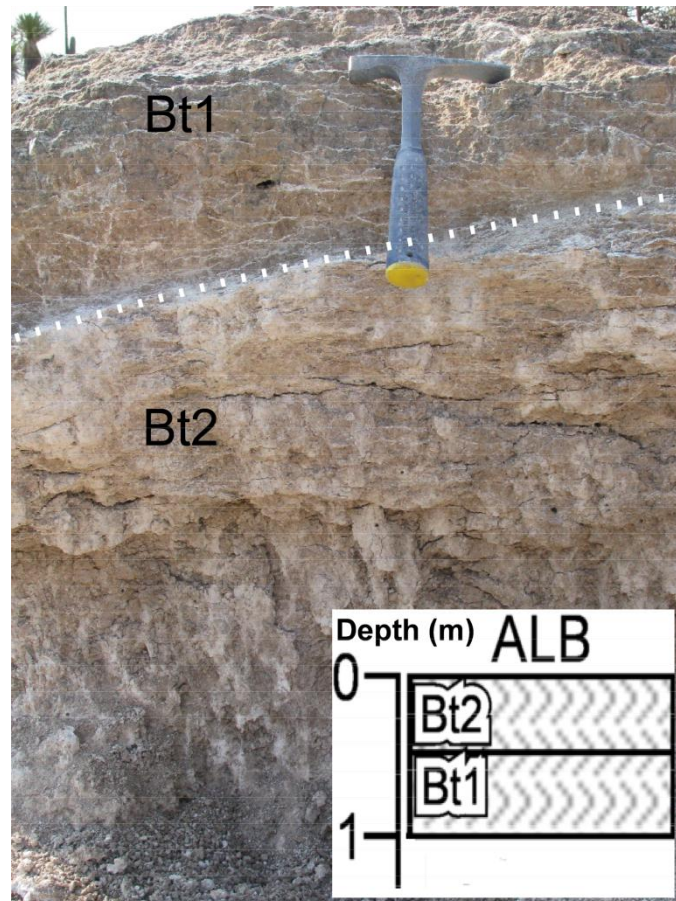
Figure 5.4.1. Sedimentary section ALB showing the different morphologies of carbonate accumulation and schematic representation of the soil profiles and depths. Codes of the graphic patterns as in Figure 5.4.14.

morphological accumulation of clay, typical of B horizons. Powder type calcrete of non-pedogenic groundwater origin can be observed along the palaeosol profile. In the Bt1 horizon, a very friable (powder-like) calcrete forms roughly horizontal sheets and coatings at the planar vertical surfaces of the blocky aggregates. At the lower part of the B horizon the powder calcrete is more concentrated. The carbonates precipitated form vertical stake-like threads at the lowermost Bt2 horizon, which has a columnar structure and a similar OM content as the horizon above (6.22 %). The presence of clay coatings were more developed in the Bt2. No radiocarbon dates were obtained from this section but a correlation was established with the top palaeosol of the sedimentary section TFR because both share the same macro-morphologic

characteristics and position in the landscape. The development of this palaeosol is considered evidence of a period of landscape stability under wetter than present conditions, considering that soil cutans observed involve illuviation of clay enhanced by water infiltration and that this process contrasts with the poor soil development under the present day arid climate. No carbonate nodules or other features of carbonate accumulation of pedogenic origin described by Gile *et al.* (1966) are observed indicating that this calcrete is related to carbonate saturated horizontal water migration near the soil surface. A more detailed outline of this calcretised palaeosol will be given in section 5.4.7 as this palaeosol correlates with the top unit of TFR section.

5.4.2. Section BIS

The sedimentary section BIS is a more than 9 metres incision of a QaII alluvial terrace and is composed of a series of different deposits (Fig. 5.4.2). It is located at the base level of the southern sub-basin (2026551N-647764W; 1684 masl), forming a gentle slope (SJR-Geomorphology map-Appendix A2). The section covers sedimentary and paedogenetic phases of the last 28,550 years (Table 5.4.2). Four units labelled BIS-I to BIS-IV, can be distinguished forming this section,showing contrasting sedimentary (Fig. 5.4.2), granulometric (Fig. 5.4.2.1) and/or morphologica features (Fig. 5.4.2.2).

5.4.2.1. BIS-I

The basal unit BIS-I (840 to 980 cm depth) shows characteristics of three environmental related processes: alluvial sedimentation, groundwater carbonates precipitation and gypsum crystals formation. A lack of sedimentary structures of poorly sorted fine sediment of medium silt mean size, ranging from pebbles to clay and skewed towards the coarser fractions, indicate alluvial
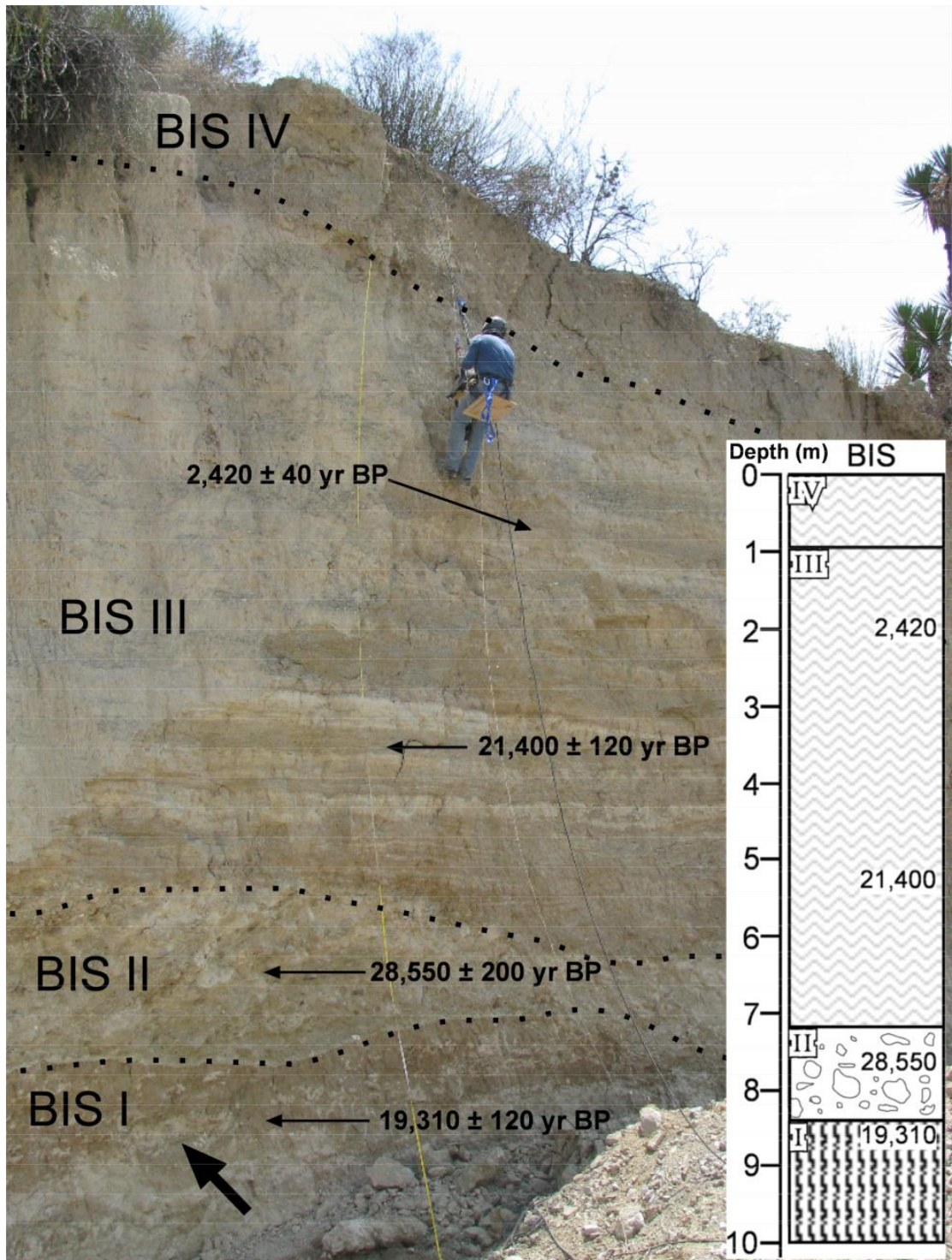
Figure 5.4.2. Sedimentary section BIS and schematic representation of the strata. Solid arrow pointing to the left indicates the place where *Glyptotherium sp*. fossil was exposed. Codes of the graphic patterns as in Figure 5.4.14.

deposition under low energy current (Fig. 5.4.2.1). Post-depositional processes involved precipitation of carbonates, forming indurate nodules clearly visible by differential erosion, forming nearly horizontal nodules (Fig. 5.4.2.3). Although

similar structures have been interpreted as rhizoconcretions (Haddoumi *et al.*, 2008) this unit does not show evidence of prolonged soil development. According to Gile *et al.* (1966) pedogenic carbonate accumulation occurs in four distinguishable morphological stages. First, carbonates form as filaments and as thin coatings on individual small grains (stage I) that later develop into nodular coatings and extend to form thin films underneath gravel sized clasts (stage II). In arid environments, stage I can be reached in the order of hundreds of years, while up to 8,000 to 15,000 years are needed to reach stage II (Gile *et al.*, 1981, 1998). As carbonate accumulation progresses and pore spaces are filled, a plugged petrocalcic horizon forms stage III. Later in the process, thin laminar structures give rise to stage IV (Gile *et al.*, 1966). An example of stage III in a group of soils in New Mexico shows that this stage can take 25,000 years to develop, while longer times are needed for later thickening of the horizontal laminae (Bachman & Machette, 1977). None of these morphologies is observed in unit BIS-I, indicating a non-pedogenic origin for the carbonate accumulation under marked arid conditions. Instead, precipitation of calcrete associated with lateral migration of water near the surface is inferred. The presence of isolated and scarce gypsum crystals indicates that the sediment was part of a poorly drained area of the basin and experienced high evaporation rates that caused precipitation of gypsum crystals. Because gypsum is highly soluble in water and calcretization takes place in its presence, calcrete formation is assumed to pre-date gypsum occurrence.

During the field exploration carried out by the author during March 2008, a megafaunal mammal fossil was discovered at the bottom of the section. The fossil was exposed after the recent collapse of part of the section (Fig.5.4.2.4).

The skull and back armour osteoderms allowed the identification of the fossil at genus level, determining that it corresponds to *Glyptotherium sp.* (Xenarthra, Glyptodontidae). The radiocarbon age obtained from the bulk sediment of BIS-I was 19,310 ± 120 ^{14}C yr BP.
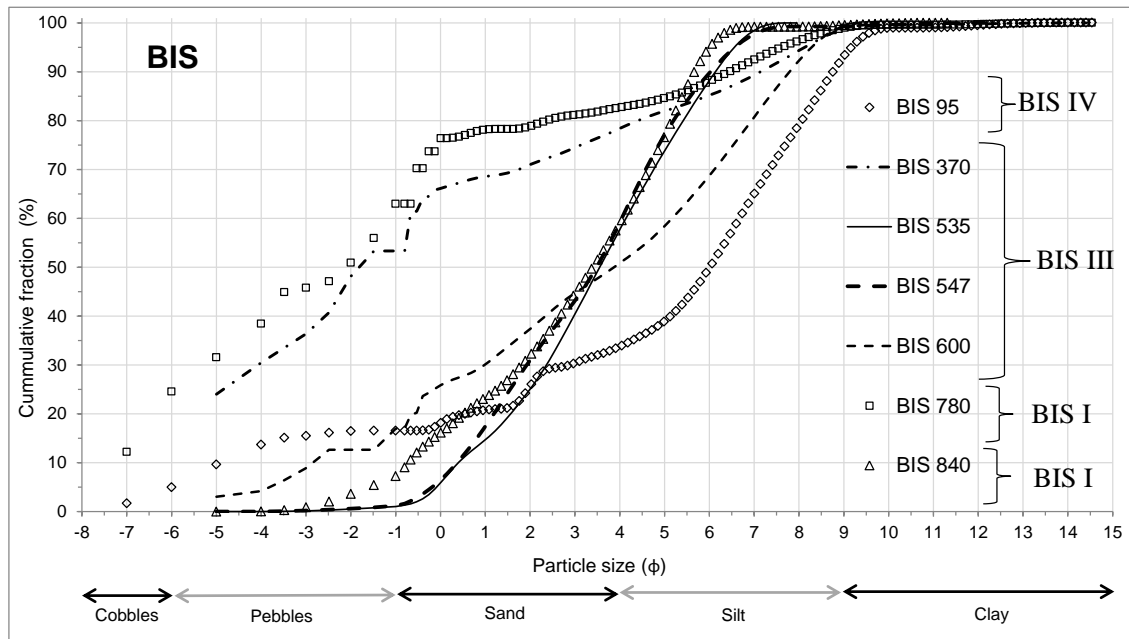
Figure 5.4.2.1. Cumulative percentage of the grain size composition for different facies of the BIS section. Numbers in the code indicate sample depth. Statistical parametres are presented in Table 5.4.2.–Appendix B.

Figure 5.4.2.2. Close view of a hand specimen of the deposit BIS-I. Calcretisation is not homogeneous and in this case it shows at the top of the sample. Tray for scale is 7.5 cm.

Table 5.4.2. Radiocarbon dates obtained from the sedimentary section BIS. The sample code includes section name and depth from which dated sample was taken.

Sample	Dated material	Technique	Measured radiocarbon age (yr BP)	Conventional radiocarbon age (yr BP)	Laboratory code
BIS III-205	Charred plant fragments	AMS	2,190 ± 40	**2,420 ± 40**	Beta-279239
BIS III-535	Organic sediment	AMS	21,310 ± 120	**21,400 ± 120**	Beta-279240
BIS II	Organic sediment	AMS	28,490 ± 200	**28,550 ± 200**	Beta279241
BIS I	Organic sediment	AMS	19,300 ± 120	**19,310 ± 120**	Beta-245128

5.4.2.2. BIS-II

The contact between BIS-I and the overlain BIS-II (720-840 cm depth) stratum is an erosional contact (Fig. 5.4.2; 5.4.2.4 A). The BIS-II is a slightly indurated deposit, characterised by extremely poorly sorted pebbles and cobbles included in a silty sand matrix. The average size class is very fine pebbles (-1.86 Φ). The multimodal frequency distribution shows that the most represented clast sizes are very coarse sand, medium pebbles and large cobbles (Fig. 5.4.2.1; Appendix B) which were probably transported as a debris flow-type sediment by a high energy current in a short period of time, eroding the surface of BIS-I. Support for this comes from the abrupt contact with the overlaid BIS-I unit, which can be interpreted as an erosional surface. However, this idea is challenged because BIS-II gave an age of 28,550 ± 200 ^{14}C yr BP, considerably older than the stratum below. Two possible scenarios can explain this age reversal. The first hypothesis needs the assumption that the radiocarbon dates provided correct ages and that after deposition of BIS-II a lateral incision of the sedimentary section occurred, leaving a cavity in the vertical wall. The erosional surface between BIS-I and BIS-II would be the upper part of the cavity. A later sedimentary flow carrying the glyptodont would have filled the cavity. This phenomenon was frequently observed along the river incisions in other parts of
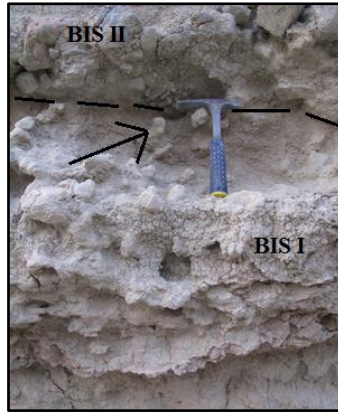
Figure 5.4.2.3. Facies BIS-I showing the carbonate nodules exposed by differential erosion (arrow). Hammer for scale.
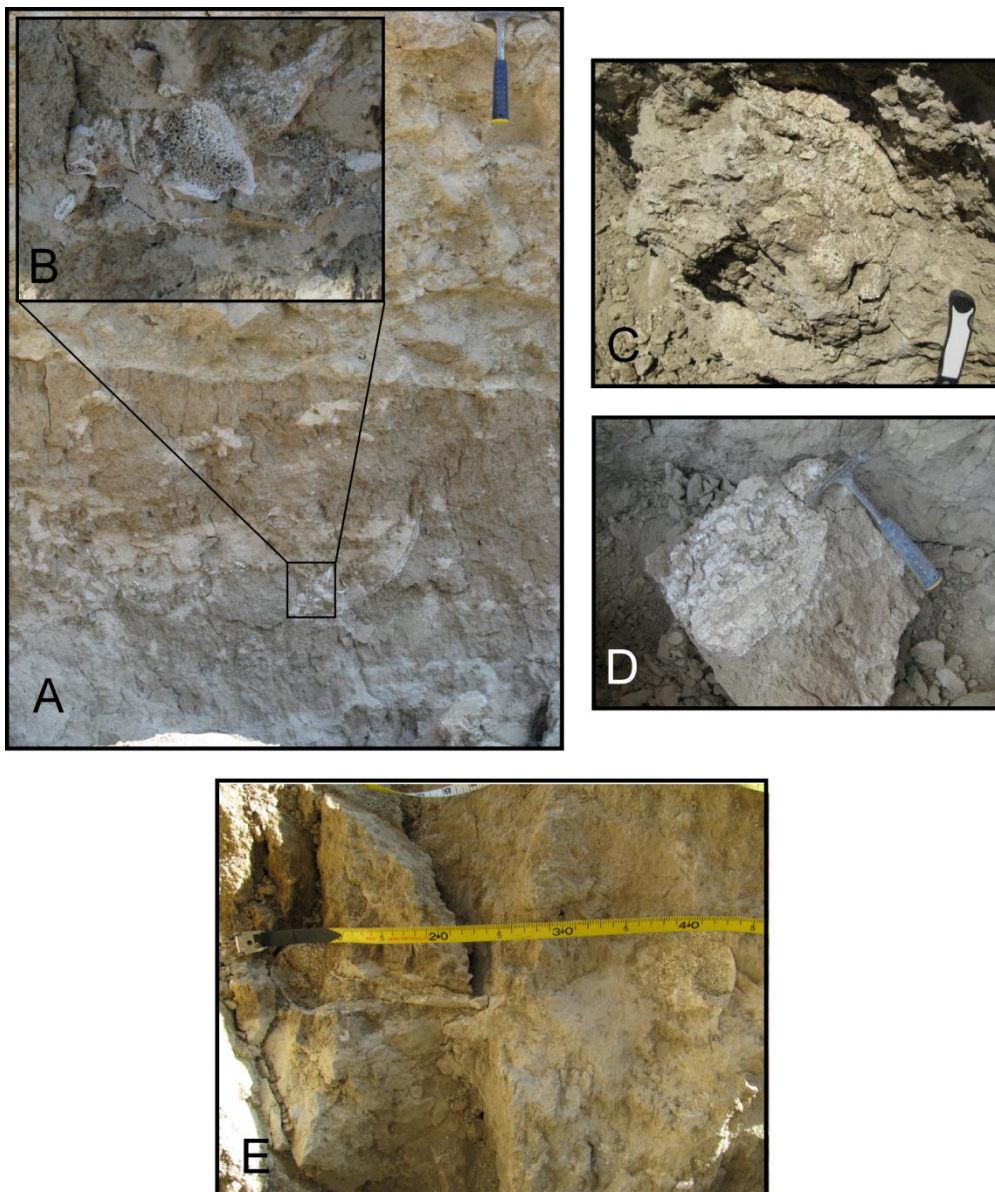
Figure 5.4.2.4. A: Exposed bones of *Glyptotherium sp.* in the sedimentary unit BIS-I and detail of a vertebra (B). Armour osteoderms from the back (C) and head (D) were also exposed. A femur is shown in E. Measuring tape in E is in cm.

the basin where the bottom part of the profile corresponded to recent incrusted fluvial material. Alternatively, the earlier age of BIS-I could be related to contamination with more recent carbon. Nowadays BIS-I is in contact with the modern river bed and under the current semi-arid climate its bottom part is intermittently exposed to high moisture during rain episodes and afterwards high evaporation rates (during the rescue of the fossil remains, while the collapsed block containing the fossil was removed from the river bed after consolidation, around 50 cm of the river bed in contact with BIS-I was dug up, showing that the BIS-I continued below the modern channel level and that it contained a considerable amount of moisture). The water transported by these intermittent rivers is enriched with organic matter from the upper parts of the basin and can possibly be percolated inside the sedimentary profile. This later hypothesis is supported by the high organic matter content in BIS-I (the highest in the section-see Table 5.4.2.1 in Appendix B). On the other hand, the presence of gypsum crystals ($CaSO_4$) reveals surface or near surface evaporation of highly concentrated saline water, which normally occurs as part of a lake body or pond in closed basins under arid conditions (Warren, 2010), but not as part of a fluvial environment. If the gypsum crystals were not formed *in situ*, but inherited from facies above (abundant gypsum crystals were found between640-650 m depth- BIS-III) the first hypothesis would be favoured. Because in the present study the material dated was bulk organic sediment, further radiocarbon age determination of fossil bone and/or an alternative dating technique (*i. e.* OSL) are necessary to clarify the actual age of BIS-II and the sedimentary processes involved.

5.4.2.3 BIS-III

BIS-III unit extends from 95 cm to 720 cm in depth and groups a series of distinctive layers of which individual thickness varies from 5 to 45 cm (Fig. 5.4.2). The radiocarbon date from bulk organic sediment collected at 535 cm of depth yielded an age of 21,400 ± 120 ^{14}C yr BP, while charcoal fragments at 205 cm were dated at 2,420 ± 40 yr BP. The main difference among facies is the grain size and the post depositional characteristics. One representative example of each sedimentary facies is explained here and listed in Table 5.4.2 (Appendix B). The coarse layer at 370 cm corresponds to an extremely poorly sorted mixture of ungraded sands and gravels (80% in volume) with a minor content of silt and clay and low organic matter content (Fig. 5.4.2.1, Table 5.4.2.-Appendix B). The mean grain size falls in the very coarse sand category. The shape of the gravel in this deposit varies from angular to sub rounded. On the other hand, the fine-grained facies can be separated in two groups on the basis of small differences in the grain size parameters, being very similar in terms of sedimentary features and OM content. The finest facies, at 547 cm, have a graphic mean of 5.5 Φ, coarse silt and a bimodal distribution at coarse sand and medium silt. Small gypsum crystals were identified in these facies and also at the facies at 640-650 cm depth. For the coarser facies (600 cm depth) the mean size is 3.8 Φ, which corresponds to very fine sand, and the grain size distribution shows a multimodal behaviour with the most prominent peaks in fine pebbles, very coarse, fine sand and fine silt. In profile view, the former facies showed a pale colour, which contrasted with the reddish facet of some fine-grained deposits, like the deposit at a depth of 535 cm. The granulometric characteristics of the 535 cm facies are the same as those at 547 cm deep, but

differ in terms of colour (10 YR 7/2 at 535 cm vs 2.5 Y 8/2 at 547 cm) and the incipient soil properties like poorly developed blocky structure, incipient clay cutans and root cavities. At this level, small gypsum fragments were identified. The similar value in OM supports the idea of a poorly developed palaeosol.

5.4.2.4. BIS-IV

The top facies BIS-IV (0-95 cm depth) is also a mixture of clasts of different size and form with no clear spatial arrangement in profile view, ungraded and with no other sedimentary features (Table 5.4.2.1-Appendix B, Fig. 5.4.2). This deposit can be classified as alluvial and does not follow the layering of the unit it overlays. It is also a coarser grained deposit than most of the facies of unit BIS-III. The finding of a pottery fragment near the bottom of the deposit may indicate that this unit was under pre-Columbian agriculture.

5.4.3. Section CAP

An exposed sequence at the southwest part of the basin represents some sedimentary and pedogenic processes related to the southern highlands. This section, coded CAP, (2025249N-644077W, 1770 masl) is part of an incised alluvial terrace deposited along a river at the southwest hills. Three distinctive units (I, II and III) can be distinguished by their pedogenic development (Fig. 5.4.3), whereas unit II has two sedimentary sub-facies (Fig.5.4.3.1).

5.4.3.1. CAP-I

The lowermost sedimentary facies CAP-I (235 to 315 cm depth) can be distinguished by its greyish colour (7.5 YR 5/1) and by its textural properties. It is the unit with the coarsest sediments in the section, with more than 50 % of the grain population being fine sand or larger in size (Fig. 5.4.3.1). In sedimentological terms this unit corresponds to an alluvial deposit of very poorly
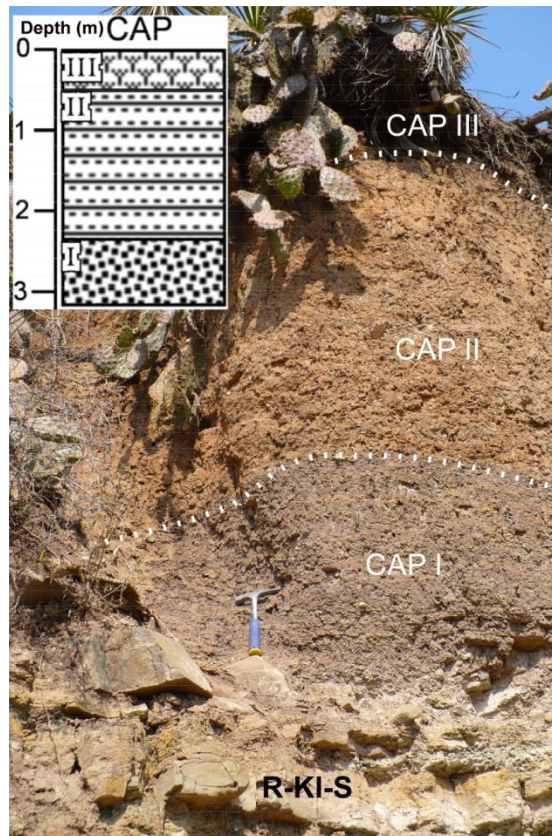
Figure 5.4.3. Sedimentary section CAP and schematic representation of the strata. The basal CAP-I overlays a sandstone bedrock (R) of the San Juan raya Formation (KI-S). Codes of the graphic patterns as in Figure 5.4.14.

sorted sand and small pebbles in lower proportions, included in a silty matrix. The presence of sub-blocky aggregates and cutans indicate pedogenesis. This unit rests directly on a sandstone bedrock of the KI-S. No radiocarbon dates were obtained from this sedimentary section but, given its topographic position, a late Pleistocene age is inferred.

5.4.3.2. CAP-II

CAP-II (50-235 cm depth) shows a rhythmic alternation of two types of facies, RA and RB. RA facies are thin layers of sandy appearance (Fig. 5.4.3.2), normally 1 cm thick although some can reach 4 cm. They are formed of poorly sorted alluvial sediments whose biggest clasts are of fine pebble size (Fig. 5.4.3.1), very friable and show no pedogenic features or aggregates. Facies RB are finer in particle size and slightly more organic than RA (Fig. 5.4.3.1; Table

5.4.3 Appendix B). The columnar blocks of this facies are hard, have abundant calcified root-like filaments and developed clay cutans (Fig. 5.4.3.2). These cutans and the reddish colour (7.5 YR 5/3) suggest a certain level of soil development. The regular alternation of RA and RB layers indicates a rhythmite type deposition of very thin layers varying slightly in grain size, but contrasting in pedogenic development. Sedimentation of medium to small particles in this part of the landscape must result from low energy alluvial transportation, alternated with stability periods when paedogenesis took place.

5.4.3.3. CAP-III

The CAP-III covers the top 50 cm and is a very organic modern soil (MO = 7.4 %) composed of very poorly sorted clasts ranging in size from small pebbles to clay. It shows no grading or stratification and the aggregates are small and of granular shape. Fragments of eroded calcrete are abundant in this soil.
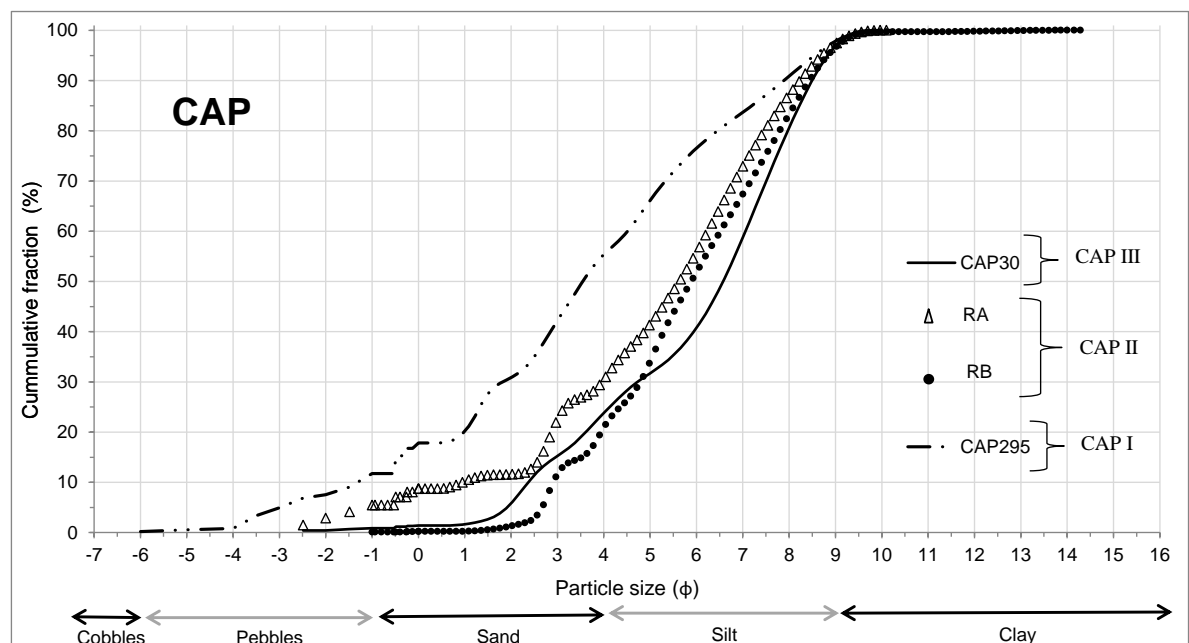
Figure 5.4.3.1. Cumulative percentage of the grain size composition for different facies of the CAP section. Numbers in the code indicate sample depth. Statistical parametres are presented in Table 5.4.3.–Appendix B.
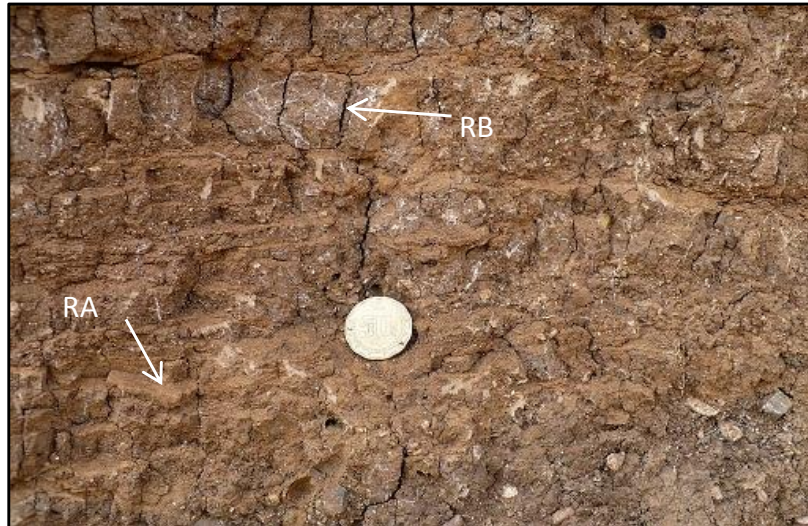
Figure 5.4.3.2. Close-up view of the rhythmite facies RA and RB of the sedimentary unit CAP-II.

5.4.4. Section SLT

Section SLT (5.5 m depth) is located in the central part of the southern sub-basin (2027026N-648474W; 1695 masl), at the contact between a QaII alluvial terrace and the QaIII alluvial fan (Fig.5.3.3.3; Appendix A). Its exposure is due to a fault at the contact between both fans. The top 30 cm of SLT section correspond to the distal part of QaIII, clearly distinguished by its whitish very fine silty material. A few metres upstream, to the east of the fracture this deposit thickens and overlays a series of poorly sorted anastomosed alluvial channels of the QaIII fan, of which the lithology is almost entirely lutite. In contrast, to the west of the fracture the underlain deposits are a palaeosol, a calcrete layer and a series of alluvial deposits of different structure and lithology, including fluvial-like lenses containing sub-rounded limestone clasts (Fig. 5.4.4). SLT section is 550 cm in depth and composed of six units (Fig. 5.4.4; Table 5.4.4-Appendix B). No radiocarbon dates were obtained from this section, but the possible stratigraphic correlation with other sedimentary sections of the basin on the basis of the volcanic ash and the top facies are discussed in a later section.

5.4.4.1. SLT-I

The bottom unit SLT-I (480 to 550 cm) is an ungraded, unstratified alluvial deposit of coarse silt material with a low content of gravel and pebbles. Although no stratification was visible in profile view, the bottom part of the unit showed inclusions of coarse cobble-sized clasts, while the medium and top part were made of finer material (Fig. 5.4.4.1). Table 5.4.4-Appendix B shows the granulometric characteristics of one sample from the bottom and close to the top of this unit. A distinctive facies at the upper part of SLT-I is a volcanic ash layer (Fig. 5.4.4), characterised by poorly sorted fine material ranging from clay to very fine sand with a median and mean size of very coarse silt (Fig. 5.4.13-Section 5.4.13). This tephra is included in the SLT-I unit and the fact that it is not mixed with alluvial material indicates an age contemporaneous with SLT-I, and that the terrace was formed by episodic depositional events. The tephra was deposited during a pause in alluvial sedimentation. Similarly, the tephra layers in sections TFR and CAN (see Section 5.4.13) are deposited near the upper boundary of an alluvial unit. However because the age of the tephras has not been numerically confirmed that their used as an index deposit for correlation is very limited. As will be seen in section 5.4.13., a preliminary age of early Holocene, between 9 to 8.5 kyr BP is designated to these volcanic ashes.

5.4.4.2. SLT-II

The abrupt transition from the fine material of SLT-I to the clast supported overlain alluvium indicates an erosion event and the beginning of deposition of the SAL-II (270-480 cm depth), which shows fine and coarse facies (Fig.5.4.4). The finegrained facies are made up mostly of lime (mean = 5.7 Φ, median = 5.6 Φ) with no sedimentary structures, very friable and no pedogenic features. The basal facies of the unit is clast supported alluvial clasts, some reaching the size

limit between cobbles and boulders and with only around 30 % of sand and finer particles. No grading or stratification was observed. The other coarse lenses are mostly pebbles and cobbles, very poorly sorted with neither grading nor stratification. The fine-grained facies indicate lower energy transport with most sediments carried in suspension, while alluvial debris of the coarsest facies shows likely sudden changes in erosion and transportation in high energy currents.
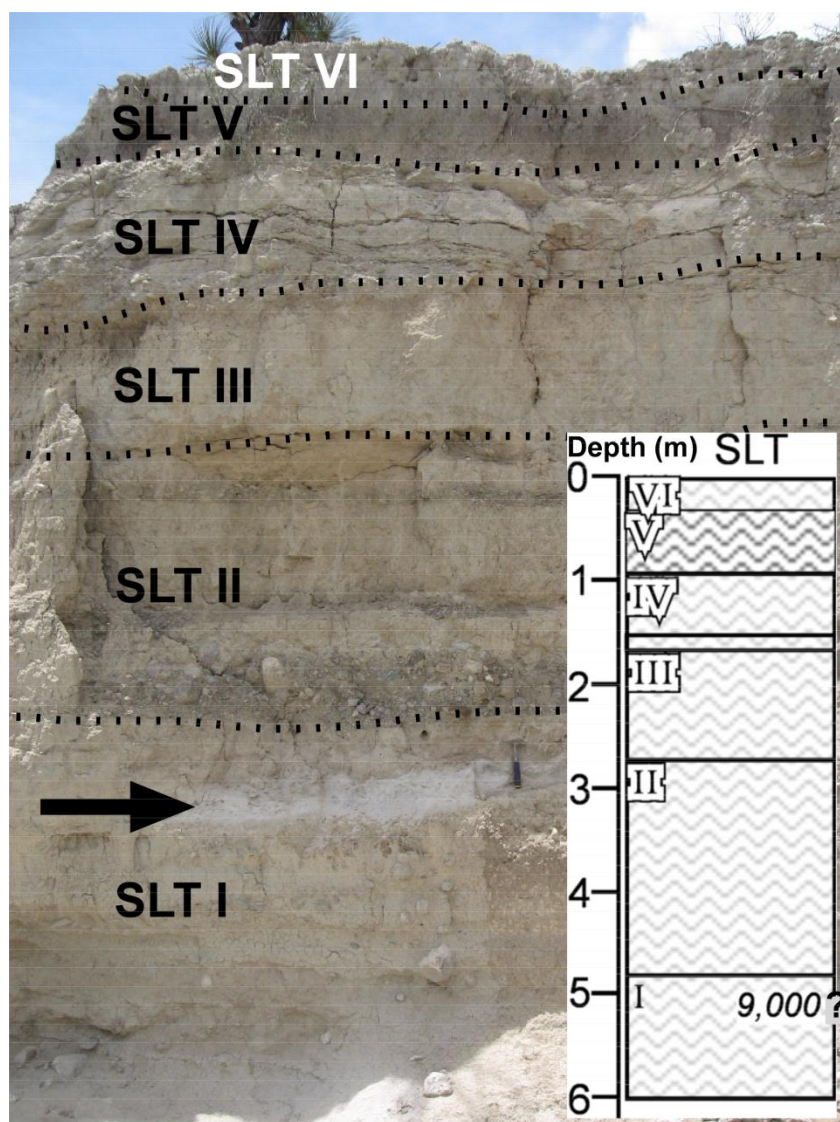
Figure 5.4.4. Sedimentary section SLT and schematic representation of the strata. The arrow indicates the level of the tephra deposit. Hammer for scale. Codes of the graphic patterns as in Figure 5.4.14. Statistical parametres are presented in Table 5.4.4.– Appendix B.
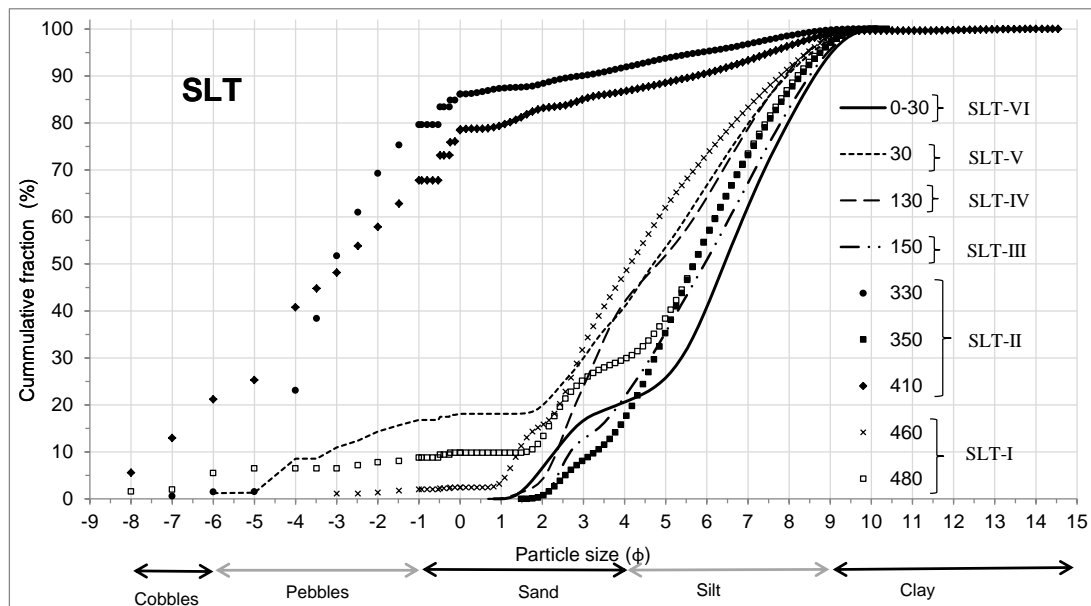
Figure 5.4.4.1. Cumulative percentage of the grain size composition for different facies of the SLT section. Numbers in the code indicate sample depth.

5.4.4.3. SLT-III

The sedimentary unit SLT-III (150-270 cm) is a homogeneous deposit made of approximately 70 % silt and with particles no coarser than medium sand (Fig.5.4.4.1). The structure of this unit is massive with very small and scarce vesicular porosity (>5 %). No pedogenic or sedimentary structures are visible. Datable material was not found in this unit and no other means of correlation were possible. The lack of sedimentary and pedogenic structure suggest continuous low energy deposition and rapid burial by subsequent alluvial deposits.

5.4.4.4. SLT-IV

SLT-IV (90-150 cm depth) is fine sediment with powder calcrete, capped by laminar calcrete (Fig. 5.4.4). In profile view, the exposed wall is covered by a relatively fragile calcrete which, once broken releases very fine (mean & median = very coarse silt) loose and reddish sediment (10YR 8/2- very pale brown). At the top of the unit the calcrete is layered and highly fragmented. This calcrete has no pedogenic morphologies and its origin is probably related to water table

108

fluctuations. However, a micromorphological analysis is necessary to determine the origin. No datable material was found in this unit.

5.4.4.5. SLT-V

The unit SLT-V (30-90 cm) is an extremely poorly sorted group of particles ranging in size from sand (~40 %) to clay. It forms very porous aggregates of granular shape. This facies has higher organic matter content than other units but shows no clear evidence of soil development. Some sand-sized carbonate concretions are visible but their origin is not clear. However, as no pedogenic features are present, a water table related origin is assumed. Because of the lack of radiocarbon dating this facies cannot be correlated in numerical terms. However, as unit SLT-I is assumed to be early Holocene and SLT-VI corresponds to the top layer of TPX, with a minimum date of 3,680± 40 ^{14}C yr BP, units II to V of this stratigraphic section are assumed to be middle Holocene.

5.4.4.6. SLT-VI

The top stratum SLT-VI (0-30 cm) is a very poorly sorted white silt deposit derived from the distally transported alluvial fan QaIII (Table 5.4.4-Appendix B). This facies has no sedimentary or paedogenetic features and can be followed downstream until it becomes the top unit of the stratigraphic section TPX. In SLT profile this sedimentary unit has a thickness of no more than 30 cm, which is a very small fraction compared with the more than 8 metres that it reaches in TPX. This unit dates at late Holocene, as will be seen in Section 5.4.8.

5.4.5. Section SJII

An alluvial surface of south provenance reaches its distal part close to the SJRv. Here, a series of modern intermittent rivers cut the deposits exposing a

series of pedo-stratigraphic units. Section SJII is composed of only five units, covering from before the LGM and middle Holocene (2025405N- 646549W, 1718 masl) (Fig. 5.4.5). The soil properties shown along this section account for more stable episodes that allowed soil development.

5.4.5.1. SJII-I

In textural terms the unit SJII-I at the base of the section (580-620 cm) is a sand and silt dominated deposit (Fig. 5.4.5.1; Table 5.4.5-Appendix B). Despite not showing sedimentary structures the very poorly sorted character of the particles and the abundance of fine grains indicates alluvial deposition under low energy current, uncapable to transport coarse fragments available in the south slopes. This facies is distinctive because in profile view the erosion preserved macroscopic calcretized nodules and removed non-cemented particles (Fig. 5.4.5), showing a very similar morphology to the base unit of section BIS. The former characteristics indicate precipitation of carbonates after alluvial deposition.

5.4.5.2. SJII-II

The former facies is overlain by a finer deposit, SJII-II (470-580 cm), of very poorly sorted silty material that shows no mature pedogenic structures but has accumulated carbonates as poorly developed powder calcrete and carbonate nodules of less than 1 mm in diameter. The aggregates formed are very porous (20 %) and friable. The bulk sediment of this deposit yielded a date of 19,480 ± 90 ^{14}C yr BP (Table 5.4.5.1-Appendix B).

5.4.5.3. SJII-III

Above the former deposit, from 390 to 470 cm in depth, there is a reddish palaeosol (7.5YR 6/3- light brown) labelled SJII-III, primarily made of very poorly
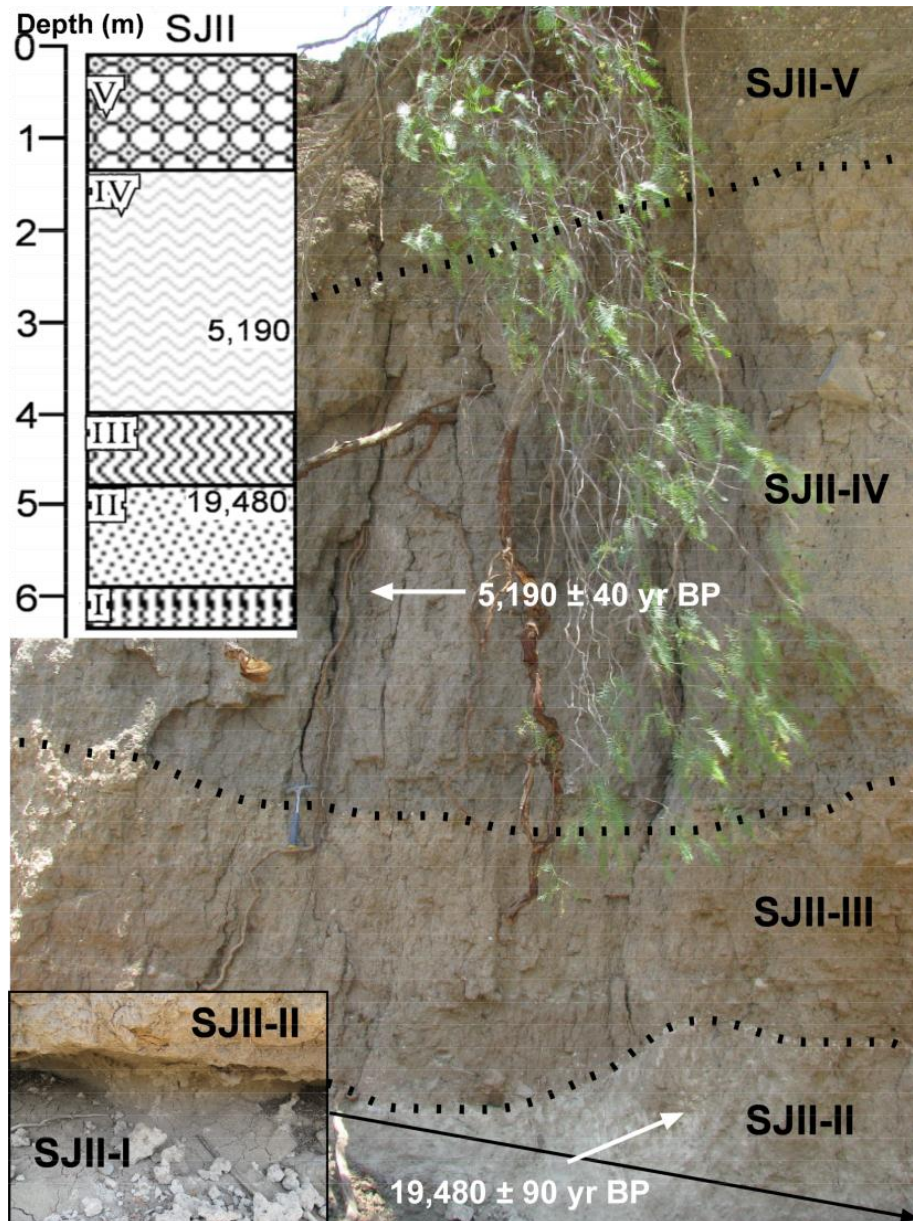
Figure 5.4.5. Sedimentary section SJII and schematic representation of the strata. Hammer for scale. Codes of the graphic patterns as in Figure 5.4.14.

sorted fine alluvial sediments which after pedogenesis acquired a columnar structure. Although no clay coatings were observed, root-like porous and rhizo-concretions evidence plant colonisation and pedogenesis. The reddish colour indicates higher oxidation compared with the other palaeosols in the section. This palaeosol could visually be followed approximately 10 m downstream and it was observed that it enclosed a tephra layer (Figs. 5.4.5.2; 5.4.13). As this tephra is bracketed between latest Pleistocene and middle Holocene, it is likely

that it correlates with the ones found in other sections and corresponds to the event at 9 to 8.5 kyr BP aruption of Citlaltepetl (Section 5.4.13). A gradual transition upwards to the SJII-IV palaeosol in sedimentological terms contrasts with the abrupt change in colour. The difference in grain size between both palaeosols is minor, being both very poorly sorted silt alluvium (Table 5.4.5-Appendix B; Fig. 5.4.5.1).

5.4.5.4. SJII-IV

The palaeosol SJII-IV (125-390 cm) shows a grey colour (10YR 6/2- light brownish grey) indicating a dominance of reduction conditions, a more developed columnar structure and clay cutans. Few carbonate nodules of less than 5 mm are present. A radiocarbon age of 5,190 ± 40 yr BP (Table 5.4.5.1) was obtained from the bulk organic sediment of this unit at a depth of 300 cm. The contact between SJII-IV and the upper unit, SJII-V is mediated by an erosional surface at 125 cm (Fig. 5.4.5).

5.4.5.5. SJII-V

The top unit (0-125 cm depth) corresponds to a fluvial-like deposit, very poorly sorted with pebbles and sand making up almost 70% of its mass volume (Fig. 5.4.5.1). The grain size mean and median values of this deposit follow the coarse sand and very fine sand categories respectively (Table 5.4.5-Appendix B), contrasting with the lower units in which silt-sized sediments dominated the textural composition. The top part of the unit SJII-V (0-20 cm) contains clasts of the same characteristics as the lower part of the unit, mixed with the finer material, and rich in organic matter compared to the lower part of the unit. In adjacent fields, a few metres away, it was observed that this terrace level had

been subjected to agriculture practices during recent times, suggesting that the top 20 cm of unit SJII-V have been altered by agriculture.

Figure 5.4.5.1. Cumulative percentage of the grain size composition for different facies of the SJII section. Numbers in the code indicate sample depth. Statistical parametres are presented in Table 5.4.5.–Appendix B.


Figure 5.4.5.2. Palaeosol of unit SJ-III showing an incrusted tephra layer. The top part of the unit was decapitated by a modern deposit after the back of the section was recently excavated by local people.

Table 5.4.5.1. Radiocarbon dates obtained from the sedimentary section SJII. The sample code includes section name and depth from which dated sample was taken.

Sample	Dated material	Technique	Measured radiocarbon age	Conventional radiocarbon age	Laboratory code
SJII300	Organic sediment	AMS	5,030 ± 40 yr BP	**5,190 ± 40 yr BP**	Beta-279242
SJII470	Organic sediment	AMS	19,400 ± 90 yr BP	**19,480 ± 90 yr BP**	Beta-279243

5.4.6. Section STC

The profile STC is located at the distal part of an alluvial fan of north provenance (QaII). The exposed section in a river cut (2026276N – 647057W; 1694 masl) shows more than 6 metres of a series of deposits divided into four sedimentary units (Fig. 5.4.6; Table 5.4.6-Appendix B). No radiocarbon dates were obtained from this sedimentary section, constraining the establishment of stratigraphic relationships with other events. The relative position in the landscape of this alluvial surface allowed its indentification as an alluvial terrace of possible Holocene age.

5.4.6.1. STC-I

The lowermost STC-I unit (660-430 cm in depth) is composed of very poorly sorted silt material with a prismatic structure and vertical changes in colour. As these changes vary slightly from grey, it is suggested that they took place under different conditions of reduction. No grading or stratification is visible in this unit. Small fragments of calcrete (sand size) are present, but are most likely inherited from the alluvial material and not formed *in situ*. The basal facies has no soil characteristics and is coarser than the other members of the unit (Fig. 5.4.6.1), while the samples at 570 and 430 cm show clay coatings (cutans) and root galleries. At a depth of 510 cm a gastropod shell was found (Fig. 5.4.6.2). Sinestral growth and a thin ornate shell observed in this fossil are diagnostic characteristics of the Physidae family, a group of common freshwater

114
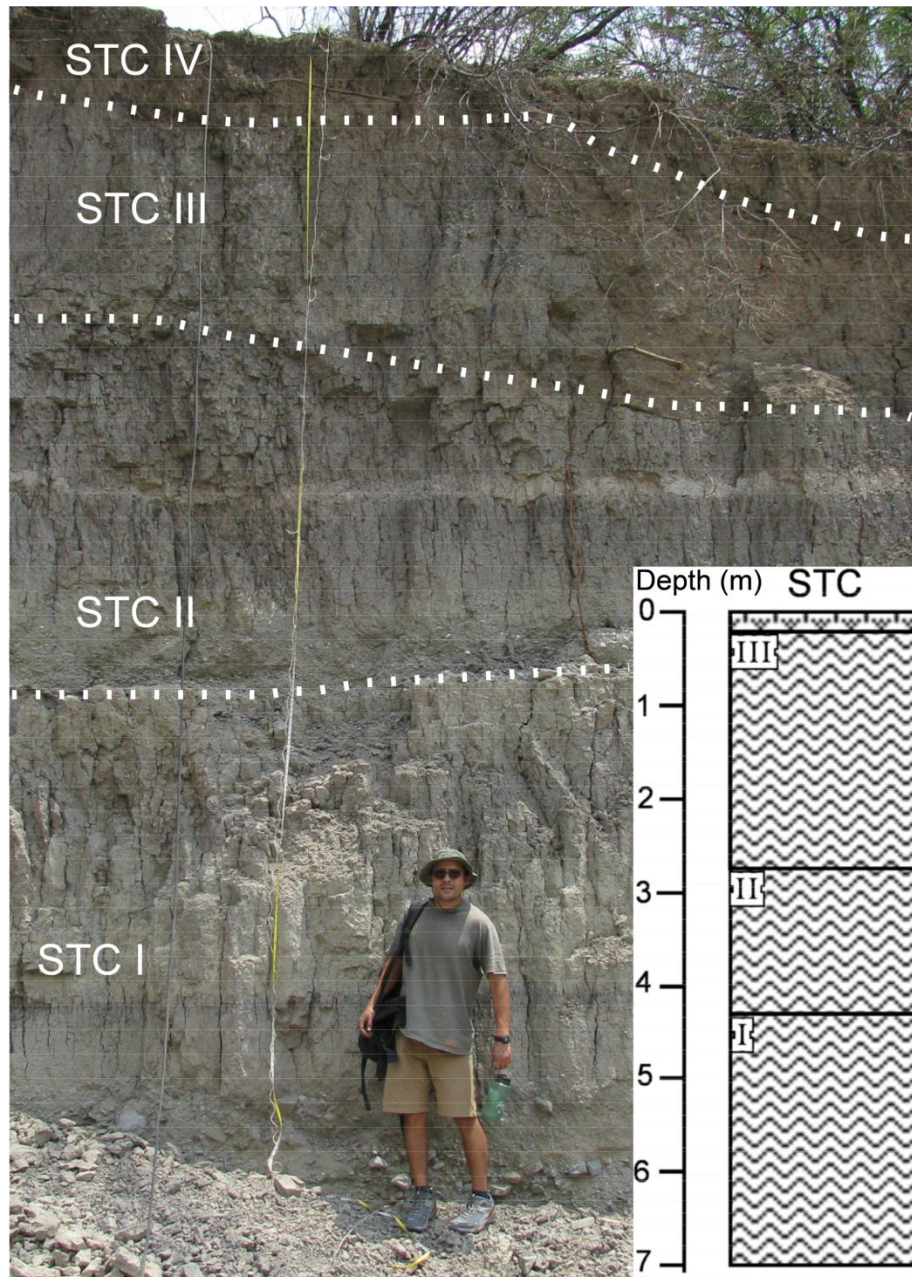
Figure 5.4.6. Sedimentary section STC and schematic representation of the strata. Codes of the graphic patterns as in Figure 5.4.14.

pulmonate gastropodos, abundant in the Americas and which probably originated in the pacific coast of Mexico (Strong *et al.*, 2008). Identification at lower levels (Genus, species) was not pursued because it has proved to be difficult on the basis of the shell only and morphological reproductive features are needed to eliminate uncertainties (Taylor, 2003; Wethington, 2004). Reports of Physidae in Mexico indicate that the common habitat for these snails is
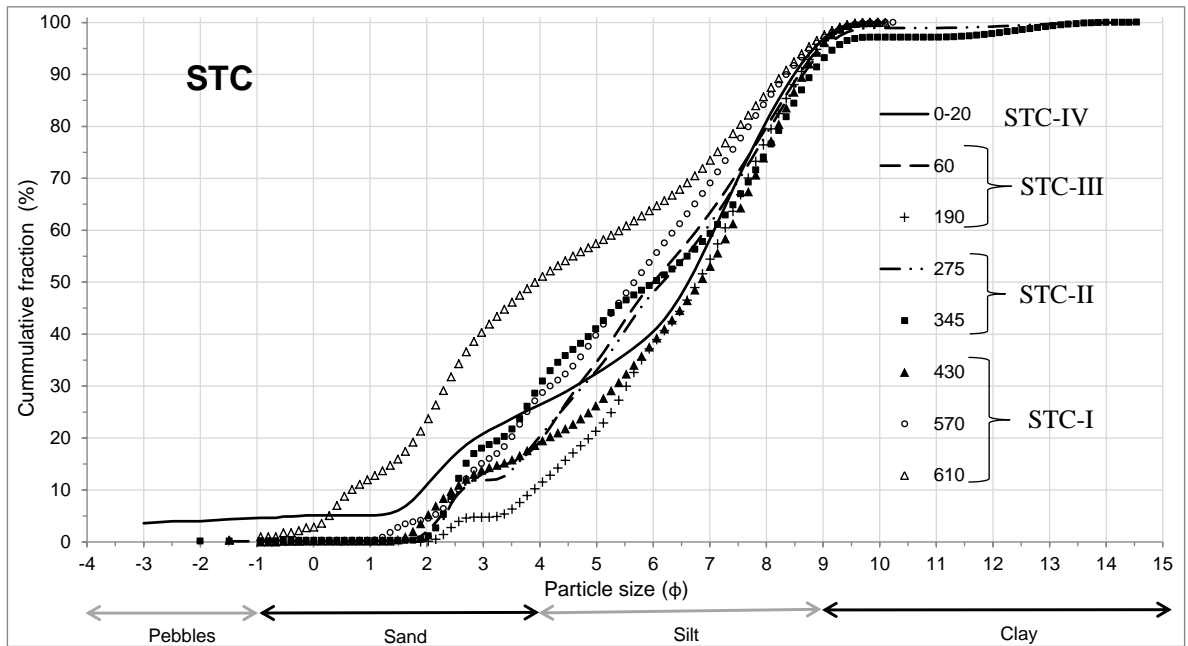
Figure 5.4.6.1. Cumulative percentage of the grain size composition for different facies of the STC section. Numbers in the code indicate sample depth. Statistical parameters are presented in Table 5.4.6–Appendix B.

Figure 5.4.6.2. Mollusc shell found at the STC-I unit. Scale bar is 5 cm.

freshwater vegetation in rivers, ponds, springs and sometimes wet mud around the water bodies (Naranjo-García, 2003), although temporary inundated environments can also be suitable (Strong *et al.*, 2008). This is more probable

116

considering that the grey colour of the sedimentary unit is most likely as a result of reduction conditions.

5.4.6.2. STC-II

Units STC-I and STC-II (275-430 cm depth) are separated by a clear erosional surface (Fig.5.4.6). The sedimentary unit STC-II is also a very poorly sorted alluvial material with no stratification but is composed of two facies that differ in terms of grain size. The basal facies is coarser and has less OM (Table 5.4.6.), while the upper part shares the same granulometric characteristics as the fine facies of the underlain unit, and higher organic content. However, the textural differences are not substantial. In both cases silt is the dominant grain size and reflects low energy alluvial current.

5.4.6.3. STC-III

The unit STC-III (20-275 cm depth) is very similar to the unit described below in terms of sedimentological composition, structure, colour and pedological features. The difference is given by the less developed columnar structure, compared with the prismatic blocks of STC-II. STC-III is also more friable and organic, but still shows greyish colours, a typical reduction condition of inundated environments.

5.4.6.4. STC-IV

The uppermost unit (STC-IV; 0-20 cm) is a more organic modern soil, which has been under recent cultivation, as was seen a few metres up fan at the surface. The organic matter content, 10.69 %, is considerably higher than the other facies of the section. The lack of sedimentological structures and poorly developed soil characteristics could be attributed to recent and intense agricultural management. This surface represents the last phase of alluvial

deposition from the southern highlands, which probably occurred during the late Holocene.

5.4.7. Section TFR

The four-metre sedimentary section TFR is located to the southwest part of the SJRv (2025720N – 645151W; 1735 masl), and is exposed along a river cut primarily produced by a rock fracture. This relatively small profile has different facies, each representing a particular depositional and environmental event (Fig. 5.4.7).

5.4.7.1. TFR-I

The basal unit TFR-I (190-400 cm) is a grey alluvial deposit formed of different facies (Fig. 5.4.7.1; Table 5.4.7-Appendix B). These sub-units are only recognised at close range by their textural composition and slight variations in colour. The facies sampled between 320 to 380 cm in depth are very poorly sorted material of medium silt mean grain size and show a reddish appearance (10YR 6/2- light brownish grey), incipient pedogenic development, with blocky aggregates, root vesicles and a slightly higher organic matter content than the facies above. The middle facies (275 cm), is also medium silt in mean size, but shows a higher degree of sorting than the previous facies and normal grading in hand specimen. This facies presents similar pedogenic characteristics to the underlain facies. The upper part of the TFR-I is a coarser and extremely poorly sorted mixture of particles ranging from big pebbles to clay (Fig. 5.4.7.1; Table 5.4.7-Appendix B). In this sediment no root cavities were found. Some of the pebble-sized particles are clearly weathered in this facies, showing weak cleavage and purple and yellow colours. Considering this feature and the
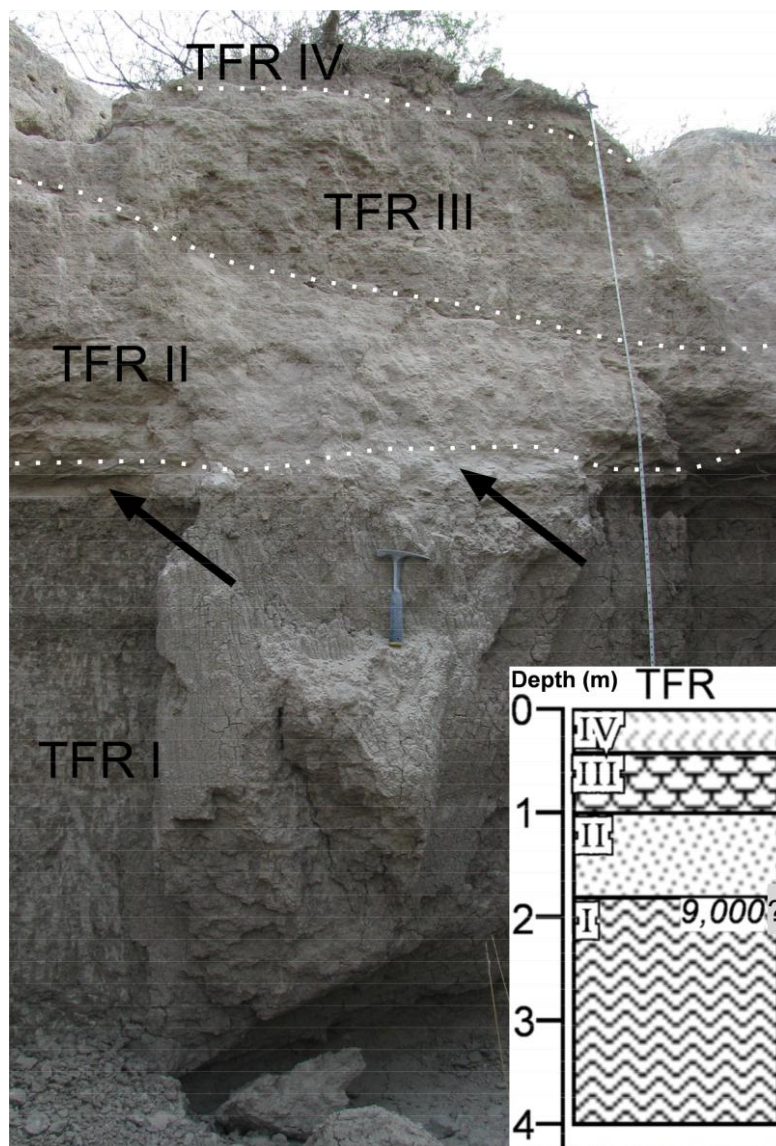
Figure 5.4.7. Sedimentary section TFR and schematic representation of the strata. Arrows indicate the level of the tephra deposit. The age of the tephra (9,000?) has been assigned on the basis of Holocene eruptions of surrounding volcanos (See section 5.4.13). Hammer for scale. Codes of the graphic patterns as in Figure 5.4.14.

greyish colour, an inundated environment is inferred. A tephra deposit is found at the upper part of TRF-I (Figs. 5.4.7 & 5.4.13).

5.4.7.2. TFR-II

The unit TFR-II (90-190- cm depth) is also composed of two sedimentary facies (Fig. 5.4.7.1). Statistical parameters of the grain size distribution of the facies sampled at 100 and 180 cm are not very different except in the bigger grains present in the facies at 100 cm (Table 5.4.7-Appendix B). The main

characteristic of these facies is their pale appearance caused by the presence of a powder calcrete whose development decreases with depth.

5.4.7.3. TFR-III and TFR-IV

TFR-III (10-90 cm in depth) unit represents a layered and well developed white (7.5YR 8/1) and massive layered and very friable calcrete. Because of the lack of petrocalcic features, as outlined in section 5.4.2, this calcrete seems to have been formed by precipitation of carbonates from saturated groundwater, affecting also the palaeosol of TFR-IV (0-10 cm depth) unit, which shows the same morphological characteristics of the palaeosol of section ALB. The tephra layer and the deposits in which it is enclosed, do not show evidence of carbonate deposition, suggesting that the water table, which could have given rise to the calcrete, was above these sediments and that the calcrete was of non pedogenic origin but of sub-superficial. According to Carlisle's model (1983), if the carbonate-rich water table is very shallow, a non pedogenic calcrete can overlap with soil formation, as commonly occurs in alluvial fans and sloped landforms. However, in order to describe the actual sequence of events, it is necessary to find out if pedogenesis and calcretization were contemporaneous. For example, carbonate and clay coatings covering clay coatings in the palaeosol fabric would prove later formation of the calcrete, while alternated concentric coatings would suggest contemporaneous formation. The idea that the volcanic ashes of the different sections (CAP, TFR, SJII & SLC) are correlate and correspond to the early Holocene Citlaltepetl eruption, will be discussed in detail in section 5.4.13. Assuming that this age is correct, the calcrete formation occurred simultaneously in TFR and ALB palaeosol after 8,500-9,000 years ago. A rapid calcrete formation would also

support a non-pedogenic origin. Valley calcretes can form as rapidly as 1.3 to 2 metres/kyr (Nash & McLaren, 2003). The most likely source of these salts could be dissolution of carbonates from the limestone of the Cretaceous highlands.
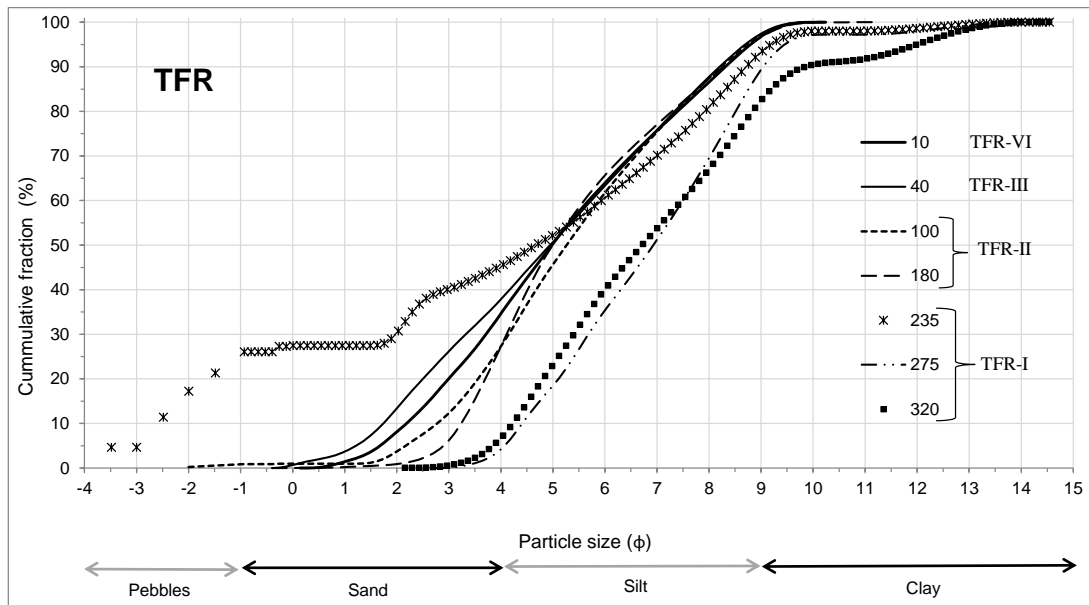
Figure 5.4.7.1. Cumulative percentage of the grain size composition for different facies of the TFR section. Numbers in the code indicate sample depth. Statistical parameters are presented in Table 5.4.7–Appendix B.

5.4.8. Section TPX

The 19-metre deep section TPX is located at the most distal part of the QaIII alluvial fan (2026650N – 648735W; 1662 masl) (Geomorphology map-Appendix A2) and is exposed by a river incision of the named "Barranca Agua la Iglesia" river which runs along the southern sub-basin in a west to east trend (Fig.5.3.2). The section is composed of seven facies (Fig. 5.4.8). Details of its position in the landscape and the tectonic origin of this fan were detailed in Section 5.3.3.2.

5.4.8.1. TPX-I

At the bottom of the section, from 1785 to 1900 cm in depth, a very poorly sorted sandy silt facies, TPX-I, shows a grey colour indicating reduction conditions and no paedogenesis. The characteristics of grey deposits are
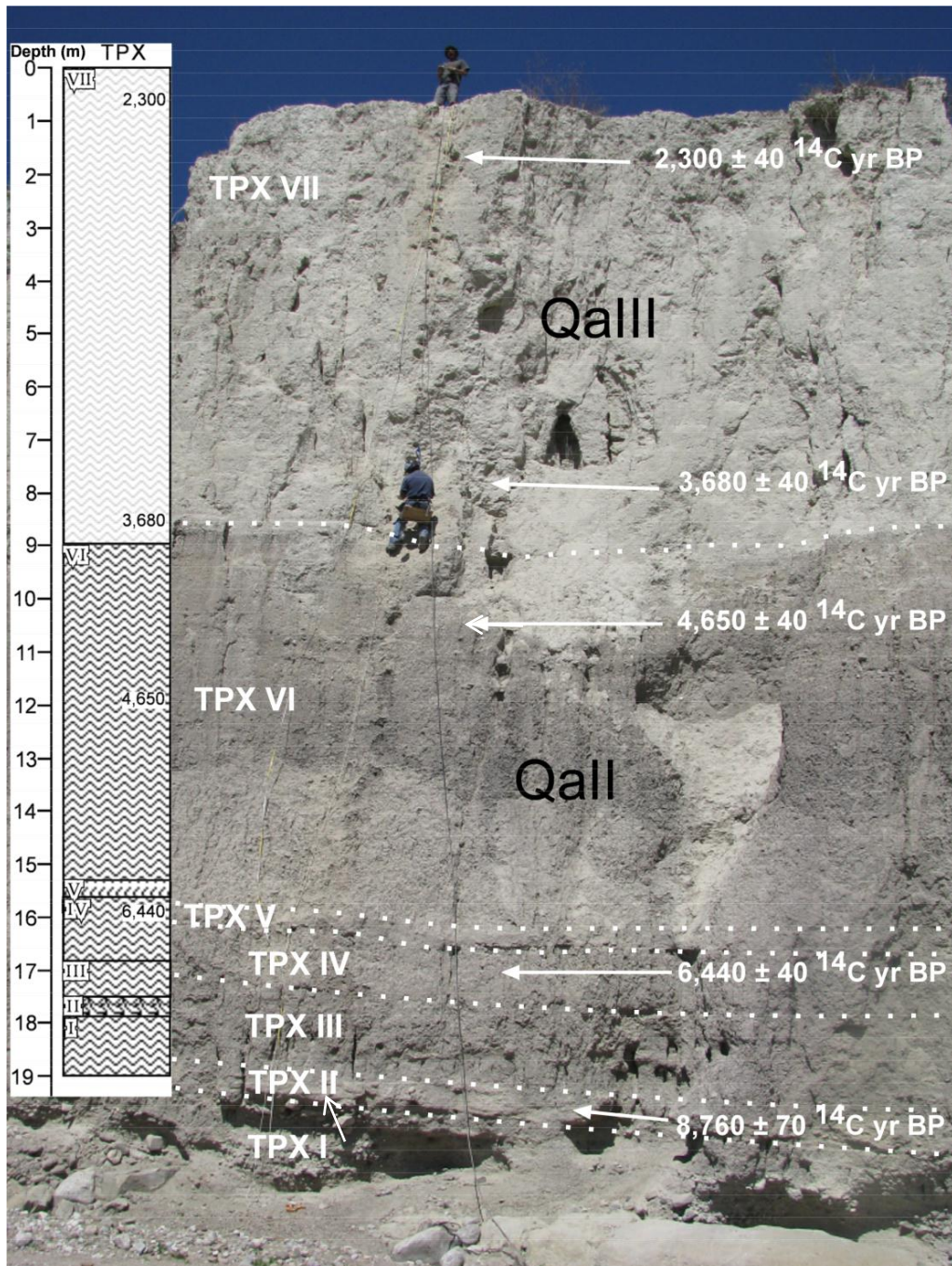
Figure 5.4.8. Sedimentary section TPX showing the main stratigraphic units and schematic representation of the strata. Arrow indicates the tufa outcrop. Codes of the graphic patterns as in Figure 5.4.14.

consistent with those found in other parts of the basin, such as in the stratigraphic section STC. TPX-I pre-dates 8 ky BP and suggests inundation conditions probably as a result of poor drainage that dominated the valley floor before this part of the Holocene. Although reduction features are present in overlain facies of this section, they are more pronounced in this bottom facies.

5.4.8.2. TPX-II

Overlaying TPX-I, there is a tufa outcrop, named unit TPX-II, of around 35 cm (1750 – 1785 cm). This tufa was not examined in sedimentological terms, but numerous plant stem cavities were observed, indicating precipitation of carbonates under non thermal water spring flow (Ford & Pedley, 1996). This unit outcrops laterally for more than 15 metres maintaining its thickness, indicating that it was formed *in situ* and during a relatively short period, most likely as a result of an increase in precipitation. The radiocarbon age of this tufa was 8,760 ± 70 yr BP (Table 5.4.8.1).

5.4.8.3. TPX-III

Above the tufa there is an alluvial deposit (1680-1750 cm) named TPX-III, composed of silty material of medium silt mean size, poorly sorted (Fig. 5.4.8.1; Table 5.4.8-Appendix B). In profile view this unit shows clearly exposed vertical cavities due to differential erosion (Fig. 5.4.8), and considering this feature and the presence of sharp edges and clay cutans in the aggregates, it is suggested that it is a palaeosol. However, the colour of this facies is grey (2.5Y 6/1), indicating poor oxidation and likely reduction of iron instead. In fact all the facies below 940 cm in depth show a grey colour (2.5Y), with variations only between 5 to 7 in value and the same chroma (1).

5.4.8.4. TPX-IV

From 1560 to 1680 cm there is a sediment unit of very poorly sorted material (TPX-IV), with mean and media sizes in the coarse silt range. This sediment is hard with a poorly developed columnar structure and similar to other facies of the unit TPX-VI in textural terms, colour and lack of sedimentary grading and stratification (Table 5.4.8-Appendix B; Fig. 5.4.8). Organic sediment of this deposit was dated at 6,440 ± 40 ^{14}C yr BP (Table 5.4.8.1).
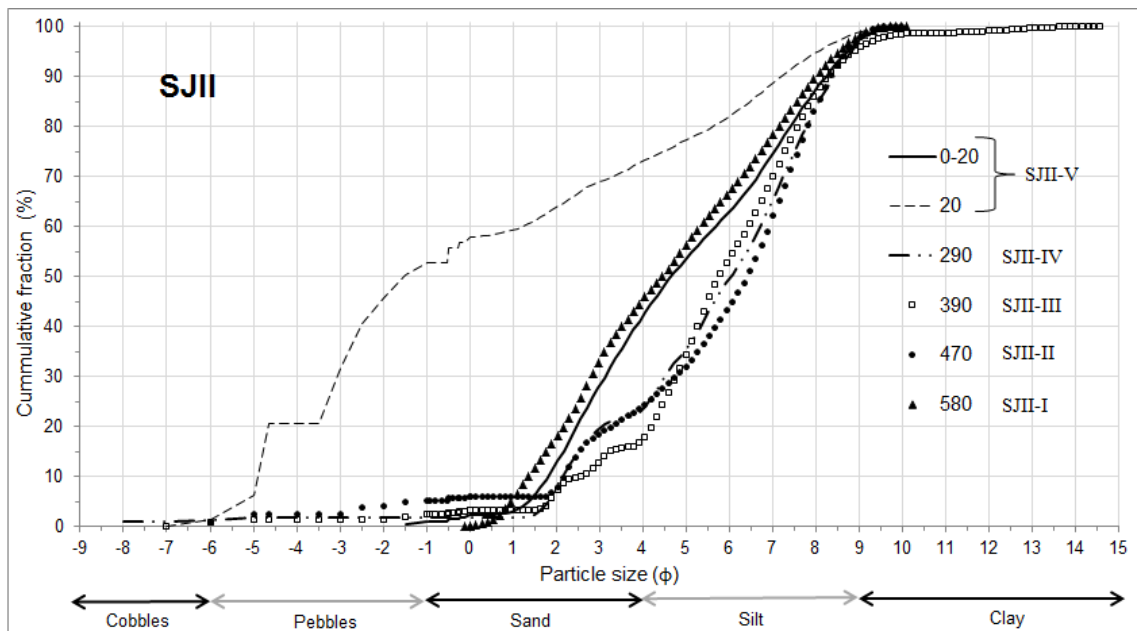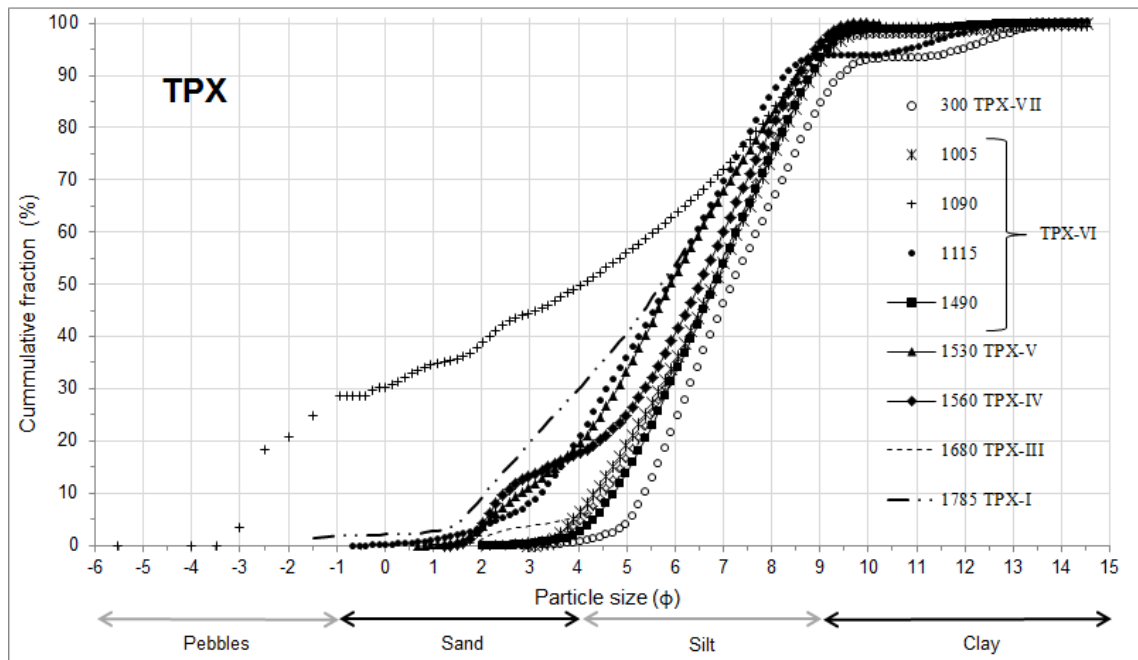
Figure 5.4.8.1. Cumulative percentage of the grain size composition for different facies of the TPX section. Numbers in the code indicate sample depth. Statistical parameters are presented in Table 5.4.8–Appendix B.

5.4.8.5. TPX-V

A prominent facies is found between 1530 and 1560 cm. This unit TPX-V appears to be more resistant to erosion, probably because of its harder condition contrasting with the higher friability of the facies above and below. This unit is more compact, has a weak columnar structure and no grading or stratification. The grain size distribution is very similar to most of the facies in this stratigraphic section. The mean and median corresponds to coarse silt, whereas sorting is very poor, showing a symmetric normal distribution. Pedogenic alteration of this alluvial material is low, but higher than any other deposits along the profile.

5.4.8.6. TPX-VI

Unit TPX-VI extends from 897 to 1530 cm depth in the section. It is formed of a series of alluvial facies of different average grain size. In profile view these facies show horizontal continuity, but there are no clear horizontal sharp boundaries or erosional surfaces. Most of the facies are composed of fine

124

sediments, with a median following in the silt category and a mean grain size also belonging to the silt class, except for the coarsest facies at 1090 cm, whose mean grain size is very fine sand and around 25 % is composed of pebble-sized sediments (Table 5.4.8-Appendix B; Fig. 5.4.8). The statistical parameters of the grain size distribution vary from poorly sorted for the fine facies to extremely poorly sorted in the coarsest one, indicating an alluvial origin and transportation by low energy currents. A date of 4,650 ± 40 ^{14}C yr BP was obtained from bulk organic sediment of this facies at 1190 cm (Table 5.4.8.1). Incision of this unit occurred before deposition of the overlain TPX-VII (Fig. 5.4.8.2).

5.4.8.7. TPX-VII

A massive depositional unit, labelled TPX-VII, covers the top 897 cm of the TPX section. The ages constraining the deposition of this white silty unit are 2,300 ± 40 ^{14}C yr BP and 3,680± 40 ^{14}C yr BP, from samples obtained at 75 and 860 cm respectively (Table 5.4.8.1). No stratification, grading or other sedimentological features are visible in profile view (Fig. 5.4.8). However, hand specimens show very thin (less than 2 mm) and irregular laminations and planar surfaces. Low porosity, light grey colour (5Y 7/1) massive condition and very high friability are other uniform characteristics across the unit. In terms of the grain size parameters, the unit shows little vertical variation. Grain size values and OM of a representative sample are reported in Table 5.4.8-Appendix B. In sedimentological terms this unit has the finest grain composition of all the facies included in this study. The mean and median correspond to fine silt (Table 5.4.8) and is the only positively skewed distribution across the facies. Particles dispersion indicates that the facies is poorly sorted (Table 5.4.8-Appendix B).
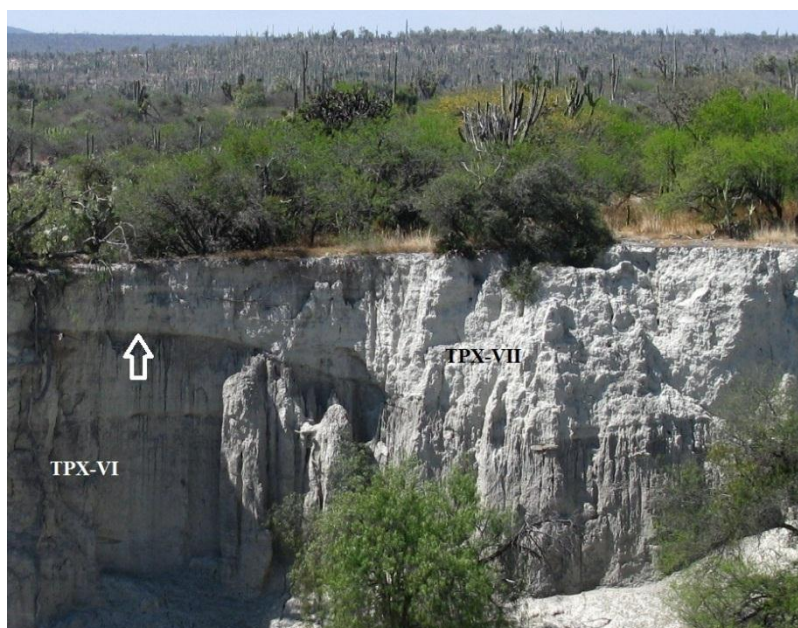
Figure 5.4.8.2. Lateral view of the top sedimentary units of TPX section showing the erosional contact between units TPX-VI and TPX-VII.

Table 5.4.8.1. Radiocarbon dates obtained from the sedimentary section TPX. The sample code includes section name and depth from which dated sample was taken.

Sample	Dated material	Technique	Measured radiocarbon age (yr BP)	Convention al radiocarbon age (yr BP)	Laboratory code
TPX75	Charred plant fragments	AMS	2,080± 40	**2,300 ± 40**	Beta-270095
TPX860	Charred plant fragments	AMS	3,490 ± 40	**3,680± 40**	Beta-270095
TPX1190	Organic sediment	AMS	4,510 ± 40	**4,650 ± 40**	Beta-237048
TPX1590	Organic sediment	AMS	6,370 ± 40	**6,440 ± 40**	Beta-237049
TPX1750	Tufa	Radiometric	8,420 ± 70	**8,760 ± 70**	Beta-279244

Given that this deposit corresponds clearly to an alluvial fan of tectonic origin, the sedimentary characteristics of TPX-VII that differ from other facies could be related to the grain size composition of the original detrital material. This material comes almost exclusively from the lutite of Kl-S in the centre of the basin, as detailed in Section 5.3.3.2. However, it cannot be stated that such differences could be attributed solely to the tectonic origin in the sense that they represent a diagnostic feature.

126

5.4.9. Section CAN

Candelilla section (3 metres deep) was studied by Canúl (2008) in palynological terms as explained in Chapter II. It is located at a dissected QaI alluvial terrace. At profile view three units are defined by differences in structure, colour and differential erosion (Fig. 5.4.9). The lowest unit CAN-I (300-140 cm depth) was dated at 9,310 ± 110 ^{14}C yr BP and is a silty alluvial deposit with the same facies characteristics as those shown by the TFR-I units of section TFR. Near the top part of the unit there is a tephra layer (Figs. 5.4.9; 5.4.13). The unit CAN-II (140-20 cm depth) has similar textural characteristics but the difference in colour indicates a higher organic matter content. Evidence of pedogenic development in CAN-II includes sub-angular aggregates, rizho-concretions, high organic matter and evidence of root penetration. Two radiocarbon dates from this unit are reported by Canúl (2008). Ages of 7,270 ± 90 ^{14}C yr BP and 6,040 ± 50 ^{14}C yr BP were obtained at depths of 105 and 65 cm. The uppermost unit CAN-III is a modern soil composed of mixed alluvial medium grained sediments.
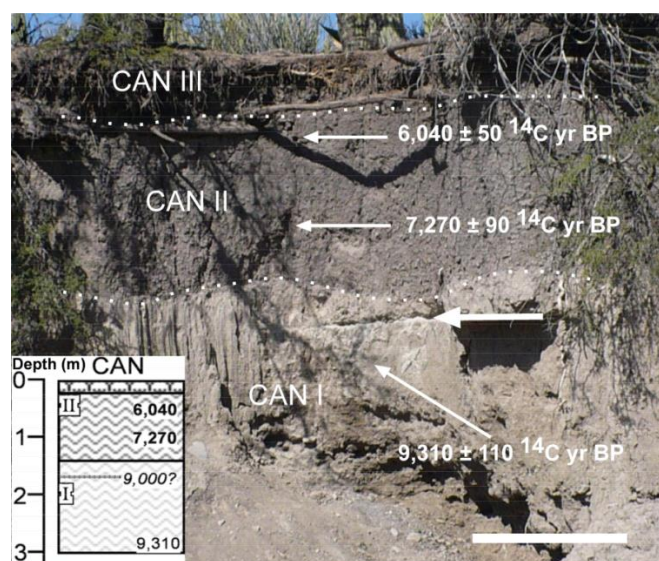
Figure 5.4.9. Sedimentary section CAN and schematic representation of the strata. The open arrow indicates the location of the volcanic ash. The vertical line for scale is 1 m. Graphic pattern codes as in Figure 5.4.14.

5.4.10. Section PV

Downstream from the TPX section, where the QAIII fan joins the alluvial terraces along the BAI, a radiocarbon date was obtained from the upper part of the deposit, giving an age of 1,160 ± 40 ^{14}C yr BP (Valiente-Banuet, pers. comm). The field description of the section is a very fine alluvial material with no pedogenic development, but no quantitative data is available at present (Valiente-Banuet, pers.comm). The geographic coordinates and topographic location of this section, a few hundred metres downstream of TPX fan (QaIII), indicate that it could be a re-worked deposit of the former sedimentary unit.

5.4.11. Section SLC

A pollen-based reconstruction by Canúl (2008) included the study of the SLC section. Four radiocarbon dates have been obtained previously, providing ages of 25,220 ± 160, 12,980 ± 190, 6,790 ± 60 and 5,020 ± 70 ^{14}C yr BP at 760, 480, 360 and 100 cm deep respectively (Canúl, 2008). A field-based description of the sedimentary features of SLC section carried out as part of the present thesis indicates that it is formed of a series of parallel beds of alluvial origin varying in thickness from 10 to 90 cm (Fig. 5.4.10). The lower half of the section up to 440 cm in depth shows different facies, but no clear bedding. The alluvial deposit SLC-I pre-dates the LGM (750-780 cm depth) and is composed of extremely poorly sorted sediments, silty matrix and with very angular clasts of up to 35 cm in diameter, showing a high energy transport. The facies SLC-II and SLC-III are sandy deposits, also with no sedimentary structures and poorly sorted. From 440 cm in depth upwards clear bedding is given by two types of deposits. The most common and of greater thickness are composed of poorly sorted and ungraded deposits, and texturally dominated by sandy silt matrix and gravel. The other type of facies has the same sedimentary characteristics but
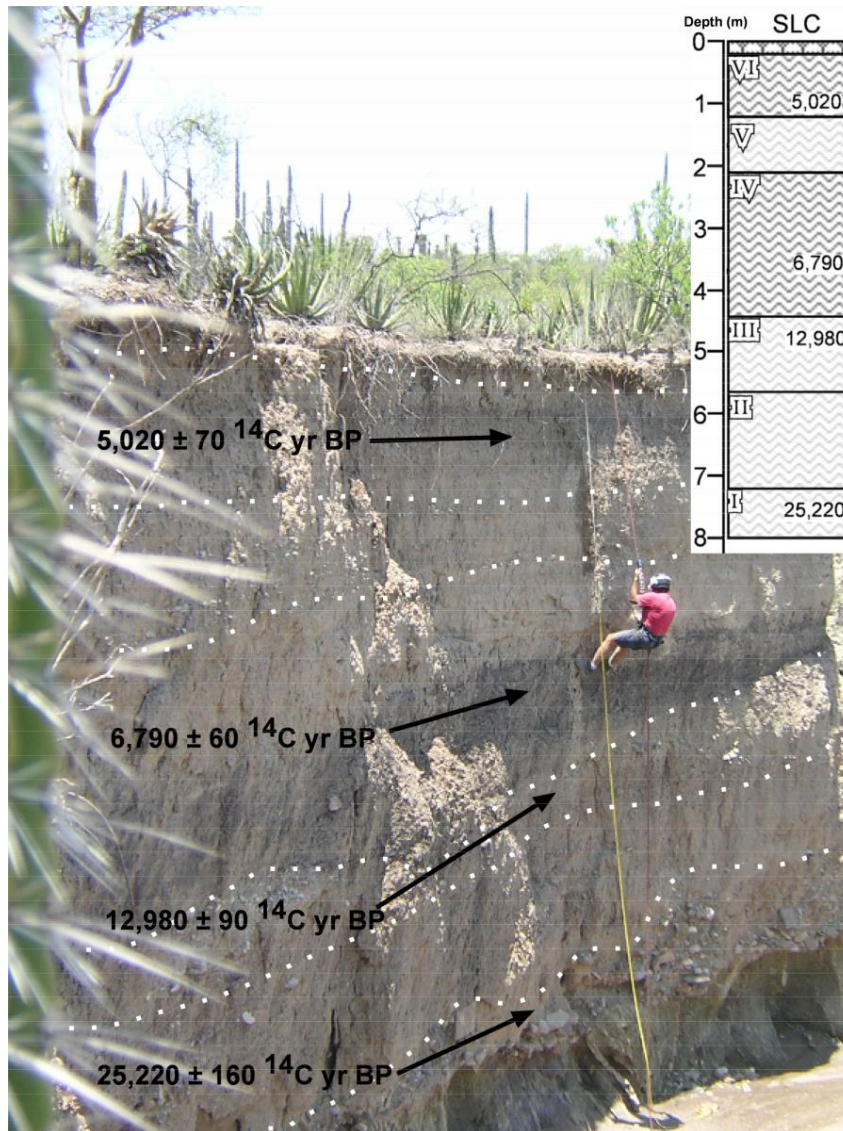
Figure 5.4.10. San Lucas sedimentary section and schematic representation of the strata. Codes of the graphic patterns as in Figure 5.4.14.

can be described as matrix supported gravel, pebbles and small cobbles. The facies between 320-410 cm (6,790 ± 60 ^{14}C yr BP) and 80-115 cm (5,020 ± 70 ^{14}C yr BP) share the same bedding of alternating facies with minor textural changes and are prominent in profile view because of their high organic matter content. Both are poorly sorted polymodal sediments with no internal stratification. These two units show pedogenic features like sub-angular (80-115 cm) or columnar (320-410 cm) structured aggregates, vesicular and root-like

carbonate concretions. At the top part of the section a modern soil has developed from a sedimentary collection similar to the facies profile down.

5.4.12. Carbon stable isotopes.

The carbon stable isotopes ^{12}C and ^{13}C ratio (reported in the standard notation as $\delta^{13}C$) were obtained for dated samples as part of the standard radiocarbon dating procedures (Fig. 5.4.12; Table 5.4.12). A clear, and statistically significant ($p= 0.0064$; $df = 1, 9$), relationship can be observed between $\delta^{13}C$ and radiocarbon age for organic sediments and charcoal dated samples. Values older than the LGM are intermediate between C_3 and C_4, while Holocene samples reflect carbon stable isotopes typical of plants with C_3 photosynthesis. Because of the lack of data, the carbon stable isotopes represent a gap of more than 12,000 years in the chrono-stratigraphy of the SJRB, between the LGM to middle Holocene. The $\delta^{13}C$ for tufa and glyptodont fossils were not included as part of the regression in the context of likely vegetation changes because they are formed by different biological and physicochemical processes.

Table 5.4.12. Sample provenance, type of material and age associated to the carbon stable isotopes plotted in Figure 5.4.12. * Unconfirmed data, from Arroyo-Cabrales (pers. com.). [a] Indirectly measured from the sediment in which the fossil was deposited.

Sample code	Type of material	13C/12C ratio (0/00)	Conventional radiocarbon age (yr BP)
BIS205	Charred plant fragments	-10.9	2,420 ± 40
BIS535	Organic sediment	-19.4	21,400 ± 120
BIS770	Organic sediment	-21.3	28,550 ± 200
BIS840	Organic sediment	-24.3	19,310 ± 120
SJII300	Organic sediment	-15.1	5,190 ± 40
SJII470	Organic sediment	-19.9	19,480 ± 90
TPX75	Charred plant fragments	-11.5	2,300 ± 40
TPX860	Charred plant fragments	-13.2	3,680± 40
TPX1190	Organic sediment	-16.3	4,650 ± 40
TPX1590	Organic sediment	-20.8	6,440 ± 40
TPX1750	Tufa	-3.9	8,760 ± 70
PVM3	Organic sediment	-16.4	1,660 40
Glyptoptherium	Armour rosett	-9.67*	19,310 ± 120[a]
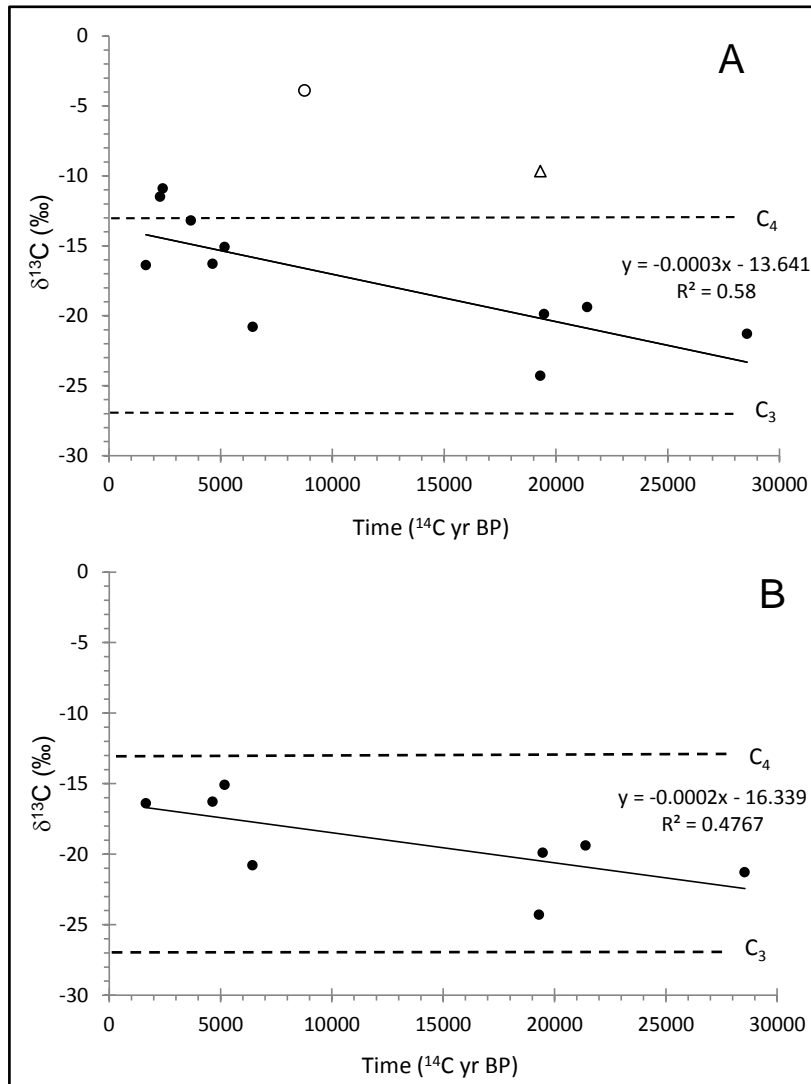
Figure 5.4.12. A: Relationship between age and carbon stable isotopes ratio (δ^{13}C) of late Quaternary sediments and charred material (closed circles), Glyptotherium rosette (open triangle) and tufa (open circle) from the SJRB. Only sediment values were included in the regression in A (p = 0.0064; df = 1, 9). B: Regression of δ^{13}C values for sediment organic matter only (p = 0.058; df = 1,6). The horizontal dotted lines indicate the δ^{13}C for pure C$_3$ and C$_4$ plant assemblages according to Sternberg _et al._ (1984).

5.4.13. Tephra deposits and constraints for correlation

Volcanic ash was present in a number of sedimentary sections- CAN, SJII, SLT and TFR. No organic material suitable for radiocarbon dating, or sanidine crystals bigger 200 μm for ^{40}Ar/^{39}Ar, were found in this tephra, making it impossible to obtain an absolute age. However, the radiocarbon dates of the CAN section constrain the tephra deposit between 7,270 ± 90 ^{14}C yr BP and 9,310 ± 110 ^{14}C yr BP. Other volcanic ash layers of similar thickness and grain

131

size (Fig. 5.4.13) in sections CAN and TFR may indicate contemporaneous deposition. Extensive literature research about the late Quaternary volcanism in neighbouring areas indicates that the closest active volcano is the Citlaltepetl (50 km from SJRB, Fig. 1), also known as Pico de Orizaba. A well dated plinian eruption of this volcano between 8,580 ± 80 and 8,980 80 ± [14]C yr BP (Carrasco-Núñez & Rose, 1995), seems to be the most likely source of these ash deposits. Other active volcanoes were Itztaccihuatl, which was active until late Pleistocene (Nixon *et al*, 1987), Popocatepetl, whose last major eruption was dated at 23,000 ^{14}C yr BP (Siebe, *et al*., 1996) and Nevado de Toluca which erupted at 28,000 and 11,600 ^{14}C yr BP (Bloomfield & Valastro, 1977). The stratigraphic position of the volcanic ashes in CAN, SAL and TFR near the top of an alluvial deposit indicate that they were all deposited during an advanced phase of alluvial activity, providing another line of evidence to establish a probable correlation and a tentative age of between 8,500 and 9,000 years.
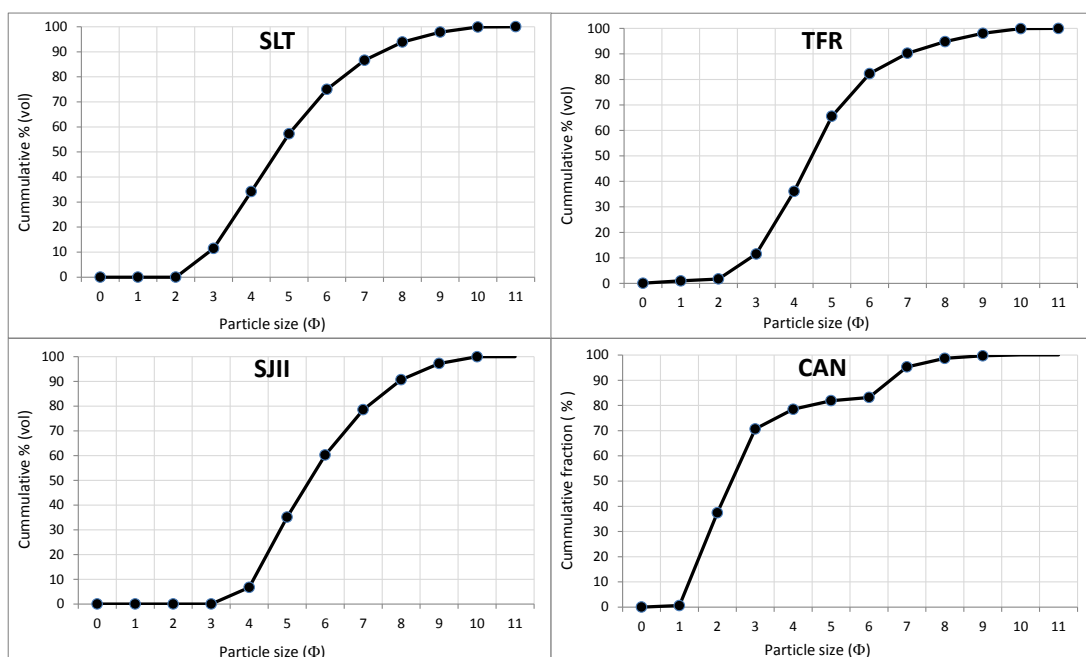
Figure 5.4.13. Cumulative curves of the tephra deposits from sections SLT, TFR, SJII and CAN.

5.4.14. Summary and key findings-Depositional and environmental records

Eleven sedimentary sections of alluvial and pedogenic origin along the basin alluvial system of the SJRB provided a sedimentary and environmental record for the last 28,550 years (Figure 5.4.14). These sections contain a series of facies of alternating periods of alluvial deposition and soil formation as well as chemical deposits and fossils. Different sections showed different sequences of facies, indicating that depositional processes varied with the position in the landscape. The earliest Quaternary deposits represented in the sedimentary sections correspond to the re-working of the QaI surfaces from the north highlands and debris material from the south slope. These deposits indicate the activation of alluvial activity and an early phase of valley filling. Environments at and before 28 kyr (BIS profile) indicate semi-arid conditions, dominance of C_3 vegetation and relatively low basin filling that continued until at least after 25 kyr (SLC profile). These deposits are composed of very poorly sorted material ranging from clay to cobbles and boulders, typical of debris flow type sediments. At around 21 kyr alluvial processes continued but only as low energy flows. Post-depositional processes implicated that this finer alluvial material was subjected to high evaporation rates (gypsum in BIS) under a geomorphic system of a closed and poorly drained basin. The LGM and particularly the end of the Pleistocene were periods of very low deposition and incipient soil development. The re-activation of sedimentary activity occured at least during the latest Holocene around 12 kyr, although different deposits across sedimentary sections suggest that this lasted until after 8 kyr. This period seemed to relate to more available moisture than previously because of the generalised deposition in different parts of the basin and the presence of a tufa

deposit. Apparent geomorphic stability lasted until approximately 7 kyr, when alluviation was re-activated. This middle Holocene active deposition apparently occurred under more humid than present conditions which promoted higher plant biomass and more OM in palaeosols. Deep incision of late Holocene deposits occurred before 3,680 14C yr BP. After incision, localised tectonic activity in the central part of the basin together with climatic instability, produced the displacement of the structural blocks along the Barranca Salitrillo and released the sediment that formed the fine-grained QAIII surface. Since after 2,300 ^{14}C yr BP a period of deep incision and erosion was established in the SJRB and persists until present. Some palaeosols preserved just above the valley bottom (CAP and ALB) also show characteristics of semi-arid environments. However, their stratigraphic position in the Quaternary context was not feasible because of the lack of numerical chronologies.
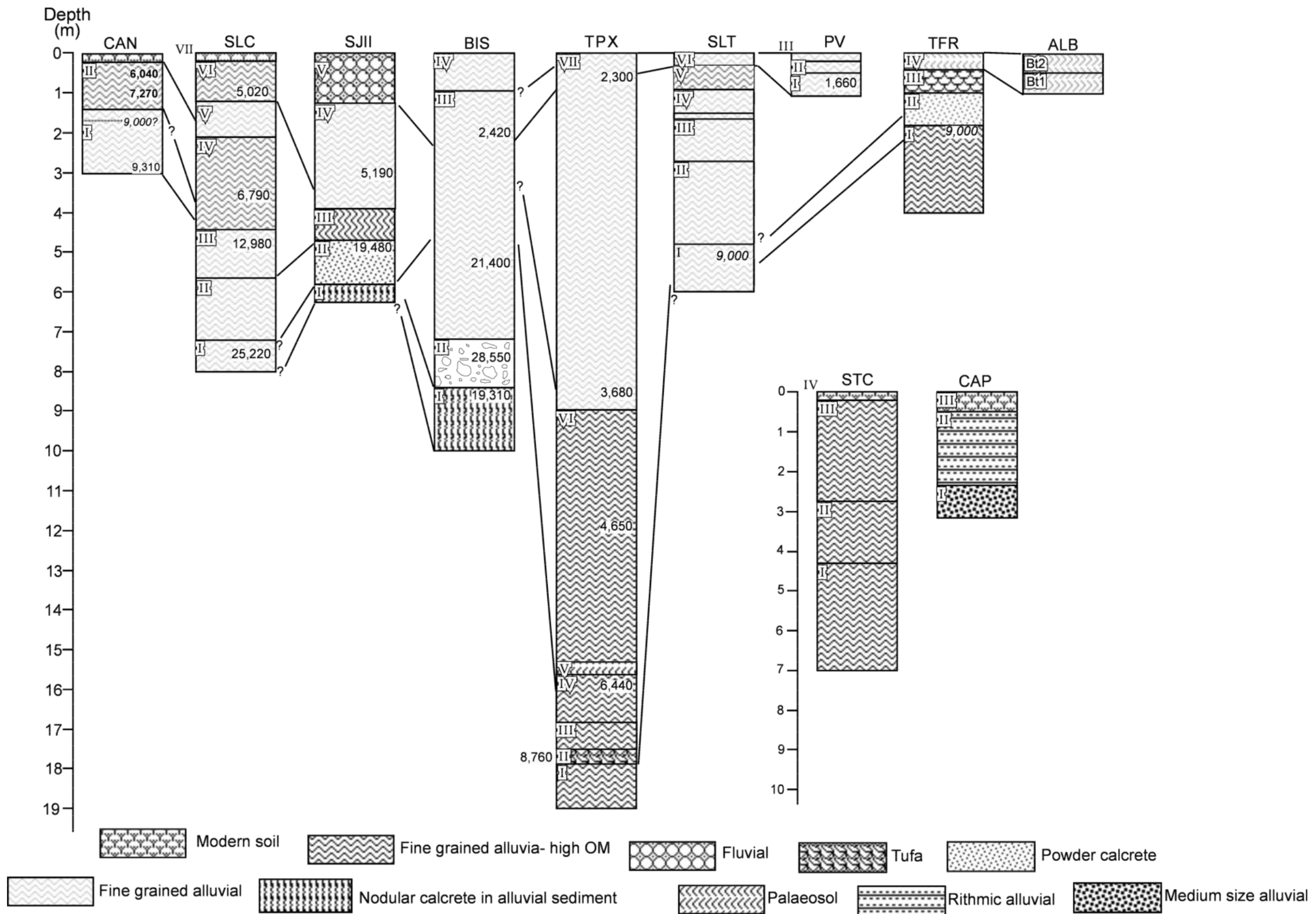
Figure 5.4.14. Late Quaternary stratigraphy of the SJRB. Data from CAN and SLC sections after Canúl (2008). Capital letters correspond to sedimentary units and the numbers indicate radiocarbon dates and are located at the depths from which they were obtained.

CHAPTER VI

DISCUSSION

6.1. Cenozoic regional geological evolution

Intramontane sedimentary basins can form by confining areas inside water divides during the orogenic uplift of structural blocks (Lu *et al.*, 2010), because of horizontal rotation along lateral faults (Christie-Blick & Biddle, 1985) or by vertical displacement of rock blocks associated with inverse (Wysocka, 2009) or normal faulting (Campos-Enriquez *et al.*, 1999). This last type of faulting seemed to be responsible for forming the internal basins of the SMS (Silva-Romo *et al.*, 2000) that occurred after the uplift and folding of the basal Palaeozoic and Mesozoic rocks (Cerca *et al.*, 2007). Numerous folds of the basal late Cretaceous rocks of the Kl-S are clearly exposed (SJR-Geology map-Appendix A1), confirming this tectonic shortening and the initiation of the continental evolution of the SJRB. According to Nieto-Samaniego *et al.*, (2006) and Cerca *et al.* (2007) the first regional episode of shortening (Coniacian-earliest Paleocene) was oriented in an east to west trend and was followed by weaker compression in northeast to southwest until the Eocene. These deformation phases are consistent with the northwest to southeast orientation of the anticline and syncline axial planes observed in the Kl-S (SJR-Geology map-Appendix A1). The structural interpretations of the SJRB by Buitrón and Barceló-Duarte (1980) and Mauvoise (1977) already showed these anticlines and synclines as northwest to southeast oriented. After the orogeny that gave rise to the SMS mountain range, the prevailing tectonic activity was extensional (Nieto-Samaniego *et al.*, 2006). However, the fault system that defines the

136

geometry of the SJRB is difficult to reconcile with the previously described pattern, appearing to be more complex. Different lines of evidence support an alternative model for the tectonic opening of the SJRB: 1) the alignment of the local fault system, 2) the depositional hiatus between Cretaceous and late Quaternary, 3) the likely Miocene overriding of the CIP-Fm and 4) the faulting of the late Eocene-early Oligocene igneous rocks. The results of this thesis indicate that a complex system of faults, oriented ENE-WSW and NE-SW formed the SJRB and probably the ZDLSB after and independent of the tectonic opening of surrounding basins (Table 6.1). Sedimentary rocks of Tertiary age in the SJRB are of igneous origin, with no evidence of fluvial or alluvial activity during the Cretaceous-Quaternary hiatus. Deposits of this type have been extensively reported for the adjacent basins of Zapotitlan and Tehuacan to the east and Tepexi and Coatzingo to the west.

At a wider scale, the SJRB and the ZDLSB are structural depressions that interrupt the continuity of the Zapotitlan range and because their contact borders are faults, a tectonic origin is inferred. However, the major faults that accommodate the displacement of the structural blocks and consequently the opening trend of the basin are oriented ENE to WSW (Fig.5.2.4). These structures are interpreted as normal faults on the grounds of the relative topographic and stratigraphic position of the blocks. The Kl-C limestone block shows contrasting forms. In the central part they are fractured and faulted forming a several hundred metre-high scarp. On the other hand, to the northeast and northwest flanks, the same rocks show conical forms at the summits and lower pronounced slopes towards the basin floor, indicating that these shapes were dominated by erosion processes and not tectonics.

Table 6.1. Summary of the geologic history of the SMS highlands after Nieto-Samaniego *et al.* (2006); Cerca *et al.* (2007) & Silva-Romo *et al.* (2000) [A] and this thesis [B]. TB-Tehuacan Basin; CTB- Coatzingo-Tepexi basin.

Time			Geologic evolution of the Tehuacan region			
			Marine phase	Continental phase		
				Shortening-orogeny	Basin opening	
Era	Period	Epoch	Marine sedimentation [A]	[A]	[A] E-W extensional tectonics	[B] NW-SE extensional tectonics
Cenozoic	Quaternary	Holocene			Active sedimentary basins TB, CTB	Active sedimentary basins SJRB / Fluvial capture by the TB
		Pleistocene				
	Neogene	Pliocene				
		Miocene				
	Paleogene	Oligocene				
		Eocene				
		Palaeocene				
Mesozoic	Cretaceous	Upper				
		Lower				

6.1.1. Geological evolution of the SJRB

Under the tectonic setting proposed in the present work (Fig. 5.2.4.1) the Cipiapa limestone corresponds to the foot wall, whereas the hanging wall corresponds to the KL-S rocks, which constitutes the most extensive outcrop in the basin. The Cipiapa calcareous limestone massifs outcropping between San Juan Raya and San Lucas Tetetitlan towns (CG, CM & CS) were first interpreted as tectonic klippes by Mauvois (1977). According to this author, the Kl-C shows a maximum thickness of 600 metres. The maximum altitude of these rocks in the north slope can reach more than 2,700 masl, while the outcrops at the centre (tectonic klippes known as Cerro Garambullo, Cerro

Mezquite and Cerro Salado) show a maximum altitude of 2,120 masl. This difference means that the tectonic klippes are negatively displaced, harmonising with the idea of a normal fault and a graven setting. Mauvois (1977) observed that the Kl-C does not show the same folding pattern as the rocks which it unconformably covers, Kl-S and Kl-Z, and he claims that the Cipiapa limestone overrode the early Cretaceous rocks during the Miocene. This conclusion was based on the re-interpretation of the geological mapping of the SJRB and other areas of central Mexico located in Guerrero, Morelos, Michoacan and Hidalgo states. Because the Cipiapa rocks rest on Miocenic outcrops of the Tehuacan Formation, Mauvois (1977) assigned a Miocene age to the overriding event. Although it is clear that the Cipiapa rocks were not folded by the same thrust that affected early Cretaceous formations, the Miocene extensional tectonism in the region demonstrated by more recent studies (Nieto-Samaniego *et al.*, 2006; Cerca *et al.*, 2007) indicates that the regional structural thrust had ceased by then, making the inferred overriding of the Cipiapa rocks on younger formations suggested by Mauvois (1977) difficult to understand on the lack of thrusting forces. Although a more detailed geological study is necessary to clarify this uncertainty, a tentative explanation could be to place this overriding during the Paleogene as part of an extended thrust after the shortening of the previously formed rocks and after the most active extensional activation of regional structures.

6.1.2. Tectonic evidence

The faults to the south and east edges (NNE-SSW oriented) of the basin are also marked by scarps. Notably, these faults cut not only the marine Cretaceous limestones, but also the late Oligocene-early Miocene igneous rocks (see

Section 5.2.3), demonstrating that this faulting post-dates the Miocene. Following a similar pattern to the north border of the basin, the footwall blocks are located broadly north of the hanging wall blocks, suggesting that the SJRB is a half graben system (Fig.5.2.4.1). Another major fault runs along the central part of the basin, defining the path of the main river (BAI) (Fig. 5.2.4). Although evidence of this fault is provided by observed slicken-sides, the directions and magnitude of its kinetics are unclear. As this fault is located at the bottom of the basin, the unconsolidated cover does not expose the relative displacement of the blocks strata. In the model proposed here, this fault is part of the same half graben and could also have had normal fault behaviour because the block to the south deepens/subsides at this contact. However, some lateral displacement cannot be discarded. The presence of normal faults indicates that the basin was, and/or is, subjected to extensional tectonism and it is suggested that the SJRB started opening as a tectonic basin at some point after the early or middle Miocene (Table 6.1).

6.1.3. Stratigraphic evidence

The confirmation of the lack of continental basin rocks in the stratigraphic record of the SJRB also supports the former idea. It has been reported that the Tehuacan and Cuayuca-Tepexi basins have been opening since the Eocene and that by the Oligocene and Miocene (see Section 2.3.1) they were actively functioning as continental endorheic basins (Ramírez-Arriaga *et al.*, 2006; Davalos-Álvarez *et al.*, 2007). In contrast, the SJRB does not have records of pre-Quaternary deposition in a continental basin environment. During the extensive field excursions along the valley bottom of the SJRB and ZDLSB, the Cretaceous rocks were found to be overlaid by unconsolidated Quaternary

sediments. If Paleogene-Neogene sedimentary landforms had been formed and intensively eroded afterwards, some remnants should be observed above the basin bottom, as commonly occurs in these types of tectonically active systems (Zhang *et al.*, 2004; Wakabayashi & Sawyer, 2001). However, this is not the case in the SJRB, where the only post-Cretaceous activity is of igneous nature. It has been recorded in other basins that depositional hiatuses caused by intense erosion are common during tectonic compression and extension (Sarmiento *et al.*, 2008). In the Tehuacan basin the most active shortening phase correlates with the lack of basin deposits (Davalos-Álvarez *et al.*, 2007). The hypothesis derived from the observed stratigraphy of the SJRB is that the hiatus between the late Cretaceous and late Quaternary is related to active tectonism and intense erosion. The topographic generalisation and fault pattern of the SJRB and ZDLSB show similar geometric arrangements (Figs. 4.1; 4.1.2). Field observations along Barranca Grande in the ZDLSB also revealed that unconsolidated deposits of Quaternary age cover the Cretaceous rocks in the absence of Tertiary strata, which suggests a likely common tectonic origin for both basins. According to this hypothesis the SJRB and ZDLSB formed part of the highlands until their drainage was probably redirected and captured by the TB after the Eocene-Miocene extension. This process should have implied the transverse crossing of the range that separates the ZDLSB and the TB. According to the synthesis by Douglas *et al.* (2009), four different mechanisms can give rise to transverse drainage. Piracy seems to suit more in this case because it involves abrupt tectonic opening of the upper basins, which we infer from the E-W central fault, and cross cutting and erosion of the topographic highs (Douglas *et al.*, 209).

Although this model was based on the geomorphology of the SJRB, the processes involved can hardly be constrained to superficial local phenomena, and more studies on the internal forces of the crust for this region are needed. The opening of the SJRB should have causes related to a crust mechanism which have not been identified. However, numerous basins of California and the Basin and Range province in south western USA and northern Mexico (Campos-Enriquez *et al.*, 1999; Mack *et al.*, 2003; 2006) provide analogues for these types of processes in which post-orogenic tectonism occurs as a sequence of phases of adjustments displacing magmatic activity and opening tectonic basins at different times due to the activation of new faulting zones (Blair & Bilodeau, 1988; Dickinson, 2002). A number of examples come from other parts of the world (Hudec & Jackson, 2002; Tranos *et al.*, 2008; Yin *et al.*, 2008). In this work a vertical displacement of the bedrock helped to infer normal faulting as the main type. However, is likely that inverse and/or strike-slip faulting could be also involved in the basin deformation as structural blocks kinematics can also change through time. Varying the style of faulting, i.e. transpresional to transtensional, during the process of Cenozoic basin opening is a common phenomenon (Tranos *et al.*, 2008). This type of faulting needs to be revisited by field measurements to determine the rate and direction of displacement, as this can help in understanding the deformation phases of the SJRB.

It is important to consider that this is not a study on structural geology and that because of the lack of data from previous studies on the internal geometry of the geological structures, the hypothesis of Cenozoic tectonic evolution needs to be tested by future surveys. These studies need to focus on

the use of geophysical methods (seismic, gravity, etc.) to describe the sub-surface geometry and the palaeo and neo-tectonic activity. Also, more regional studies are needed to clarify the kinematic behaviour of the faults that opened the SJRB as well as the timing of their activity.

6.1.4. Summary of the geologic evolution of the SJRB

The processes experienced by the SJRB under the influence of regional tectonics during the Cenozoic are summarised below.

1) Folding and lifting of the Mesozoic rocks during the late Cretaceous as part of the Palaeogene orogeny (Nieto-Samaniego *et al*., 2006; Cerca *et al*., 2007).

2) Overriding of the Cipiapa Formation over the San Juan Raya Formation (Mauvois, 1977), before the regional Miocene extensional phase.

3) Post-Paleogene (middle-late Miocene?) activation of the ENE-WSW and NNE-SSW normal faults and opening of the basin by means of a half-graben system (this thesis).

4) Intense erosion during the Miocene-Pleistocene associated to active tectonics and basin opening (this thesis).

5) Capture of the SJRB and ZDLSB drainage by the TB during the Pliocene-Pleistocene (this thesis).

6) Establishment of the approximate current geometric structure of the basin during the Pleistocene and active formation of alluvial deposits and, to a lesser extent, fluvial activity during the Quaternary (this thesis).

6.2. Geomorphological processes

Internally the SJRB shows different generations of alluvial landforms. QaII terraces are found in both sub-basins of the SJRB and represent generalised

alluvial episodes, while the QaI and QaIII fans correspond to a localised tectonic process. A first observation of the alluvial landforms suggests that their size and shape are a function of the catchment area and relief of the highlands up-stream. However, these alluvial fans and terraces can be potentially formed and modified by different factors. The difficulty in unravelling the relative contribution of each one has long been recognised. Alluvial and fluvial deposits can be produced by climate (Waters *et al.*, 2010) or tectonics (Viseras *et al.*, 2003), although often both play concomitant roles (Fontana *et al.*, 2008; Charreau *et al.*, 2009). Tectonics provides the sediment load, sets the relief and changes the potential energy of the sources (Viseras *et al.*, 2003), whereas climate influences detritus transport energy and landform architecture (Bull, 1991; Harvey, 1996; 1999a). In order to succeed in explaining the causes of sedimentary landforms, independent records of climate (Briant *et al.*, 2005.) or tectonics (Quigley *et al.*, 2007) should be provided. For example, a reliable chronology and well-known climatic long-term cycles allowed Maddy *et al.* (2005) to correlate and infer climate driven changes observed in alluvial erosion and sedimentation pulses and distinguish them from tectonics. Even in cases where the tectonic variable has little effect, the type of climatic signal imprinted in depositional landforms shows no uniform patterns. Alluvial fan deposition in some parts of the southwest USA has been attributed to changes from wet to dry in a chain of events (Wells, 1987; Bull, 1991). Increasing aridity is followed by vegetation cover reduction, which in turn enhances the loss of soil mechanical stability (loss of soil colloids, reduced water infiltration) and makes it more susceptible to erosion, finally enhancing alluviation. The inverse climatic change can also produce alluvial landforms. Transitions from dry to wet in the

144

same region, in Baja California in Mexico (Harvey *et al.*, 1999b; Armstrong *et al.*, 2010) and southern Spain (Harvey *et al.*, 1999a) have been accompanied by intensification of monsoon rains in the form of storms which have enhanced erosion and alluvial fan formation.

6.2.1. Quaternary alluvial history of the SJRB

The Quaternary sedimentary landforms of the SJRB seem to have been formed by different aggradational episodes with tectonics and climate involved. Local differences in fault activity such as the ones observed in the SJRB can produce tectonic controlled sediments distinguishable from climatic driven ones in a short distance (Wysocka, 2009). These tectonic patterns seem to explain the distinctive geometry of the different alluvial generations of the SJRB. The first generation (QaI) formed more than 28 kyr ago probably because of an active phase of normal faulting that released important amounts of debris affecting the north sector of the SJRB. In theory, active tectonics can increase the relief gradient supplying a constant level of detritus (Harvey *et al.*, 1999a), which finally feeds deposition. The faulting of the KI-C (north scarp) provided high angle slopes and more exposed bedrock surfaces susceptible to high rates of erosion, which can explain the presence of big areas of badlands and the lack of colluvial deposits in the mountain front. This indicates also that sediments produced there entered rapidly into the alluvial process that created the extensive QaI, which lay directly on Cretaceous rocks. Later episodes of alluvial deposition are represented by late Pleistocene-Holocene QaII terraces and a single fan QaIII of middle Holocene age.

6.2.2. Pleistocene-surfaces QaI

At first sight, the most noticeable feature of the Qf landforms is their asymmetry (Appendix A2). It has been accepted that in asymmetric half graben systems, alluvial fans originating from the hanging wall and foot wall show marked differences (Mack & Stout, 2005). In half graben systems fans are generally steeper and smaller in the active side of the graben (*i.e.* footwall scarps) due to higher rates of subsidence (Blair & McPherson, 2009) and a generally smaller catchment area (Mack & Stout, 2005); or near the mountain front if the rate of uplift and sediment yield exceed that of denudation (Ortega-Ramírez *et al.*, 2001). This pattern can be observed where an extended valley floor is well defined; which is not the case in the SJRB due to more complex basal structures. Here the alluvial fans developed from the south facing slope extend widely with a gentle slope because of a higher catchment area and more pronounced slopes. This difference is assumed to result from a higher rate of subsidence in the hanging wall in the north sector of the basin. Slower rates of subsidence of the southern block and more gentle slopes could explain why QaI fans of south provenance were not formed. Alluvial fans normally develop in a valley area where the slope gradient decreases and a repose angle allows flowing sediments to settle. However, QaI distal parts are found at a certain distance from the present day lowest basin level. Progradation observed in the most distal part of the west QaI, facing the SJRv (Fig. 5.3.3.1), indicates a higher base level at the time of QaI formation compared to its present location. It is common that base level decreases in the distal fan and causes distal dissection (Harvey *et al.*, 1999a), which agrees with the pattern observed in both QaI fans.

6.2.3. Pleistocene-Holocene-surfaces QaII

The lowering of the base level by means of late Pleistocene activation of the E-W fault could also explain a relatively small displacement of the structural blocks separated by this fault and the initiation of QaII formation. A change in base level can trigger the formation of alluvial fans (Schumm *et al* 2000; Harvey, 2002) and/or their deformation (Harvey, 2002). The shift from deposition of QaI surfaces to their incision-erosion plus formation of fine-grained and smaller QaII surfaces, filling the newly created valley floor, are interpreted as low magnitude tectonic lowering of the base level. Because the surface of QaI fans is capped by calcrete and has not been eroded from their central part it is assumed that faulting directed incision to the distal fan and lateral margins. Sediments eroded from QaI were re-deposited as topographically lower alluvial terraces, forming sheets of fine sediments under medium to low energy flow. The cessation of strong alluvial activity (QaI), the lack of contemporaneous fans sourced from the southern highlands and the change of base level at the central part of the SJRB suggest that tectonics was the main control for Pleistocene QaI fans.

Different lines of evidence suggest that QaII surfaces have been climatically controlled. Theoretically, tectonism can be important in the long-term whereas climatic changes can occur drastically (Ritter *et al.*, 1995), being the main force for alluvial deposition. The time span covered by QaII is the last 28 kyr years and during this interval the results suggest a decrease in tectonically produced detritus from the highlands, alluvial re-working of QaI and fluvial incision. This idea is supported by the small volume of QaII deposits compared with QaI, by the vertical and horizontal dominance of fine-grained facies of QaII and the high erosion of QaI. Also, QaII deposits have not been

disturbed by axial or longitudinal faulting; an argument commonly used to infer tectonic quiescence (Ridente *et al.*, 2008). For example, Maher & Harvey (2008) found that in Rio Alias, southern Spain, the Quaternary alluvial deposits were modified by very active tectonics, causing an increase in tortuosity of the meandering channels mediated by lateral migration, incision and rupture of the sedimentary landforms by perpendicular faulting. Also local incision was attributed to tectonics given the opposite regional deposition caused by climate change. No evidence of this type was found affecting QaII landforms.

With the change of base level in the central part of the SJRB, the process of filling the valley bottom was initiated (QaII). Beds conforming these small fans and terraces include fine and medium grained alluvial layers alternated with a number of poorly developed palaeosols. These deposits form almost continuous sheets that can be followed hundreds of metres along the "Barrancas" even at relatively high levels in the south and east highlands (See geomorphology map). Deposition along highland channels happens because transport capacity decreased as a result of the lowering of the channel slope gradient (Schumm *et al.*, 2000) or because sediment supply increases beyond the stream discharge capacity (Blum & Törnqvist, 2000). The oblique tilt of the southern block implicates uplift with respect to the adjacent block of the ZDLSB and deepening towards the central part of the SJRB. The formation of QaII terraces along highland channels does not fit with an increase in subsidence of this block, which would produce a more pronounced slope and higher channel gradients preventing accumulation. Because little change in subsidence is inferred, a climatic control on QaII is more plausible.

6.2.4. Holocene- surfaces QaIII

In the lowest part of the floodplain the sedimentary sections BIS, STC, SLC & SJII reach depths between 6.3 and 10 metres. The bottom facies yielded ages of 28 kyr whereas near surface sediments date back to between 5 and 2.4 kyr and provide a rough idea of the sedimentation rate (although it is not constant, as can be seen by the numerous vertical discontinuities). These sections correspond to QaII surfaces and contrast with QaI fan-TPX section in which nearly 18 metres of fine sediment were deposited in only 8.7 kyr, with a broad sedimentation rate of 2.4 metres per millennia. Such a difference can be explained by the tectonic activation of a central block, which locally lowered the base level probably during the early Holocene, enhancing erosion and deposition of QaIII. Considering the proximity of SLT and BIS sections (Appendix A), the differences in facies sequence under the correlation scheme presented in Figure 5.4.14, cannot be explained by differential landscape position without referring to the fault system surrounding QaIII. As explained in Section 5.4.8, this alluvial fan was fed by fine sediments released from the faulted lutite of the central highlands of CS. Intermittent continuous deposition and soil development until after 2.4 kyr observed in BIS suggests climatic fluctuations. Hence, QaIII development is interpreted as being caused primarily by tectonics and secondly by climate.

6.3. Palaeoenvironmental change

The evidence of climatic signals in the sedimentary records of the SJRB is complex. As discussed previously, the main factor that produced the unconsolidated sedimentary record was initially tectonic. However, it is likely that climatic changes could account for the contrasting facies seen in the profile view of QaI fans. Alternating beds of alluvial deposits of different

149

sedimentological characteristics and palaeosols could have been formed as a result of contrasting environments. It was observed that most of the sediments deposited had suffered little or no subsequent alteration, suggesting rapid rates of deposition during the late Quaternary, whereas the lack of induration of those deposits indicates that they were deposited, and palaeosols developed, probably during the late Pleistocene.

6.3.1. Pleistocene-climatic pattern

The Pleistocene is represented by the oldest unconsolidated sediments in the SJRB and corresponds to a period of global interglacial condition. However, a lack of detailed palaeoclimatic reconstructions in adjacent regions, together with the likely tectonic origin of QaI, mean that the environmental reconstruction for that period in the Tehuacan region is highly constrained. Under the scenario proposed from the results of this research, sediments were released at a high rate because of very active tectonics in the north sector and mobilised rapidly to form the extended and deep QaI alluvial fans. High volumes of sediment were deposited because the transport capacity of the fluvial network was exceeded. This Pleistocene deposition occurred at a higher base level of the basin compared to the present depocentre. Brief episodes of geomorphic stability allowed some sedimentary facies to develop incipient paedogenesis during the Pleistocene. Further chronological controls as well as detailed studies of those sedimentary sequences of QaI group are necessary in order relate those changes to climatic patterns. It is known that the late Pleistocene was characterised by shifts from cold interstadial events to warmer periods in cycles in the order of thousands of years (Dansgaard *et al.*, 1993). Such changes had a global impact on Earth Surface Systems by modifying climate regimes even in

subtropical regions. However, there is almost no data on their effects on subtropical central Mexico. In general, the last 8 kyr are considered to be a period of relative climatic stability only comparable to a short warm period (at least as warm as the Holocene) that occurred around 125 kyr ago (GRIP members, 1993). It is likely that active tectonics and rapid climate shifts during the late Pleistocene were involved in the initial filling of the SJRB. Dating the depositional episodes of QaI is a necessary first step towards the analysis of the likely influence of Pleistocene climatic oscillations on local environmental conditions.

6.3.2. Calcretes in Pleistocene surfaces

Another insight into the environmental conditions related to QaI fans could come from the presence of surface calcretes, which can potentially hold a climatic signal. It has been discussed that calcretes can have an environmental significance depending on the processes involved in their formation, pedogenic or non-pedogenic. The most important factors forming calcretes are the presence of a water table, concentration of solutes, physicochemical conditions (CO_2 degassing, evaporation rates) and the amount and type of biological activity. With the information available to-date, it is problematic to distinguish the factors involved in the formation of calcrete on QaI, and perhaps the most challenging is to disentangle whether it was formed in a soil environment or related to underground water. According to Wright *et al.* (2007) this distinction can be achieved despite the fact that they often overlap. Calcretes capping the QaI fans are highly indurated and show a platy structure overlapping a massive hardpan, characteristics that could either be paedogenetic or water table related (Wright *et al.*, 2007).

Although pedogenic calcretes can form in diverse environments, their presence in the SJRB could indicate enhanced arid conditions. The carbonate source for pedogenic calcrete formation is mainly atmospheric dust, although plants, microbial activity and weathered clasts can also contribute (Dixon & McLaren, 2009). Pedogenic calcretes form in arid and semi-arid lands by illuviation and precipitation of carbonates, favoured by high evapotranspiration rates (Gile *et al.*, 1966). This type of calcrete requires geomorphic stability for long periods of time. In the southwest USA, soils derived from non-carbonaceous rocks can show initial morphological expression of pedogenic calcrete in only 100 years, while for indurate pedogenic hardpans (stages III of Gile *et al.*, 1966), like those developed in QaI, it can take more than 25 kyr to develop (Gile *et al.*, 1998). QaI calcretes show no morphological evidence of the initial stages of the K horizon which suggests that, if they are pedogenic, they were developed over thousands of years under long-term landscape stability and an arid climate. Although to-date this form of development cannot be discarded, other characteristics of the QaI surfaces suggest possible groundwater origin.

In the model proposed in this thesis after deposition of QaI fans, their location in the landscape locates them as a surface of transit of water and sediment from the north calcareous limestone highlands. For non-pedogenic calcretes groundwater is the main contributor of solutes (Dixon & McLaren, 2009). QaI Calcrete could have developed because of non-pedogenic precipitation of carbonates from water infiltrated through the calcareous limestone. The development of a thin tufa stratum at the bottom of the TPX section around 8.7 kyr (see Section 5.4.8) can be considered a smaller scale

analogue of carbonate precipitation derived from saturated ground water flow. Although the processes of tufa precipitation differ from those of calcretes, this demonstrates the underground migration and discharge of water captured in the highlands. If the calcrete of QaI was developed in a groundwater environment, it would suggest that the climate was semi-arid, but more humid and perhaps with a weak seasonality compared to the present. This would seem to be inconsistent with Alonso-Zárza's revision (2003), where she indicates that intermittent heavy rains are associated with more developed groundwater tables. However, it must be considered that the SJRB is a first order basin of small size and that rainfall moisture is rapidly transferred to the adjacent basins and infiltrated. This constrains the development of a groundwater system to locally received rain; whereas for higher order basins the water table can be sustained by more prolonged water inputs after episodic rains. Low intensity and more evenly distributed rains in the SJRB would maintain a higher level of the water table in the alluvial fans and would not be a factor of strong head-ward erosion. This calcrete could have developed in a relatively short period of time, which would be consistent with the proposed tectonic change of base level. In terms of environmental setting, soil associated calcretes are more common in fine-grained substrates, while those developed close to the water table tend to form in more permeable substrates like alluvial fans (Wright *et al.*, 2007; Mack *et al.*, 2000). Dixon & McLaren (2009) indicate that calcrete can precipitate rapidly because of a decrease in groundwater level or on a drainage surface, conditions that could probably have been established in QaI surfaces during the Pleistocene. Laminar flow in the alluvial fans is a condition that could have occurred in QaI and that is typical of calcretes formed in these types of

landforms (Nash & McLaren, 2003). After the change of base level and incision of Qal, the distal part of these fans did not receive laminar flow, and drainage had since been confined to rivers, supporting the idea that those calcretes are Pleistocenic.

The former scenario is outlined as the most plausible explanation; however, more detailed studies need to be conducted to test those hypotheses and to clarify the environmental conditions during their formation. A detailed study of the calcretes is necessary to disentangle their nature. Micromorphology analysis would be of high value to test the alternative environmental scenarios during their genesis. If formed under soil conditions, the micro-fabrics of the calcretes would show biological influence of calcite precipitation (alpha fabrics), whereas their absence and other characteristics associated with groundwater formation, like type of spar and micrite forms (McLaren, 2004; Nash & Smith, 2003; Wright *et al.*, 2007; Zhou & Chafetz, 2009), would lead to different landscape interpretations.

6.3.3. Late Pleistocene-Holocene-climatic correlations

The stratigraphic correlation of the sections studied recapitulates the late Pleistocene and Holocene palaeoenvironmental records of the SJRB (Fig. 5.4.14). The lowest unit (BIS-I) corresponds to the earliest known alluvial valley filling after the tectonic lowering of the base level. This deposit and the one dated at 28.5 kyr were probably formed as a product of the drastic changes in temperature and precipitation that accompanied the changes towards a glacial phase (see Table 1). Between approximately 35 and 27.5 kyr ago four highly defined and interstadial events took place (interstadials 8 to 5) (Dansgaard *et al.*, 1993), characterised by abrupt shifts to milder conditions from previous

colder stages (Bond *et al.*, 2001). These milder interstadial events, which started rapidly and shifted gradually towards cooling cycles, had an impact in the North Atlantic Ocean circulation (Johnsen *et al.*, 1992). As explained in Section 2.3.2, warmer climates enhanced circulation in the Circum-Caribbean region, carrying more moisture to central Mexico. The extent to which these shifts towards mild conditions, and the atmospheric response time (Phillips, 2009), led to enhanced precipitation in the Tehuacan is unclear given the high variability of these events (Johnsen *et al.*, 1992). It is still possible that one of those shifts produced higher precipitation and more sediment movement towards the basin bottom. High erosion rates were likely to have been prevented because denser vegetation was present in the SJRB as suggested by the stable isotope results. Very negative δ^{13}C values suggest that at this time vegetation was mainly composed of trees and shrubs, while the presence of *Glyptotherium sp.* indicates open spaces in which grasses and other C_4 plants developed. This clearly suggests higher moisture availability compared to the present. Locally, colder than present temperatures, compatible with a higher abundance of pine pollen (Canúl, 2008), and semi-arid conditions are inferred before the LGM. The possible landscape was of a closed basin with very brief periods of inundation in the valley area. The development of calcrete nodules in BIS-I indicates the presence of a groundwater table and high evaporation rates which, together with the well preserved *Glyptotherium sp.* which indicates no pedogenic development, support the idea of a semi-arid environment. During the last stages of BIS-I, before deposition of BIS-II, the basin could have experienced longer periods of inundation and enhanced evaporation under a dry climate that provided conditions for precipitation of gypsum crystals. Again,

excursion to mild periods during the interstadial prior to LGM could account for more precipitation and higher evapotranspiration rates. The suggested environment of a poorly drained basin with a sporadic water body at the valley level is supported also because, as no plants colonised the valley, soils were not formed either. The depositional event recorded at 25 kyr (section SLC) coincides with interstadial event 4, and probably represents an analogue deposition produced by a rapid increase in precipitation, which shifted again to colder conditions (Johnsen *et al.*, 1992).

An evaporative closed basin under a semi-arid climate is supported by the presence of megafaunal fossils, which are commonly found in the proximity of water bodies. Although the identification of the glyptodont to species level was not possible because of the poor preservation condition of the exposed osteoderms, the extinct species *Glyptotherium mexicanum* and *Glyptotherium cylindricum* of known Mexican distribution are the likely candidates. Preliminary isotope results suggest that this glyptodont had a mixed diet ($\delta^{13}C_{VPDB}$ -9.67; $\delta^{18}O_{V\text{-}SMOW}$ -3.83) (Arroyo-Cabral, per. comm.) and studies of the masticatory apparatus indicate that these animals were probably grazers (Fariña & Vizcaino, 2001). Fariña and Vizcaino (2001) suggested that because of the lack of tooth enamel and the low position of the jaw, glyptodonts' mechanical masticatory systems were no less efficient than normal grazers and that to compensate they should have enough available plant biomass. Considering their significant weight (up to 2 tons), they would need a denser vegetation than the one presently established. These animals were commonly found in grasslands and open savannahs (Gillette & Ray, 1981). As there are no modern analogues it is difficult to obtain a precise environmental reconstruction of the

ecological requirements (Bago, 2003); however, according to Gillette and Ray (1981), glyptodonts lived in the proximity of currents or water bodies, supporting the idea of a variable water body in the central part of the SJRB. Mead *et al.* (2007) indicate that the external armour of glyptodonts provided poor insulation for thermal conductance and hence needed a warm climate. Even at their northernmost distribution in the USA, they were restricted to tropical and sub-tropical locations along the Gulf of Mexico. The glyptodont was not found in South American localities that showed very arid conditions, whereas its close relative *Panpatherium* was commonly found in these locations and also evidenced grazing anatomy better adapted to this type of environment. The fact that glyptodonts required a permanent source of water and have been reported in the tropical and sub-tropical southeastern USA and Mexico (Mead *et al.*, 2007) but not in Arizona and New Mexico in LGM deposits, also suggests that there was water available under a semi-arid climate.

The period between 25.5 to 19.4 kyr was of relative geomorphic and climatic stability with constant and very low rate deposition filling the valley floor, suggesting low intensity rain or perhaps low seasonality. In section BIS thin fine-grained alluvial beds alternate with young palaeosols indicating instability and stability periods. Seasonal inundation and filling of the basin floor with fine sediments took place under high evaporation rates, while lateral groundwater (carrying solutes from the southern limestone highlands) promoted calcretization of the sediments located at higher levels of the basin floor (SJII). The poor soil development and low organic matter across palaeosols could also be indicative of low productivity and semi-arid conditions; although higher effective moisture than present could be responsible for the negative δ^{13}C

values, which indicate that vegetation was still dominated by trees and shrubs. In Section 3.3.3 the hypothesis presented indicates that global cold conditions and weaker thermohaline circulation could probably cause low precipitation and seasonality in central Mexico, and this is possibly the cause of that geomorphic stability. Sea levels decreased by around 100 m and because the Gulf of Mexico is a passive margin with a gentle slope, a decrease in sea level could also translate into a lateral migration of many km, most likely enhancing aridity. Increased aridity during the LGM could cause a gradual decrease in vegetation cover, and slow slope erosion because rains remained weak, not very seasonal and locally reduced by the rain shadow (Table 1).

No drastic sedimentary or important pedogenic activity was identified between the LGM and latest Pleistocene, indicating relative geomorphic stability and perhaps decreasing precipitation. However, because few erosional events were identified for this period across the sedimentary sections, a very low rate of deposition until the latest Pleistocene is attributed to relatively stable conditions. This is surprising if we consider that the end of the Pleistocene was characterised by high climatic instability, especially during the phases of LIS melting, and that hypothetical instability was expected (Table 1). Although pollen variations (Canúl, 2008) and the observed decline in C_4 plants clearly suggest a climatic deterioration, the lack of sediments between the LGM and the Holocene do not allow us to follow the trend during this period. Perhaps the response and resilience of the ecosystem account for the apparent geomorphic stability, including the soil factor, and the fact that colder than present conditions prevailed for most of the end of the Pleistocene. Another factor that could have contributed was that high seasonal rains were not established at that time,

implying less risk of erosion. Weak rain during the late Plesitocene may have caused little sediment mobility and deposition along the hill slope rivers and valley floor, causing gradual slope denudation. The presence of filling in the headwaters zone is normally temporal as they tend to be removed rapidly (Mial, 1981); however the presence of alluvial terraces located at middle altitudes at the south and east slopes of the SJRB can only be explained by low intensity rains and a stable soil mantle supported by vegetation cover. The opposite condition is present today, in which vegetation has been reduced and clear signs of soil erosion can be observed. Under the modern highly seasonal climatic pattern, rains occur as short episodes of high intensity which dissect the alluvial surfaces carrying a vast sediment load. These massive flows composed of a mixed load of sediments are known locally as "barrancadas" and year after year change the shape of the lower parts of the alluvial terraces. An inverse pattern from Pleistocene-middle Holocene basin filling to a late Holocene-modern time erosion and dissection is clear.

Sediments dated at 12.9 kyr (SLC) correspond to alluvial deposition and are perhaps one of the last depositional faces of the relatively stable end of the Pleistocene. Despite the date de-phasing, the only important climatic phenomenon during that period is the Younger Dryas, which ended 10,700 years ago (Dansgaard *et al.*, 1989). This event, however, was a high-magnitude regression to cold conditions during the transition to a warmer Holocene. The link between this event and the deposit mentioned is not clear and requires more detailed analysis. It has been argued that the North Atlantic region responded rapidly (sometimes in the scale of decades) to climate changes (Dansgaard *et al.*, 1993). However, because SST and circulation processes

affecting the SMS are mediated by those high latitude oceanic patterns, the response may take longer and become out of phase, masking the effect.

6.3.4. Holocene-climatic correlations

Conditions turned more humid during the Holocene; time marked by the re-activation of depositional events of various intensities recorded across the sedimentary sections around 9 to 8 kyr. It was during this high insolation period that perhaps more moisture penetration caused soil erosion and deposition on the valley floor (see Table 1). This was enhanced by the decrease in plant cover and perhaps gradual change of vegetation during the end of the Pleistocene. The high organic matter in the sediments corresponding to middle Holocene also suggests more productivity and higher available moisture than before.

Hill slope rivers in the SJRB also accumulated sediment and presented an alluvial behaviour during the early and middle Holocene, suggesting that although summer pattern and increased precipitation prevailed, the rain pattern was not markedly seasonal and storms were of lower intensity compared to present conditions. Increasing precipitation has been related to shifts in river morphology from alluvial to fluvial, accompanied by deep incision (Springer *et al.*, 2009). According to Bull (1991), a self-enhancing mechanism of hill slope erosion and alluvial aggradation can result from a rapid change from moist to arid conditions, such as those that occurred between 11 to 6 kyr in the American southwest and northern Mexico. Prolonged droughts translate into reduced plant cover, which in turn triggers soil erosion. Bull (1991) observed that this accelerated sediment transport shifted river behaviour from a "degradational to an aggradational mode of operation", producing basin filling and alluvial fan formation. Low energy flows in the SJRB during the Holocene

160

are the likely cause of aggradation, while high energy produced debris or degradation (Bull, 1999).

The Holocene was the most active time period in the SJRB with sediments yielding ages at millennial scales. Across the sections, the Holocene represents between three and 6 metres of sediments, except for section TPX, in which at least 18 metres of sediment were deposited since 8.7 kyr. CAN section records the resuming of basin filling with alluvial sediments as early as 9.3 kyr. A preliminary age for the tephra layers in different sections is assigned between 8,500-9,000 years ago on the basis of their stratigraphic position and the reported plinian eruption of the Citlaltepetl volcano at that time (see Section 5.4.13). The deposits in which these ashes are incrusted correspond to increasing runoff and intermittent alluvial deposition and no later pedogenic or diagenetic alteration. The tufa outcrop from TPX was dated at 8,780 ^{14}C yr BP, indicating likely wetter than previous conditions. Sedimentation during the early Holocene was not continuous, but interrupted since 9,000 years ago. This is inferred because several sections show an abrupt contact with the superimposed facies, indicating a pause in sedimentation (CAN & TFR) or erosion (SLT). Holocene alluvial deposition re-started at least since 7.2 kyr, and was followed by paedogenesis as shown by the organic palaeosols of CAN and SLC. In fact, SLC shows that this soil development was interrupted by an increase in runoff and later re-establishment of similar pedogenic conditions at middle Holocene that led to the upper organic palaeosol. Key characteristics like high organic matter and pedogenic features of the SJII-IV palaeosol (dated at 5.1 kyr) as well as middle Holocene pedogenic facies of TPX which reconcile with this idea. Palaeosols between 7 kyr and 5 kyr could indicate more biomass

productivity and periods of wetter than previous weather, interrupting the trend towards more arid conditions. The dominance of CAM and C_3 functional groups can also be considered proof of this tendency (see Section 5.4.12).While the type and thickness of middle Holocene deposits are more or less uniform across sedimentary profiles, noticeable high rates of deposition are recorded in TPX after 6,440 ± 40 ^{14}C. More than 15 metres of alluvial facies showing almost no pedogenic evidence represent a broadly continuous sedimentation until late Holocene. Two main sedimentary units correspond to this time. The lower is composed of alluvial deposits with higher organic matter and variations of bedding main grain size, from fine to medium sized clast. The upper part is almost 9 metres thick and was deposited between 3,680 and 2,300 yr BP. A phase of relatively shallow incision occurred just before the TPX-VII unit was deposited, which had taken place between around 3.6 to 2.3 kyr. In order to understand the presence of this massive deposit the tectonic evidence must be considered. The TPX-VII corresponds to the QaIII alluvial fan mapped and described in section 5.3.3. It is bound by normal faults, including the Cerro Salado fault (see photo showing triangular facets-section 5.3.3), and lies on the collapsed block, which was filled by the sediment yielded by the Cerro Salado lutite. According to the model proposed in this thesis, active normal tectonism lowered the base level on which TPX-VII currently lies. These active tectonics released fine-grained sediment from the limestone of Cerro Salado and bigger clasts from Cerro Mezquite. Under higher than present precipitation, alluvial debris flow-type fan formation was enhanced before the Holocene fine-grained alluvial deposition took place. Late Pleistocene intense erosion was followed by normal faulting and deposition of early Holocene alluvium. This tectonic vertical

motion preserved the debris flow deposits containing boulders of the Cerro Mezquite dolomite exposed at the western limit of QaIII-TPX. Under a climatic regime of higher precipitation than present, medium energy alluvial deposits formed the QaIII fan, fed exclusively of lutite.

Since at least 2,300 ± 40 ^{14}C yr BP the geomorphic phenomena characterising the SJRB has been of intense head-ward erosion and incision of alluvial fans and terraces. It is inferred that the modern climate of aridity and high seasonality was established after the middle Holocene. Establishment and/or intensification of monsoon rains can cause deep channel incision of alluvial surfaces (Narayanapanicker *et al.*, 2007), which seems to have occurred regionally during the late Holocene. Palaeocurrents are not widely distributed in the basin floor or hill slope rivers, confirming the dominance of alluvial processes before the deep incision phase.

6.3.5. Vegetation changes

The changes we observed in the stable isotope values also suggest vegetation changes. According to Brunner (1982) the LGM represented the lowest temperature of the last 40,000 years, after a gradual decline in temperature since around 35,000 years ago, while the Holocene is the warmest period during the last 90,000 years. The usefulness of δ^{13}C in the sedimentary record for reconstructing physiological patterns of palaeovegetation is well-known (Cerling *et al.*, 1989). Groups of plants with contrasting physiological pathways, C$_3$ (*i.e.* trees, shrubs), C$_4$ (*i.e.* grasses) and CAM (*i.e.* cacti) incorporate carbon stable isotopes in different ways. Positive values indicate enrichment in the high mass isotope (^{13}C) relative to the standard (Koch, 1998). For pre-industrial times, the carbon stable isotopes of the atmospheric CO$_2$ (δ^{13}C) were around -

163

6‰ (Cerling, 1984). Vegetation composed purely of C_3 plants would have a $\delta^{13}C$ a value of -27 ‰, whereas -13 ‰ is the norm for C_4 plants, with CAM plants having intermediate values, varying from -11 to -22 ‰ (Sternberg *et al.*, 1984). When this plant biomass becomes part of the sedimentary record, it carries the signature of the dominant metabolic pathway.

Viewed in very simple terms the stable isotopes results (section 5.4.12) suggest that significant vegetation changes have occurred in the SJRB over the last 28 kyr. Broadly, between 28 to 19 kyr ago the $\delta^{13}C$ values correspond to C_3 type vegetation, while the middle and late Holocene witnessed the local dominance of C_4 plants. Given that C_3 plants such as most trees and shrubs are less efficient under arid conditions than C_4 grasses and some CAM plants, changes towards more positive $\delta^{13}C$ have been related to increasing aridity (*i.e.* Nordt, *et al.*, 1994). However, some important points must be discussed considering that the $\delta^{13}C$ data was obtained from bulk sediment or charcoal.

Firstly, for a reliable interpretation of the carbon isotope ratio, the source of the material analysed as well as its likely contamination and/or diagenetic alteration must, at best, be known. In sedimentary sequences, the stable isotope extraction from palaeosols, alluvium and carbonates is common. Organic carbon and carbonates are the potential records of $\delta^{13}C$ in sediments. Pedogenic carbonates in soils form when carbon from soil CO_2 is incorporated to minerals like calcite. This CO_2 comes mainly from soil respiration and secondarily from atmospheric diffusion, plus a contribution from dissolved minerals derived from parent rocks (Cerling & Quade, 1993). Although carbonate $\delta^{13}C$ depends on soil biological activity and constitutes useful palaeorecords, they can contain allochthonous carbon (Birkeland, 1984). In fact,

the carbonate $\delta^{13}C$ can be enriched by between 14 to 16 ‰ (more positive) with respect to that of soil organic matter (Cerling *et al.*, 1989). In the case of SJRB isotopes, all the samples were treated with acid washes to eliminate carbonates before the determination of isotopes (as specified in the radiocarbon date report from Beta Analytic), so that $\delta^{13}C$ values are assumed to represent only organic carbon. Also, potential contamination from modern roots was also controlled by the physical removal of non-bulk sediment.

Potential contamination can come from edaphic micro-organisms and allochthonous carbon (Xie *et al.*, 2004), eventually modifying the isotopic composition and obscuring the purely autochthonous stable and radiogenic carbon. Neglected contamination by older and/or younger organic carbon for the alluvial (not palaeosol) samples of the SJRB is also assumed because there is no evidence of post-depositional alteration of the alluvial sediments. In the case of palaeosols they show very little pedogenic development, indicating short periods of landscape stability and no post burial alteration. Data on $\delta^{13}C$ of the SJRB is assumed to be a good indicator of plant isotopic fractionation, with alluvial sediments indicating preservation of the organic carbon, mainly derived from local vegetation. For the $\delta^{13}C$ of palaeosols, these would also be good indicators of the plant assemblages established locally at the time of pedogenesis. This is because in semi-arid conditions low water availability limits carbon recycling and microbial activity to short periods during the rainy season. Another point to support the reliability of the inference is that the palaeosols of the SJRB experienced relative short periods of pedogenesis and show no post-burial alteration.

The $\delta^{13}C$ of the rosette of the glyptodont contrasts with that of the related sediment in which it was buried. The rosette isotopic composition corresponds to C_4 plants, and agrees with the grazing behaviour (Fariña & Vizcaino, 2001) and the associated habitat of grasslands and open savannahs (Gillette & Ray, 1981). The fact that sediment organic carbon corresponds to C_3 plants group could denote that the glyptodont had a selective feeding behaviour, misrepresenting the dominant metabolic path at community level.

Comparisons with the carbon stable isotope ratio of tufa of the TPX section (-3.9 ‰) are constrained because the tufa formation involves carbon fixation from CO_2 dissolved in water, biological intake and physicochemical processes (Vázquez-Urbez *et al.*, 2010). Because the water solute composition and the micro and macro-organisms can be highly diverse and variable in different systems, it is unclear what governs the $\delta^{13}C$ the isotope fraction of the TPX tufa. In semi-arid lands, the tufa physicochemical deposition rate is greater under rapid water flow as mechanical degassing (CO_2) of running water causes carbon release for calcite precipitation (Chen *et al.*, 2004). On the other hand, in slow flowing environments, the role of macro and micro-organisms can be more important (Chen *et al.*, 2004) because the biological contribution to super-saturation is mediated by CO_2 plant uptake from water (for photosynthesis) (Chen *et al.*, 2002 in Chen *et al.*, 2004). A more detailed study on the type of plants (*Tipha sp.*, algae, etc.) and/or physicochemical processes involved in this tufa formation and the use of oxygen isotopes is crucial to understand the true meaning of the stable carbon isotopes ratio of this rock.

Despite the low temporal resolution of palaeosols in detecting rapid changes in vegetation, the presence of other alluvial sediments in the

stratigraphic record of the SJRB and the δ^{13}C pattern clearly reconcile with the current vegetation, which is mostly composed of C_3 and CAM plants (Valiente-Banuet *et al.*, 2009). In fact, in arid lands CAM plants can have very similar δ^{13}C values to C_4 plants (Ehleringer & Monson, 1993), which would explain the clustering of the δ^{13}C values close to the typical C_4 range. The present day landscape is very patchy with plant communities dominated by columnar cacti forests with densities of up to1,200 individuals per hectare (Valiente-Banuet *et al.*, 1991) and other CAM plants like *Beaucarnea sp.* (Valiente-Banuet *et al.*, 2009). Trees (*Prosopis*, *Acacia*) typical of C_3 metabolism (Cerling, 1984) are confined to deep alluvial terraces or form a smaller proportion of the biomass of the plant communities in other landforms, compared to the contribution made by C_4 and CAM plants. The δ^{13}C values close to the LGM also agree with the general hypothesis of a wetter than present scenario and support the idea of a change from a relatively wetter environment with an open tropical deciduous forest during the late Pleistocene towards a shift to a semi-desert scrub and cacti vegetation under more arid conditions since the middle Holocene. The presence in the SJRB of isolated trees (*Bursera morelensis*, *Fouquieria formosa*, etc.) typically found in the more humid parts of the Tehuacan region, forming tropical deciduous forest, support this scenario.

6.3.6. Palaeoenvironments from non-correlated sections

More information about the palaeoenvironmental evolution of the SJRB is available from sections such as ALB, STC and CAP. However, the lack of radiocarbon dates and index strata constrain their inclusion in the overall interpretation. The ALB profile is a highly calcretized palaeosol located near the central western limit of the basin. The position in the landscape in which this

palaeosol developed, out of the areas of recent alluvial fans formation, prevented it from being eroded. Based on its main characteristics this unit is interpreted as a well-developed palaeosol, probably originally evolved in a more humid than present environment. It has been established that down profile clay migration (illuviation) and clay cutans development occur at very low rates in arid climates (Yaalon, 1983). The ALB palaeosol is well structure and shows brownish colour, and abundant and well-formed clay coatings, contrasting with typical Holocene semi-arid climate soils, which show poor soil structure and very low organic matter content. This palaeosol is highly calcretized. The presence of $CaCO_3$ precipitates forming ex-ped horizontal laminations and rhizo-concretions suggest that this soil was developed under relatively humid conditions and was later subjected to an arid phase of rapid calcrete development. This assumption is based on indirect evidence. First, a palaeosol showing the same characteristics is found at the top of section TFR, allowing the correlation of both facies as probably contemporaneous. This palaeosol lies above two differentiated deposits, one of them being contemporaneous with a deposition of volcanic ash. This ash, although not directly dated, is also probably correlated with others found in sections SAL and CAN. In section STC, the presence of a freshwater molluscs and reduction features in the sediments indicate wetter conditions in the past and that the basin sustained a sporadic shallow water body.

6.4. Cenozoic environmental evolution

The SJRB has evolved as a tectonic and sedimentary basin during the Quaternary. The main processes have been the active opening out of phase with other regional adjacent basins, probably because of neo-tectonic events

not previously identified. It was until the Late Pleistocene when this Earth Surface System started acting as a sedimentary basin, although the characteristics of the sedimentary landforms suggest very active tectonics. The end of the Pleistocene and Holocene seemed to be less active in tectonic terms, shifting the erosional and sedimentary regimes to climate control. The apparent response of the SJRB to the climate changes during the last glacial period, prior to the LGM, appeared to be in terms of geomorphic instability, under a colder and wetter than present climate. The vegetation was likely mixed, composed of more trees, perhaps resembling the tropical deciduous forests which presently develop in the more humid micro-habitats of the region. The presence of high volumes of sediment deposited during the last 12 kyr, and the change in the isotopic composition of sediments, also suggest important climatic changes during the late Pleistocene and Holocene. The presence of humans in the region and their hypothetical land management practices cannot explain by itself the drastic erosion and alluvial deposition as proposed by McAuliffe *et al*. (2001), meaning that tectonic and climatic factors were the predominant causes. Hunter-gathering practices in the Valley of Mexico were still common during the middle Holocene, and it is very unlikely that the initial agriculture development in the Tehuacan region, estimated after early Pleistocene (Sluyter & Dominguez, 2006), caused such dramatic changes in the landscape. It is more likely that those climatic and geomorphic changes had a strong impact on the cultural development. The inferred changes in vegetation should have translated into the rapid loss of plant and animal resources. The presence of some isolated drought-tolerant elements of tropical deciduous forests in the area (like *Bursera sp.* and *Fouquieria sp.* trees) suggest also that

the change in vegetation implied elimination of those species with physiological and reproductive characteristics which did not allow them to persist given the increase in aridity during the last several thousand years.

CHAPTER VII

CONCLUSIONS

The SJRB is a complex ESS that has experienced a long history of tectonic and environmental change. The evidence obtained from this research suggests that this basin was opened by neo-tectonic activity in a fault pattern which had not been described before. Regional basins were opened by normal faulting which was particularly active during the Oligocene-Miocene period. However, the fault pattern, the relative positions of the structural blocks, and the Tertiary depositional hiatus observed in the SJRB indicate a probably late Tertiary-Pleistocene opening of the basin. However, this idea needs to be confirmed through more detailed studies of geology and geophysics. Data on the thickness of the deposits and structural blocks, as well as measurements on fault directions and rates of movements, is essential to test the validity of the basin configuration proposed in Figure 5.2.4.1. The only evidence of continental basin activity in the SJRB is the collection of Quaternary landforms. These landforms are a complex mosaic, reflecting the influence of tectonics and climate. Three cohorts of alluvial events were established on the basis of topographic position and numerical dates. The oldest alluvial fans (QaI) pre-date the latest Pleistocene and impose a clear asymmetry to the basin because they originated from the north slope, suggesting a tectonic origin. On the other hand, the alluvial terraces QaII represent a more generalised movement of sediment from the highlands and older alluvial surfaces and basin filling, probably related to climate changes. The active deposition before the LGM indicates a semi-dry environment, which was wetter and less seasonal than present, followed by an enhanced drought and reduced alluvial activity during

the LGM and until the latest Pleistocene. Sedimentary records and fossils indicate that at least some of the lower parts of the basin were inundated for long periods, allowing the development of gley conditions. This was probably due to the regional increase in precipitation after the LGM, and the lower seasonality maintained until the middle Holocene. The establishment of current conditions of enhanced aridity, dissection of alluvial landforms and massive sediment movement out of the basin occurred between 3 to 2.5 kyr BP.

A geological reconstruction of past environments requires a reliable interpretation of the evidence preserved in the landscape. Given that landforms result from the evolving geometric arrangement of the earth's surface (Phillips, 2009), we recognise that in order to understand how they have been shaped, they must be studied as dynamic products of past and/or present processes of formation, deformation and fragmentation of the exposed lithology, in constant interaction with biotic, climatic and human factors. Also, it must be considered that stochastic and purely physical properties of the landscape can explain some changes in the geomorphology (Murray *et al.*, 2009). The final interpretation of the evolution of a landscape depends on detecting the relative importance of the individual forces in determining landform dynamics. This varies according to the system studied and also depends on the type of approach and the researchers' interests, with final conclusions often biased by preconceived hypotheses (Inkpen & Wilson, 2009). In arid systems, such the study area, climate and tectonics have been considered first order factors that constantly modify the shallow morphological expression of the rocks (Bull, 1991). Stated in other words, tectonics and climate share the distinguishable feature of imprinting their influence on the geomorphology of arid environments.

However, a non *a priori* belief approach can be the best working strategy for environmental reconstruction (Inkpen & Wilson, 2009), especially when dealing with a system whose past is mostly unknown. The approach adopted in this thesis allowed an integral analysis of the SJRB as a system. However, it was limited because of a lack of information on basic aspects such as tectonics and climate on a more regional scale. Also, it was not possible to be conclusive in many aspects and some explanations were given on the basis of the best possible interpretation, given the available data and the complexity and diversity of the studied records. For example, palaeosols can be a valuable source of information on past environments but in order to extract such information, more detailed analyses are necessary. Similar considerations should be given to the widely spread calcretes, isotope records, volcanic ashes and fossils. On the other hand, this approach was positive because it allowed a first insight into the Cenozoic history of the basin. It also gave evidence of the high potential of those palaeorecords to provide answers to crucial questions, generating a wide perspective for future research and calling attention to this complex but unique region.

Future studies should consider that the SJRB is a complex Earth Surface System in which its internal sub-systems interact dynamically. Landforms and sedimentary records suggest that tectonics and climate have been major forces of change. However, to demonstrate clearly the contribution of each factor this study needs to be extended. Climate can have more spatial influence while tectonics could be more local, so one way to resolve the relative contribution of tectonics and climate in the SJRB is by extending this study to nearby areas with contrasting tectonic history. For example, if during the late Quaternary,

tectonics in the SJRB were no more active than in adjacent basins, the presence of correlative alluvial stratigraphic records could be related to climate. Daniels (2010) expresses this possibility arguing that it is possible to discard autogenic causes as a variable of changes in the alluvial record by defining the time and space in which autogenic changes can operate and cannot be explained by allogenic forces, mainly climate change

This thesis is the first study aiming to understand the change of this Earth Surface System in an integrative way. However, an important number of questions remain unanswered, and many new more new ones were raised. It is desirable to continue studying this system because it has proved to be a very interesting model of Earth surface change. Also, given current environmental changes it is crucial to understand how this important system of southern Mexico has responded to previous changes and which future actions should be taken in order to preserve the outstanding biodiversity and cultural heritage.

In particular, studies on pollen of the described sedimentary sections should be carried out in order to obtain data on past vegetation, considering that the geomorphological and sedimentological contexts have been provided. Studies on modern erosion are urgently needed. Radiocarbon dates and observations clearly indicate that the present day process of dissection of the alluvial surfaces and the intensive erosion in the hills have been established relatively recently. The long-term effects of this generalised loss of soil can have irreversible implications on the local biodiversity. To date the rate and volume of soil eroded every year and the mechanical resistance (in the sense of ESS) of the soils in the region is unknown. This thesis demonstrates that the SJRB is a very dynamic system that responds to different forces. It is unknown how those

changes can affect the current mechanisms and we should move towards exploring the long-term function of this important ESS given the close relationships between all of its components.

Our knowledge on the Geology of Mexico is still far from perfect.

SAN JUAN RAYA GEOLOGIC MAP

Scale 1:50,000

Univeristy of Leicester

Department of Geography

Author:
Javier Medina-Sánchez

October 2010

Quaternary
Pleistocene/
Holocene
Qa — Alluvial

Oligocene?
O-Ba — Basaltic andesite

Upper Cretaceous
Limestone
Dolomite
Brecha

Lower Cretaceous
Mudstone
Sandstone
Sandstone/ Mudstone
Limestone   Barremnian

UK-C — Cipiapa Formation
LK-S — San Juan Raya Formation
LK-Z — Zapotitlan Formation

Lithology

Fault   Plateau
Scarp   Intermitent river

Structural features

176

Appendix A2

SAN JUAN RAYA GEOMORPHOLOGICAL MAP

177

Appendix B
Sedimentological characteristics of selected stratigraphic sections

Table 5.4.2. Granulometric parameters and OM of the sedimentary units of section BIS. Capital letters before and after dash indicate relative size (VF = fine, F = fine, M = medium, C = coarse, VC = very coarse) and class grain size (C = clay, SI = silt, Sn = sand, Pb = pebbles) respectively. Dispersion is indicated by the degree of sortedness (P = poor, VP = very poor, EP = extremely poor). Skewness: VN = very negative, N = negative, SYM = symmetric, P = positive, VP = very positive). Kurtosis: VL = very leptokurtic, L = leptokurtic, M = mesokurtic, P = platikurtic.

Unit	Depth (cm)	OM (%)	Graphic mean (phi)		Median (phi)		Dispersion		Skewness		Kurtosis	
BIS-IV	95	4.3	4.5	VC-SI	6.0	C-SI	5.0	EP	-0.6	VN	1.0	M
BIS-III	370	2.77	-0.1	VC-Sn	-1.4	VF-Pb	4.3	EP	0.5	VP	0.6	P
	535	3.58	5.7	C-SI	5.7	C-SI	2.1	VP	-0.0	SYM	0.8	P
	547	3.22	5.5	C-SI	5.7	C-SI	2.1	VP	-0.0	SYM	0.8	P
	600	3.14	3.8	VF-Sn	4.3	VC-SI	3.7	VP	-0.1	N	0.6	P
BIS-II	780	2.17	-1.8	VF-Pb	-2.0	F-Pb	4.9	EP	0.2	P	1.0	M
BIS-I	840	7.72	6.2	M-SI	6.6	M-SI	2.4	VP	-0.2	N	0.7	P

Table 5.4.3. Main statistical parameters of the particle size composition of the different facies of the CAP section. Capital letters before and after dash indicate relative size (VF = fine, F = fine, M = medium, C = coarse, VC = very coarse) and class grain size (C = clay, SI = silt, Sn = sand, Pb = pebbles) respectively. Dispersion is indicated by the degree of sortedness (P = poor, VP = very poor, EP = extremely poor). Skewness: VN = very negative, N = negative, SYM = symmetric, P = positive, VP = very positive). Kurtosis: VL = very leptokurtic, L = leptokurtic, M = mesokurtic, P = platikurtic.

Unit	Depth (cm)	OM	Median (phi)		Mean (phi)		Dispersion		Skewness		Kurtosis	
CAP-III	30	7.42	6.60	M-SI	6.05	M-SI	2.34	VP	-0.36	VN	0.82	P
CAP-II RA	180	3.97	4.05	VC-SI	4.72	VC-SI	2.30	VP	0.40	VP	0.85	P
CAP-II RB	185	4.81	5.93	C-SI	5.87	C-SI	2.05	VP	-0.04	SYM	0.79	P
CAP-I	295	4.16	3.51	VF-Sn	3.55	VF-Sn	3.57	VP	-0.08	SYM	1.07	M

Table 5.4.4. Main statistical parameters of the particle size composition of the different facies of the SLT section. Capital letters before and after dash indicate relative size (VF = fine, F = fine, M = medium, C = coarse, VC = very coarse) and class grain size (C = clay, Sl = silt, Sn = sand, Pb = pebbles) respectively. Dispersion is indicated by the degree of sortedness (P = poor, VP = very poor, EP = extremely poor). Skewness: VN = very negative, N = negative, SYM = symmetric, P = positive, VP = very positive). Kurtosis: VL = very leptokurtic, L = leptokurtic, M = mesokurtic, P = platikurtic.

Unit	Depth	OM	Median (phi)		Mean (phi)		Dispersion		Skewness		Kurtosis	
SLT-VI	0-30	6.7	6.47	M-Sl	6.09	M-Sl	2.39	VP	-0.31	N	1.09	M
SLT-V	30	10.48	4.72	VC-Sl	4.15	VC-Sl	4.14	EP	-0.39	VN	1.28	L
SLT-IV	130	7.95	4.85	VC-Sl	4.93	VC-Sl	2.15	VP	0.09	SYM	0.70	P
SLT-III	150	7.25	5.93	C-Sl	5.83	C-Sl	2.12	VP	-0.07	SYM	0.86	P
SLT-II	330	4.25	-3.00	M-Pb	-2.39	F-Pb	2.60	VP	0.55	VP	1.78	V-L
	350	8.27	5.66	C-Sl	5.77	C-Sl	1.91	P	0.05	SYM	0.94	M
	410	4.38	-3.00	M-Pb	-2.22	F-Pb	4.78	EP	0.27	P	1.11	M
SLT-I	460	5.95	4.18	VC-Sl	4.36	VC-Sl	2.40	VP	0.16	P	0.87	P
	480	5.22	5.66	C-Sl	5.27	C-Sl	3.62	VP	-0.42	VN	1.45	L

Table 5.4.5. Main statistical parameters of the particle size composition of the different facies of the SJII section. Capital letters before and after dash indicate relative size (VF = fine, F = fine, M = medium, C = coarse, VC = very coarse) and class grain size (C = clay, Sl = silt, Sn = sand, Pb = pebbles) respectively. Dispersion is indicated by the degree of sortedness (P = poor, VP = very poor, EP = extremely poor). Skewness: VN = very negative, N = negative, SYM = symmetric, P = positive, VP = very positive). Kurtosis: VL = very leptokurtic, L = leptokurtic, M = mesokurtic, P = platikurtic.

Unit	Depth (cm)	OM	Median (phi)		Mean (phi)		Dispersion		Skewness		Kurtosis	
SJII-V	0-20	4.07	4.7	VC-Sl	4.8	VC-Sl	2.5	VP	0.08	SYM	0.73	P
	20	2.28	-1.4	VF-Sn	0.2	C-Sn	4.5	EP	0.49	VP	0.68	P
SJII -IV	290	5.01	6.0	M-Sl	5.7	C-Sl	2.4	VP	-0.27	N	0.85	P
SJII -III	390	4.66	5.7	C-Sl	5.7	C-Sl	2.0	VP	-0.06	SYM	1.01	M
SJII -II	470	3.6	6.4	M-Sl	5.8	C-Sl	2.9	VP	-0.50	VN	1.25	L
SJII -I	580	2.8	4.4	VC-Sl	4.5	VC-Sl	2.5	VP	0.08	SYM	0.74	P

Table 5.4.6. Main statistical parameters of the particle size composition of the different facies of the STC section. Capital letters before and after dash indicate relative size (VF = fine, F = fine, M = medium, C = coarse, VC = very coarse) and class grain size (C = clay, SI = silt, Sn = sand, Pb = pebbles) respectively. Dispersion is indicated by the degree of sortedness (P = poor, VP = very poor, EP = extremely poor). Skewness: VN = very negative, N = negative, SYM = symmetric, P = positive, VP = very positive). Kurtosis: VL = very leptokurtic, L = leptokurtic, M = mesokurtic, P = platikurtic.

Unit	Depth (cm)	OM	Median (phi)		Mean (phi)		Dispersion		Skewness		Kurtosis	
STC-IV	0-20	10.69	6.6	M-SI	5.88	C-SI	2.83	VP	-0.47	VN	0.96	M
	60	6.11	6.06	M-SI	5.94	C-SI	2.14	VP	-0.1	N	0.8	P
STC-III	190	5.54	6.73	M-SI	6.54	M-SI	1.83	P	-0.2	N	0.86	P
	275	5.5	6.19	M-SI	6	M-SI	2.19	VP	-0.12	N	0.78	P
STC-II	345	3.44	6.06	M-SI	5.84	C-SI	2.45	VP	-0.12	N	0.67	P
	430	4.72	6.87	M-SI	6.33	M-SI	2.25	VP	-0.40	VN	0.91	M
	570	4.29	5.66	C-SI	5.59	C-SI	2.21	VP	-0.06	SYM	0.74	P
STC-I	610	2.41	3.91	VF-SI	4.41	VC-SI	2.87	VP	0.19	P	0.70	P

Table 5.4.7. Main statistical parameters of the particle size composition of the different facies of the TFR section. Capital letters before and after dash indicate relative size (VF = fine, F = fine, M = medium, C = coarse, VC = very coarse) and class grain size (C = clay, SI = silt, Sn = sand, Pb = pebbles) respectively. Dispersion is indicated by the degree of sortedness (P = poor, VP = very poor, EP = extremely poor). Skewness: VN = very negative, N = negative, SYM = symmetric, P = positive, VP = very positive). Kurtosis: VL = very leptokurtic, L = leptokurtic, M = mesokurtic, P = platikurtic.

Unit	Depth (cm)	OM	Median (phi)		Mean (phi)		Dispersion		Skewness		Kurtosis	
TFR-V	10	7.01	4.99	VC-SI	5.12	C-SI	2.39	VP	0.07	SYM	0.80	P
TFR-IV	40	5.26	4.99	VC-SI	4.99	VC-SI	2.52	VP	-0.01	SYM	0.79	P
TFR-III	100	4.87	5.26	C-SI	5.41	C-SI	2.11	VP	0.08	SYM	0.87	P
TFR-II	180	5.1	4.99	VC-SI	5.38	C-SI	1.92	P	0.30	P	0.80	P
	235	4.75	4.72	VC-SI	3.93	VF-Sn	4.40	EP	-0.29	N	0.59	VP
TFR-I	275	4.84	6.87	M-SI	6.84	M-SI	1.79	PS	-0.04	SYM	0.78	P
	320	5.27	6.74	M-SI	6.86	M-SI	2.37	VP	0.18	P	0.98	M

Table 5.4.8. Main statistical parameters of the particle size composition of the different facies of the TPX section. Capital letters before and after dash indicate relative size (VF = fine, F = fine, M = medium, C = coarse, VC = very coarse) and class grain size (C = clay, Sl = silt, Sn = sand, Pb = pebbles) respectively. Dispersion is indicated by the degree of sortedness (P = poor, VP = very poor, EP = extremely poor). Skewness: VN = very negative, N = negative, SYM = symmetric, P = positive, VP = very positive). Kurtosis: VL = very leptokurtic, L = leptokurtic, M = mesokurtic, P = platikurtic.

Unit	Depth (cm)	OM (%)	Median (phi)		Mean (phi)		Dispersion		Skewness		Kurtosis	
TPX-VII	300	2.91	7.14	F-Sl	7.28	F-Sl	1.90	P-S	0.25	P-Sk	1.18	Lk
TPX-VI	1005	4.82	6.87	M-Sl	6.72	M-Sl	1.74	P-S	-0.14	N-Sk	0.80	Pk
	1090	2.56	4.05	VC-Sl	3.35	VF-Sn	4.46	EP-S	-0.20	N-Sk	0.56	V-Pk
	1115	4.42	5.80	C-Sl	5.78	C-Sl	2.31	VP-S	0.08	SYM	1.15	Lk
	1490	4.63	6.87	M-Sl	6.83	M-Sl	1.58	P-S	-0.05	SYM	0.82	Pk
TPX-V	1530	5.03	5.93	C-Sl	5.89	C-Sl	2.13	VP-S	-0.08	SYM	0.89	Pk
TPX-IV	1560	4.97	6.47	M-Sl	6.20	M-Sl	2.18	VP-S	-0.26	N-Sk	1.05	Mk
TPX-III	1680	5.11	6.74	M-Sl	6.74	M-Sl	1.64	P-S	-0.08	SYM	0.89	Pk
TPX-I	1785	4.14	5.66	C-Sl	5.51	C-Sl	2.45	VP-S	-0.11	N-Sk	0.76	Pk

BIBLIOGRAPHY

Aguilera, J.G. 1906. Excursión de Tehuacan a Zapotitlan y San Juan Raya Mexico. *Xº Congreso Internacional de Geología. Libreto guía,* 7:1-27.

Aguilera, J.G., Ordoñez, E. and Buelna, R.J. 1896. Bosquejo Geológico de Mexico. *Boletín del Instituto Geológico de Mexico,* 4-6:83-93.

Alonso-Zarza, A.M. 2003. Palaeoenvironmental significance of palustrine carbonates and calcretes in the geological record. *Earth Science Reviews,* 60: 261-298.

Armstrong, P.A., Perez, R., Owen, L.A. and Finkel, R.C. 2010. Timing and controls on late Quaternary landscape development along the eastern Sierra El Mayor range front in northern Baja California, Mexico. *Geomorphology,* 114: 415-430.

Asmeron, Y., Polyak, V., Burns, S., and Rassmussen, J. 2007. Solar forcing of Holocene climate: New insights from a speleothem record, southwestern United States. *Geology,* 35 (1):1-4.

Bachman, G.O. and Machette, M.N. 1977. Calcic soils and calcretes in the southwestern United States. *US Geological Survey Open Report.*

Bargo, S.M. 2003. Biomechanics and palaeobiology of the Xenarthra: The state of the art. *Senckenbergiana Biologica,* 83(1): 41-50.

Beraldi-Campesi, H., Cevallos-Ferriz, S.R.S., Centeno-García, E., Arenas-Abad, C and Fernández, L.P. 2006. Sedimentology and palaeoecology of an Eocene-Oligocene alluvial-lacustrine arid system, Southern Mexico. *Sedimentary Geology,* 191: 227-254.

Berrio, J.C., Hooghiemstra, H., van Geel, B. and Ludlow-Wiechers, B. 2006. Environmental history of the dry forest biome of Guerrero, Mexico, and human impact during the las c. 2700 years. *The Holocene,* 16(1): 62-80.

Birkeland, P. W. 1984. *Soils and geomorphology*. Oxford University Press. EUA.

Blair, T.C. and Bilodeau, W.L. 1988. Development of tectonic cyclothems in rift, pull-apart, and foreland basins: sedimentary response to episodic tectonism. *Geology,* 16: 517-520.

Blair, T.C. and McPherson, J.G. 2009. Processes and forms of alluvial fans. In: Parsons, A.J. and Abrahams, A.D. (eds.). 2009. *Geomorphology of Desert Environments*. 2nd ed. Springer, 413-466.

Bloomfield, K, and Valastro, J.R. 1974. Late Pleistocene eruptive history of Nevado de Toluca Volcano, Central Mexico. *Gelogical Society of America Bulletin,* 85(6): 901-906.

Blum, M.D. and Törnqvist, T.E. 2000. Fluvial response to climate and sea level-change: a review and look forward. *Sedimentology,* 47 (supplement 1): 2-48.

Bond, G., Kromer, B., Beer, J., Muscheler, R., Evans, M.N., Showers, W., Hoffmann, S., Lotti-Bond, R., Hajdas, I. and Bonani, G. 2001. Persitent solar influence on North Atlantic climate during the Holocene. *Science,* 294: 2130-2136.

Bradbury, J.P. 2000. Limnologic history of Lago de Pátzcuaro, Michoacán, Mexico for the past 48,000 years: impacts of climate and man. *Palaeogeography, Palaeoclimatology, Palaeoecology,* 163: 65–95.

Briant, R.M., Bateman, M.D., Coopel, R.G. and Gibbard, P.L. 2005. Climatic control on Quaternary fluvial sedimentology of a Fenland Basin river, England. *Sedimentology,* 52: 1397-1423.

Brunet, J. 1967. Geological studies. In: Byers, D.S. (ed.). *The prehistory of the Tehuacan Valley. Vol. I. Environment and subsistence*. University of Texas Press, 66-90.

Brunner, C.A. 1982. Paleoceanography of surface waters in the Gulf of Mexico during the Late Quaternary. *Quaternary Research,* 17: 105-119.

Brunner, C.A. and Cooley, J.F. 1976. Circulation in the Gulf of Mexico during the last glacial maximum 18,000 yr ago. *Geological Society of America Bulletin,* 87: 681-686.

Buitrón, B.E. and Bareló-Duarte, J. 1980. Nereidos (Mollusca-Gastropoda) del Cretácico inferior de la región de San Juan Ray, Puebla. *Revista del Instituto de Geología UNAM,* 4(1): 46-55.

Bull, W.B., 1991. *Geomorphic Response to Climatic Change*. Oxford University Press, Oxford. USA.

Byers, D. 1967. Climate and hydrology. In: Byers, D. (ed.). *The Prehistory of the Tehuacan Valley*. Vol. I. Environment and subsintence. University of Texas Press, 48-65.

Caballero, M., Lozano-García, S., Ortega-Guerrero, M., Urrutia-Fucugauchi, J. and Macias, J.L. 1999. Environmental characteristics of Lake Tecomulco, northern basin of Mexico, for the last 50,000 years. *Journal of Paleolimnology,* 22: 399-411.

Calderón-García, A., 1956, Bosquejo geológico de la región de San Juan Raya, Puebla: Mexico. *Congreso Geológico Internacional, Excursión A-11*, 9-33.

Camardi, G. 1999. Charles Lyell and the uniformity principle. *Biology and Philosophy,* 14: 537-560.

Campa, U.M.F. and Coney, P. J. 1983. Tectonostratigraphic terranes and mineral resourcedistribution of Mexico: *Canadian Journal Earth Sciences*, 20: 1040-105.

Campos-Enríquez, J.O., Ortega-Ramírez, J., Alatriste-Vilchis, D., Cruz-Gática, R. and Cabral-Cano, E. 1999. Relationship between extensional tectonic style and the paleoclimatic elements at Laguna El Fresnal, Chihuahua Desert, Mexico. *Geomorphology,* 28: 75-94.

Canúl, M.M.E. 2008. Reconstrucion paleoclimatica (Cuaternario-tardío) de la porción occidental del valle de Tehuacan, Puebla: Estudio palinológico. MSc thesis. UNAM, Mexico.

Caran, S.C. and Neely, J.A. 2006. Hydraulic engineering in prehistoric Mexico. *Scientific American,* 295(4): 78-85.

Carlisle, D. 1983. Concentration of uranium and vanadium in calcretes and gypcretes. *Geological Society of London, Special Publications,* 11: 185-195.

Carrasco-Núñez, G. and Rose, W.I. 1995. Eruption of a major Holocene pyroclastic flow at Citlaltépetl volcano (Pico de Orizaba), Mexico, 8.5-9.0 ka. *Journal of Volcanology and Geothermal Research,* 69: 197-215.

Centeno-García, E., Mendoza-Rosales, C.C. and Silva-Romo, G. 2009. Sedimentología de la Formación Matzitzi (Paleozoico superior) y significado de sus componentes volcánicos, región de Los Reyes Metzontla-San Luis Atolotitlán, Estado de Puebla. *Revista Mexicana de Ciencias Geológicas,* 26(1): 18-36.

Cerca, M., Ferrari, L., López-Martínez, M., Martiny, B., and Iriondo, A. 2007. Late Cretaceous shortening and early Tertiary shearing in the central Sierra Madre del Sur, southern Mexico: Insights into the evolution of the Caribbean–North American plate interaction. *Tectonics,* 26: TC3007.

Cerling, T.E. 1984. The stable isotopic composition of modern soil carbonate and its relationship to climate. *Earth and Planetary Science Letters,* 71: 229-240.

Cerling, T.E. and Quade, J. 1993. Stable carbon and oxygen isotopes in soil carbonates. In: Swart, P.K., Lohmann, K.C., McKenzie, J. and Savin, S. (eds.). *Climate change in Continental Isotope Records, Geophysical Monographs.* American Geophysical Union, 78: 217-231.

Cerling, T.E. and Quade, J., Wang, Y. and Bowman, J.R. 1989. Carbon isotopes in soils and palaeosols as ecology and palaeoecology indicators. *Nature,* 341: 138-139.

Charreau, J., Gumiaux, C., Avouac, J-P., Augier, R., Chen, Y., Barrier, L., Gilder, S., Dominguez, S., Charles, N. and Wang, Q. 2009. The Neogene Xiyu Formation,

a diachronous prograding gravel wedge at front of the Tianshan: climatic and tectonic implications. *Earth and Planetary Science Letters,* 287: 298-310.

Chen, J., Zhang, D.D., Wang, S., Xiao, T. and Huang, R. 2004. Factors controlling tufa deposition in natural waters at waterfall sites. *Sedimentary Geology,* 166: 535-366.

Christie-Blick, N. and Biddle, K.T. 1985. Deformation and basin formation along strike-slip faults. pp. 1-34. In Christie-Blick, N. and Biddle, K.T. (eds.). Strike-slip deformation, basin formation and sedimentation. *Society of Economic Paleontologists and Mineralogists. Special publication No. 37,* 386 p.

Clark, P.U., Marshall, S.J., Clarke, G.K.C, Hostetler, S.W., Licciardi, J.M. and Teller, J.T. 2001. Freshwater Forcing of Abrupt Climate Change During the Last Glaciation. *Science,* 293: 283-287.

CLIMAP, Climap project members. 1976. The surface of the Ice-Age earth. *Science,* 191: 1131-1137.

Conserva, M.E. and Byrne, R. 2002. Late Holocen vegetation change in the Sierra Madre Oriental of Central Mexico. *Quaternary Research,* 58: 122-129.

Corona-Esquivel, R. J. J. 1983, Estratigrafía de la región de Olinala-Tecocoyunca, noreste del Estado de Guerrero: *Revista del Instituto de Geología UNAM,* 5(2): 17-24.

Curtis, J.H., Brenner, M. and Hodell, D.A. 1999. Climate change in the Lake Valencia Basin, Venezuela, ~12 000 yr BP to present. *The Holocene,* 9(5): 609-619.

Curtis, J.H., Hodell, D.A., and Brenner, M. 1996. Climate variability on the Yucatan peninsula (Mexico) during the past 3500 years, and implications for Maya cultural evolution. *Quaternary Research,* 46: 37-47.

Daniels, J.M. 2010. Distinguishing allogenic from autogenic causes of bed elevation change in late Quaternary alluvial stratigraphic records. *Geomorphology,* 101: 159-171.

Dansgaard, W., Johnsen, S.J., Clausen, H.B., Dahl-Jensen, D., Gunderstrup, N.S., Hammer, C.U., Hvidberg, C.S., Steffensen, J.P., Svelnbjornsdottir, A.E., Jouzel, J. and Bod, G. 1993. Evidence of general instability of past climate from a 250-kyr ice core record. *Nature,* 364: 218-220.

Dansgaard, W., White, J.W.C. and Johnsen, S.J. 1989. The abrupt termination of the Younger Dryas event. *Nature,* 339: 532-534.

Dávalos-Álvarez, O.G. 2006. Evolución Tectónica Cenozóica en la Porción Norte de la Falla de Oaxaca. MSc thesis. UNAM, Mexico.

Dávalos-Álvarez, O.G., Nieto-Samaniego, A.F., Alaníz-Álvarez, S.A., Martínez-Hernández, E. and Ramírez-Arriaga, E. 2007. Estratigrafía cenozóica de la region de Tehuacan y su relación con el sector norte de la falla de Oaxaca. *Revista Mexicana de Ciencias Geológicas,* 24(2): 197-215.

Dávila, A. P., Villaseñor, R. J. L., Medina, L. R., Ramírez, R. A., Salinas, T. A., Sánchez, K. J. and Tenorio, L. P. 1993. *Flora del Valle de Tehuacan-Cuicatlán.* Listados florísticos de Mexico X. Instituto de Biología. UNAM, Mexico.

Dávila, A.P., Arizmendi M.C., Valiente-Banuet, A., Villaseñor, J.L., Casas, A. and Lira, R. 2002. Biological diversity in the Tehuacan-Cuicatlán Valley, Mexico. *Biodiversity and Conservation,* 11: 421–442, 2002.

de Cserna, Z. 1989. An outline of the geology of Mexico. In Ball, A.W. and Palmer, A.R. The Geology of North America: an overview. Vol. A. *Geological Society of America Special Paper*, 233-264.

deMenocal, P.B., Ortiz, J., Guilderson, T. and Sarnthein, M. 2000. Coherent high- and low-latitude climate variability during the Holocene warm period: *Science,* 288: 2198–2202.

Dickinson, W.R. 2002. The Basin and Range province as a composite extensional domain. *International Geology Review,* 44: 1-38.

Dixon, J.C. and McLaren, S. 2009. Duricrusts. In: Parsons, A.J. and Abrahams, A.D. (eds.). 2009. *Geomorphology of Desert Environments.* 2nd ed. Springer, 123-151.

Douglas, J., Meek, N., Dorn, R.I. and Schmeeckle, M.W. 2009. A criteria-based methodology for determining the mechanism of transverse drainage development, with application to the southwestern United States. *Geological Society of America Bulletin,* 121(3-4): 586-598.

Ehleringer, J.R. and Monson, R.K. 1993. Evolutionary and ecological aspects of photosynthetic pathway variation. *Annual review of Ecology and Systematics,* 24: 411-439.

Elías-Herrera, M. and Ortega-Gutiérrez, F., 2002, Caltepec fault zone: An Early Permian dextral transpressional boundary between the Proterozoic Oaxacan and Paleozoic Acatlán implications: *Tectonics,* 21(3): TC001278.

Emiliani, C., Gartner, S., Lidz, B., Eldridge, K., Elvey, D. K., Huang, T. C., Stipp, J. J., and Swanson, M. F., 1975, Paleoclimatological analysis of Late Quaternary cores from the northeastern Gulf of Mexico: *Science,* 189: 1083–1088.

Emiliani, C., Rooth, C. and Stipp, J.J. 1978. The late Wisconsin flood into the Gulf of Mexico. *Earth and Planetary Science Letters,* 41: 159-162.

Englehart, P.J. and Douglas, A. 2001. The role of north Pacific tropical storms in the rainfall climatology of western Mexico. *International Journal of Climatology,* 21: 1357-1370.

Fariña, R.A. and Vizcaíno, S.F. 2001. Craved teeth and jaws: How glyptodonts masticated. *Acta Palaeontologica Polonica,* 46(2): 219-234.

Feldman, R.M., Martínez-López, L., González-Rodríguez, K.A., González-León, O. and Fernández-Barajas, M. 2007. Crustacea from the Muhi quarry (Albian–Cenomanian), and a review of Aptian Mecochiridae (Astacidea) from Mexico. *Annals of the Carnegie Museum,* 76(3): 145–156.

Ferrusquilla-Villafranca, I. 1976. Estudios geoloógico-paleontoloógicos en la región Mixteca, Parte 1: Geología del área Tamazulapan- Teposcolula-Yanhuitlán, Mixteca Alta, Estado de Oaxaca, Mexico. *Boletín del Instituto de Geología UNAM,* 97:160-191.

Flower, B.P., Hastings, D.W., Hill, H.W. and Quinn, T.M. 2004. Phasing of deglacial warming and Laurentide Ice Sheet meltwater in the Gulf of Mexico. *Geology,* 32(7): 597-600.

Fontana, A., Mozzi, P. and Bondesan, A. 2008. Alluvial fans in Venetian-Friulian (north-eastern Italy): evidence of sedimentary and erosive phases during Late Pleistocene and Holocene. *Quaternary International,* 189: 71-90.

Ford, T.D. and Pedley, H.M. 1996. A review of tufa and travertine deposits of the world. *Earth Science Reviews,* 41: 117-175.

Galloway, R.W. 1983. Full-glacial Southwestern United States: mild and wet or cold and dry? *Quaternary Research,* 19: 236-248.

García, E. 1981. *Modificaciones al Sistema Climático de Köppen.* Instituto de Geografía, UNAM. Mexico.

Gates, W.L. 1976. Modeling Ice-Age climate. *Science,* 191: 1138-1144.

Gile, L. H., Peterson, F. F. and Grossman, R. B. 1966. Morphological and genetic sequences of carbonate accumulation in desert soils. *Soil Science,* 101 (5): 347-360.

Gile, L.H., Gibbens, R.P. and Lenz, J.M. 1998. Soil induced variability in root systems of creosotebush (*Larrea tridentata*) and tarbush (*Florencia cernua*). *Journal of Arid Environments,* 39: 57-78.

Gile, L.H., Hawley, J.W. and Grossman, R.B. 1981. *Soils and Geomorphology in the Basin and Range area of southern New Mexico.* Guidebook to the desert project. Memoir 39.

Gillette, D. D., and C. E. Ray. 1981. Glyptodonts of North America. *Smithsonian Contributions in Paleobiology*, 40:1-255.

Gozález-Arreola, C. 1974. Phylloceras del Cretácico inferior de San Juan Raya-Zapotitlan, Estado de Puebla, México. *Bolletin de la Sociedad Geológica Mexicana,* 35: 29-37.

González-Quintero, L. 1980. Paleoecologia de un sector costero de Guerrero, Mexico (300 años). *Memorias III Coloquio Científico Prehistórico 86.* INAH, Mexico, 133-158.

González, R.A., Sánchez, R.L., Mota, M., Arceo, F.A., Onofre, E.L., Zarate, L.J. and Soto, R.A. 2000. *Carta Geologico-minera, Oaxaca E14-9.* Servicio Geologico Mexicano, Hidalgo, Mexico. One map scale 1:250,000.

Graham, J. 1988. Collection and analysis of field data. In: Tucker, M. (ed.). 1988. *Techniques in Sedimentology.* Blackwell Scientific Publications, 5-62.

Grimm, E.C., Jacobson, G.L., Watts, W.A., Hansen, B.C.S. and Maasch, K.A. 1993. A 50,000-year record of climatic oscillations from Florida and its temporal correlation with the Heinrich events. *Science,* 261: 198-200.

GRIP members. 1993. Climate instability during the last interglacial period recorded in the GRIP ice core. *Nature,* 364: 203-207.

Haddoumi, H., Charriere, A., Andreu, B. and Mojon, P. 2008. Les depots continentaux du Jurassique moyen au Cretace inferieur dans le Haut Atlas oriental (Maroc): paleoenvironnements successifs et signification paleogeographique. *Carnets de Geologie,* 6: 1-29.

Harvey, A.M. 1996. The role of alluvial fans in the mountain fluvial systems of southern Spain: implications of climatic change. *Earth Surface Processes and Landforms,* 21: 543-553.

Harvey, A.M. 2002. The role of base level change in the dissection of alluvial fans: case studies from southeast Spain and Nevada. *Geomorphology,* 45: 67-87.

Harvey, A.M., Silva, P.G., Mather, A.E., Goy, J.L., Stokes, M. and Zazo, C. 1999a. The impact of Quaternary sea-level and climate change on coastal alluvial fans in the Cabo de Gata ranges, southeast Spain. *Geomorphology,* 28: 1-22.

Harvey, A.M., Wigand, P.E. and Wells, S.G. 1999b. Response of alluvial fan systems tolthe late Pleistocene to Holocene climatic transition: contrasts between the margins of pluvial lakes Lahontan and Mojave, Nevada and California, USA. *Catena,* 36: 255-281.

Haug, G.H., Hughen, K.A., Sigman, D.M., Peterson, L.C. and Röhl, U. 2001. Southward migration of the intertropical convergence zone through the Holocene. *Science,* 293: 1304-1308.

Higuera-Gundy, A., Brenner, M., Hodell, D.A., Curtis, J.H., Leyden, B.W. and Binford, M.W. 1999. A 10,300 ^{14}C yr record of climate and vegetation change from Haiti. *Quaternary Research,* 52: 159-170.

Hodell, D.A., Brenner, M., Curtis, J.H., Medina-González, R., Ildefonso-Chan Can, E., Albornaz-Pat, A. and Guilderson, T.P. 2005. Climate change on the Yucatan peninsula during the Little Ice Age. *Quaternary Research,* 63: 109-121.

Horton, R.E. 1945. Erosional development of streams and their drainage basins; hydrophysical approach to quantitative morphology. *Geological Society of America Bulletin,* 56: 275-370.

Howard, A.D. 1967. Drainage analysis in geologic interpretation: a summary. *American Association of Petroleum Geologists,* 51:2246-5229.

Huang, Y., Shuman, B., Wang, Y. Webb III, T., Grimm, E.C. and Jacobson Jr., G.L. 2006. Climatic and environmental controls on the variation of C3 and C4 plant abundances in central Florida for the past 62,000 years. *Palaeogeography, Palaeoclimatology, Palaeoecology,* 237: 428–435

Hudec, M.R. and Jackson, P.A. 2002. Structural segmentation, inversion, and salt tectonics on a passive margin: evolution of the Inner Kwanza Basin, Angola. *Geological Society of America Bulletin,* 114: 1222-1244.

Iltis, H.H. 1983. From teosinte to maize: the catastrophic sexual transmutation. *Science,* 222: 886–894.

INEGI. 1998a. Carta Orizaba E 14-16. Topográfica escala 1:250 000.

INEGI. 1998b. Carta Tehuacan E 14 B75. Topográfica escala 1:50 000

INEGI. 1998c. Carta Orizaba E 14-16. Geología escala 1:250 000.

Inkpen, R. and Wilson, G.P. 2009. Explaining the past: abductive and Bayesian reasoning. *The Holocene,* 19(2): 329-334.

Jansen, E. and Veum, T. 1990. Evidence for two-step deglaciation and its impact on North Atlantic deep-water circulation. *Nature,* 343: 612-616.

Johnsen, S.J., Clause, H.B., Dansgaard, W., Fuhrer, K., Gundestrup, N., Hammer, C.U., Iversen, P., Jouzel, J., Stauffer, B. and Steffensen, J.P. 1992. Irregular glacial interstadial in a new Greenland ice core. *Nature,* 539: 311-313.

Keppie, D.J. 2004. Terranes of Mexico revisited: a 1.3 billion years odyssey. *International Geology Review,* 46: 765-794.

Kirby, M.E., Mullins, H.T., Patterson, W.P. and Burnett, A.W. 2002. Late glacial–Holocene atmospheric circulation and precipitation in the northeast United States inferred from modern calibrated stable oxygen and carbon isotopes. *Geological Society of America Bulletin,* 114 (10): 1326–1340.

Koch, P.L. 1988. Isotopic reconstruction of past continental environments. *Annual Review of Earth and Planetary Sciences,* 26: 573-613.

Konert, M. and VanDenberghe, J. 1997. Comparison of laser grain size analysis with pipette and sieve analysis: a solution for the underestimation of the clay fraction. *Sedimentology,* 44:523-535.

Kutzbach, J.E. and Guetter, P.J. 1986. The influence of changing orbital parameters and surface boundary conditions on climate simulations for the past 18,000 years. *Journal of Atmospheric Science,* 43: 1726-1759.

Lachinet, M.S., Asmeron, Y., Burns, S.J., Patterson, W.P., Plyak, V.J. and Seltzer, G.O. 2004. Tropical response to the 8200 yr B.P. cold event? Speleothem isotopes indicate a weakened early Holocene monsoon in Costa Rica. *Geology,* 32(11): 957-960.

Lachniet, M.S. and Seltzer, G.O. 2002. Late Quaternary glaciation of Costa Rica. *Geological Society of America Bulletin,* 114(5): 547-558.

Leyden, B.W. 1985. Late Quaternary aridity and Holocene moisture fluctuations in the Lake Valencia Basin, Venezuela. *Ecology,* 66: 1279-1295.

Leyden, B.W., Brenner, M., Hodell, D.A. and Curtis, J.H. 1994. Orbital and internal forcing of climate in the Yucatan Peninsula for the past 36 ka. *Palaeogeography,Palaeoclimatology, Palaeoecology,* 109: 193-210.

Leyden, B.W., Brenner, M.A. and Dahlin, B. 1998. Cultural and climatic history of Coba, a lowland Maya city in Quintana Roo, Mexico. *Quaternary Research,* 49: 111-22.

Leyden, B.W., Brenner, M.A., Hodell, D.A. and Curtis, J.H. 1993. Late Pleistocene climate in Central America lowlands. In Swart, P.K., McKenzie, J. and Saving, S. (eds.). *Climate Change in Continental Isotopic Records.* American Geophysical Union, 165-178.

Lösser, H. 2009. Morphology, taxonomy and distribution of the Early Cretaceous coral genus *Holocoenia* (Scleractinia) and its first record in the Caribbean. *Revista Mexicana de Ciencias Geológicas,* 26(1): 93-103.

Lowe, J.J. and Walker, M.J.C. 1997. *Reconstructing Quaternary Environments.* 2nd ed. Prentince Hall.

Lozano-García, M.S. and Ortega Guerrero, B., 1994. Palynological and magnetic susceptibility records of Lake Chalco, central Mexico. *Palaeogeography, Palaeoclimatology, Palaeoecology,* 109: 177-191.

Lozano-García, M.S. and Ortega-Gerrero, B. 1998. Late Quaternary environmental changes of the central part of the Basin of Mexico: Correlation between Texcoco and Chalco basins. *Review of Palaeobotany and Palynology,* 99: 77-93.

Lozano-García, M.S. and Vázquez-Selem, L. 2005. A high-elevation Holocene pollen record from Iztaccíhuatl volcano, central Mexico. *The Holocene,* 15(3): 329-338.

Lozano-García, M.S., Ortega-Gerrero, B., Caballero-Miranda, M. and Urrutia-Fucugauchi, J. 1993. Late Pleistocen and Holocen paleoenvironments of Chalco Lake, central Mexico. *Quaternary Research,* 40: 332-343.

Lozano-García, M.S., Sosa-Nájera, S., Sugiura, Y. and Caballero, M. 2005. 23,000 yr of vegetation history of the Upper Lerma, a tropical high-altitud basin in central Mexico. *Quaternary Research,* 64: 70-82.

Lu, H., Burbank, D.W., Li, Y. and Liu, Y. 2010. Late Cenozoic structural and stratigraphic evolution of the northern Chinese Tian Shan foreland. *Basin Research,* 22: 249-269.

Lyell, C. 1832. *Principles of Geology*. Volume the second. John Murray. London.

Mack, G.H. and Stout, D.M. 2005. Unconventional distribution of facies in a continental rift basin: the Pliocene-Pleistocene Mangas Basin, south-western New Mexico, USA. *Sedimentology,* 52: 1187-1205.

Mack, G.H., Cole, D.R. and Treviño, L. 2000. The distribution and discrimination of shallow, authigenic carbonate in the Pliocene-Pleistocene Palomas Basin, southern Rio Grande rift. *Geological Society of America Bulletin,* 112: 643-656.

Mack, G.H., Seager, W.R. and Leeder, M.R. 2003. Synclinal-horst basins: examples fromthe southern Rio Grande rift and southern transition zone of southwestern NewMexico,USA. *Basin Research,* 15: 365-377.

Mack, G.H., Seager, W.R., Leeder, M.R., Perez-Arlucea, M. and Salyards, S.L. 2006. Pliocene and Quaternary history of the Rio Grande, the axial river of the southern Rio Grande rift, New Mexico, USA. *Earth Science Reviews,* 79:141-162.

MacNeish, R.S. 1967. A summary of the subsistence. In: Byers, D (ed.). *The Prehistory of the Tehuacan Valley*. Vol. I. Environment and subsintence. University of Texas Press, 290-331.

Maddy, D., Demir, T., Bridgland, D.R., Veldkamp, A., Stemerdink, C., van der Schriek, T. and Westway, R. 2005. An obliquity-controlled Early Pleistocene river terrace record from Western Turkey? *Quaternary Research,* 63: 339-346.

Maher, E. and Harvey, A.M. 2008. Fluvial system response to tectonically induced base-level change during the late-Quaternary: the Rio Alias southeast Spain. *Geomorphology,* 100: 180-192.

Marchitto, T.M. and Wei, K. 1995. History of Laurentide meltwater flow to the Gulf of Mexico during the last deglaciation, as revealed by reworked calcareous nannofossils. *Geology,* 23(9): 779-782.

Martínez, A.H., Zárate, B.R., Loaeza, G.J.P., Saenz, P.R. and Cardoso, V.E.A. 2001. *Carta Geológico-Minera Orizaba E14-6*. Servicio Geológico Mexicano. Mexico. One map, scale 1:250,000.

Martínez-Hernández, E. and Ramírez-Arriaga, E. 1999. Palinoestratigrafía de la region de Tepexi de Rodríguez, Puebla, Mexico-Inplicaciones cronoestratigráficas. *Revista Mexicana de Ciencias Geológicas,* 16(2): 187-207.

Martinson, D.G., Pisias, N.G., Hays, J.D., Imbrie, J., Moore, T.C. and Shackleton, N.J. 1987. Age dating and the orbital theory of the ice ages: development of a high resolution 0-300,000 year chronostratigraphy. *Quaternary Research,* 27: 1-29.

Mauvois, R. 1977. Cabalgamiento Micénico (?) en la parte centromeridional de Mexico. *Revista del Instituto de Geología UNAM,* 1(1): 48-63.

McAuliffe, J.R., Sundt, P.C., Valiente-Banuet, A., Casas, A. and Viveros, J.L. 2001. Pre-columbian soil erosion, persistent ecological changes, and collapse of a subsistence agricultural economy in the semi-arid Tehuacan n Valley, Mexico's 'Cradle of Maize'. *Journal of Arid Environments,* 47: 47–75.

McLaren, S. 2004. Characteristics, evolution and distribution of Quaternary channel calcretes, southern Jordan. *Earth Surface Processes and Landforms,* 29: 1487-1507.

McManus, J. 1988. Grain size determination and interpretation. In Tucker, M. (ed.). *Techniques in Sedimentology*. Blackwell, 63-85.

Mead, J.I., Swift, S.L., White, R.S., McDonald, H.G & Baez, A. 2007. Late Pleistocene (Rancholabrean) Glyptodont and Pampathere (Xenarthra, Cingulata) from Sonora, Mexico. *Revista Mexicana de Ciencias Geologicas,* 24(3): 439-449.

Medina-Sánchez, J. 2004. Recursos hídricos del suelo y requerimientos para la germinación de cinco cactus columnares gigantes con poblaciones segregadas en el Valle de Tehuacan. MSc thesis. Instituto de Ecología, UNAM, Mexico.

Metcalfe, S., Davies, S.J., Braisby, J.D., Leng, M.J., Newton, A.J., Terrett, N.L. and O'Hara, S.L. 2007. Long and short-term change in the Pátzcuaro Basin, central Mexico. *Palaeogeography, Palaeoclimatology, Palaeoecology,* 247: 272-295.

Metcalfe, S., Say, A., Black, S., McCulloch, R. and O´Hara, S. 2002. Wet conditions during the last glaciation in the Chihuahuan Desert, Alta Babícora Basin, Mexico. *Quaternary Research,* 57: 91-101.

Metcalfe, S.E., Bimpson, A., Courtice, A.J., O´Hara, S. and Taylor, D.M. 1997. Climate change at the monsoon/westerly boundary in Northern Mexico. *Journal of Paleolimnology,* 17: 155-171.

Metcalfe, S.E., O´Hara, S.L., Caballero, M. and Davies, S.J. 2000. Records of Late Pleistocene-Holocene climatic change in Mexico- A review. *Quaternary Science Reviews,* 19: 699-721.

Meyer, E.R. 1973. Late Quaternary Paleoecology of the Cuatro Cienegas basin, Coahuila, Mexico. *Ecology,* 54(5): 982-995.

Mial, A.D. 1981. Alluvial sedimentary basins: tectonic setting and basin architecture. In Miall, A.D. 1981. (ed.). *Sedimentation and Tectonics in Alluvial Basins.* Geological Association of Canada. Special paper No. 23, 1-33.

Morán-Zenteno, D. J., Tolson, G., Martínez-Serrano, R. G., Martiny, B., Schaaf, P., Silva-Romo, G., Macías-Romo, C., Alba-Aldave, L. A., Hernández-Bernal, M. S. and Solís-Pichardo, G. N., 1999, Tertiary arc-magmatism of the Sierra Madre del Sur, Mexico, and its transition to the volcanic activity of the Trans-Mexican Volcanic Belt: *Journal of South American Earth Sciences*, 12: 513-535.

Morán-Zenteno, D.J., Caballero-Miranda, C.I., Silva-Romo, G., Ortega-Guerrero, B. and González-Torres, E. 1993. Jurassic-Cretaceous paleogeographic evolution of the Northern Mixteca terrane, Southern Mexico. *Geofisica Internacional,* 32(3): 453-473.

Mosiño-Aleman, P.A. and García, E. 1981. The variability of rainfall in Mexico and its determination by means of the gamma distribution. *Geografiska Annaler,* 63A(1-2): 1-10.

Murray, A.B., Lazarus, E., Ashton, A., Baas, A., Coco, G., Coulthard, T., Fonstad, M., Haff, P., McNamara, D., Paola, C., Pelletier, J. and Reinhardt, L. 2009. Geomorphology, complexity, and the emerging science of the Earth's surface. *Geomorphology,* 103:496-505.

Naranjo-García, E. 2003. Moluscos continentals de Mexico: Dulceacuícolas. *Revista de Biología Tropical,* 51(Suppl. 3): 495-505.

Narayanapanicker, S., Bagati, T.N., Kumar, R. and Thakur, V.C. 2007. Evolution of Quaternary alluvial fans and terraces in the intramontane Pinjaur Dun, Sub-Himalaya, NW India: interaction between tectonics and climate change. *Sedimentology,* 54: 809-833.

Nash D.J. and McLaren S.J. 2003. Kalahari valley calcretes: their nature, origins, and environmental significance. *Quaternary International,* **111**:3–22.

Nash, D.J. and Smith, R.F. 2003. Properties and development of channel calcretes in a mountain catchment, Tabernas Basin, southern Spain. *Geomorphology,* 50:227-250.

Nieto-Samaniego, F., S.A. Alaniz-Álvarez, G. Silva-Romo, M.H. Eguiza-Castro and C.C. Mendoza-Rosales. 2006. Latest Cretaceous to Miocene deformation events in the eastern Sierra Madre del Sur, Mexico, inferred from the geometry and age of major structures. *Geological Society of America Bulletin,* 118(1-2): 238-252.

Nixon, G. T., Demant, A., Armstrong, R. L., and Harakal, J. E. 1987. K-Ar and geologic data bearing on the age and evolution of the Trans-Mexican Volcanic Belt: *Geofísica Internacional*, 26: 109–158.

Nordt, L. 1994. Late Quaternary fluvial landscape evolution in desert grasslands of northern Chihuahua, Mexico. *Geological Society of America Bulletin,* 115: 596-606.

Oldfield, F. 2005. *Environmental Change; Key Issues and Alternatives*. Cambridge University Press.

Olson, D.M. and Dinerstein, E. 1998. The global 200: A representation approach to conserving the earth's most biologically valuable ecoregions. *Conservation Biology,* 12(3): 502-515.

Omaña, L., and González-Arreola, C. 2008. Late Jurassic (Kimmeridgian) larger benthic Foraminifera from Santiago Coatepec, SE Puebla, Mexico. *Geobios,* 41: 799-817.

Ortega-Gutiérrez F., Ruiz, J. and Centeno-García, E. 1995. Oaxaquia, a Proterozoic microcontinent accreted to North America during the late Paleozoic. *Geology,* 23(12): 1127-1130.

Ortega-Gutiérrez, F. 1978. Estratigrafía del Complejo Acatlán en la Mixteca Baja, estados de Puebla y Oaxaca. *Revista del Instituto de Geología UNAM,* 2(2): 112-131.

Ortega-Gutiérrez, F. 1981. Metamorphic belts of southern Mexico and their tectonic significance. *Geofísica Internacional,* 20: 177-202.

Ortega-Gutiérrez, F., and Elías-Herrera, M., 2003, Wholesale melting of the southern Mixteco terrane and origin of the Xolapa Complex. *Geological Society of America Abstracts with Program V*, 35(4): 66-72.

Ortega-Gutiérrez, F., Elías-Herrera, M., Reyes-Salas, M. and Macías-Romo, C. 1999. Late Ordovician Early Silurian continental collisional orogeny in southern. *Geology,* 28(8): 719-722.

Ortega-Gutiérrez, F., Mitre-Salazar, L. M., Roldán-Quintana J., Aranda-Gómez, J. J., Morán-Zenteno, D., Alaniz-Álvarez, S. A., and Nieto-Samaniego, A. F., 1992, *Carta Geológica de la República Mexicana*, 5th edition, Scale 1:2 000 000: Universida Nacional Autónoma de Mexico, Instituto de Geología; y Secretaría de Energía, Minas e Industria Paraestatal, consejo de Recursos Minerales.

Ortega-Gutiérrez, F., Ruiz, J. and Centeno-García, E. 1995. Oaxaquia, a Proterozoic microcontinent accreted to North America during the late Paleozoic. *Geology,* 23(12): 1127-1130.

Ortega-Ramírez, J. 1995. Los paleoambientes holocénicos de la Laguna de Babícora, Chihuahua, Mexico. *Geofísica Internacional,* 34: 107-116.

Ortega-Ramírez, J., Maillol, J.M., Bandy, W., Valiente-Banuet, A., Urrutia-Fucugauchi, J., Mortera-Gutiérrez. and Chacón-Cruz, G.J. 2004. Late Quaternary evolution of alluvial fans in the Playa-Lake, El Fresnal region, northern Chihuahua Desert, Mexico: Palaeoclimatic implications. *Geofísica Internacional,* 43(3): 445-466.

Ortega-Ramírez, J., Maillol, J.M., Urrutia-Fucugauchi, J., Valiente-Banuet, A., Bandy, W. and Martínez-Serrano, R. 2001. Tectonic and climate change controls in Late Quaternary alluvial fan development in the Playa El Fresnal Region, North Chihuahuan Desert. *Journal of Arid Land Studies,* 11(3): 143-158.

Ortega-Ramírez, J., Valiente-Banuet, A., Urrutia-Fucugauchi, J., Mortera-Gutiérrez, C.A. and Alvarado-Valdez, G. 1998. Paleoclimatic changes during the Late Pleistocene-Holocene in Laguna Babicora, near the Chihuahuan Desert, Mexico. *Canadian Journal of Earth Sciences,* 35: 1168-1179.

Palacios-Fest, M.R., Carreño, A.L., Ortega-Ramírez, J.R. and Alvarado-Valdéz, G. 2002. A paleoenvironmental reconstruction of Laguna Babícora, Chihuahua, Mexico based on ostracode paleoecology and trace element shell chemistry. *Journal of Paleolimnology,* 27: 185-206.

Pantoja-Alor, J. 1990. Geología y paleoambientes de la cantera Tlayua, Tepexi de Rodríguez, Estado de Puebla. *Revista del Instituto de Geología UNAM,* 9(2): 156-169.

Pavon, N.P. and Briones, O. 2001. Phenological patterns of nine perennial plants in an intertropical semi-arid Mexican scrub. *Journal of Arid Environments,* 49(2): 256-277.

Phillips, J.D. 1997. Humans as geological agents and the question of scale. *American Journal of Science,* 297: 98-115

Phillips, J.D. 2009. Changes, perturbations and responses in geomorphic systems. *Progress in Physical Geography,* 33(1): 17-30.

Piperno, D.R., Moreno, J.E., Iriarte, J., Holst, I., Lachniet, M., Jones, J.G., Ranere, A.J. and Castanzo, R. 2007. Late Pleistocene and Holocene environmental history of the Iguala Valley, central Balsas watershed of Mexico. *Proceedings of the National Academy of Science,* 104(29): 11847-11881.

Piperno, D.R., Ranere, A.J., Holst, I., Iriarte, J. and Dickau, R. 2009. Starch grain and phytolith evidence for early ninth millennium B.P. maize from the Central Balsas River Valley, Mexico. *Proceedings of the National Academy of Science,* 106(13): 5019-5024.

Poore, R.Z., Dowsett, H.J. and Verardo, S. 2003. Millennial to century-scale variability in Gulf of Mexico Holocene climate records: *Paleoceanography,* 18: 26-1–26-13.

Poore, R.Z., Pavich, M.J. and Grissino-Mayer, H.D. 2005. Record of the North American southwest monsoon from Gulf of Mexico sediment cores. *Geological Society of America Bulletin,* 33(3): 209-212.

Quigley, M.C., Sandiford, M. and Cupper, M. L. 2007. Distinguishing tectonic fromclimatic controls on range-front sedimentation. *Basin Research,* 19, 491–505.

Ramírez-Arriaga, E., Prámparo, M.B., Martínez-Hernández, E. and Valiente-Baunet, A. 2006. Palynology of the Paleogene Cuayuca Formation (stratotype sections), southern Mexico: Chronostratigraphical and palaeoecological implications. *Review of Palaeobotany and Palynology,* 141: 259-275.

Ranere, A.J., Piperno, D.R., Holst, I., Dickau, R. and Iriarte, J. 2009. The cultural and chronological context of early Holocene maize and squash domestication in the Central Balsas River Valley, Mexico. *Proceedings of the National Academy of Science,* 106(13): 5014-5018.

Ridente, D., Fracassi, U., Bucci, D.D., Trincardi, F. and Valensise, G. 2008. Middle Pleistocene to Holocene activity of the Gondola Fault zone (Southern Adriatic Foreland): deformation of a regional shear zone and seismotectonic implications. *Tectonophysics,* 453: 110-121.

Ritter, J.B., Miller, J.R., Enzel, Y. and Wells, S.G. 1995. Reconciling the roles of tectonism and climate in Quaternary alluvial fan evolution. *Geology,* 23(3): 245-248.

Romero, M. 1896. Mexico. *Journal of the American Geographical Society of New York,* 28(4): 327-386.

Rosenmeier, M.F. Hodell, D.A., Brenner, M., Curtis, J.H. and Guilderson, T.P. 2002. A 4000 year lacustrine record of environmental change in the southern Maya lowlands, Petén, Guatemala. *Quaternary Research,* 57: 183-190.

Rudwick, M. 1975. Charles Lyell, F.R.S. (1797-1875) and his London lecture on Geology, 1832-33. *Notes and Records of the Royal Society of London,* 29 (2): 231-263.

Rzedowski, J. 1978. *Vegetación de Mexico.* Limusa. Mexico.

Santamaría-Díaz, A., Alaniz-Álvarez, S.A. and Nieto-Samaniego, A.F. 2008. Deformaciones cenozoicas en la cobertura de la falla Caltepec en la region de Tamazulapam, sur de Mexico. *Revista Mexicana de Ciencias Geológicas,* 25(3): 494-516.

Sarmiento, G., Gaviria, S., Hooghiemstra, H., Berrio, J.C. and Van der Hammer, T. 2008. Landscape evolution and origin of Lake Fuquene (Colombia): Tectonics, erosion and sedimentation processes during the Pleistocene. *Geomorphology,* 100: 563-575.

Sedlock, R.L., Ortega-Gutiérrez, F. and Speed, R.C. 1993. Tectonostratigraphic Terranes and Tectonic Evolution of Mexico. *Geologica Society of America Special Paper 278.*

Sedlov, S., Lozano-García, S., Soleiro-Rebolledo, E., McClung de Tapia, E, Ortega-Guerrero, B. and Sosa-Najera, S. 2010. Tepexpan revisited: A multiple proxy of local environmental changes in relation of human occupation from a paleolake shore section in central Mexico. *Geomorphology,* 122: 309-322.

Sedlov, S., Solleiro-Rebolledo, E., Terhorst, B., Solé, J., Flores-Delgadillo, M.L., Werner, G. and Poetsch, T. 2009. The Tlaxcala basin palaeosol sequence: a multyscale proxy of middle to late Quaternary environmental change in central Mexico. *Revista Mexicana de Ciencias Geológicas,* 26(2): 448-465.

Shumm, S.A., Dumont, J.F. and Holbrook, J.M. 2000. *Active Tectonics and Alluvial Rivers.* Cambridge University Press.

Siebe, C., Abrams, M., Macias, J.L. and Obenholzner, J. 2006. Repeated volcanic disasters in Prehispanic time at Popocatépetl, central Mexico: Past key to the future? *Geology,* 24(5): 399-402.

Silva-Romo, G., Mendoza-Rosales, C. and Martiny, B. 2000. Acerca del origen de las cuencas cenozóicas de la zona cortical extendida del sur de Mexico: Un ejemplo en la region Mixteca. Simposio Regional Sobre el Sur de Mexico- *Geos,* 326-327.

Sionneau, T., Bout-Roumazeilles, V., Flower, B.P., Bory, A., Tribovillard, N., Kissel, C., Van Vliet-Lanoe, B. and Montero-Serrano, J.C. 2010. Provenance of freshwater pulses in the Gulf of Mexico during the last deglaciation. *Quaternary Research,* 74: 235-245.

Sluyter, A. and Dominguez, G. 2006. Early maize (Zea mays L.) cultivation in Mexico: Dating sedimentary pollen records and its implications. *Proceedings of the National Academy of Science,* 103(4): 1147-1151.

Springer, G.S., Rowe, H.D., Hardt, B, Cocina, F.G., Edwards, R.L. and Cheng, H. 2009. Climate driven changes in river channel morphology and base level during the Holocene and late Pleistocene of southern West Virginia. *Journal of Cave and Karst Studies,* 71(2): 121-129.

Sternbergh, L.O., Deniro, M.J. and Ting, I.P. 1984. Carbon, hydrogen, and oxygen isotope ratios of cellulose from plants having intermediary photosynthetic modes. *Plant Physiology,* 74: 104-107.

Street-Perrott, F.A. and Perrot, R.A. 1990. Abrupt climate fluctuations in the tropics: the influence of Atlantic Ocean circulations. *Nature,* 343: 607-612.

Strong, E.E., Gargominy, O., Ponder, W.F. and Bouchet, P. 2008. Global diversity of gastropods (Gastropoda; Mollusca) in freshwater. *Hydrobiologia,* 595: 149-166.

Syvitski, J.M.P. (ed.). 1991. *Principles, methods, and applications of particle size analysis.* Cambridge University Press.

Taylor, D.W. 2003. Introduction to Physidae (Grastropoda: Hygrophila); biogeography, classification, morphology. *Revista de Biologia Tropical,* 5 (1-suplement 1): 1-287.

Tchakerian, V.P. and Lancaster, N. 2002. Late Quaternary arid/humid cycles in the Mojave Desert and western Great Basin of North America. *Quaternary Science Reviews,* 21: 799-810.

Tranos, M.D., Kachev, V.N. and Mountrakis, D.M. 2008. Transtensional origin of the NE-SW Simitli basin along the Strouma (Strymon) lineament, SW Bulgaria. *Journal of the Geological Society of London*, 165: 499-510.

Valiente, B.L. 1991. Patrones de precipitación en el Valle semiárido de Tehuacan, Puebla. BSc thesis. UNAM, Mexico.

Valiente-Banuet, A. and Escurra, E. 1991. Shade as a cause of the association between the cactus *Neobuxbaumia tetetzo* and the nurse plant *Mimosa luisana* in the Tehuacan Valley, Mexico. *Journal of Ecology,* 79: 961-971.

Valiente-Banuet, A., Arizmendi, M.C., Rojas-Martínez, A., and Dominguez-Canseco, L. 1996. Ecological relationships between columnar cacti and nectar feeding bats in Mexico. *Journal of Tropical Ecology,* 12: 103-119.

Valiente-Banuet, A., Solis, L., Davila, A.P., Arizmendi, M.C., Silva-Pereyra, C., Ortega-Ramírez, J., Trevino, C.J., Rangel-Landa, S. and Casas, A. 2009. *Guia de la Vegetacion del Valle de Tehuacan-Cuicatlan*. UNAM, Mexico.

Valiente-Banuet, A., Vital-Rumebe, A, Verdú, M. and Callaway, R.M. 2006. Modern Quaternary plant lineages promote diversity through facilitation of ancient tertiary lineages. *Proceedings of the National Academiy of Sciences,* 103 (45): 16812-16817.

Valiente-Banuet, A.; Casas, A., Alcántara-Eguren, A.; Dávila, P., Flores-Hernández, N., Arizmendi, M.C, Villaseñor, J.L. and Ortega Ramírez, J. 2000. La vegetación del Valle de Tehuacan-Cuicatlán. *Boletín de la Sociedad Botánica de Mexico,* 67: 17-74.

Vázquez-Selem, L. and Heine, K. 2004. Late Quaternary glaciation in Mexico. In Ehlers, J. and Gibbard, P.L. (eds). *Quaternary glaciations - extent and chronology, part II. South America, Asia, Africa, Australia, Antarctica*. Elsevier. Amsterdam, 233-242.

Vázquez-Urbez, M., Arenas, C., Sancho, C., Auque, L. and Pardo, G. 2010. Factors controlling present-day tufa dynamics in the Monasterio de Piedra Natural Park (Iberian Range, Spain): depositional environmental settings, sedimentation rates and hydrochemistry. *International Journal of Earth Sciences,* 99: 1027-1049.

Vélez, M.I., Hooghiemstra, H., Metcalfe, S., Wille, M. and Berrio, J.C. 2006. Late Glacial and Holocene environmental and climatic changes from a limnological transect through Colombia, northern South America. *Palaeogeography, Palaeoclimatology, Palaeoecology,* 234(1): 81-96.

Viseras, C, Calvache, M.L., Soria, J.M. and Fernandez, J. 2003. Differential features of alluvial fans controlled by tectonic or eustatic accommodation space. Examples from the Beltic Cordillera, Spain. *Geomorphology,* 50: 181-202.

Vita-Finzi, C. 1970. Alluvial history of central Mexico. *Nature,* 227: 596-597.

von Bertalanffy, L. 1950. An Outline of General System Theory. *British Journal for the Philosophy of Science,* 1(2): 134-165.

Wakabayashi, J. and Sawyer, T.L. 2001. Stream incision, tectonic uplift, and evolution of topography of the Sierra Nevada, California. *Journal of Geology,* 109: 539-562.

Wang, H., Follmer, L.R. and Liu, C-L.J. 2000. Isotope evidence of paleo-ENSO cycles in the loess-paleosol record in the central USA: *Geology,* 28: 771–774.

Warren, J.K. 2010. Evaporites through time: Tectonic, climatic and eustatic controls in marine and nonmarine deposits. *Earth Science Reviews,* 98: 217-268.

Waters, J.V., Jones, S.J. and Armstrong, H.A. 2010. Climatic controls on late Pleistocene alluvial fans, Cyprus. *Geomorphology,* 115: 228-251.

Watts, W.A. and Hansen, B.C.S. 1994. Pre-Holocene and Holocene pollen records of vegetation history from Florida Peninsula and their climatic implications. *Palaeogeography, Palaeoclimatology, Palaeoecology,* 109: 163-176.

Wells, S.G., 1987. A quantitative analysis of arroyo development and geomorphic processes in the Zuni River drainage basin, west-central New Mexico. Technical Report No. 327-81L. Washington.

Wethington, A.R. 2004. Family Physidae. *A supplement to the workbook accompanying the FMCS Freshwater Identification Workshop.* University of Alabama. Tuscaloosa.

Windley, B.F. 1993. Uniformitarism today: plate tectonics is the key to the past. *Journal of the Geological Society,* 150: 7-19.

Wright, V.P., Alonso-Zárza, A.M., Sanz, M.E. and Calvo, J.P. 2007. Diagenesis of late Miocene micritic lacustrine carbonates, Madrid Basin, Spain. *Sedimentary Geology,* 114: 81-95.

Wysocka, A. 2009. Sedimentary environments of the Neogene basins associated with the Cao Bang-Tien Yen Fault, Vietnam. *Acta Geologica Polonica,* 59(1): 45-69.

Xie, S., Guo, J., Huang, J., Chen, F., Wang, H. and Farrimond, P. 2004. Restricted utility of δ^{13}C of bulk organic matter as a record of paleovegetation in some loess-paleosol sequences in the Chinese Loess Plateau. *Quaternary Research,* 62: 86-93.

Yaalon, D. H. 1983. Climate, time and soil development. In: Wilding, L. P., Smeck, N. E. and Hall, G. F. (eds). *Pedogenesis and soil taxonomy. I Concepts and interactions.* Elsevier Science Publishers B. V. Netherlands, 233-251.

Yañez, P., Ruiz, J., Patchett, J., Ortega-Gutiérrez, F. and Hehrels, G.E. 1991. Isotopic studies of the Acatlan complex, southern Mexico: Implications for Paleozoic North American tectonics. *Geological Society of America Bulletin,* 103: 817-828.

Yin, A., Dang, Y., Zhang, M., Chen, X. and McRivette, M.W. 2008. Cenozoic tectonic evolution of the Qaidam basin and its surrounding regions (Part 3): Structural geology, sedimentation, and regional tectonic reconstruction. *Geological Society of America Bulletin,* 120: 847-876.

Zhang, K., Liu, K. and Yang, J. 2004. Asymmetrical valleys created by the geomorphic response of rivers to strike-slip fault. *Quaternary Research,* 62: 310-315.

Zhou, J. and Chafetz, H.S. 2009. The genesis of late Quaternary caliche nodules in Mission Bay, Texas: stable isotopic compositions and palaeoenvironmental interpretation. *Sedimentology,* 56: 1392-1410.

Web pages:

USGS-NASA, 2009. Landsat TM image. http://landsat.usgs.gov, 16/06/2009.

NASA. 2009. Shuttler Radar Topography Mission. http://dds.cr.usgs.gov/srtm/.version2_1/, 15/06/2009.